Topological magnetic structures in MnGe and CeAlGe: neutron diffraction and symmetry analysis

Vladimir Pomjakushin
Laboratory for Neutron Scattering and Imaging LNS, Paul Scherrer Institut PSI
Switzerland

Neutron wide-angle diffraction experiments:	HRPT, DMC /PSI
SANS (CeAlGe):	SANS-I/PSI, D33/LLB
Samples:	Solid State Chemistry group PSI and University of Tokyo (MnGe)
Hall effect:	University of Tokyo

MnGe: V. Pomjakushin, I. Plokhikh, J. S. White, Y. Fujishiro, N. Kanazawa, Y. Tokura, and E. Pomjakushina
Phys. Rev. B **107**, 024410 (2023)

CeAlGe: P. Puphal, V. Pomjakushin, N. Kanazawa, V. Ukleev, D.J. Gawryluk, J. Ma, M. Naamneh, N.C. Plumb, L. Keller, R. Cubitt, E. Pomjakushina and J.S. White
Physical Review Letters, **124**, 017202 (2020)

Plan

- Intro to magnetic structures/symmetries, topological textures for multi-k structures, homotopy, winding numbers, …

  For both MnGe and CeAlGe

- Samples. Neutron diffraction experiments
- Magnetic structures 1k, 2k and 3k in respective Magnetic Superspace Groups MSSG
- Calculation of topological charges
- Summary

Magnetic structure

Examples

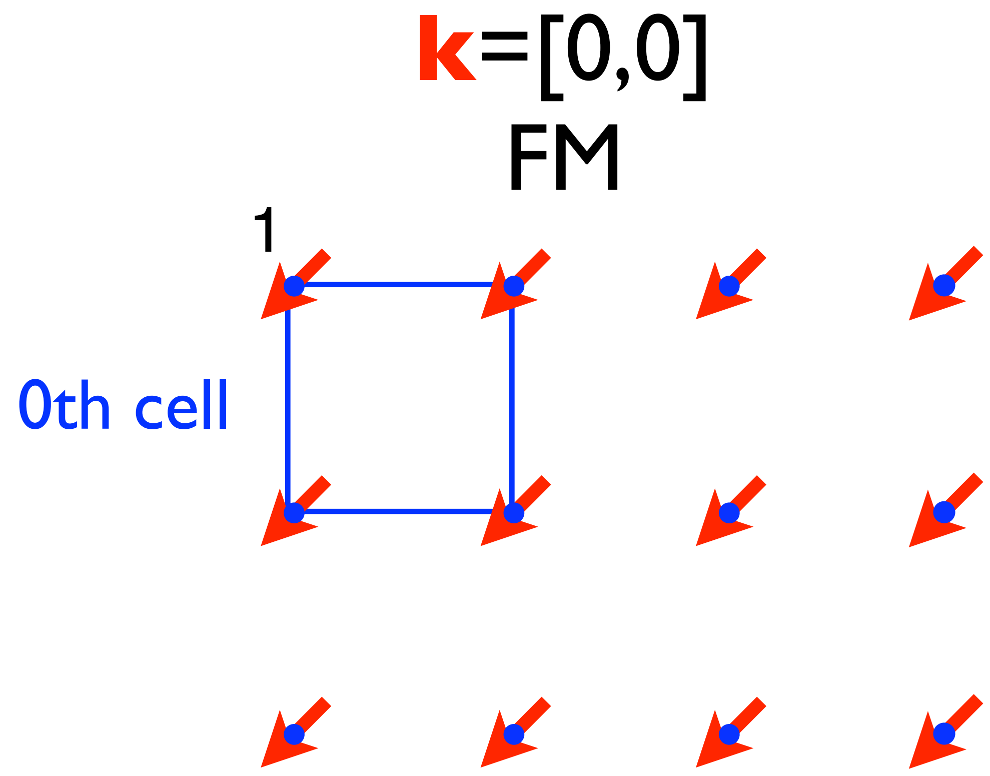

$$\mathbf{S}_{01} = \mathbf{S}_x + \mathbf{S}_y$$

Magnetic structure

Examples

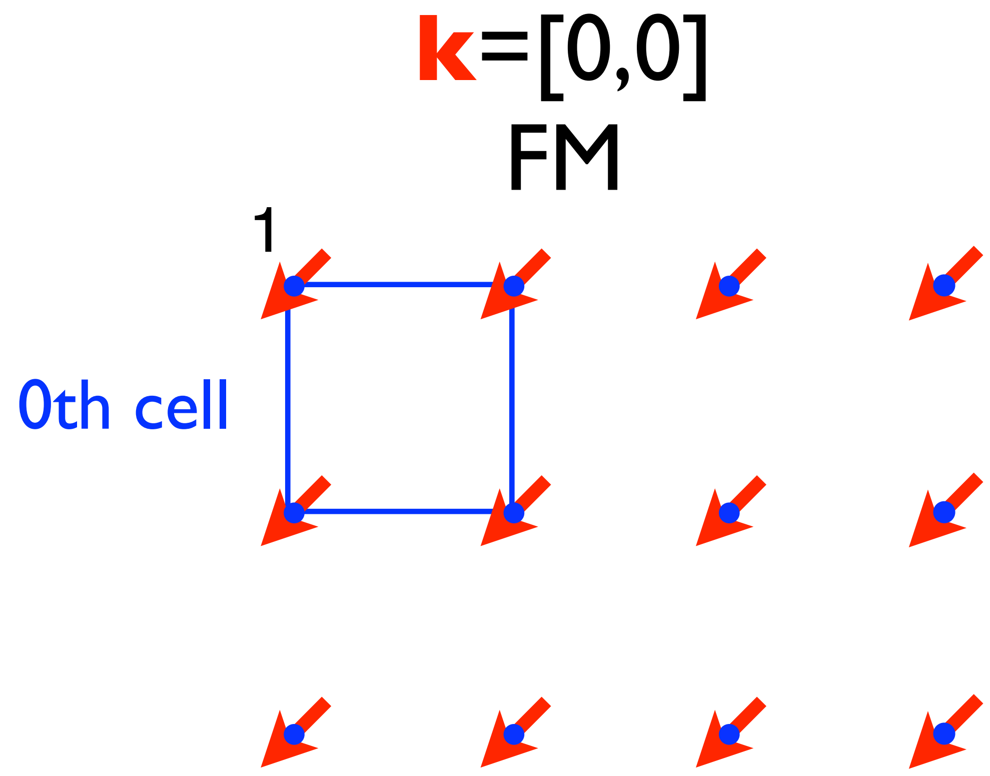

$$\mathbf{S}_{01} = \mathbf{S}_x + \mathbf{S}_y$$

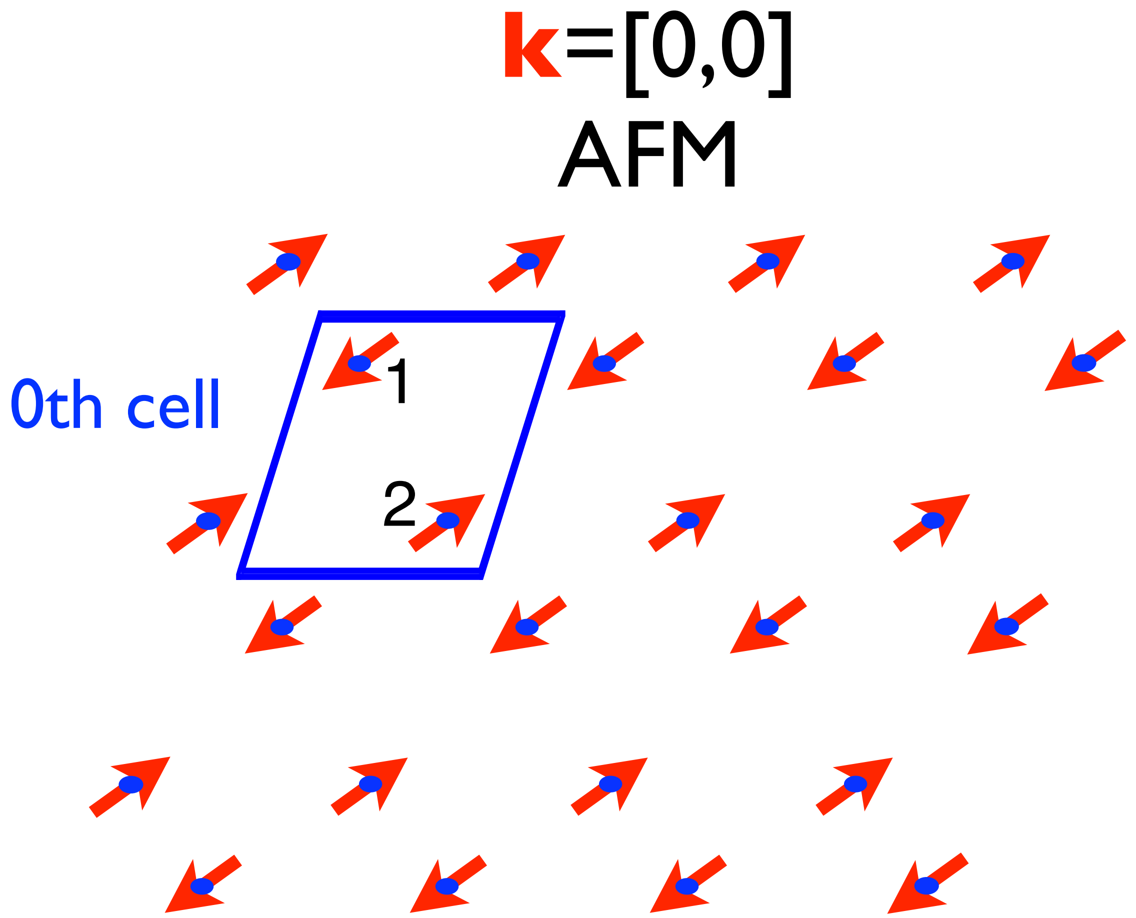

$$\mathbf{S}_{01} = \mathbf{S}_x + \mathbf{S}_y$$

$$\mathbf{S}_{02} = -\mathbf{S}_{01}$$

2k magnetic structure

Antiferromagnetic (à la cycloidal spiral) three sub−lattice ordering in $Tb_{14}Ag_{51}$

k−vector: k_K=[1/3, 1/3, 0]

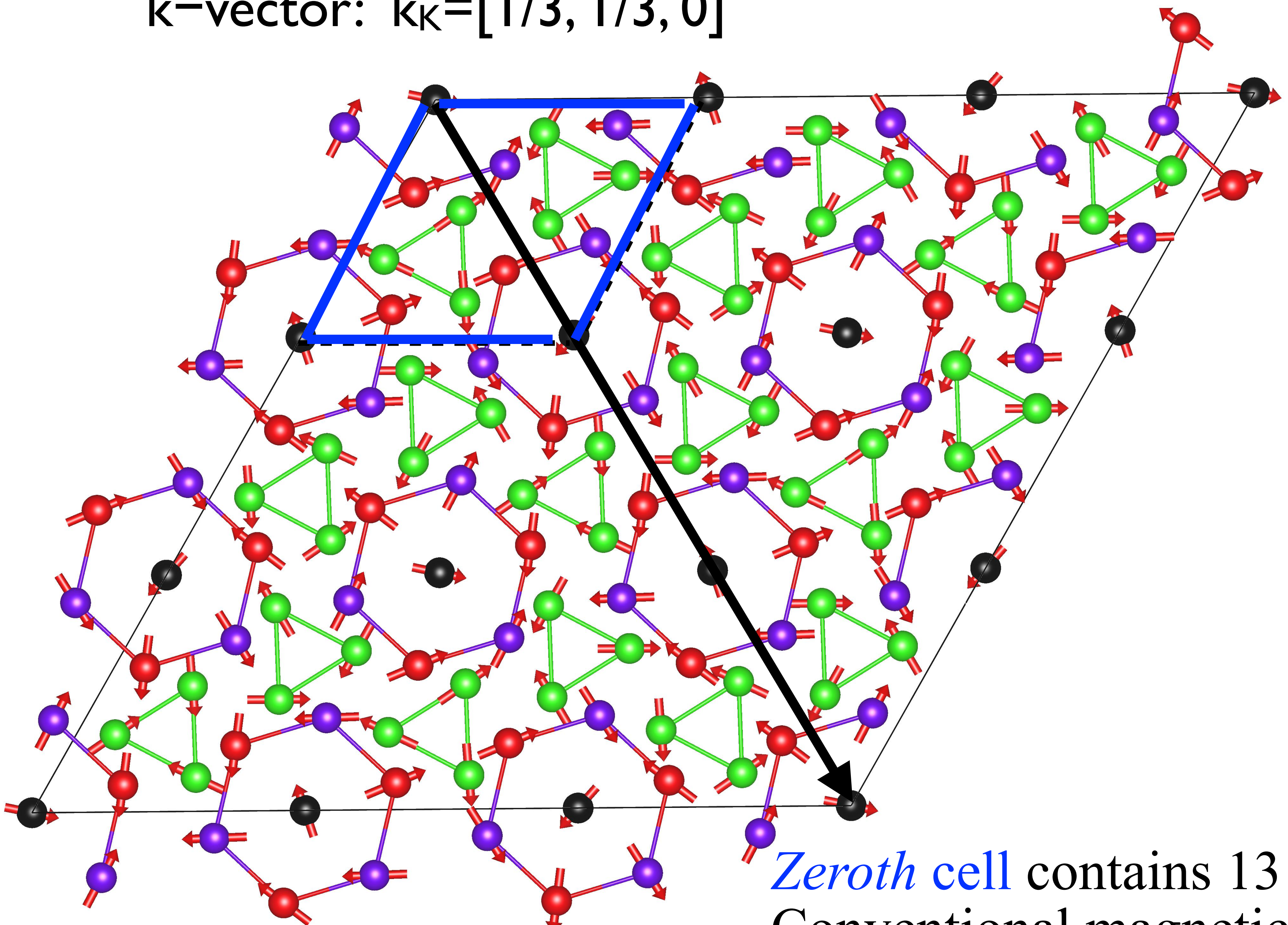

Zeroth cell contains 13 spins of Tb^{3+}.
Conventional magnetic unit cell contains 126 spins of Tb^{3+}!!

Magnetic moment amplitudes S_0
Propagation vector k of magnetic structure

position of spin in the lattice

Magnetic moment $$\mathbf{S}(\mathbf{t}_n) = \frac{1}{2}(\mathbf{S}_0 e^{+2\pi i \mathbf{t}_n \mathbf{k}} + \mathbf{S}_0^* e^{-2\pi i \mathbf{t}_n \mathbf{k}}) \equiv |S_{0\alpha}| \hat{\mathbf{e}}_\alpha \cos(2\pi \mathbf{t}_n \mathbf{k} + \phi_\alpha)$$
$$\alpha = x, y, z$$

Modulated magnetic structure

real space

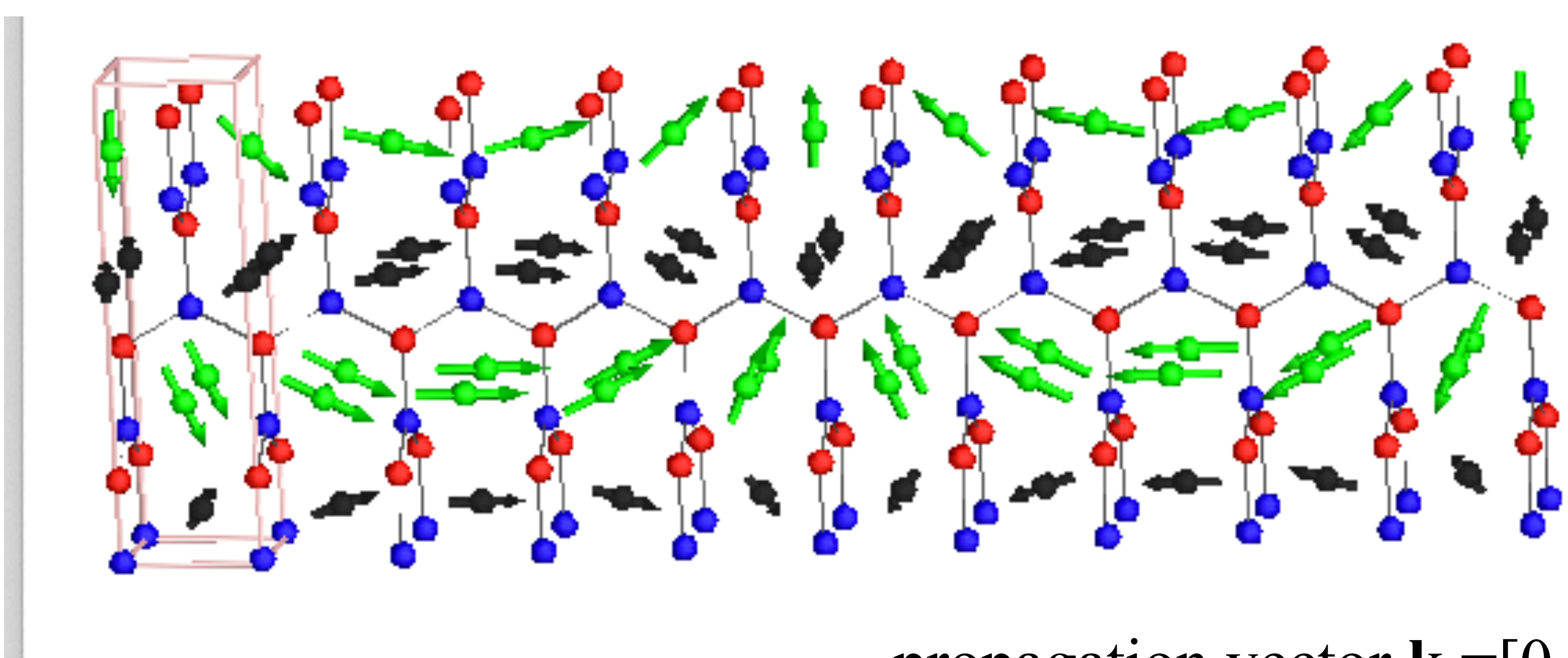

propagation vector **k** =[0,b,0]

Diffraction: reciprocal space

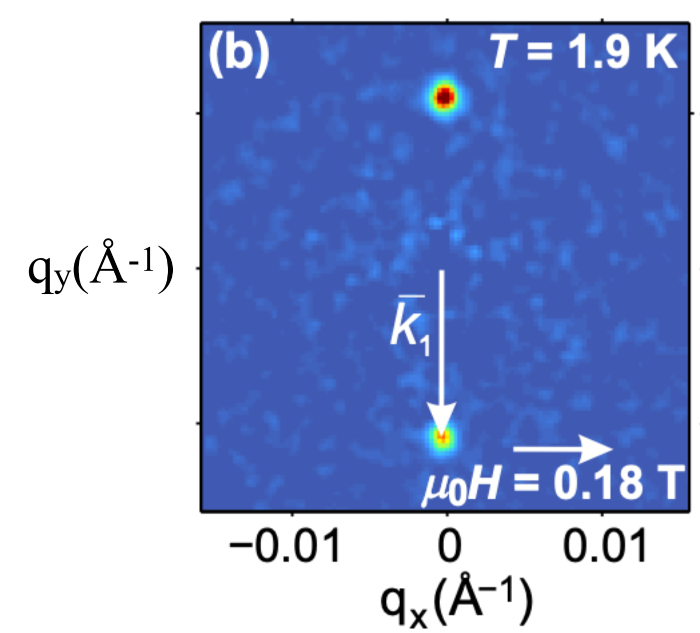

multi-k structures

$$\mathbf{S}(\mathbf{t}_n) = \sum_{l=1}^{m} |S_{0\alpha,l}| \hat{\mathbf{e}}_\alpha \cos(2\pi \mathbf{t}_n \mathbf{k}_l + \phi_{\alpha,l}), \;\; \alpha = x, y, z$$

real space

Diffraction: reciprocal space

k2=[b,0,0]

k1=[0,b,0]]

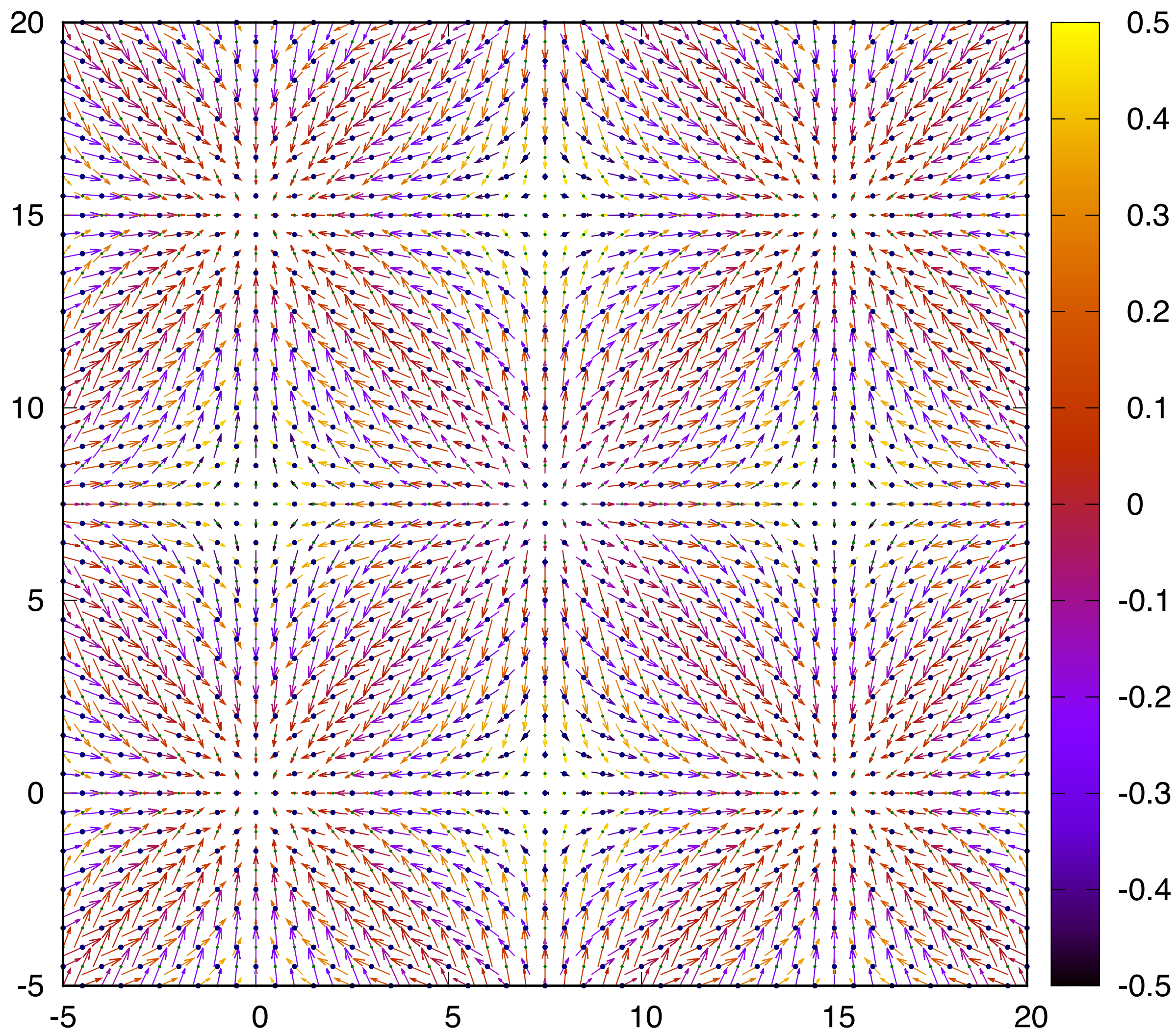

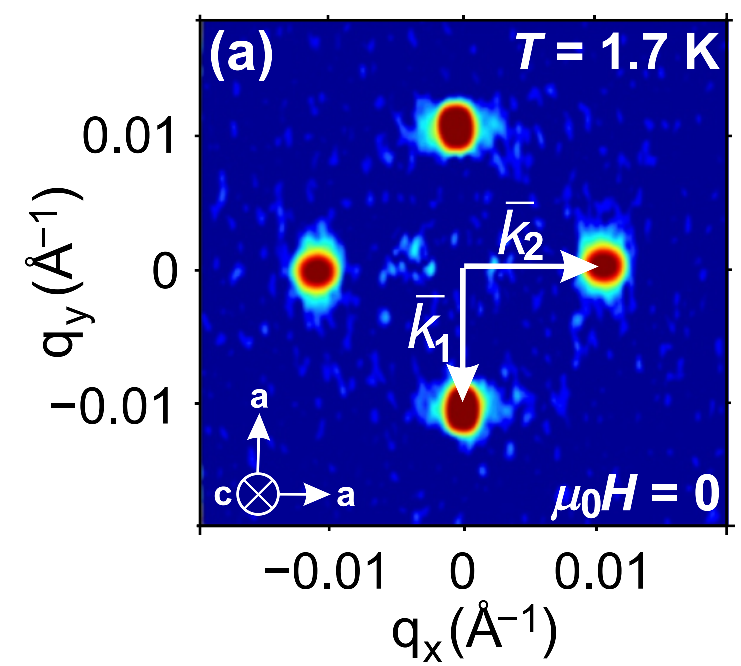

Examples of propagation vector stars

P2_13: 8 symops, three 2-fold and there 3-fold rotations

DT MnGe

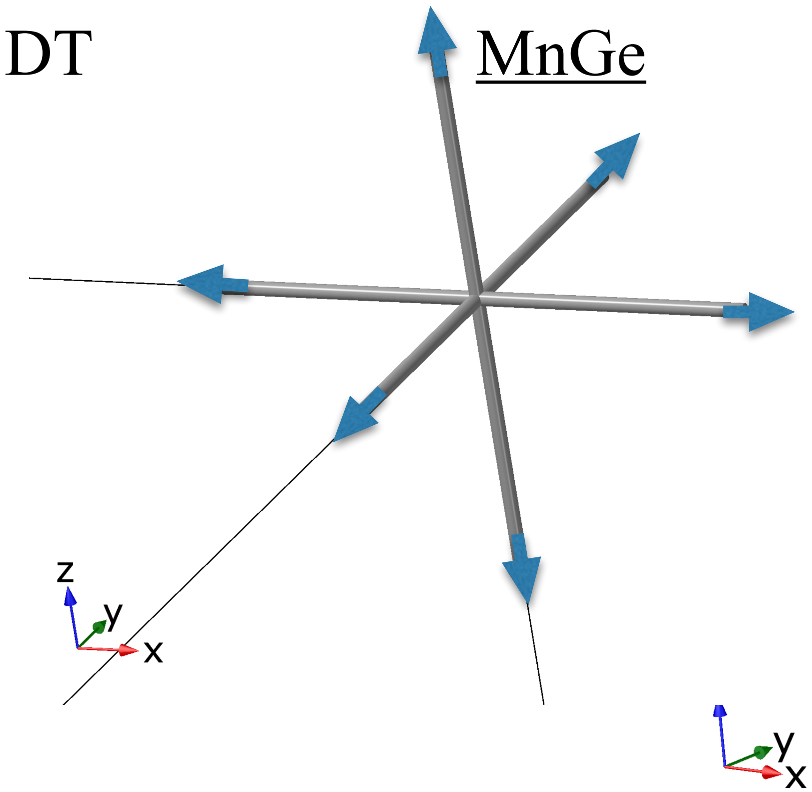

3+3=6-arms 0b0

X

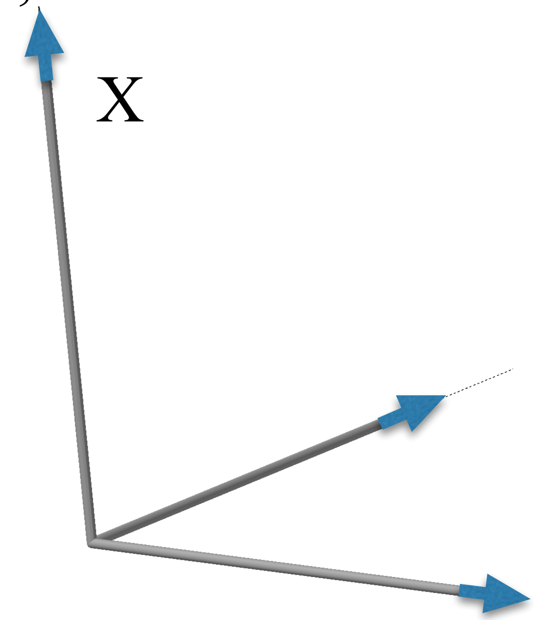

3-arms 0½0

M

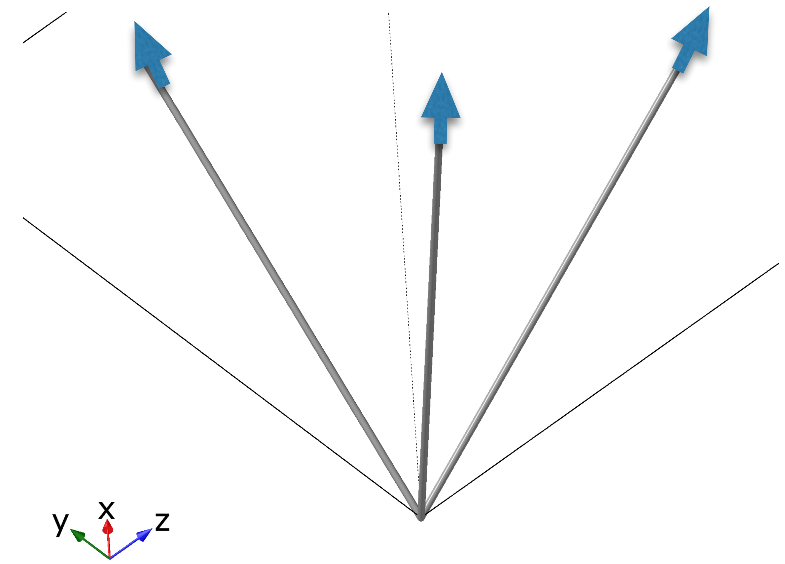

3-arms ½½0

Examples of propagation vector stars

P2_13: 8 symops, three 2-fold and there 3-fold rotations

DT <u>MnGe</u>

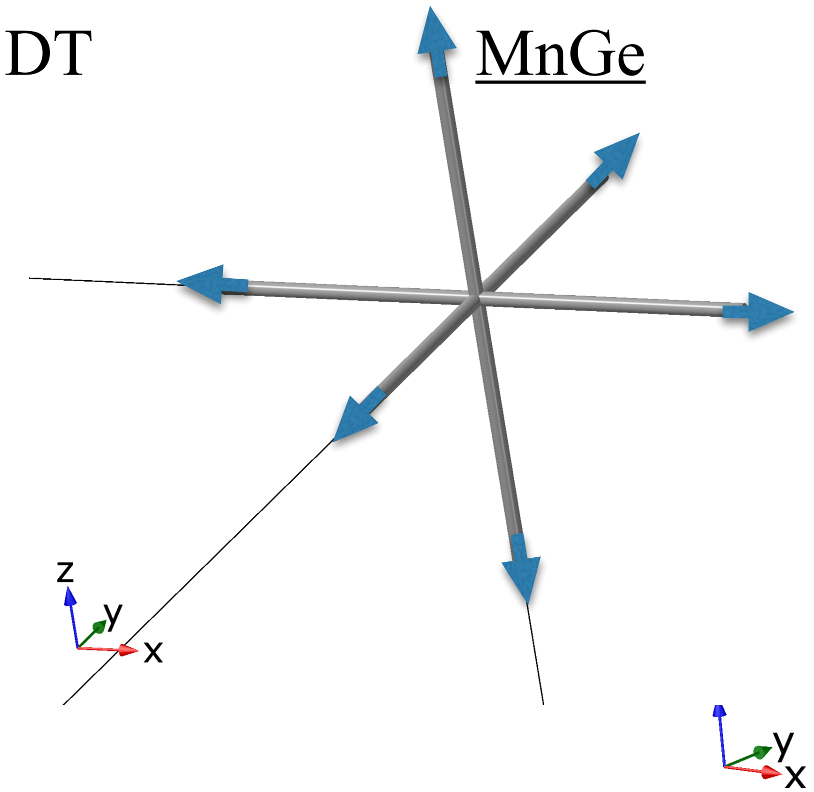

3+3=6-arms 0b0

X

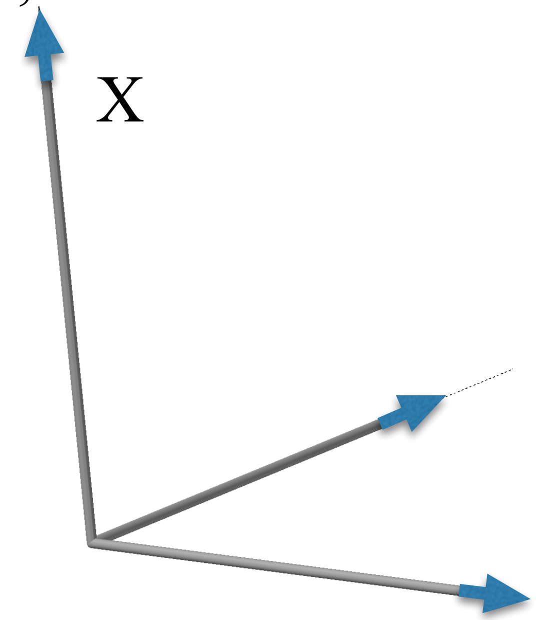

3-arms 0½0

M

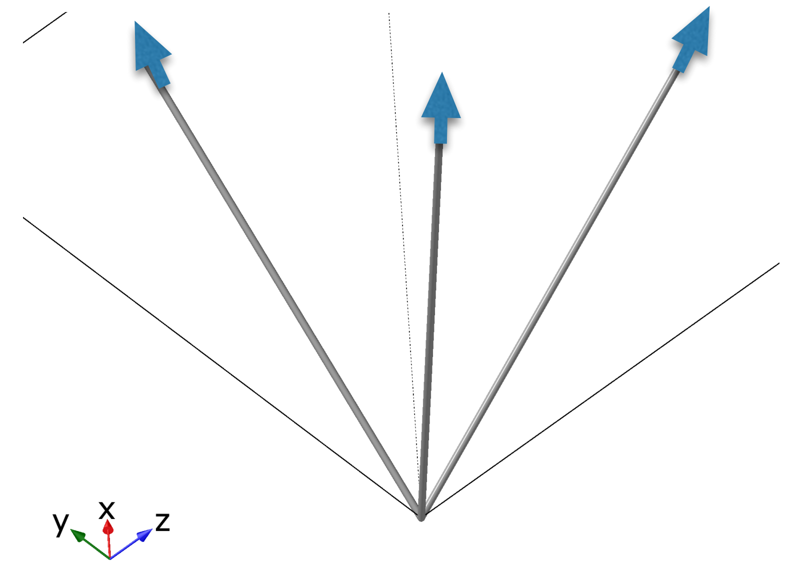

3-arms ½½0

LD <u>MnSi</u>

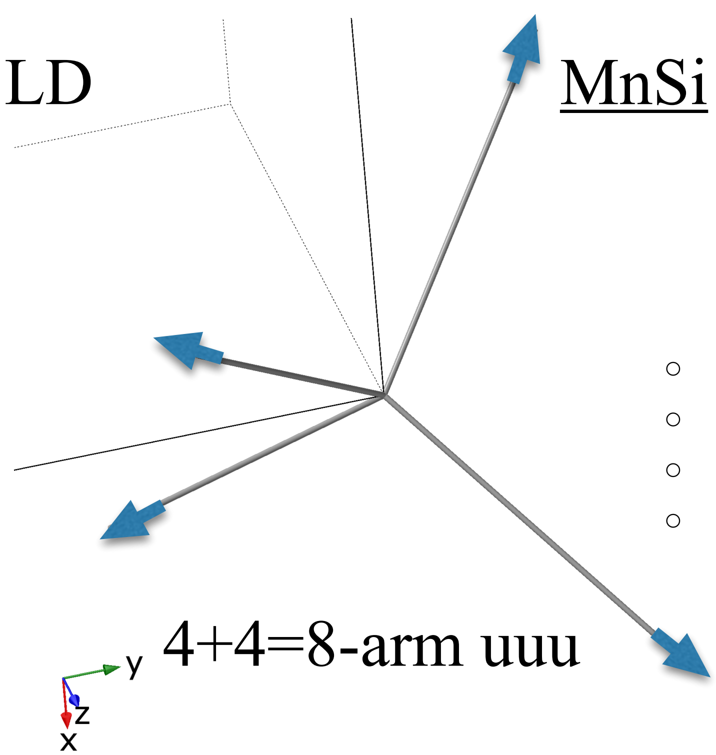

- u u u
- -u -u u
- -u u -u
- u -u -u

4+4=8-arm uuu

R

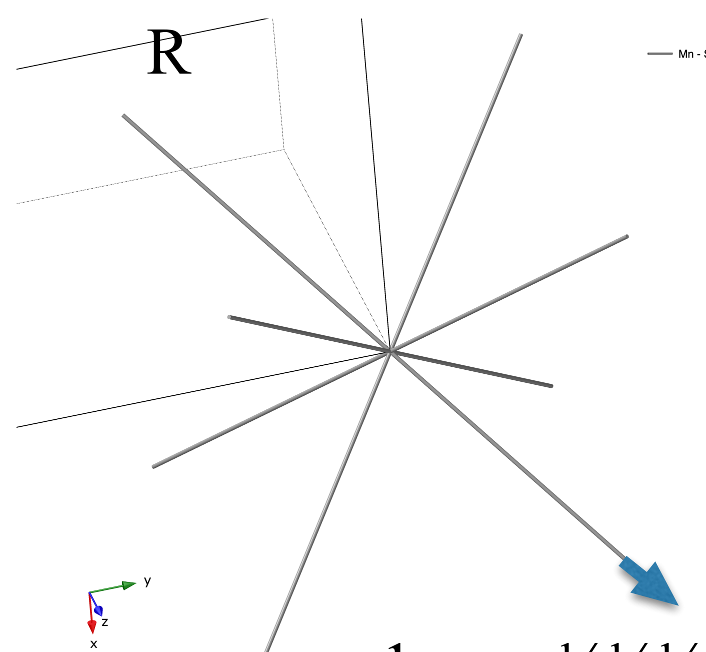

1-arm ½½½

Magnetic Space Groups MSG and propagation vector

$$\mathbf{S}(\mathbf{t}_n) = Re\left(C\mathbf{S}_0 e^{2\pi i \mathbf{t}_n \mathbf{k}}\right) \sim \cos(2\pi \mathbf{t}_n \mathbf{k} + \varphi)$$

- commensurate (C) : $|\mathbf{k}|$=m/n, m,n: integers. For large (m,n) **k** should be considered incommensurate (IC)
- incommensurate IC $|\mathbf{k}| \neq$ m/n

MSG: only 3D-crystallographic symmetry elements, e.g. no arbitrary rotation angles, only 60, 90, 120, 180 degrees

62 ***Pnma***

Pn′ma
Pnm′a
Pnma′
**Pn′m′a*
**Pnm′a′*
**Pn′ma′*
Pn′m′a′

Magnetic Space Groups MSG and propagation vector

$$\mathbf{S}(\mathbf{t}_n) = Re\left(C\mathbf{S}_0 e^{2\pi i \mathbf{t}_n \mathbf{k}}\right) \sim \cos(2\pi \mathbf{t}_n \mathbf{k} + \varphi)$$

- commensurate (C) : $|\mathbf{k}|$=m/n, m,n: integers. For large (m,n) $\mathbf{k}$ should be considered incommensurate (IC)
- incommensurate IC $|\mathbf{k}| \neq$ m/n

MSG: only 3D-crystallographic symmetry elements, e.g. no arbitrary rotation angles, only 60, 90, 120, 180 degrees

62 *Pnma*

Pn′ma
Pnm′a
Pnma′
* *Pn′m′a*
* *Pnm′a′*
* *Pn′ma′*
Pn′m′a′

modulated (in)commensurate

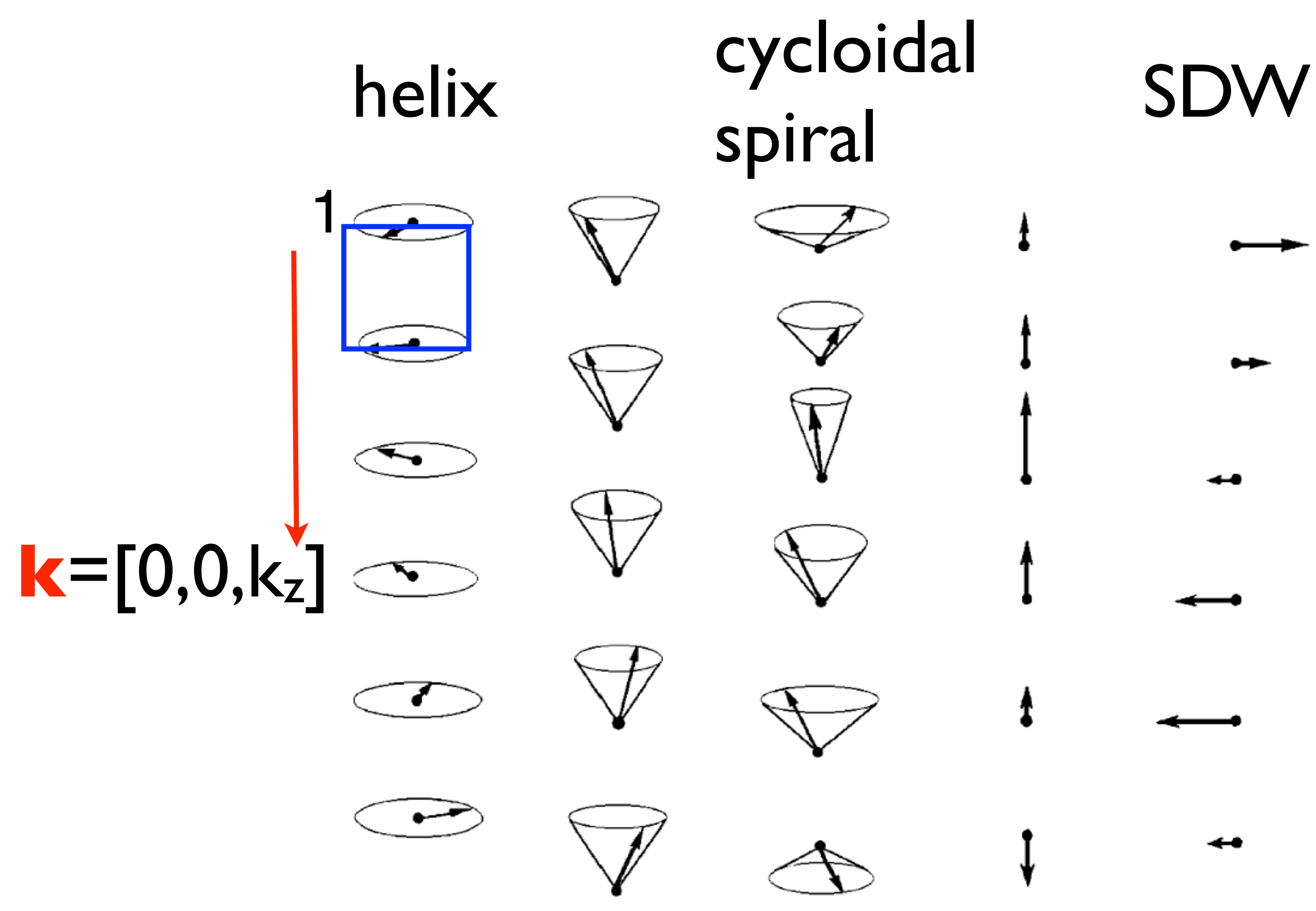

Superspace group concept

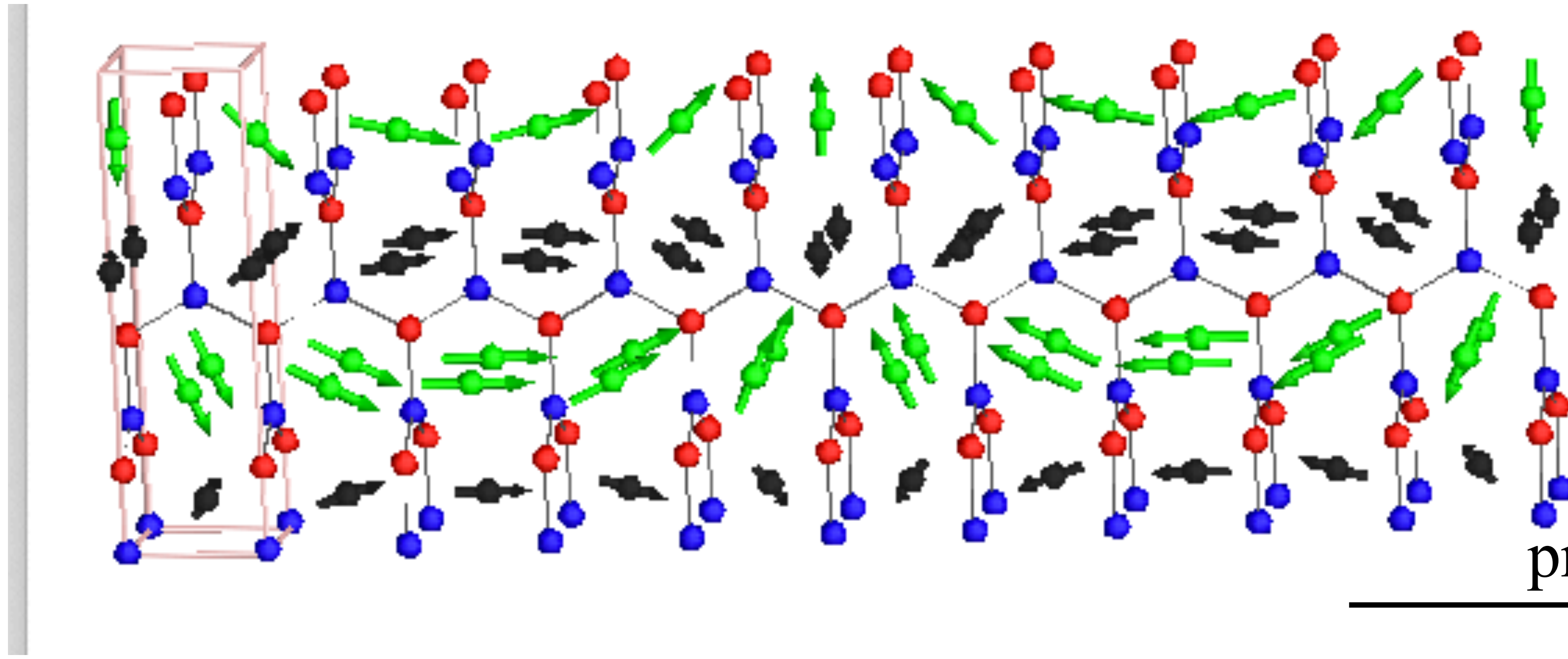

propagation vector **k**

J. Phys.: Condens. Matter **24** (2012) 163201

position $\boldsymbol{r}_{l\mu} = \boldsymbol{l} + \boldsymbol{r}_\mu$ ($\boldsymbol{l}$ being a lattice translation of the basic structure) is given by the value of the function $A_\mu(x_4)$ at $x_4 = \boldsymbol{k} \cdot \boldsymbol{r}_{l\mu}$:

$$A_{l\mu} = A_\mu(x_4 = \boldsymbol{k} \cdot \boldsymbol{r}_{l\mu}). \qquad (1)$$

These atomic modulation functions can be expressed by a Fourier series of the type

$$A_\mu(x_4) = A_{\mu,0} + \sum_{n=1,\ldots} [A_{\mu,ns} \sin(2\pi n x_4) + A_{\mu,nc} \cos(2\pi n x_4)]. \qquad (2)$$

x1 - x

x2 - y

x3 - z

x4 - internal coordinate is "just" a 2π normalised phase

Superspace group concept

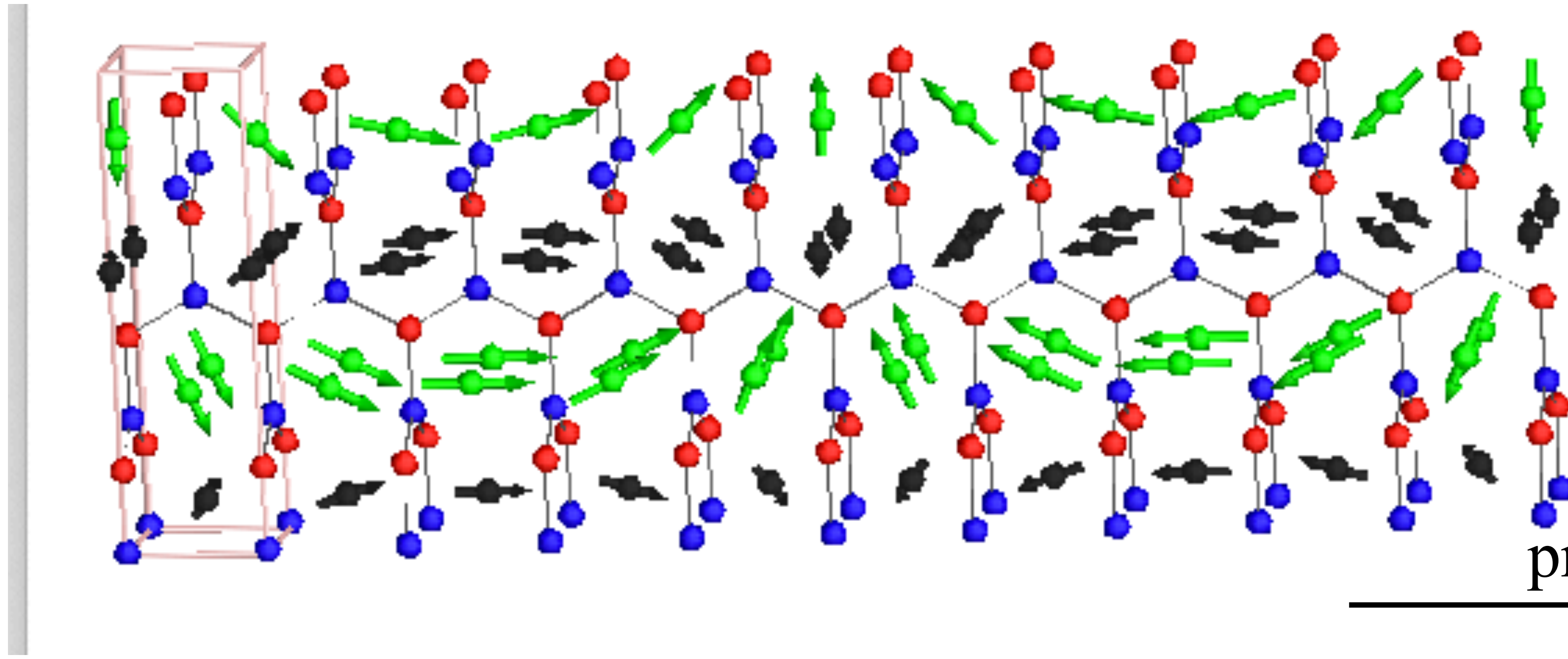

propagation vector **k**

J. Phys.: Condens. Matter **24** (2012) 163201

position $\boldsymbol{r}_{l\mu} = \boldsymbol{l} + \boldsymbol{r}_\mu$ ($\boldsymbol{l}$ being a lattice translation of the basic structure) is given by the value of the function $A_\mu(x_4)$ at $x_4 = \boldsymbol{k} \cdot \boldsymbol{r}_{l\mu}$:

$$A_{l\mu} = A_\mu(x_4 = \boldsymbol{k} \cdot \boldsymbol{r}_{l\mu}). \quad (1)$$

These atomic modulation functions can be expressed by a Fourier series of the type

$$A_\mu(x_4) = A_{\mu,0} + \sum_{n=1,\ldots} [A_{\mu,ns} \sin(2\pi n x_4) + A_{\mu,nc} \cos(2\pi n x_4)]. \quad (2)$$

x1 - x

x2 - y

x3 - z

x4 - internal coordinate is "just" a 2π normalised phase

Example of MSSGs

Table 1. Representative operations of the centrosymmetric superspace group $P\bar{1}1'(\alpha\beta\gamma)0s$ described by using generalized Seitz-type symbols (left column) and symmetry cards

$\{1\|0000\}$	x_1	x_2	x_3	x_4	$+m$
$\{\bar{1}\|0000\}$	$-x_1$	$-x_2$	$-x_3$	$-x_4$	$+m$
$\{1'\|000\frac{1}{2}\}$	x_1	x_2	x_3	$x_4+\frac{1}{2}$	$-m$
$\{\bar{1}'\|000\frac{1}{2}\}$	$-x_1$	$-x_2$	$-x_3$	$-x_4+\frac{1}{2}$	$-m$

x1 - x
x2 - y
x3 - z

Example of MSSGs

Table 1. Representative operations of the centrosymmetric superspace group $P\bar{1}1'(\alpha\beta\gamma)0s$ described by using generalized Seitz-type symbols (left column) and symmetry cards

$\{1\|0000\}$	x_1	x_2	x_3	x_4	$+m$
$\{\bar{1}\|0000\}$	$-x_1$	$-x_2$	$-x_3$	$-x_4$	$+m$
$\{1'\|000\frac{1}{2}\}$	x_1	x_2	x_3	$x_4+\frac{1}{2}$	$-m$
$\{\bar{1}'\|000\frac{1}{2}\}$	$-x_1$	$-x_2$	$-x_3$	$-x_4+\frac{1}{2}$	$-m$

x1 - x
x2 - y
x3 - z

Some simple, maybe unexpected, exemplary consequences

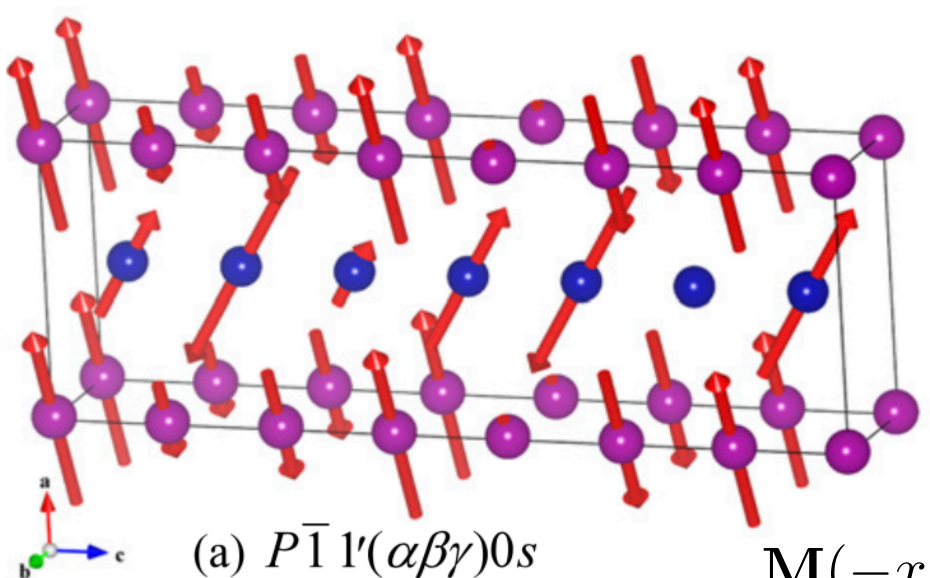

(a) $P\bar{1}\,1'(\alpha\beta\gamma)0s$

This MSSG restrict all atoms located in special positions to be in phase and only AM is allowed for them.

$$\mathbf{M}(-x_4) = \mathbf{M}(x_4) \quad \rightarrow \mathbf{M} \sim \mathbf{m} \cdot \cos(2\pi x_4)$$

1	*h*	$\bar{1}$	$\frac{1}{2},\frac{1}{2},\frac{1}{2}$
1	*g*	$\bar{1}$	$0,\frac{1}{2},\frac{1}{2}$
1	*f*	$\bar{1}$	$\frac{1}{2},0,\frac{1}{2}$
1	*e*	$\bar{1}$	$\frac{1}{2},\frac{1}{2},0$
1	*d*	$\bar{1}$	$\frac{1}{2},0,0$
1	*c*	$\bar{1}$	$0,\frac{1}{2},0$
1	*b*	$\bar{1}$	$0,0,\frac{1}{2}$
1	*a*	$\bar{1}$	$0,0,0$

Famous metallic topological materials with long magnetic periodicity

Weyl semi-metal

MnSi	CeAlGe	MnGe
	Magnetic modulation length	
200 Å	70 Å	30 Å
T_N=35K	4K	170K

Non coplanar magnetic textures $\mathbf{n}(x, y, z)$ defined by multi-k magnetic structure, have non zero topological charge Q, responsible for THE etc.

2k-structure

k1=[0,b,0], k2=[b,0,0]

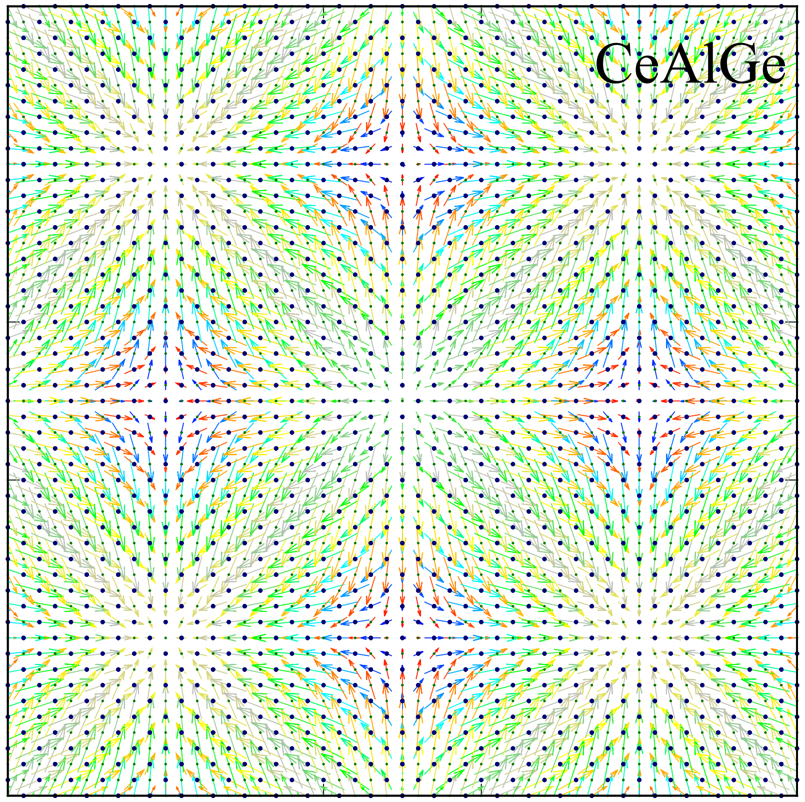

$I4_1md1'(a00)000s(0a0)0s0s$

Diffraction: reciprocal space

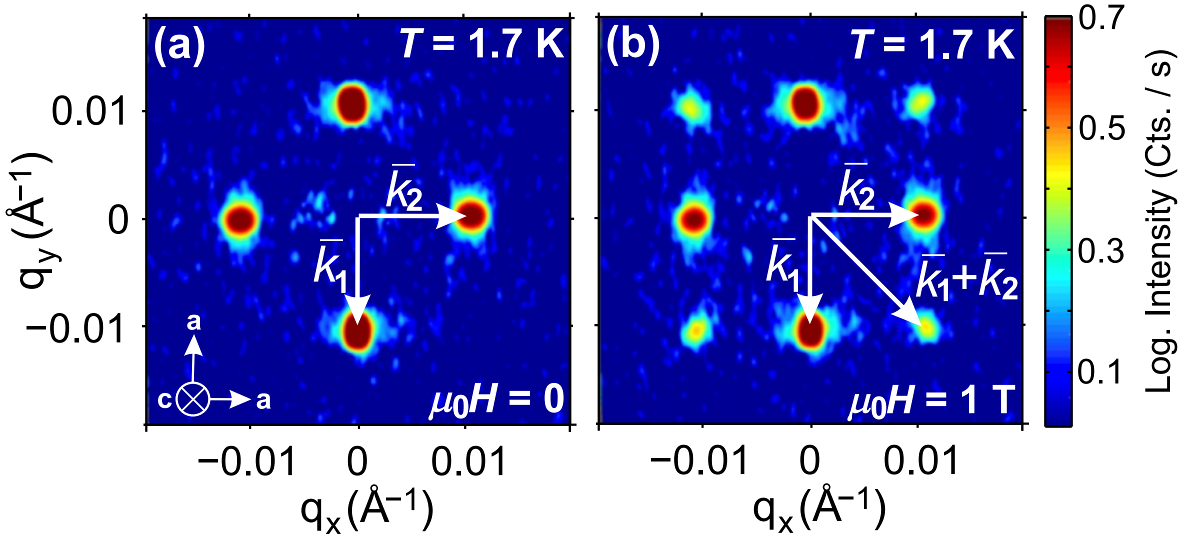

multi-arm vs. multi-k

Topology. Homotopy. Winding numbers or topological charges

Topology, homotopy

Topology is the appropriate mathematical framework for the study of spaces ($\mathbb{R}^n$, S^n)★which can (and cannot) be continuously deformed into each other. Continuous deformations include twisting and stretching but not tearing or puncturing.

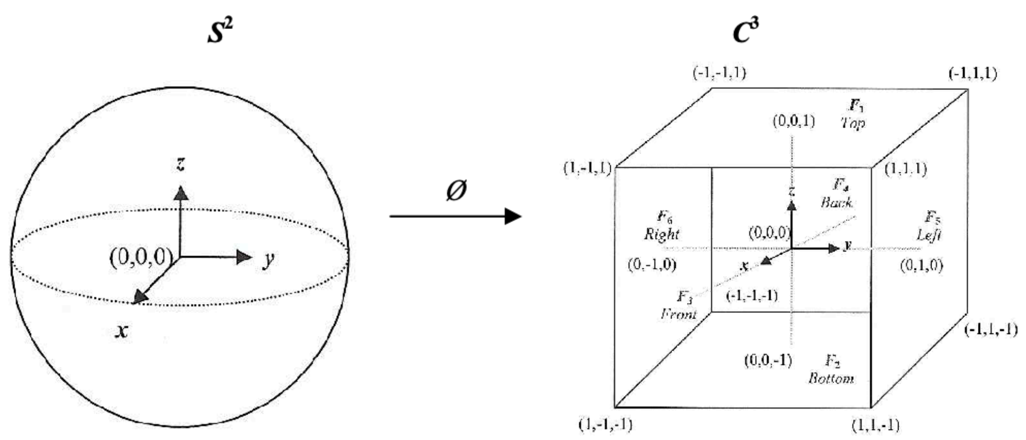

★Spaces in which topology is important are given names

a homeomorphism between sphere and cube

https://en.wikipedia.org/wiki/Homotopy

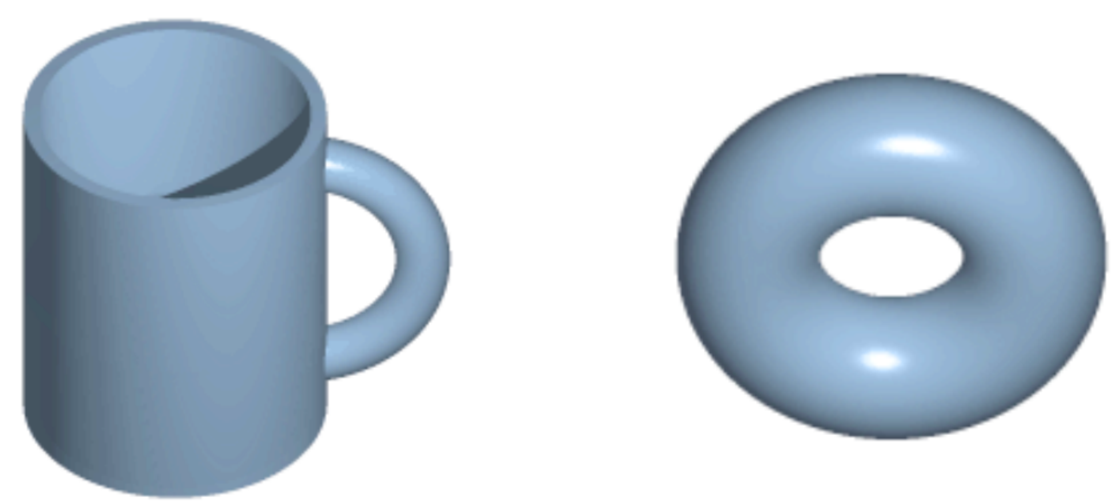

a coffee mug and a donut (torus) are homeomorphic. A homotopy between two embeddings of the torus into $\mathbb{R}^3$

An often-repeated mathematical joke is that topologists cannot tell the difference between a coffee mug and a donut

Topology, homotopy

Topology is the appropriate mathematical framework for the study of spaces ($\mathbb{R}^n$, S^n)★which can (and cannot) be continuously deformed into each other. Continuous deformations include twisting and stretching but not tearing or puncturing.

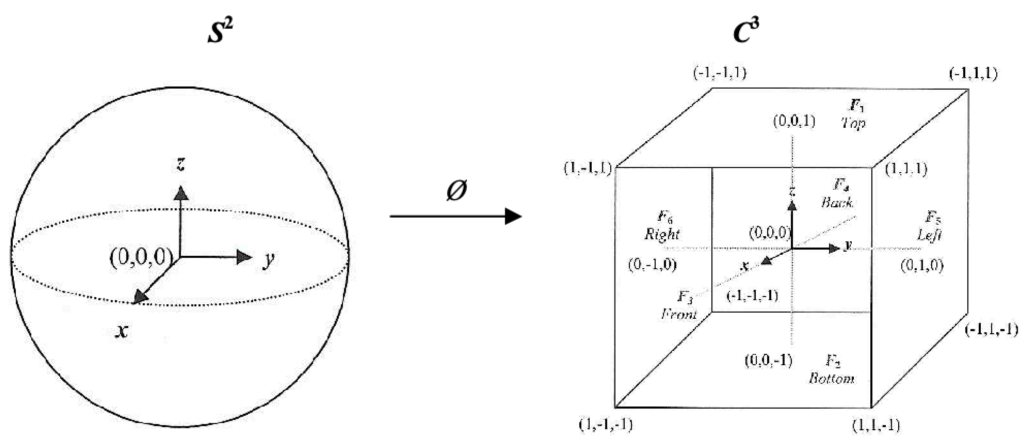

a homeomorphism between sphere and cube

★Spaces in which topology is important are given names

https://en.wikipedia.org/wiki/Homotopy

a coffee mug and a donut (torus) are homeomorphic. A homotopy between two embeddings of the torus into $\mathbb{R}^3$

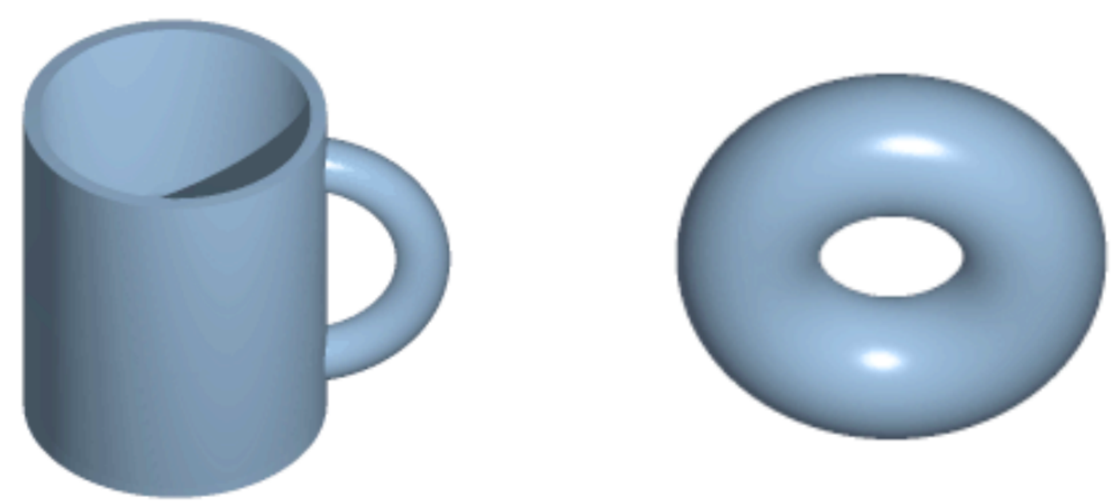

An often-repeated mathematical joke is that topologists cannot tell the difference between a coffee mug and a donut

Homotopy of paths in topological space X

Topological space X: (e.g. $\mathbb{R}^2$ or S^2)

https://en.wikipedia.org/wiki/Homotopy

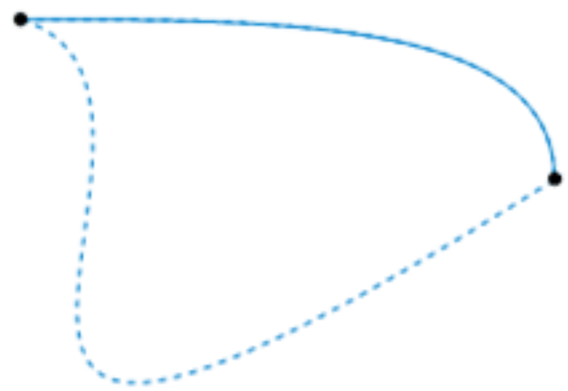

The two dashed paths shown above are homotopic relative to their endpoints. The animation represents one possible homotopy.

Homotopy of paths in topological space X

Topological space X: (e.g. $\mathbb{R}^2$ or S^2)

https://en.wikipedia.org/wiki/Homotopy

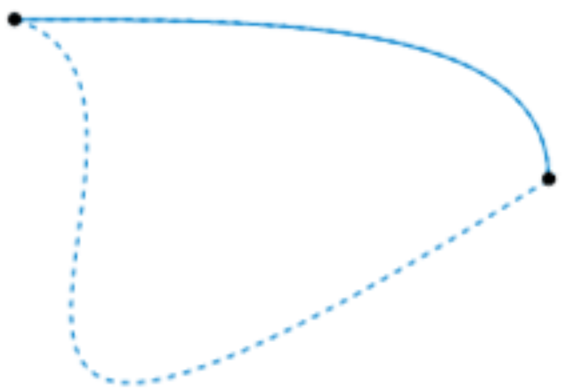

The two dashed paths shown above are homotopic relative to their endpoints. The animation represents one possible homotopy.

Homotopy of paths in topological space X

Topological space X: (e.g. $\mathbb{R}^2$ or S^2)

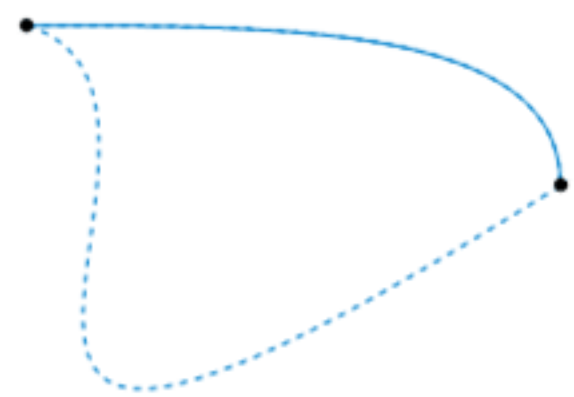

https://en.wikipedia.org/wiki/Homotopy

The two dashed paths shown above are homotopic relative to their endpoints. The animation represents one possible homotopy.

homotopy is a broader concept

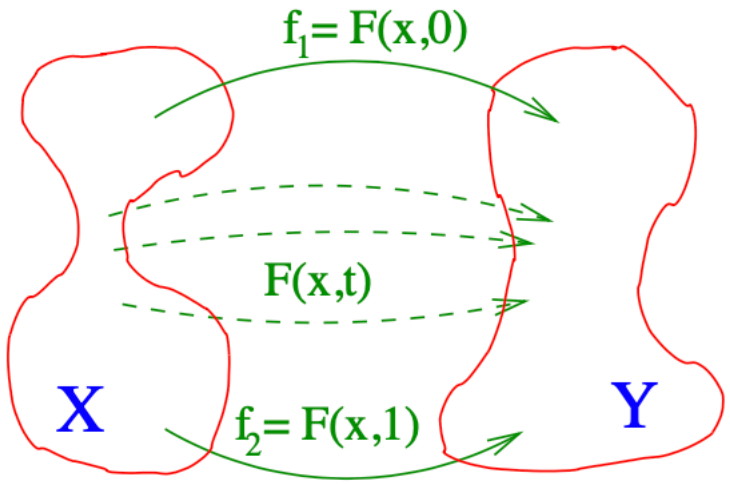

Figure 3. Representation of a homotopy $F(x,t)$ between two maps f_1 and f_2.

Condensed Matter Physics 2006, Vol. 9, No 2(46), pp. 283–304

Homotopic loops, homotopy classes

Consider the space given by the circumference of a circle S^1

make a loop by joining the ends of the path →

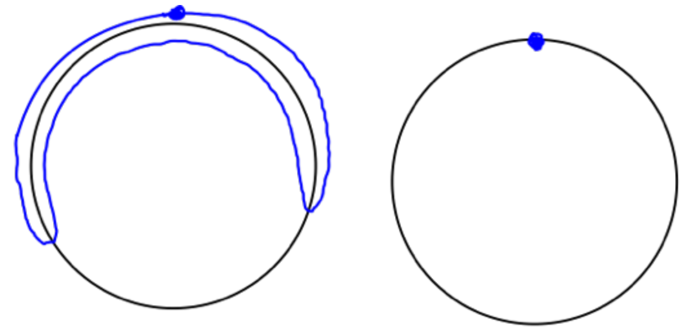

n=0

n is winding number or charge specifies a class

loops that can be continuously deformed into each other are homotopic and make a class

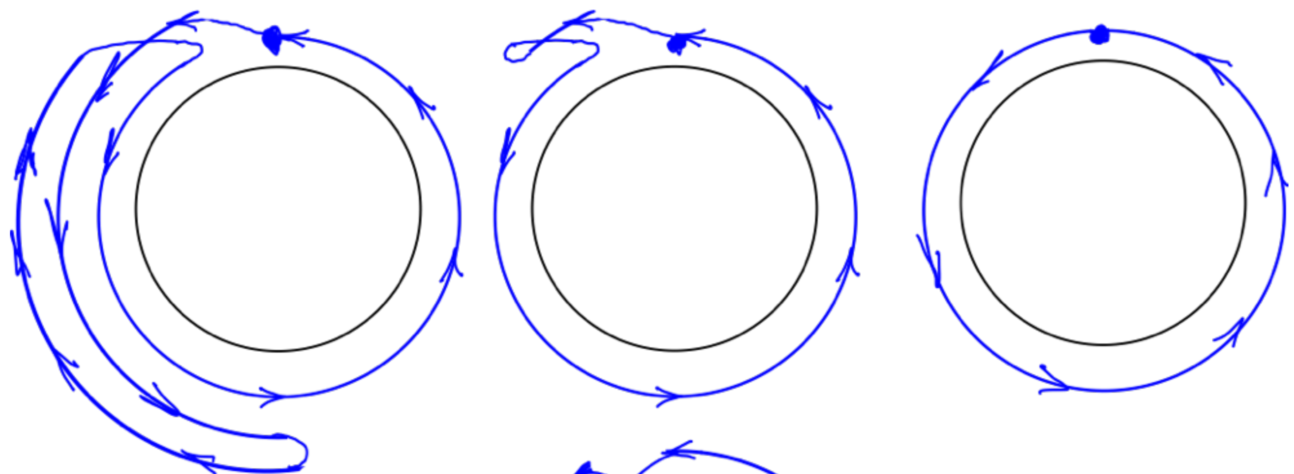

n=+1

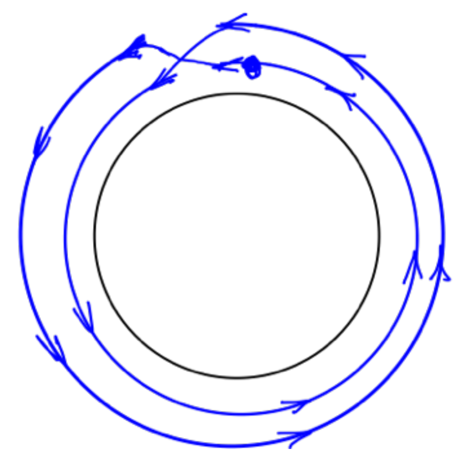

n=+2

These classes can then be mapped onto a mathematic homotopy groups (given the symbol π_1 , π_2, …)

homotopy group of a circle

$\pi_1(S^1) \simeq \mathbb{Z}$ (integers)

Homotopy. Mapping physical space to the order parameter space

a two-dimensional physical space $\mathbb{R}^2$ filled with normalised planar magnetisation **n**(x,y)

$$\mathbf{n}(x,y) = \mathbf{n}_x(x,y) \qquad + \mathbf{n}_y(x,y)$$
$$\mathbf{n}(x,y) = \hat{\mathbf{e}}_x \cos\varphi(x,y) + \hat{\mathbf{e}}_y \sin\varphi(x,y)$$

order parameter space

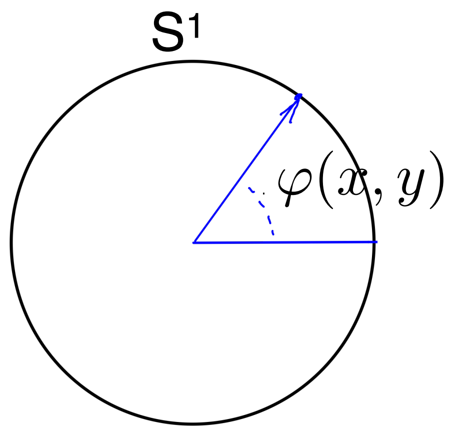

Specifying the order parameter along the contour in real space determines a mapping of that contour into order parameter space

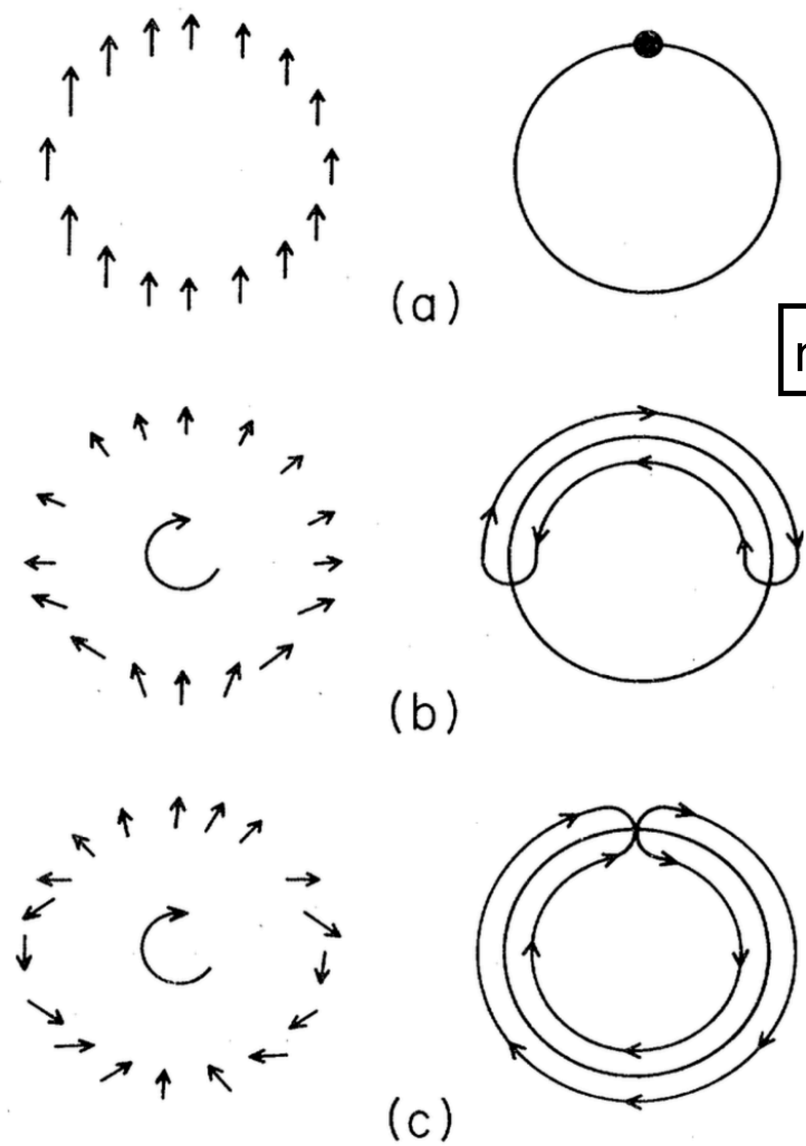

n=0

n=+2

Since **n**(x,y) is continuous on the contour this angle must be an integral multiple of 2π - winding number n

N. D. Mermin RevModPhys.51.591 (1979)

Example of isolated 2D skyrmion with Q=1

3D magnetisation texture $\mathbf{n}(x, y)$ on a 2D xy-plane

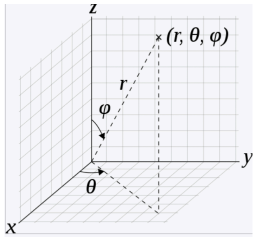

$$\mathbf{n}(x, y) = \mathbf{n}_x(x, y) + \mathbf{n}_y(x, y) + \mathbf{n}_z(x, y)$$

$$\mathbf{n}(x, y) = \mathbf{n}(\theta, \phi) = (\sin\theta\cos\phi, \sin\theta\sin\phi, \cos\theta)$$

$$\phi = Q\varphi + \eta$$

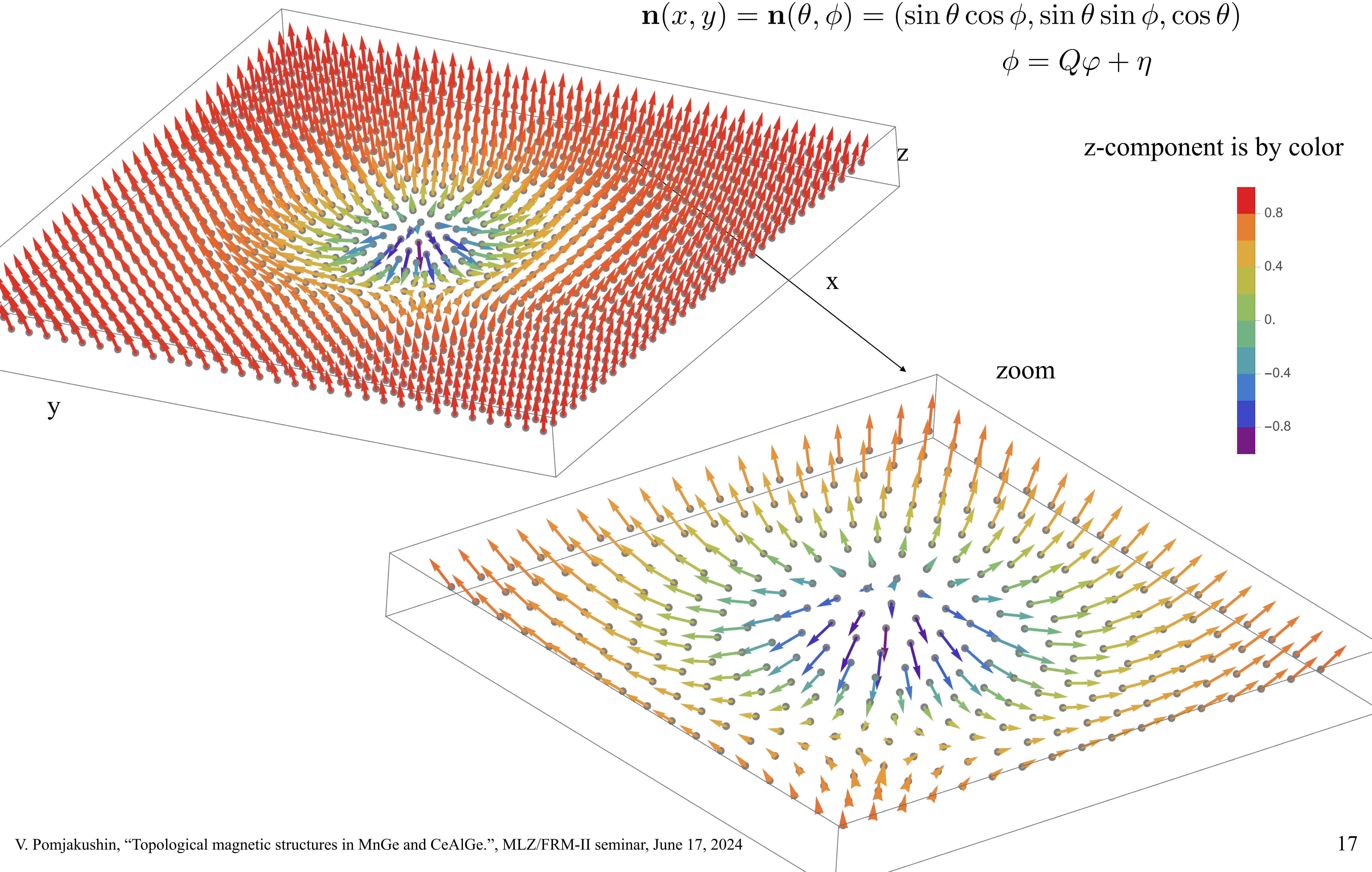

Single skyrmion★ and topological charges Q

Normalised magnetisation **n**(x,y)=**M**(x,y)/M

Single skyrmion

n||**r**

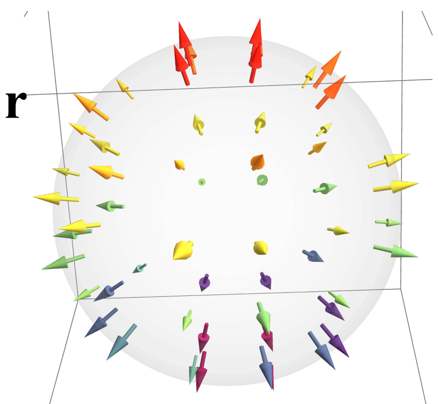

order parameter on the sphere S^2

homotopy group of a 2D-skyrmion
$\pi_2(S^2) \cong \mathbb{Z}$ (integers)

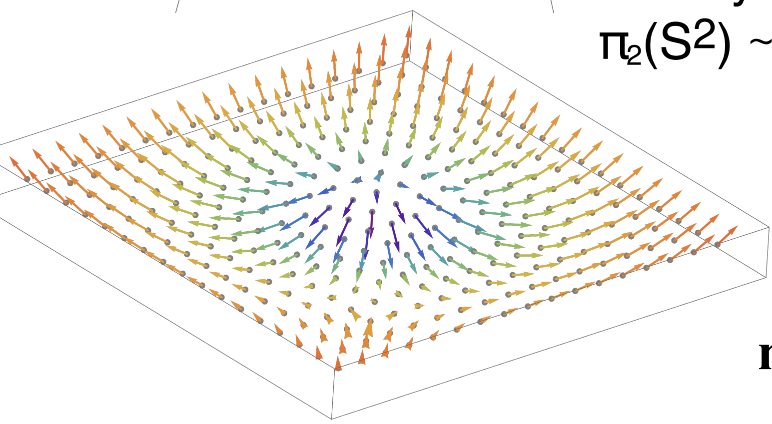

n(x,y) in infinite 2D plane $\mathbb{R}^2$

Topological charge or winding number Q counts how many times **n**(**r**) wraps S^2 (4π) as x,y spans the <u>whole</u> 2D-plane $\mathbb{R}^2$

$$Q = \iint_{\mathbb{R}^2} \frac{1}{4\pi}(\mathbf{n} \cdot [\frac{\partial \mathbf{n}}{\partial x} \times \frac{\partial \mathbf{n}}{\partial y}])dxdy$$

★ ....

- T Skyrme was a British physicist. In 1962 he proposed topological soliton to model a particle like neutron or proton. These entities would later in 1982 became known as skyrmions.
- Now it is established that proton is made of quarks… But in solid state physics we have such objects: magnetic skyrmions.

Single skyrmion★ and topological charges Q

Normalised magnetisation **n**(x,y)=**M**(x,y)/M

Single skyrmion

n||**r**

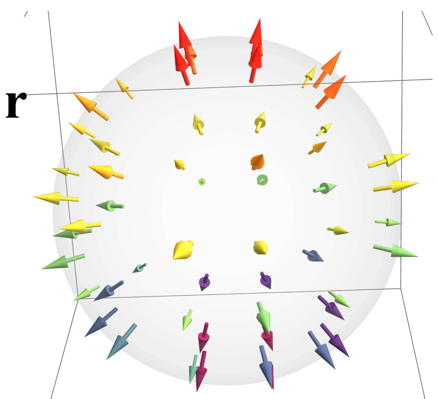

order parameter on the sphere S^2

homotopy group of a 2D-skyrmion $\pi_2(S^2) \cong \mathbb{Z}$ (integers)

or real **n** on the sphere S^2 by stereographic projection for this specific skyrmion

stereographic projection

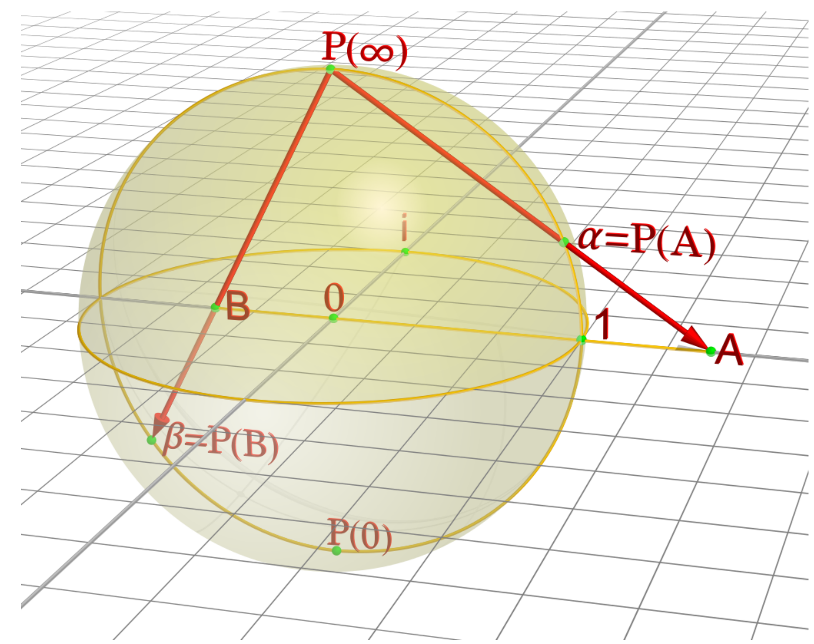

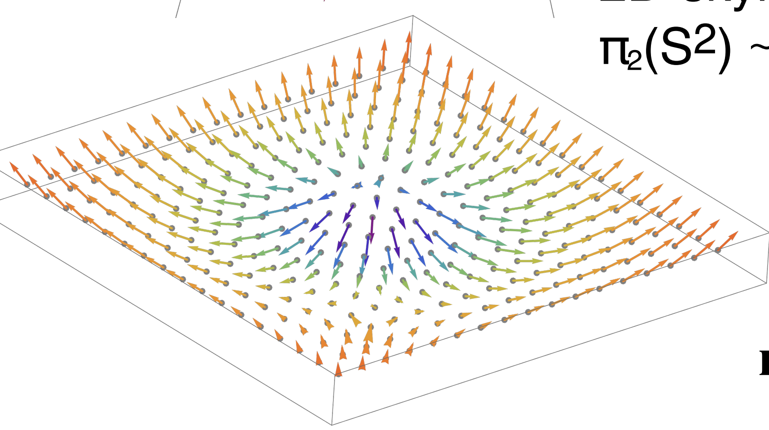

n(x,y) in infinite 2D plane $\mathbb{R}^2$

Topological charge or winding number Q counts how many times **n**(**r**) wraps S^2 (4π) as x,y spans the <u>whole</u> 2D-plane $\mathbb{R}^2$

$$Q = \iint_{\mathbb{R}^2} \frac{1}{4\pi} (\mathbf{n} \cdot [\frac{\partial \mathbf{n}}{\partial x} \times \frac{\partial \mathbf{n}}{\partial y}]) dxdy$$

★ ....

- T Skyrme was a British physicist. In 1962 he proposed topological soliton to model a particle like neutron or proton. These entities would later in 1982 became known as skyrmions.
- Now it is established that proton is made of quarks… But in solid state physics we have such objects: magnetic skyrmions.

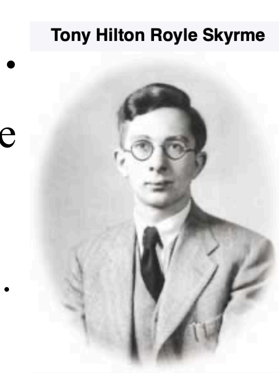

Skyrmions in magnetic materials

Neel-type   Topological skyrmion (Q=+1)   Bloch-type

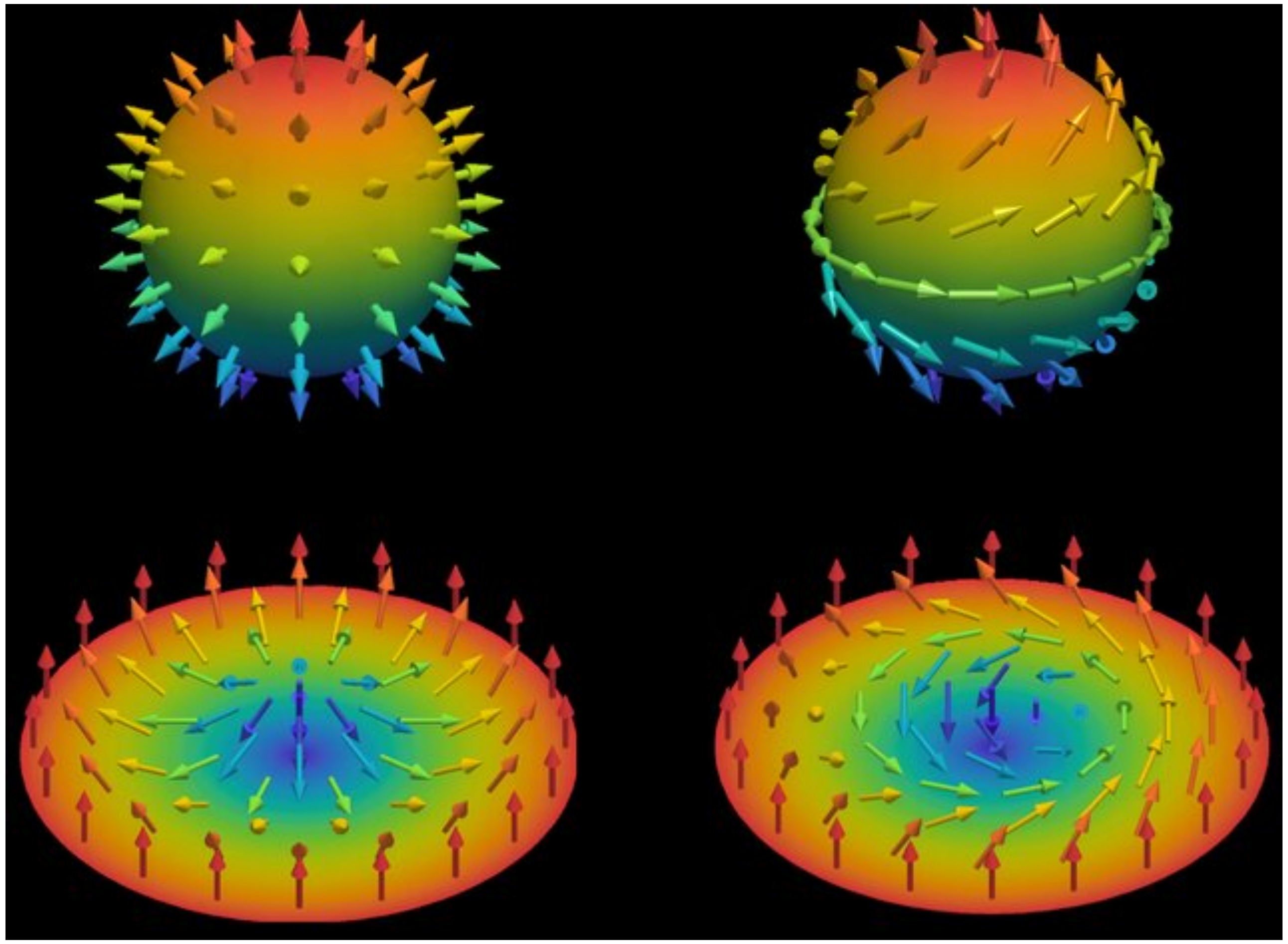

Neel antiskyrmion Q=-1

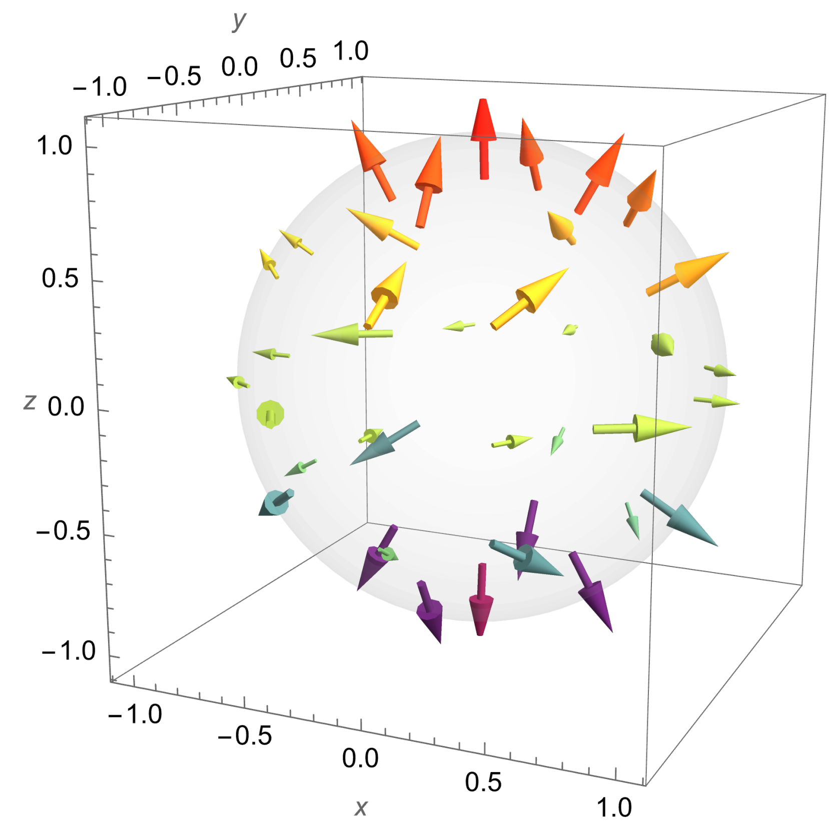

meron (Q = ±1/2)

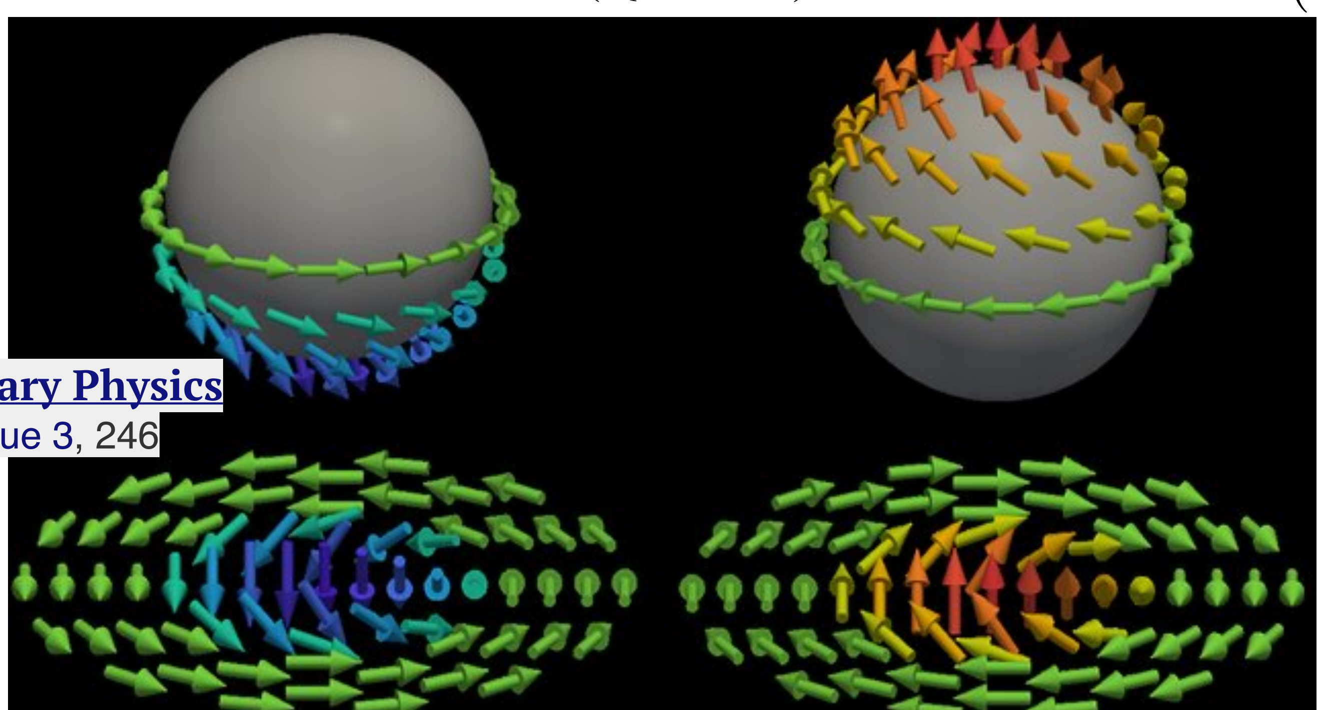

$$\mathbf{n}(x,y) = \mathbf{n}(\theta,\phi) = (\sin\theta\cos\phi, \sin\theta\sin\phi, \cos\theta)$$

$$\phi = Q\varphi + \eta$$

Contemporary Physics
60, 2019 - Issue 3, 246

Skyrmion/meron lattice vs. isolated skyrmion

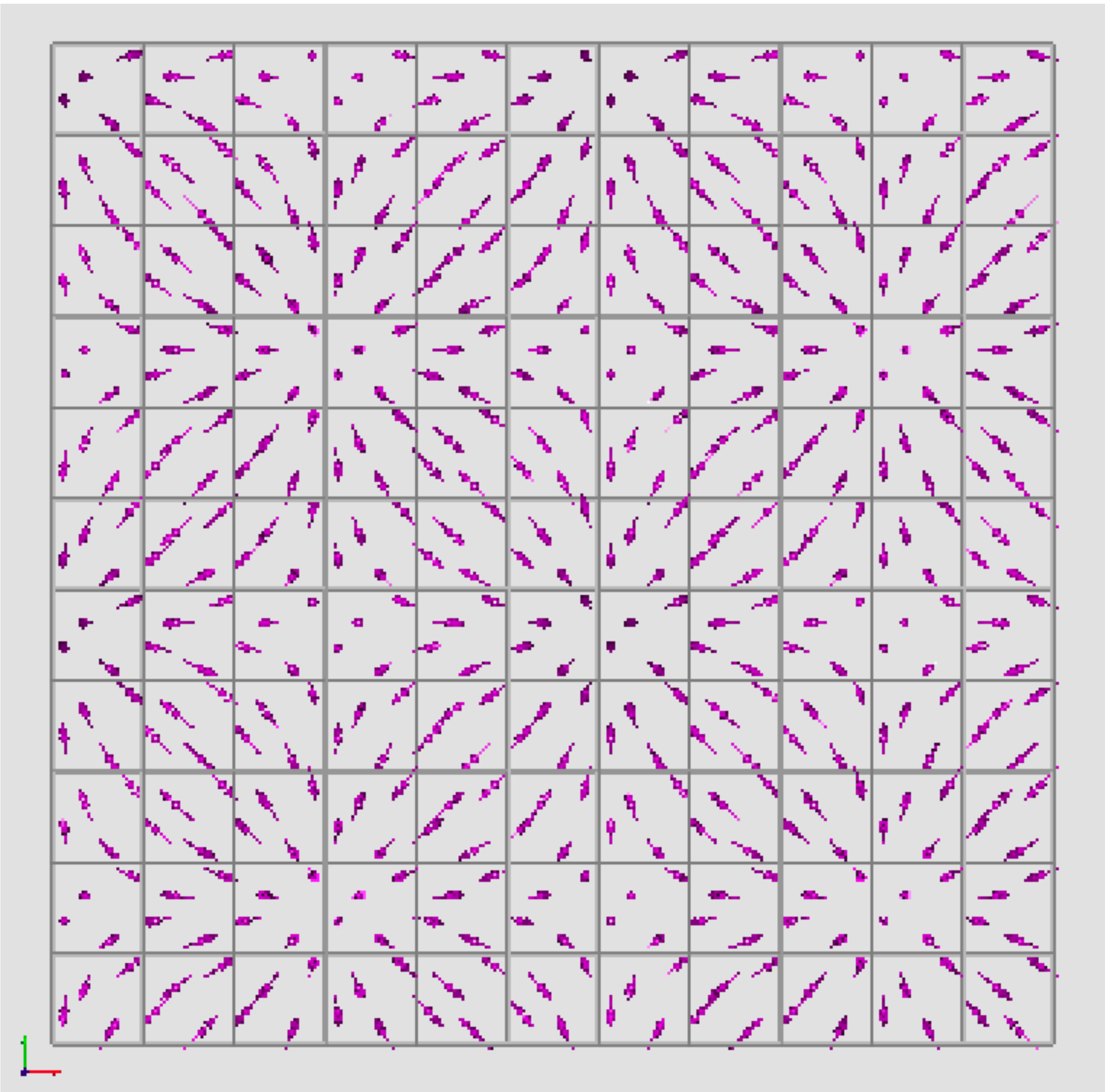

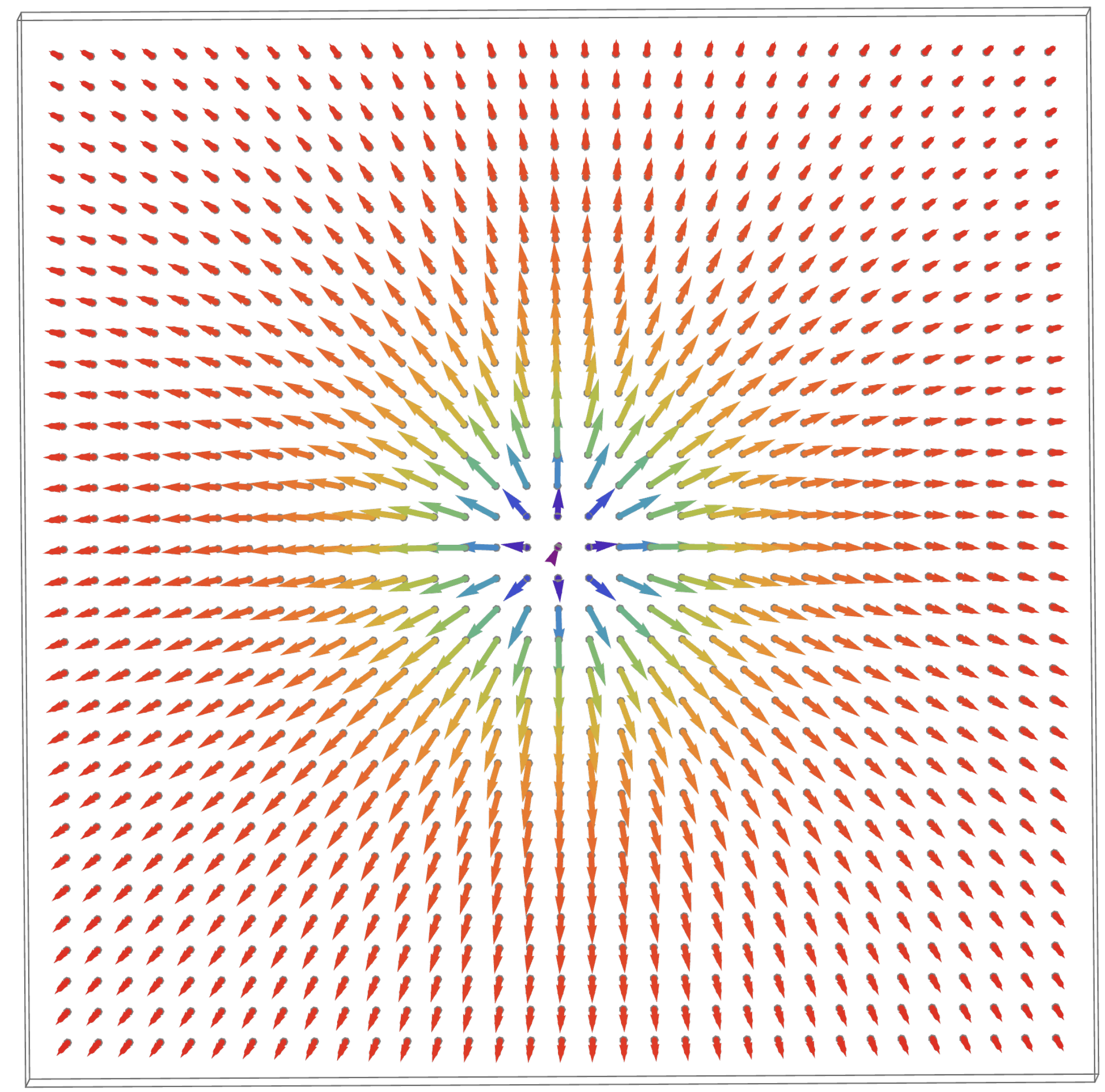

Topological charge density w(x,y)

Normalised magnetisation **n**(x,y)=**M**(x,y)/M

topological charge/winding density ~ solid angle <u>for our systems of interest</u>

$$\omega(x,y) = \frac{1}{4\pi}(\mathbf{n}\cdot[\frac{\partial\mathbf{n}}{\partial x}\times\frac{\partial\mathbf{n}}{\partial y}]) \quad \mathbf{n} = \mathbf{M}/M$$

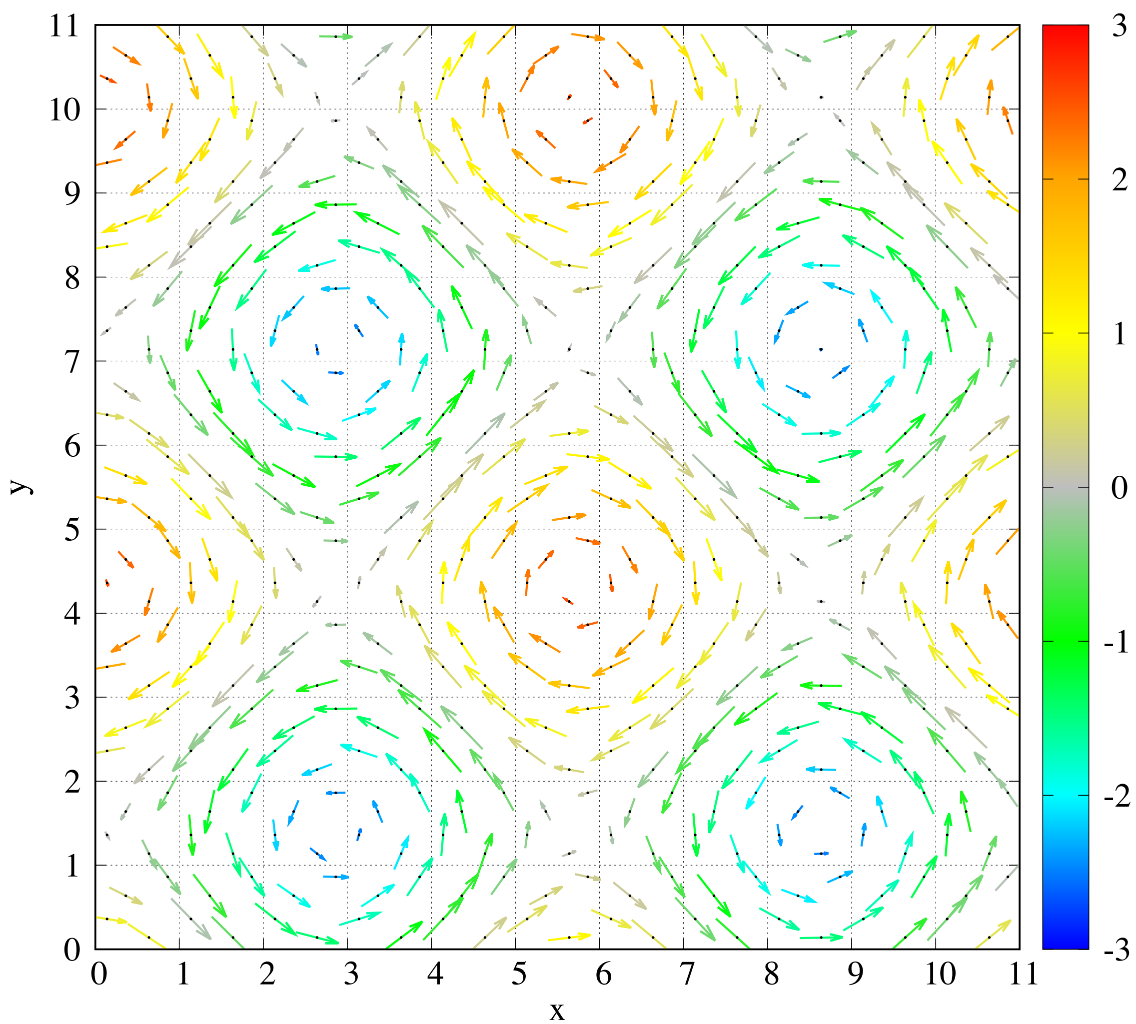

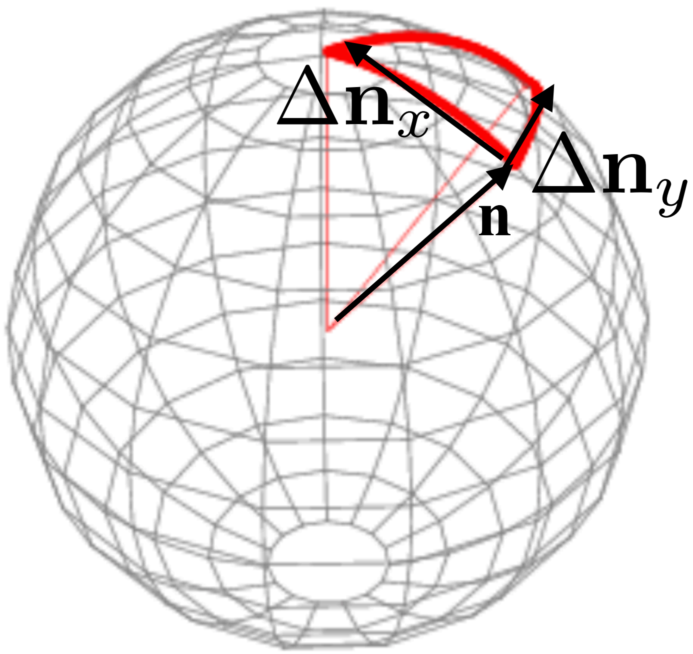

Topological number/charge over *S*

$$Q = \iint_{S\subset\mathbb{R}^2} \omega(x,y)dxdy$$

Skyrmion (Q=+1),
Antiskyrmion (Q=-1)
Meron-Antimeron (Q = ±1/2) for periodic magnetization textures.

Skyrmions and topological charges Q for the 3D-magnetisation textures given by propagation vectors

Propagation vectors define dimension of a different space where M(r) changes /twist

Normalised magnetisation $\mathbf{n}(x,y,z)=\mathbf{M}(x,y,z)/M$

1D

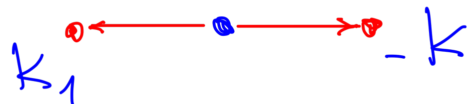

topological density/winding ~ solid angle == 0

no topological objects are expected - both $\partial\mathbf{n}/dy$ AND $\partial\mathbf{n}/dx$ must be $\neq 0$!

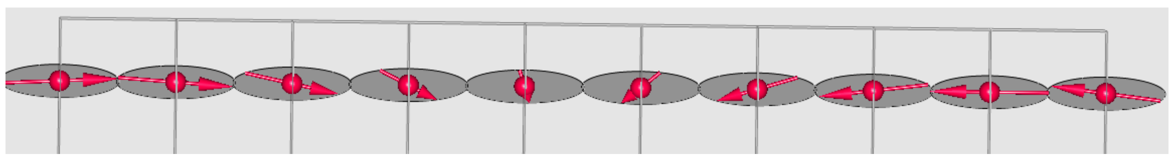

Skyrmions and topological charges Q for the 3D-magnetisation textures given by propagation vectors

Propagation vectors define dimension of a different space where M(r) changes /twist

Normalised magnetisation **n**(x,y,z)=**M**(x,y,z)/M

1D

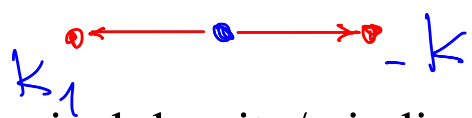

topological density/winding ~ solid angle == 0

no topological objects are expected - both ∂**n**/dy AND ∂**n**/dx must be ≠ 0!

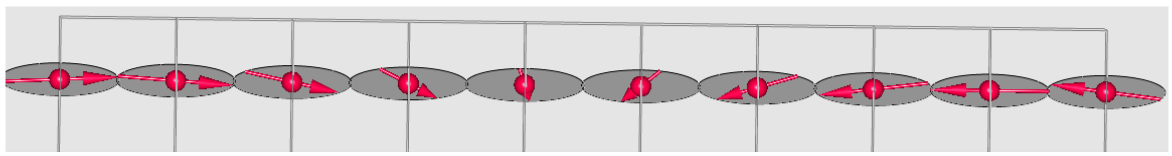

2D

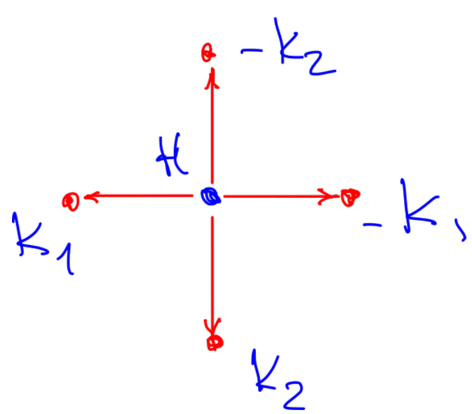

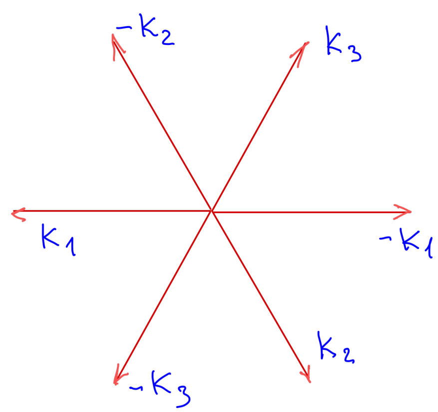

might have skyrmions and merons for non-coplanar structure

topological density/winding ~ solid angle

$$w(x,y) = \frac{1}{4\pi}(\mathbf{n}\cdot[\frac{\partial \mathbf{n}}{\partial x}\times\frac{\partial \mathbf{n}}{\partial y}]),\, Q = \int\int w(x,y)dxdy$$

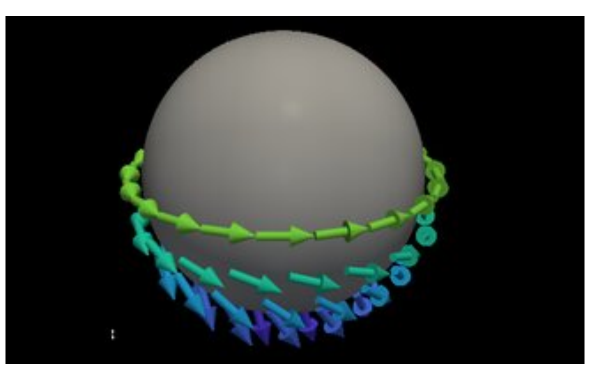

Skyrmions and topological charges Q for the 3D-magnetisation textures given by propagation vectors

Propagation vectors define dimension of a different space where M(r) changes /twist

Normalised magnetisation **n**(x,y,z)=**M**(x,y,z)/M

1D

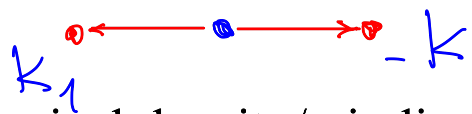

topological density/winding ~ solid angle == 0

no topological objects are expected - both ∂**n**/dy AND ∂**n**/dx must be ≠ 0!

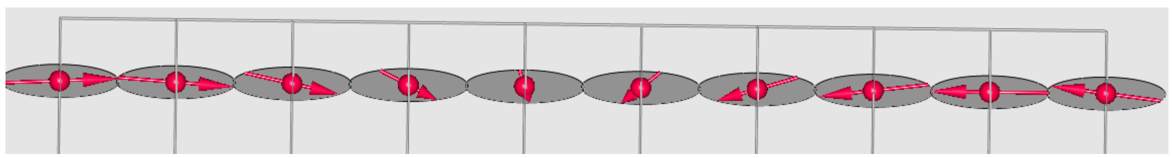

3D

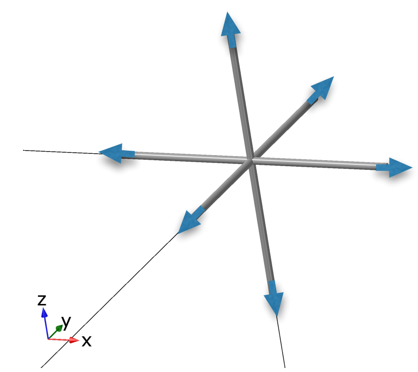

might have objects like 3D skyrmion/hedgehog/ monopole with singularity in the centre

2D

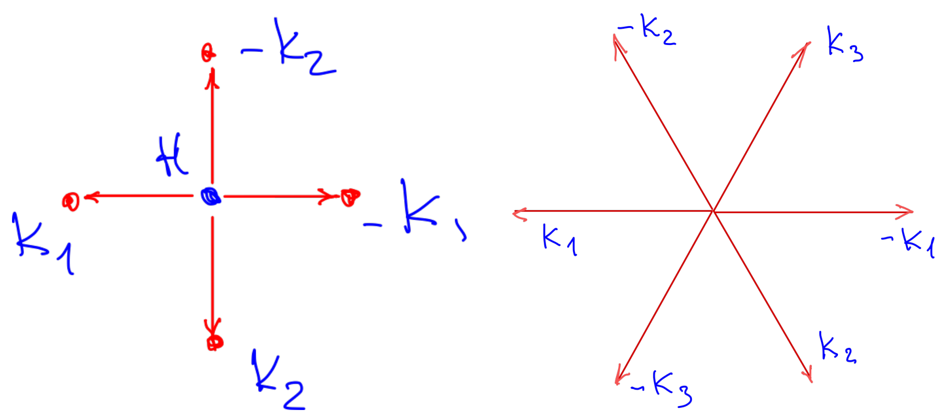

might have skyrmions and merons for non-coplanar structure

topological density/winding ~ solid angle

$$w(x,y) = \frac{1}{4\pi}(\mathbf{n}\cdot[\frac{\partial \mathbf{n}}{\partial x}\times\frac{\partial \mathbf{n}}{\partial y}]), Q = \int\int w(x,y)dxdy$$

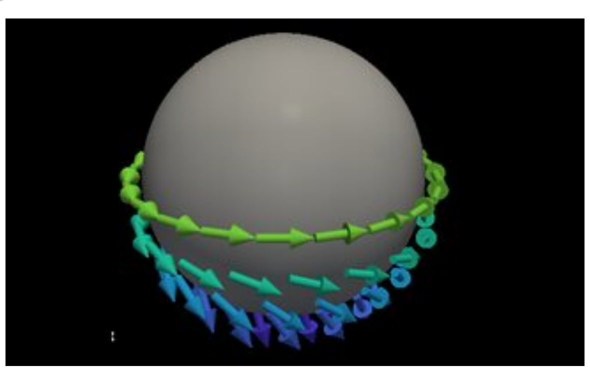

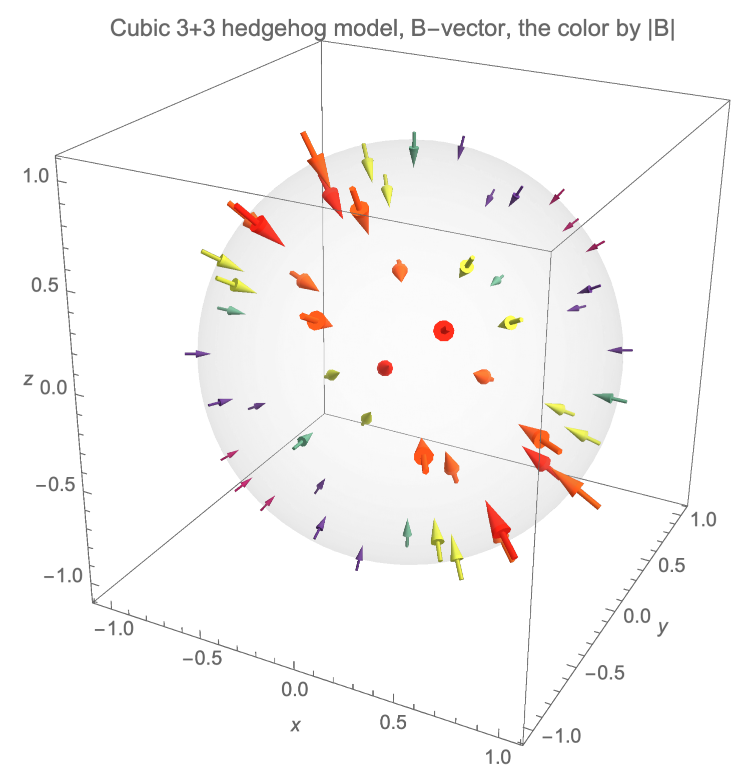

$$Q = \frac{1}{8\pi}\epsilon^{ijk}\int_S \mathrm{d}S_k \boldsymbol{n}(\boldsymbol{r})\cdot[\partial_i \boldsymbol{n}(\boldsymbol{r})\times\partial_j \boldsymbol{n}(\boldsymbol{r})] = \pm 1$$

Motivation to study MnGe

Apply a state-of-the-art analysis of all possible magnetic superspace structures allowed by the crystal symmetry in metallic MnGe (P213) that are consistent with neutron diffraction data.

MnGe has been long-studied for its remarkable phenomena related to the topological magnetic order, but surprisingly, the detailed magnetic structure underlying such phenomena was not addressed before this study.

MnGe samples

1. Single crystals are not possible to grow.
2. Powders are difficult - only high pressure (8 GPa) synthesis was known - Y. Fujishiro, N.Kanazawa

new chemical route to synthesize MnGe!

a combined mechanochemical and solid-state route at ambient pressures and moderate temperatures

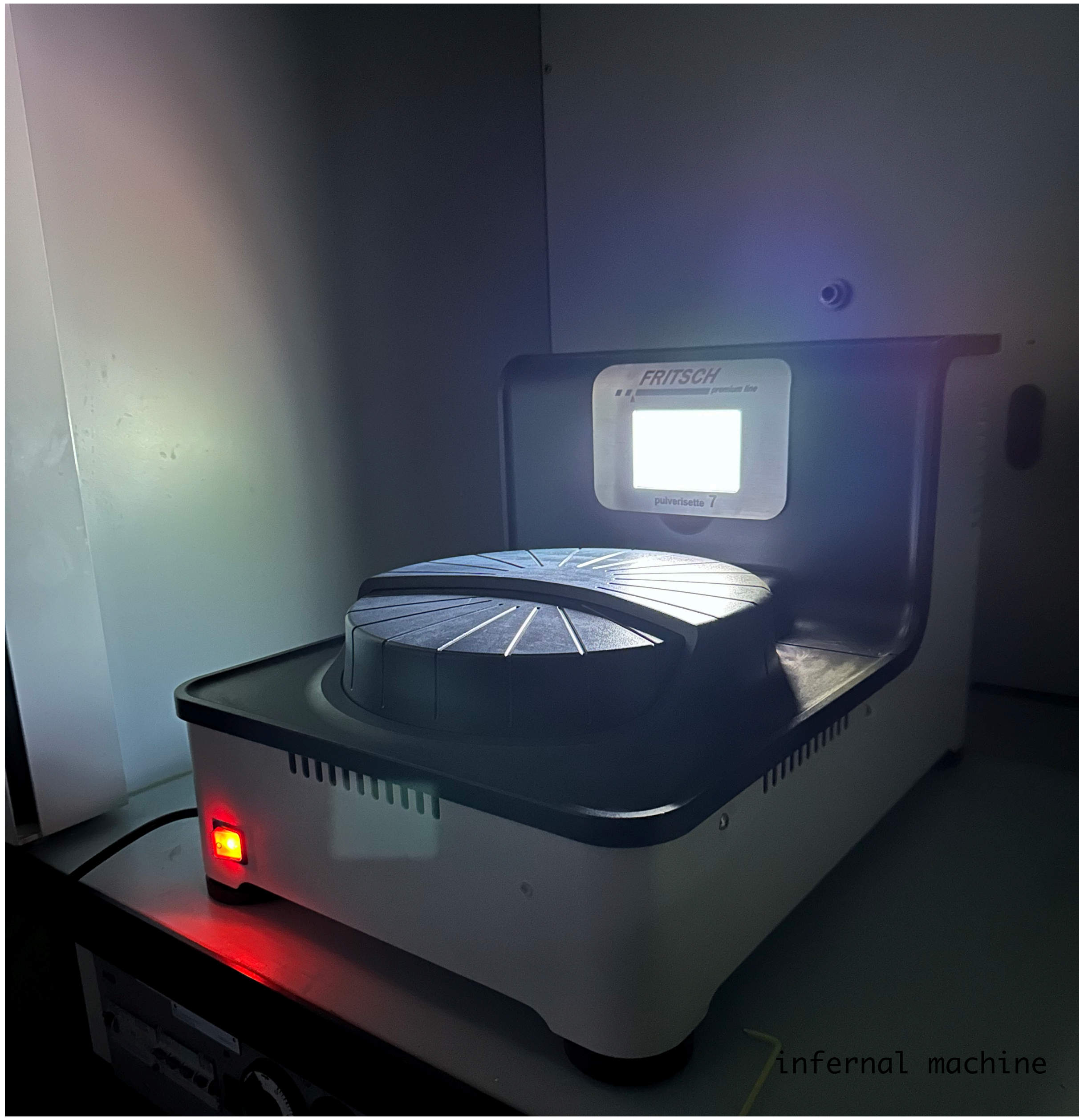

Katja Pomjakushina

Igor' Plokhikh

Crystal structure. Neutron diffraction patterns

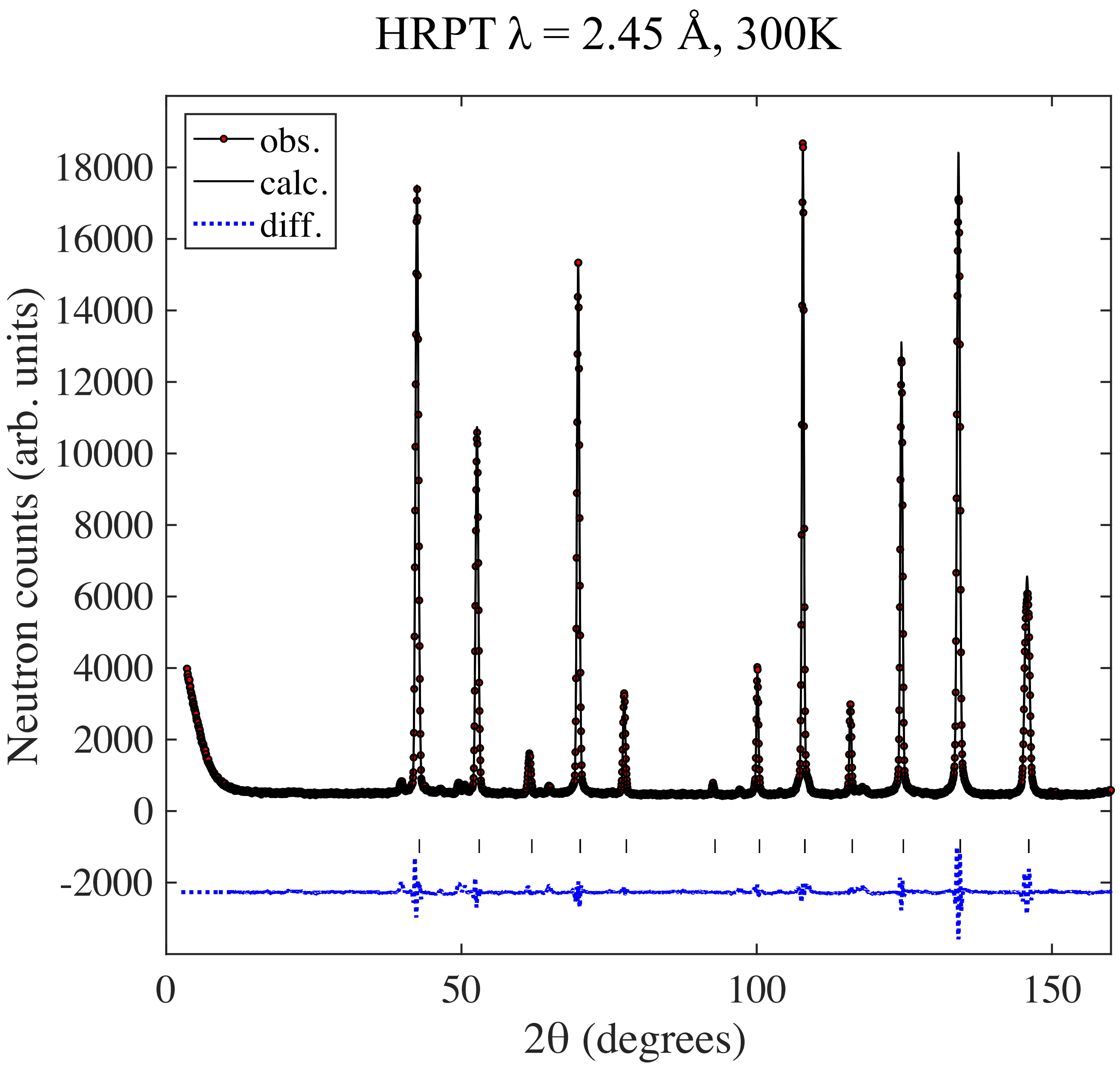

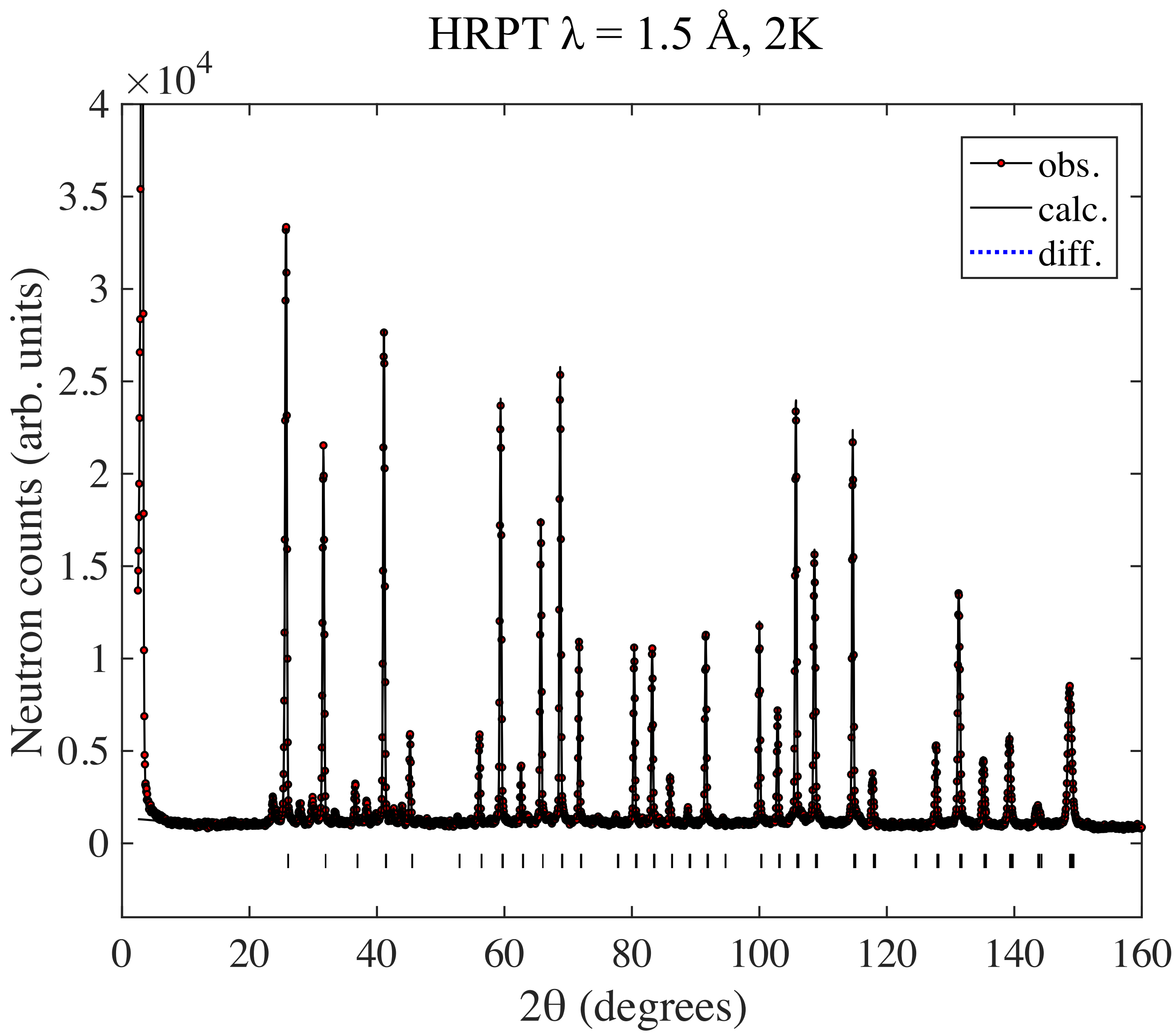

Crystal structure. P2_13 space group T=@300K

Mn (4a) (x,x,x) three 2-fold axes

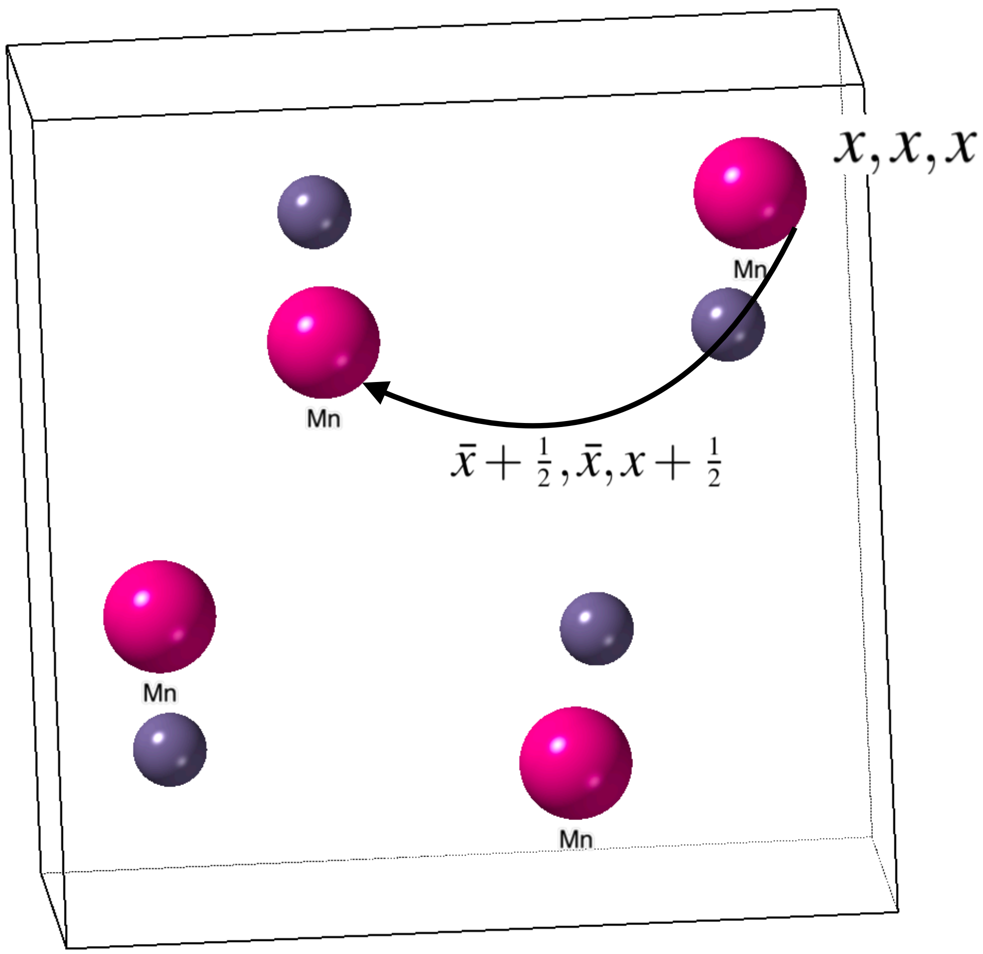

HRPT λ = 2.45 Å

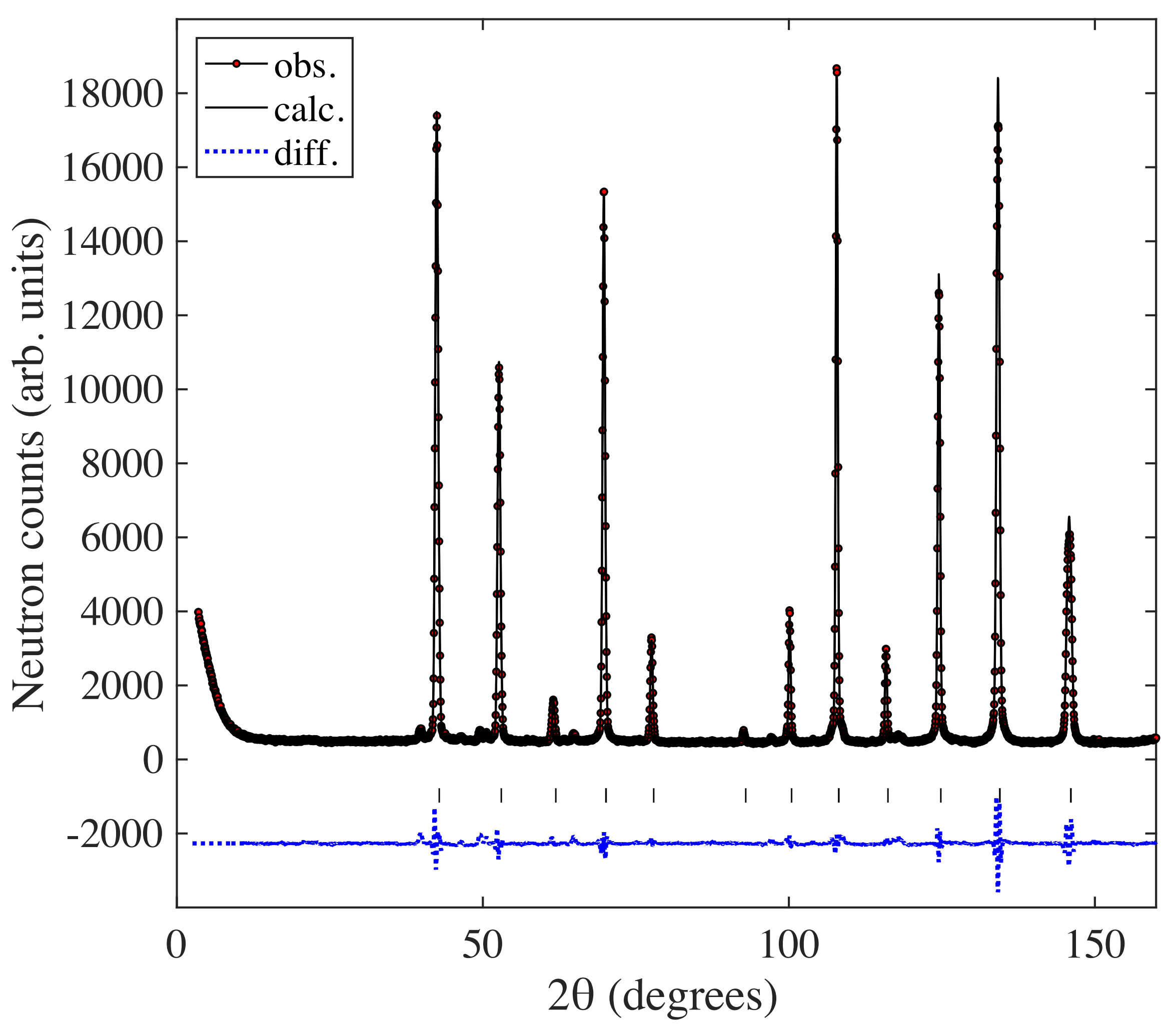

Pure magnetic neutron diffraction pattern “2K”-“300K”

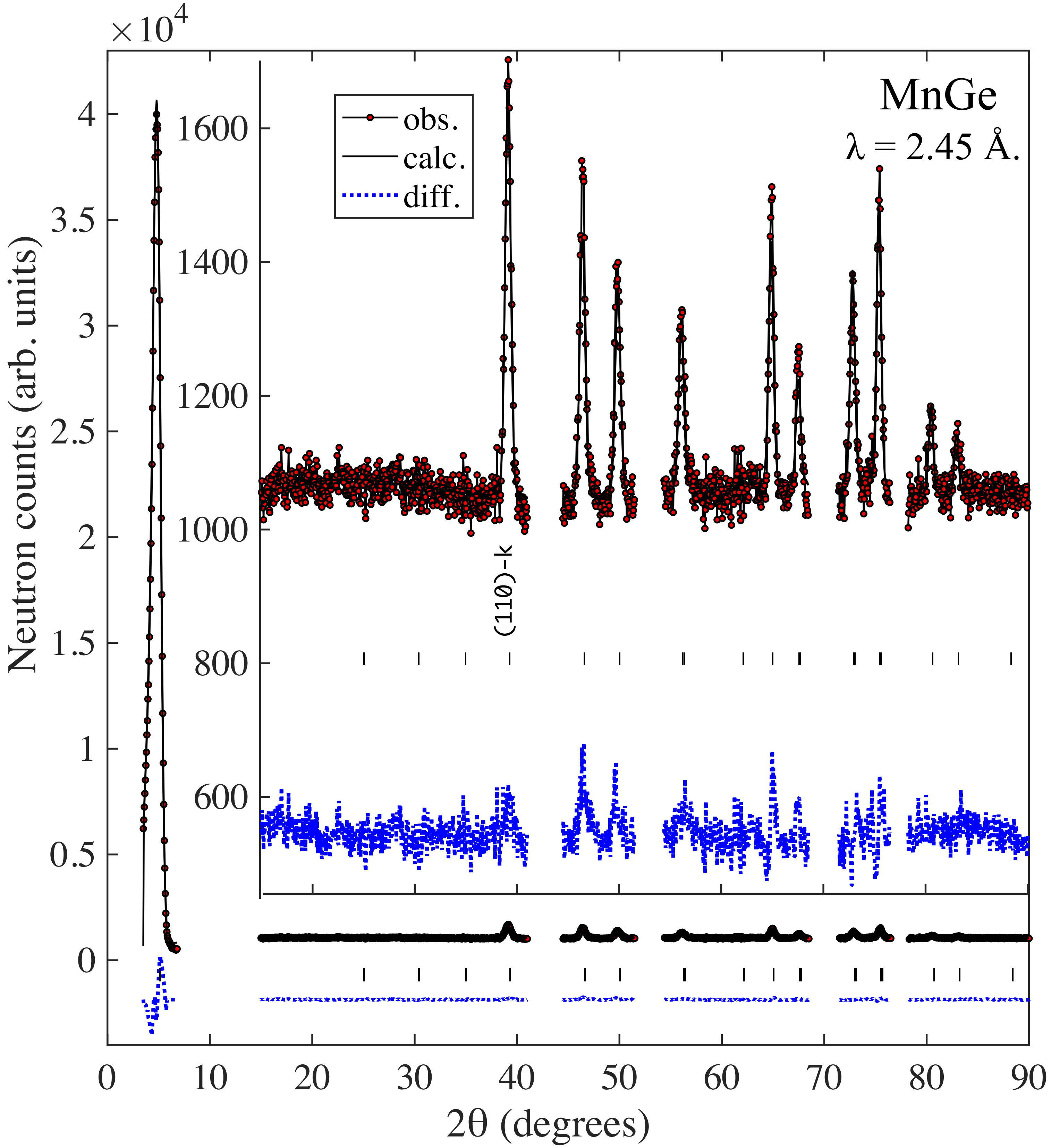

cubic P2_13

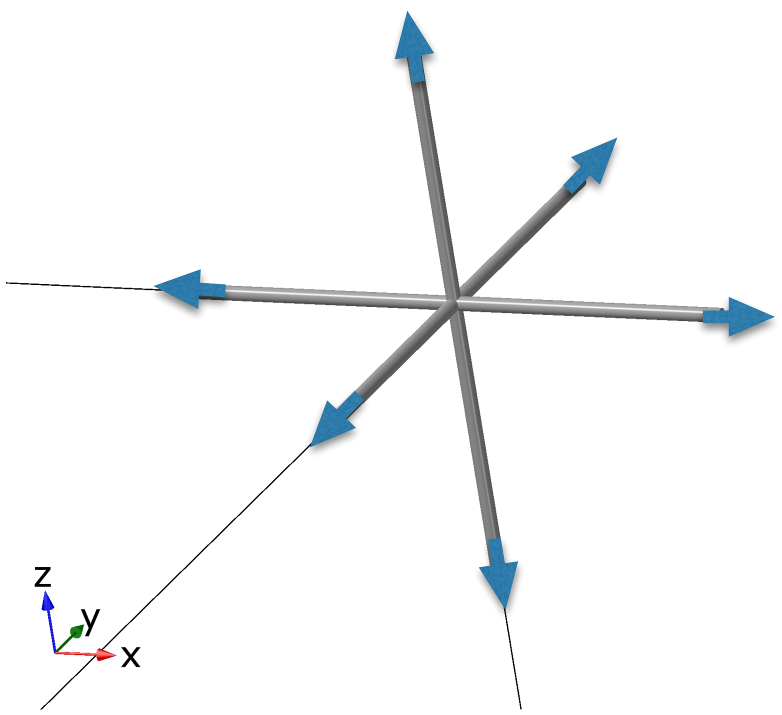

propagation vector star
3*2-arms **k** = [0b0]
Two irreps DT1, DT2

b = 0.17 → magnetic period 30 Å

magnetic domain sizes: L ≃ 520 Å

Magnetic and crystal symmetry analysis for single- and multi-k structures

Harold T. Stokes, Dorian M. Hatch, and Branton J. Campbell

ISODISTORT: ISOTROPY Software Suite http://iso.byu.edu

→ **ISOTROPY Software Suite**
Harold T. Stokes, Dorian M. Hatch, and Branton J. Campbell, Department of Physics and Astronomy, Brigham Young University, Provo, Utah 84606, USA,

BYU BRIGHAM YOUNG UNIVERSITY

M. I. Aroyo, J. M. Perez-Mato, D. Orobengoa, E. Tasci, G. de la Flor, and A. Kirov

Bilbao Crystallographic Server http://www.cryst.ehu.es/

→ bilbao crystallographic server

University of the Basque Country
Universidad del País Vasco (UPV)
Euskal Herriko Unibertsitatea (EHU)
eman ta zabal zazu

Two main web sites with a collection of software which applies group theoretical methods to the analysis of phase transitions in crystalline solids.

General tools for representation analysis, Shubnikov groups, 3D+n, and much more...

Magnetic SuperSpace subGroups for P2_13 [a,0,0]+[0,a,0]+[0,0,a]

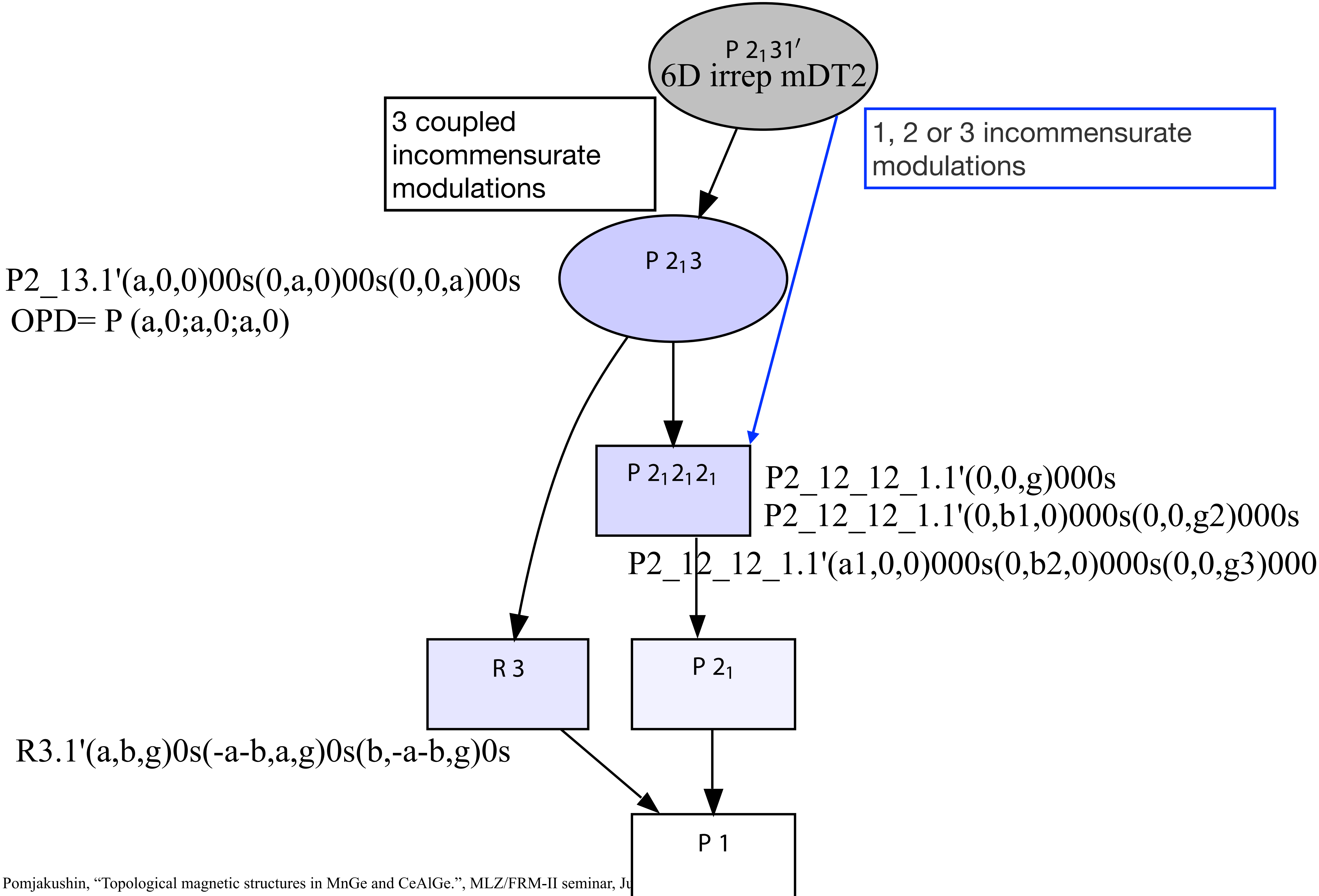

Magnetic SuperSpace subGroups for P2_13 [a,0,0]+[0,a,0]+[0,0,a]

Data analysis★:

1. Simulated annealing search for 3D+3, 3D+2 and 3D+1 MSSG
2. standard LSQ fit

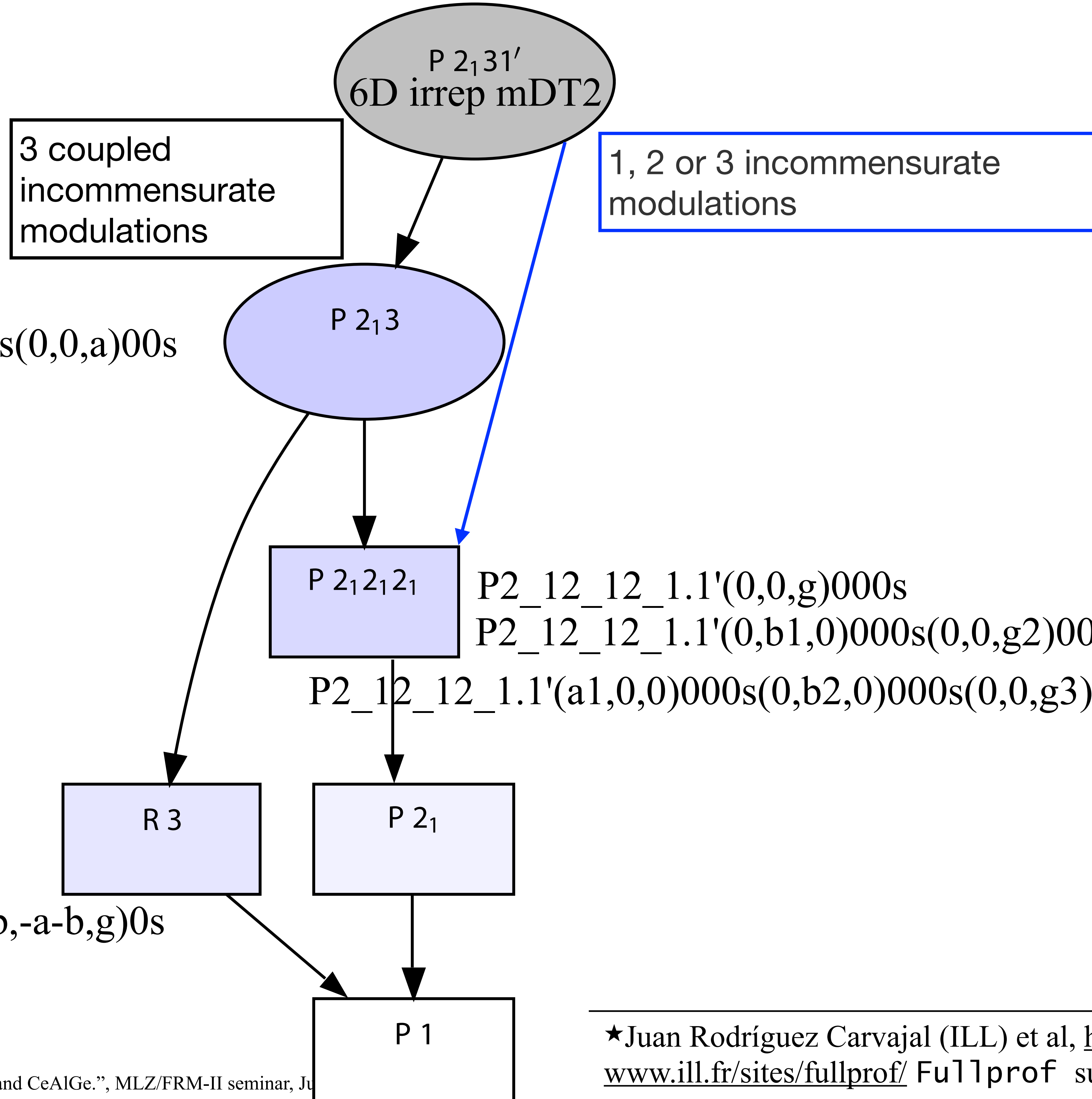

P2_13.1'(a,0,0)00s(0,a,0)00s(0,0,a)00s

OPD= P (a,0;a,0;a,0)

P2_12_12_1.1'(0,0,g)000s

P2_12_12_1.1'(0,b1,0)000s(0,0,g2)000s

P2_12_12_1.1'(a1,0,0)000s(0,b2,0)000s(0,0,g3)000s

R3.1'(a,b,g)0s(-a-b,a,g)0s(b,-a-b,g)0s

★Juan Rodríguez Carvajal (ILL) et al, http://www.ill.fr/sites/fullprof/ `Fullprof` suite

3D+3 General formula for magnetic moments

Magnetic moments on four Mn (4a) (x,x,x) - six parameters to find: m_1, m_2, m_3 , α_1 , α_2 , α_3

P2_13.1'(a,0,0)00s(0,a,0)00s(0,0,a)00s

1st arm 2nd arm 3rd arm

$$[M_x, M_y, M_z]_1 = [m_1\cos(\tilde{y}+\alpha_1) + m_3\cos(\tilde{z}+\alpha_3) + m_2\cos(\tilde{x}+\alpha_2), \quad \leftarrow \text{Mx}$$
$$m_2\cos(\tilde{y}+\alpha_2) + m_1\cos(\tilde{z}+\alpha_1) + m_3\cos(\tilde{x}+\alpha_3), \quad \leftarrow \text{My}$$
$$m_3\cos(\tilde{y}+\alpha_3) + m_2\cos(\tilde{z}+\alpha_2) + m_1\cos(\tilde{x}+\alpha_1)] \quad \leftarrow \text{Mz}$$

$$[M_x, M_y, M_z]_2 = [m_1\cos(\tilde{y}-\alpha_1) + m_3\cos(\tilde{z}+\alpha_3) - m_2\cos(\tilde{x}-\alpha_2),$$
$$m_2\cos(\tilde{y}-\alpha_2) + m_1\cos(\tilde{z}+\alpha_1) - m_3\cos(\tilde{x}-\alpha_3),$$
$$-m_3\cos(\tilde{y}-\alpha_3) - m_2\cos(\tilde{z}+\alpha_2) + m_1\cos(\tilde{x}-\alpha_1)]$$

$$[M_x, M_y, M_z]_3 = [m_1\cos(\tilde{y}+\alpha_1) - m_3\cos(\tilde{z}-\alpha_3) + m_2\cos(\tilde{x}-\alpha_2),$$
$$-m_2\cos(\tilde{y}+\alpha_2) + m_1\cos(\tilde{z}-\alpha_1) - m_3\cos(\tilde{x}-\alpha_3),$$
$$m_3\cos(\tilde{y}+\alpha_3) - m_2\cos(\tilde{z}-\alpha_2) + m_1\cos(\tilde{x}-\alpha_1)]$$

$$[M_x, M_y, M_z]_4 = [m_1\cos(\tilde{y}-\alpha_1) - m_3\cos(\tilde{z}-\alpha_3) - m_2\cos(\tilde{x}+\alpha_2),$$
$$-m_2\cos(\tilde{y}-\alpha_2) + m_1\cos(\tilde{z}-\alpha_1) + m_3\cos(\tilde{x}+\alpha_3),$$
$$-m_3\cos(\tilde{y}-\alpha_3) + m_2\cos(\tilde{z}-\alpha_2) + m_1\cos(\tilde{x}+\alpha_1)]$$

$$\tilde{y} = 2\pi k y$$

Usually in crystallography one uses sin and cos-components:

$$m_1\cos(\tilde{y}+\alpha_1) = m_1\cos\alpha_1 \cos\tilde{y} - m_1\sin\alpha_1 \sin\tilde{y}$$
$$= m_c \cos\tilde{y} + m_s \sin\tilde{y}$$

Models 3D+3, 3D+2

TABLE II. Magnetic structure parameters for MnGe for the different 3+3 and 3+2 models explained in Sec. IV D. See caption of Table I for details. The total moment amplitude, which is a sum over all k-vector components, is $\sqrt{6}$ and 2 times larger than the component given for a single k-vector for hedgehog and skyrmion structures, respectively. For the 3+2 structure, m_5 and m_6, are not given, because they are constrained to be equal to m [illegible] 0 in formula (3).

Model	m_{xc}, m_{xs}, μ_B	m_{yc}, m_{ys}, μ_B	m_{zc}, m_{zs}, μ_B	M, μ_B
3+3 (F) SA	−0.8616, −0.0217	0.0028, 0.0711	0.1653, 1.2014	
3+3 (F) hedgehog	1.048(1), 0	0, 0	0, −1.048(1)	2.567(3)
R_{wp}, R_{exp}, χ^2, R_B		3.67, 1.63, 5.08, 0.634		
3+3 (1) hedgehog	0.950(1), 0	0, 0	0, −0.950(1)	2.327(3)
R_{wp}, R_{exp}, χ^2, R_B		7.60, 3.37, 5.07, 2.22		
3+3 (1) x	1.344(2), 0.14(12)	0, 0	0, 0	2.328(3)
R_{wp}, R_{exp}, χ^2, R_B		7.60, 3.37, 5.07, 2.17		
3+3 (F) xz	1.42(5), 0	0, 0	0.28(3), 0.41(2)	2.56(6)
R_{wp}, R_{exp}, χ^2, R_B		3.62, 1.63, 4.95, 0.589		
3+3 (F) x	1.481(2), 0.19(3)	0, 0	0, 0	2.58(3)
R_{wp}, R_{exp}, χ^2, R_B		3.64, 1.63, 5.01, 0.569		
3+2 (F) skyrmion	1.283(1), 0	0, 0	0, −1.283(1)	2.566(2)
R_{wp}, R_{exp}, χ^2, R_B		3.67, 1.63, 5.08 , 0.643		

Models 3D+3, 3D+2

TABLE II. Magnetic structure parameters for MnGe for the different 3+3 and 3+2 models explained in Sec. IV D. See caption of Table I for details. The total moment amplitude, which is a sum over all k-vector components, is $\sqrt{6}$ and 2 times larger than the component given for a single k-vector for hedgehog and skyrmion structures, respectively. For the 3+2 structure, m_5 and m_6, are not given, because they are constrained to be equal to m … 0 in formula (3).

Model	m_{xc}, m_{xs}, μ_B	m_{yc}, m_{ys}, μ_B	m_{zc}, m_{zs}, μ_B	M, μ_B
3+3 (F) SA	−0.8616, −0.0217	0.0028, 0.0711	0.1653, 1.2014	
3+3 (F) hedgehog	1.048(1), 0	0, 0	0, −1.048(1)	2.567(3)
R_{wp}, R_{exp}, χ^2, R_B		3.67, 1.63, 5.08, 0.634		
3+3 (1) hedgehog	0.950(1), 0	0, 0	0, −0.950(1)	2.327(3)
R_{wp}, R_{exp}, χ^2, R_B		7.60, 3.37, 5.07, 2.22		
3+3 (1) x	1.344(2), 0.14(12)	0, 0	0, 0	2.328(3)
R_{wp}, R_{exp}, χ^2, R_B		7.60, 3.37, 5.07, 2.17		
3+3 (F) xz	1.42(5), 0	0, 0	0.28(3), 0.41(2)	2.56(6)
R_{wp}, R_{exp}, χ^2, R_B		3.62, 1.63, 4.95, 0.589		
3+3 (F) x	1.481(2), 0.19(3)	0, 0	0, 0	2.58(3)
R_{wp}, R_{exp}, χ^2, R_B		3.64, 1.63, 5.01, 0.569		
3+2 (F) skyrmion	1.283(1), 0	0, 0	0, −1.283(1)	2.566(2)
R_{wp}, R_{exp}, χ^2, R_B		3.67, 1.63, 5.08 , 0.643		

Models 3D+3, 3D+2

TABLE II. Magnetic structure parameters for MnGe for the different 3+3 and 3+2 models explained in Sec. IV D. See caption of Table I for details. The total moment amplitude, which is a sum over all k-vector components, is $\sqrt{6}$ and 2 times larger than the component given for a single k-vector for hedgehog and skyrmion structures, respectively. For the 3+2 structure, m_5 and m_6, are not given, because they are constrained to be equal to m … 0 in formula (3).

Model	m_{xc}, m_{xs}, μ_B	m_{yc}, m_{ys}, μ_B	m_{zc}, m_{zs}, μ_B	M, μ_B
3+3 (F) SA	−0.8616, −0.0217	0.0028, 0.0711	0.1653, 1.2014	
3+3 (F) hedgehog	1.048(1), 0	0, 0	0, −1.048(1)	2.567(3)
$R_{wp}, R_{exp}, \chi^2, R_B$		3.67, 1.63, 5.08, 0.634		
3+3 (1) hedgehog	0.950(1), 0	0, 0	0, −0.950(1)	2.327(3)
$R_{wp}, R_{exp}, \chi^2, R_B$		7.60, 3.37, 5.07, 2.22		
3+3 (1) x	1.344(2), 0.14(12)	0, 0	0, 0	2.328(3)
$R_{wp}, R_{exp}, \chi^2, R_B$		7.60, 3.37, 5.07, 2.17		
3+3 (F) xz	1.42(5), 0	0, 0	0.28(3), 0.41(2)	2.56(6)
$R_{wp}, R_{exp}, \chi^2, R_B$		3.62, 1.63, 4.95, 0.589		
3+3 (F) x	1.481(2), 0.19(3)	0, 0	0, 0	2.58(3)
$R_{wp}, R_{exp}, \chi^2, R_B$		3.64, 1.63, 5.01, 0.569		
3+2 (F) skyrmion	1.283(1), 0	0, 0	0, −1.283(1)	2.566(2)
$R_{wp}, R_{exp}, \chi^2, R_B$		3.67, 1.63, 5.08 , 0.643		

Models 3D+3, 3D+2

TABLE II. Magnetic structure parameters for MnGe for the different 3+3 and 3+2 models explained in Sec. IV D. See caption of Table I for details. The total moment amplitude, which is a sum over all k-vector components, is $\sqrt{6}$ and 2 times larger than the component given for a single k-vector for hedgehog and skyrmion structures, respectively. For the 3+2 structure, m_5 and m_6, are not given, because they are constrained to be equal to m [illegible] 0 in formula (3).

Model	m_{xc}, m_{xs}, μ_B	m_{yc}, m_{ys}, μ_B	m_{zc}, m_{zs}, μ_B	M, μ_B
3+3 (F) SA	−0.8616, −0.0217	0.0028, 0.0711	0.1653, 1.2014	
3+3 (F) hedgehog	1.048(1), 0	0, 0	0, −1.048(1)	2.567(3)
R_{wp}, R_{exp}, χ^2, R_B		3.67, 1.63, 5.08, 0.634		
3+3 (1) hedgehog	0.950(1), 0	0, 0	0, −0.950(1)	2.327(3)
R_{wp}, R_{exp}, χ^2, R_B		7.60, 3.37, 5.07, 2.22		
3+3 (1) x	1.344(2), 0.14(12)	0, 0	0, 0	2.328(3)
R_{wp}, R_{exp}, χ^2, R_B		7.60, 3.37, 5.07, 2.17		
3+3 (F) xz	1.42(5), 0	0, 0	0.28(3), 0.41(2)	2.56(6)
R_{wp}, R_{exp}, χ^2, R_B		3.62, 1.63, 4.95, 0.589		
3+3 (F) x	1.481(2), 0.19(3)	0, 0	0, 0	2.58(3)
R_{wp}, R_{exp}, χ^2, R_B		3.64, 1.63, 5.01, 0.569		
3+2 (F) skyrmion	1.283(1), 0	0, 0	0, −1.283(1)	2.566(2)
R_{wp}, R_{exp}, χ^2, R_B		3.67, 1.63, 5.08 , 0.643		

#D+3 Hedgehog model: refined by LSQ

P2_13.1'(a,0,0)00s(0,a,0)00s(0,0,a)00s

	m1 =-m3=0.950(1)μ_B , α1 =0		m3=0.950(1)μ_B , α3 =π/2	
	m_{xc}, m_{xs}, μ_B		m_{zc}, m_{zs}, μ_B	M, μ_B
3+3 (1) hedgehog	0.950(1), 0	0, 0	0, -0.950(1)	2.327(3)

$$[M_x, M_y, M_z] = 0.95[\cos\tilde{y} - \sin\tilde{z}, \cos\tilde{z} - \sin\tilde{x}, \cos\tilde{x} - \sin\tilde{y}]\mu_B$$

$\tilde{y} = 2\pi k y$ …,etc

Hedgehog 3D+3 magnetic structure - one refined parameter

cubic MSSG 198.3.206.1.m10.2 P2_13.1′ (a,0,0)00s(0,a,0)00s(0,0,a)00s

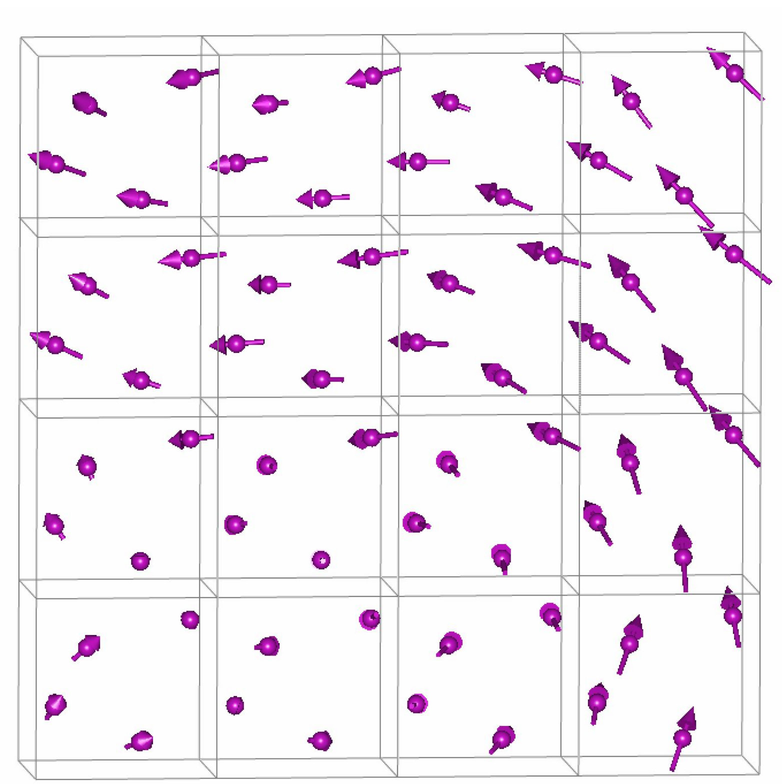

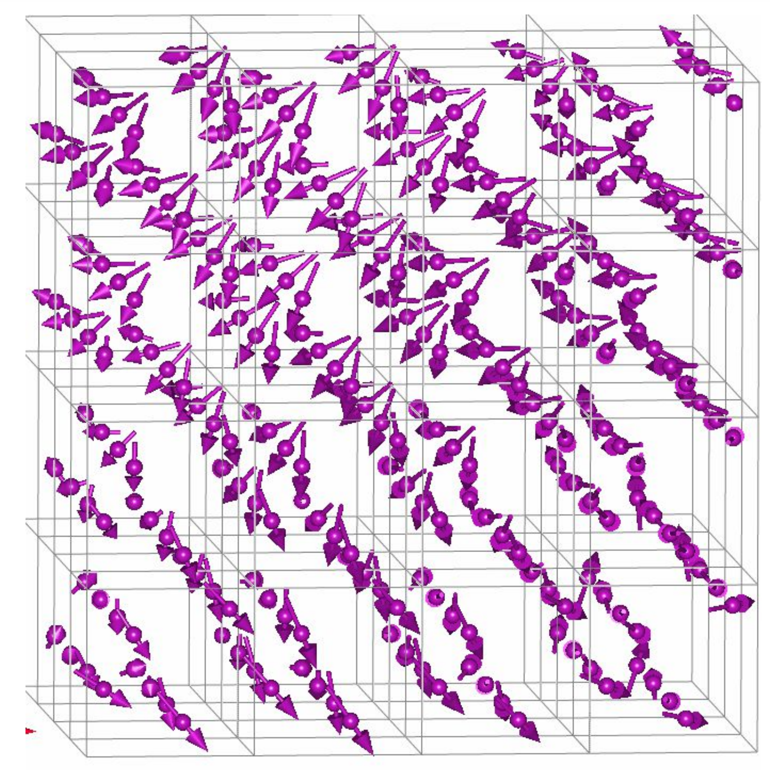

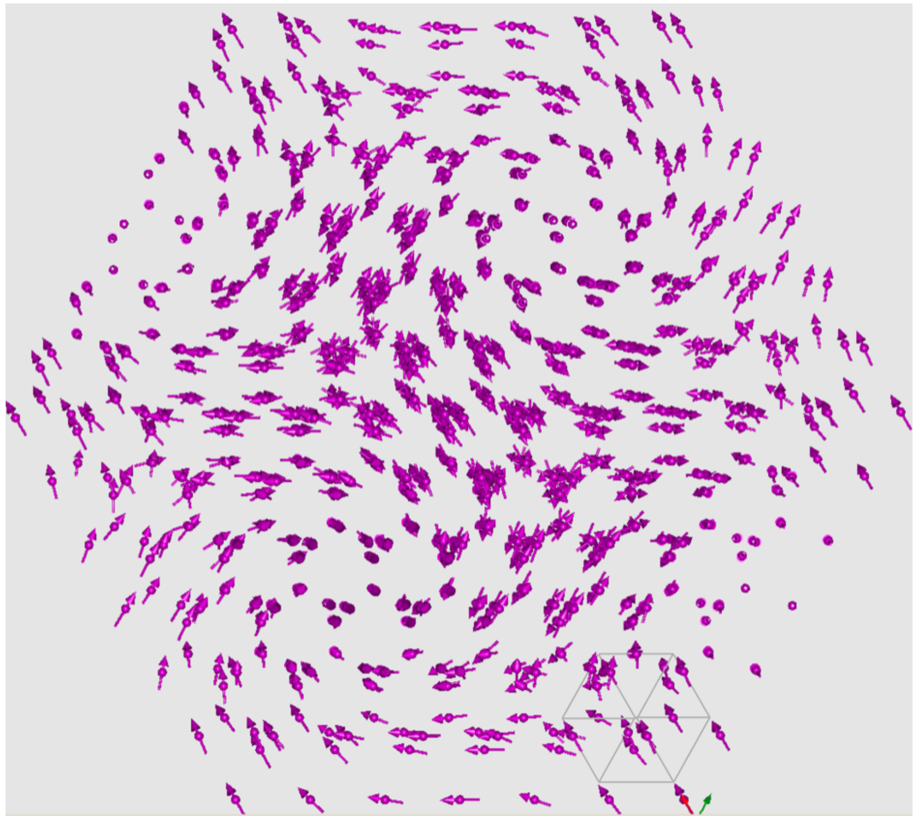

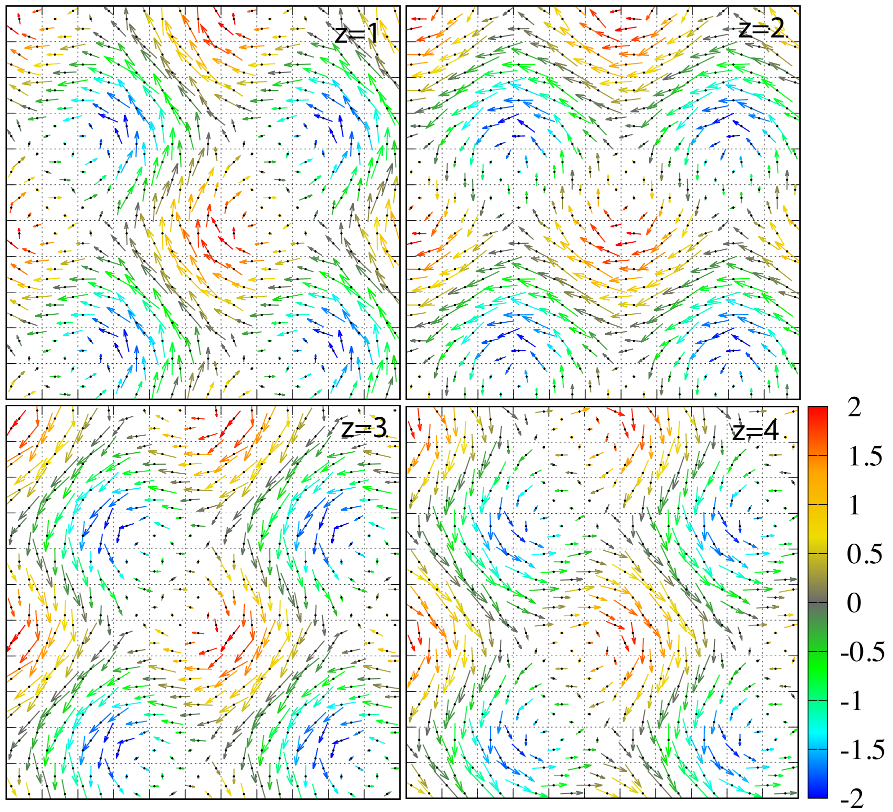

Hedgehog 3D+3 magnetic cell contains 8 monopoles

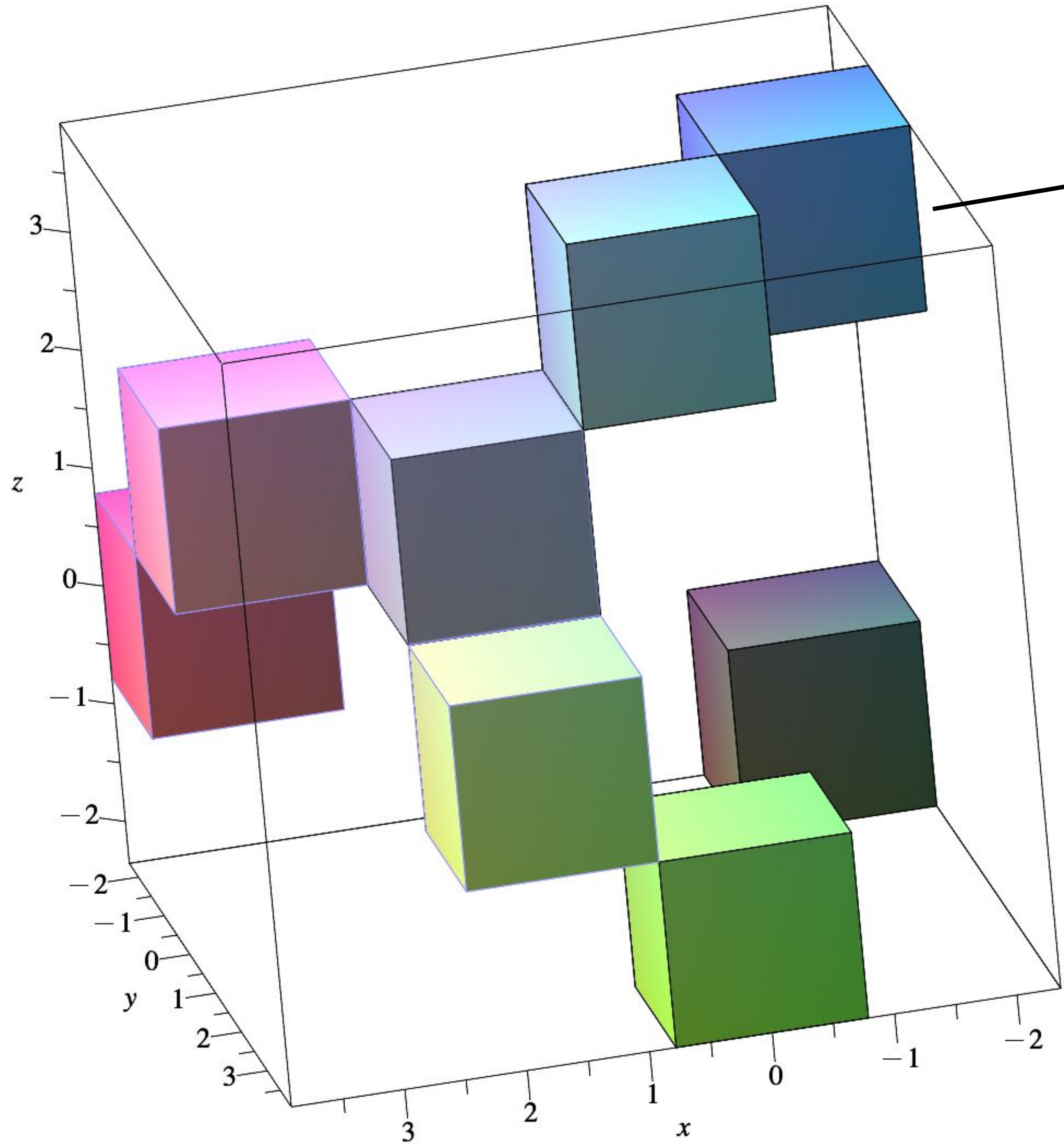

Hedgehog 3D+3 magnetic cell contains 8 monopoles. Each with |Q|=1

cubic MSSG 198.3.206.1.m10.2 P2_13.1′ (a,0,0)00s(0,a,0)00s(0,0,a)00s

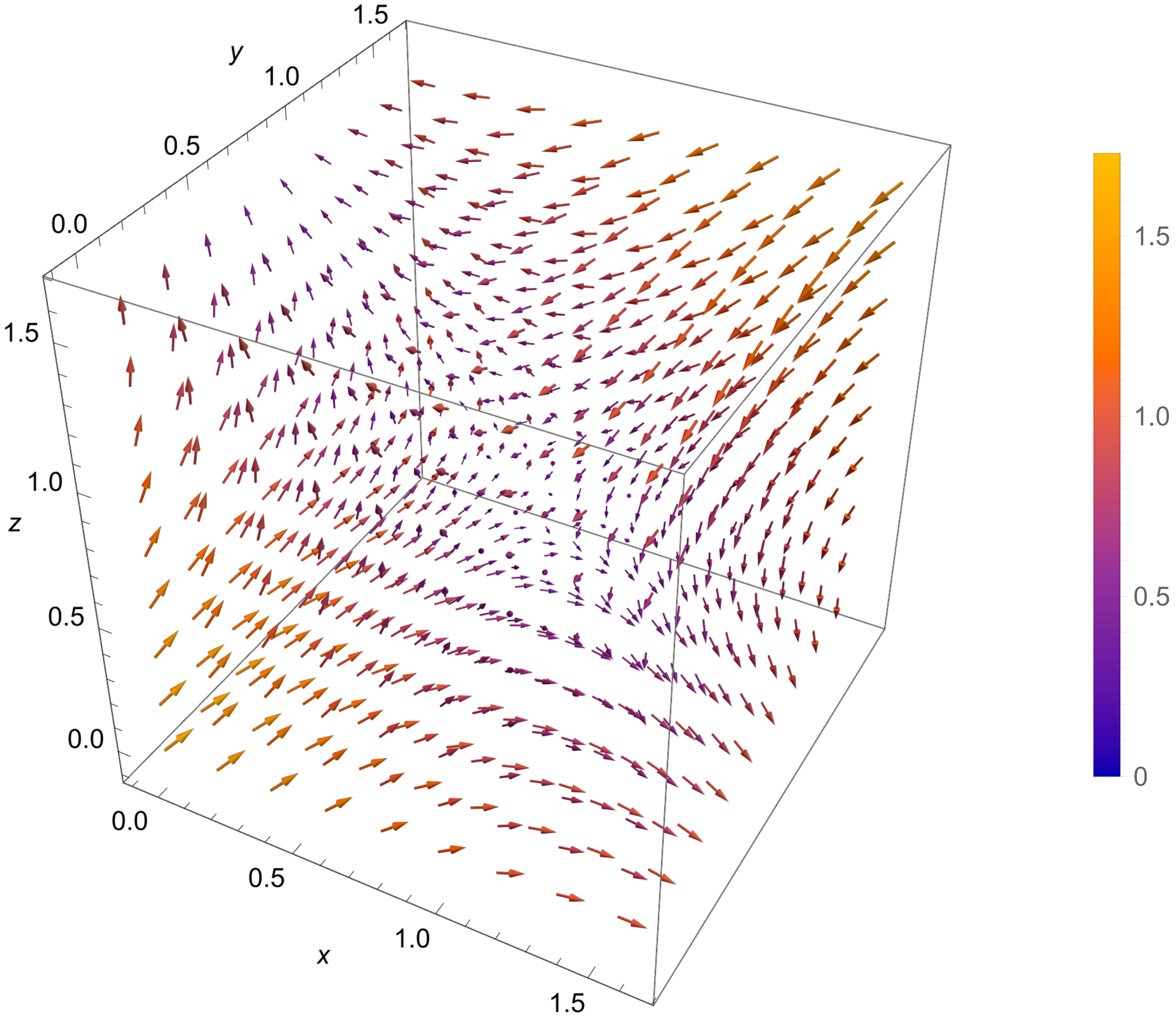

Fragment of magnetization (edge π /2 around the center π/4,π/4,π/4). The total solid angle spanned on the cube faces is Q = +/−1 in 4π units. The color indicates the size of the magnetization.

Normalized Linearized Magnetization on unity sphere

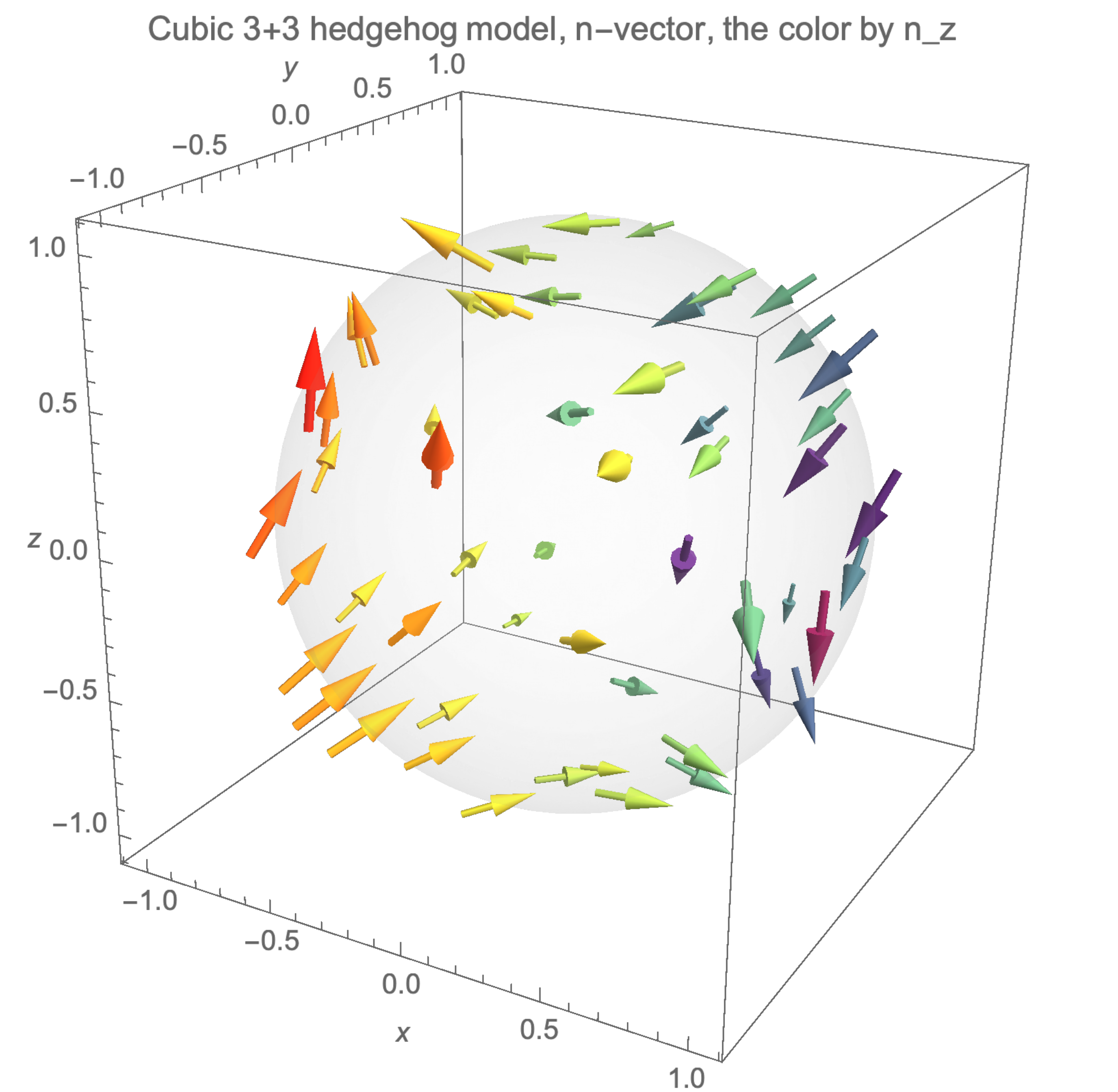

“Bloch” skyrmion (meron) 3D+2 magnetic structure

orthorhombic MSSG 19.2.29.2.m26.3 P2_12_12_1.1′ (0,b1,0)000s(0,0,g2)000s

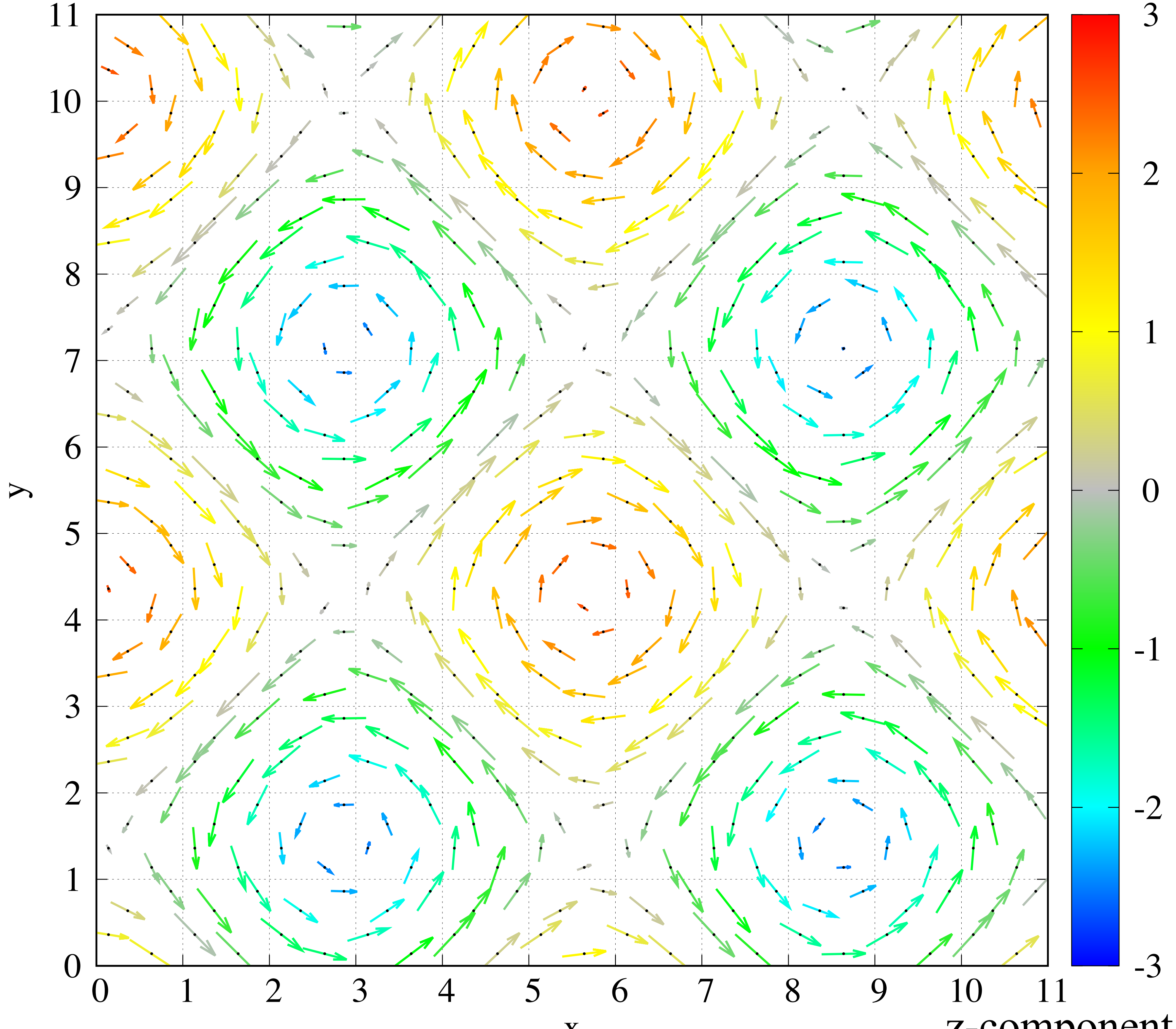

z-component by color

$$w(x,y) = \frac{1}{4\pi}\left(\mathbf{n}\cdot\left[\frac{\partial \mathbf{n}}{\partial x}\times\frac{\partial \mathbf{n}}{\partial y}\right]\right)$$

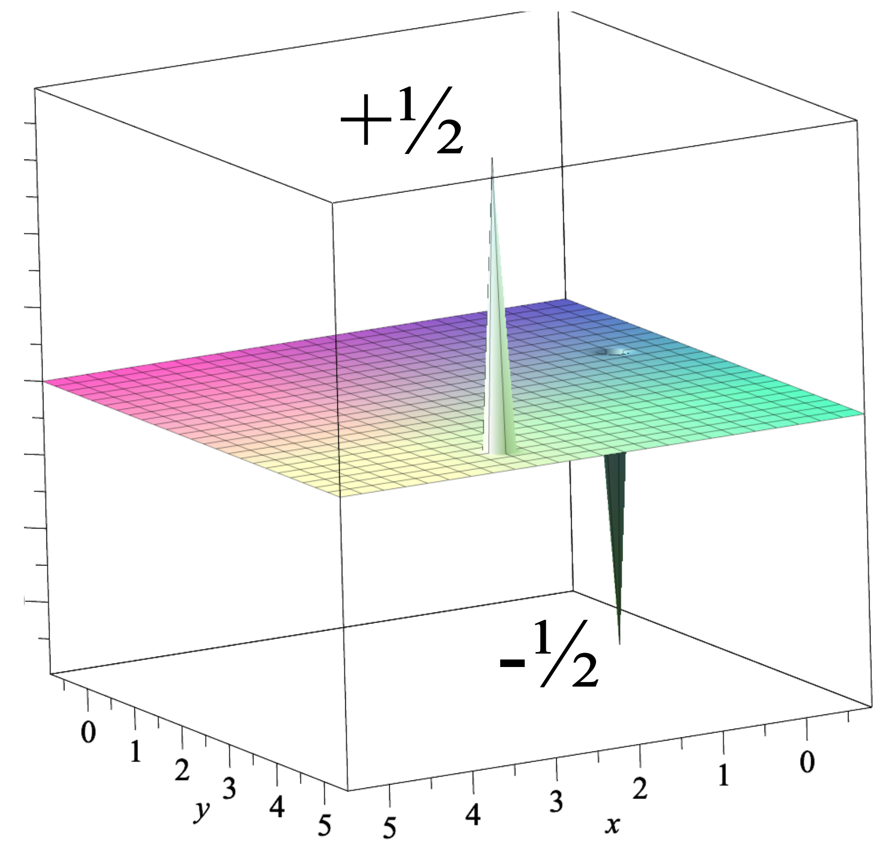

The total topo-charge Q = 0 in zero field.

“Bloch” skyrmion (meron) 3D+2 magnetic structure

orthorhombic MSSG 19.2.29.2.m26.3 P2_12_12_1.1′ (0,b1,0)000s(0,0,g2)000s

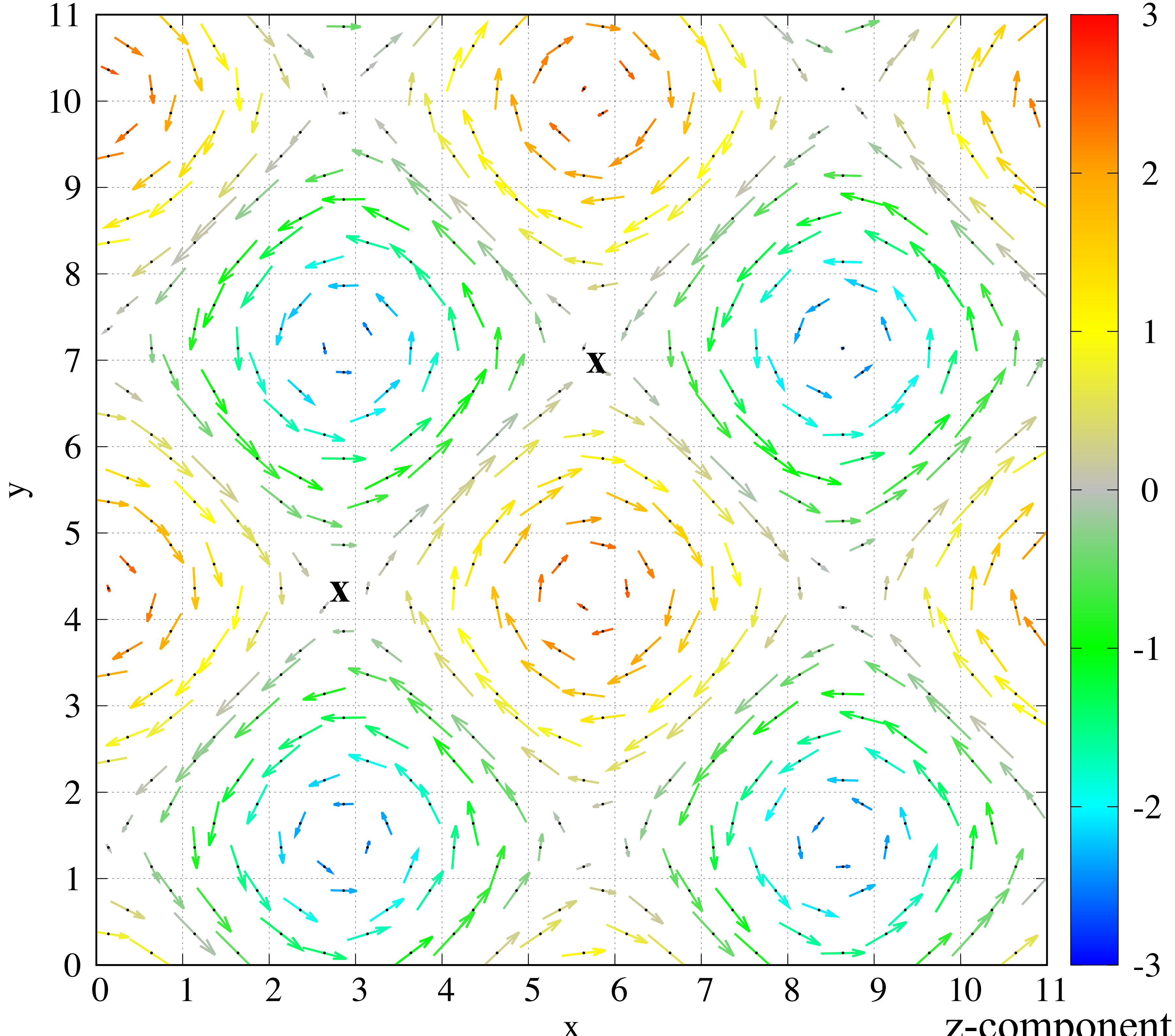

z-component by color

$$w(x,y) = \frac{1}{4\pi}\left(\mathbf{n}\cdot\left[\frac{\partial \mathbf{n}}{\partial x}\times\frac{\partial \mathbf{n}}{\partial y}\right]\right)$$

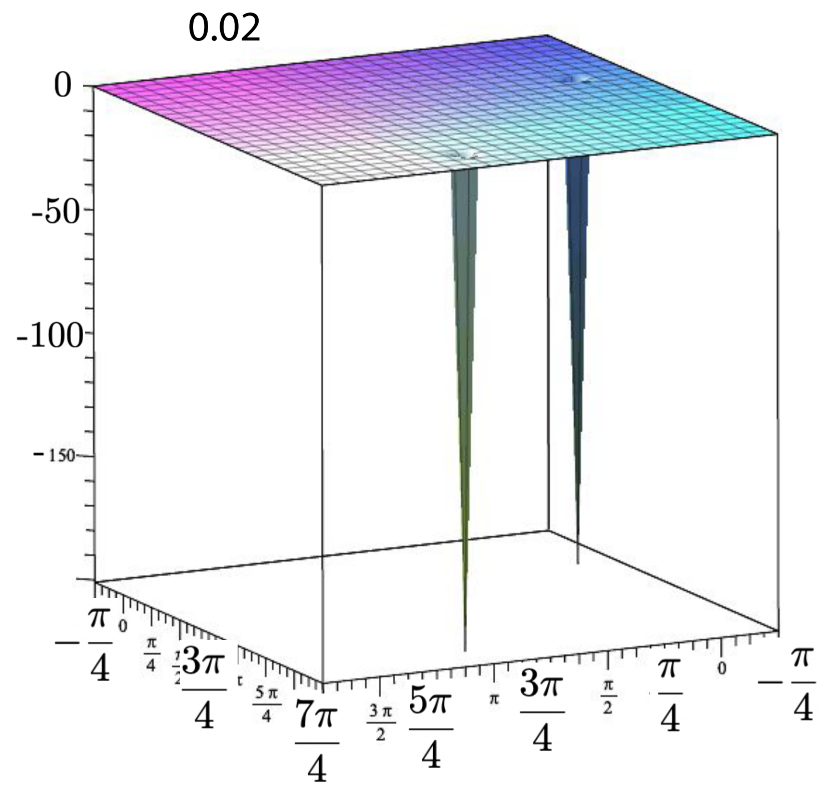

The total topo-charge Q = −1 in infinitesimal field.

Topological charges in MnGe in external field

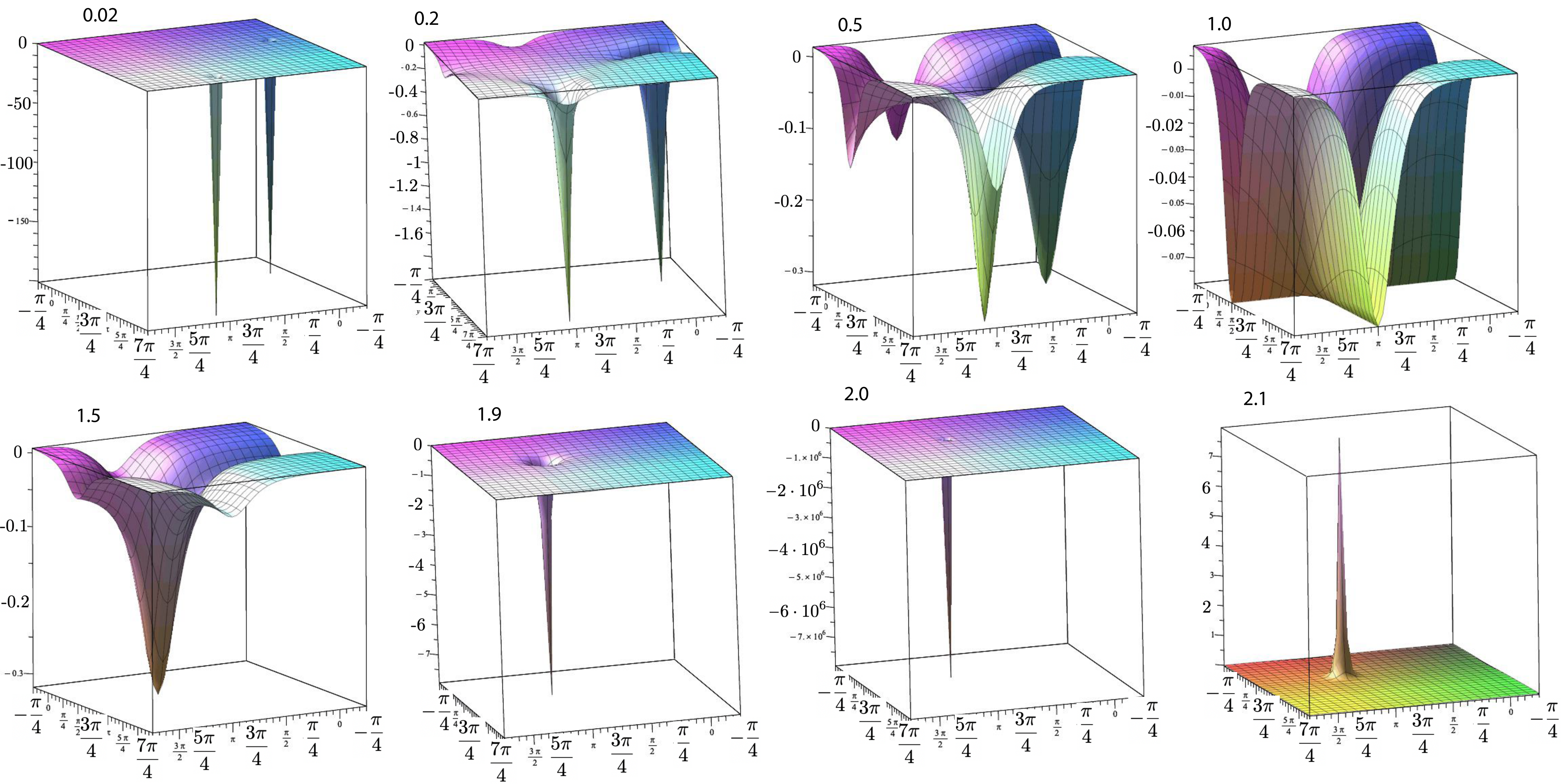

FIG. 8. Density of topological charge $w(x, y)$ calculated using formula (6) for the magnetic structure in the orthorhombic 3+2 model given by formula (5) (to avoid singularities the coefficient for cosine of the z component was chosen to be 1.0001) with a ferromagnetic component along the z axis $m_f = 0.02, 0.2, 0.5, 1, 1.5, 1.9, 2.0, 2.1$. One modulation period between $-\pi/4 \cdots 2\pi - \pi/4$ is shown, corresponding to about 6 unit cells in Fig. 7. Each peak carries topological charge $Q = -1/2$ for infinitely small m_f. The total topological charge per cell is $Q = -1$ for $m_f \leqslant 2$ and $Q = 0$ for $m_f > 2$.

Superspace magnetic structure and topological charges in Weyl semimetal CeAlGe

Motivation to study CeAlGe

CeAlGe was predicted theoretically to be an easy-plane FM type-II Weyl semimetal (WSM)*.

It is still not clear if it is WSM… Instead, we have found that CeAlGe is an antiferromagnet with rich phase diagram

It has topologically nontrivial magnetization textures in real-space ==> topological Hall effect (THE).

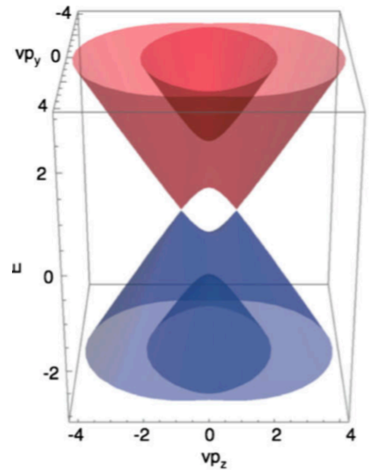

* G. Chang, B. Singh, S.-Y. Xu, G. Bian, S.-M. Huang, C.-H. Hsu, I. Belopolski, N. Alidoust, D. S. Sanchez, H. Zheng, et a Physical Review B 97 (2018).

WSM has gapless electronic excitations Weyl fermions that are protected by topology and symmetry.

Samples CeAlGe: single crystals & powders

BULK SINGLE-CRYSTAL GROWTH OF THE … PHYSICAL REVIEW MATERIALS **3**, 024204 (2019)

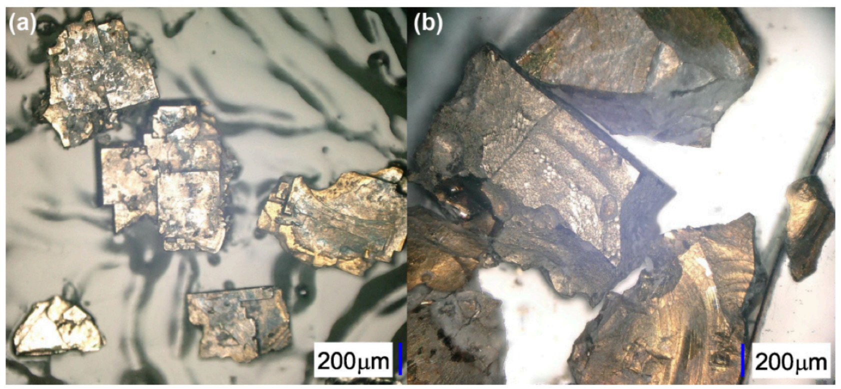

FIG. 2. Pictures of the flux-grown crystals of (a) CeAlGe and (b) PrAlGe right after flux removal using NaOH-H_2O, and before subsequent annealing

FIG. 3. Photos of (a) the cast CeAlGe rod, and the floating-zone-grown crystals of (b) CeAlGe and (c) PrAlGe.

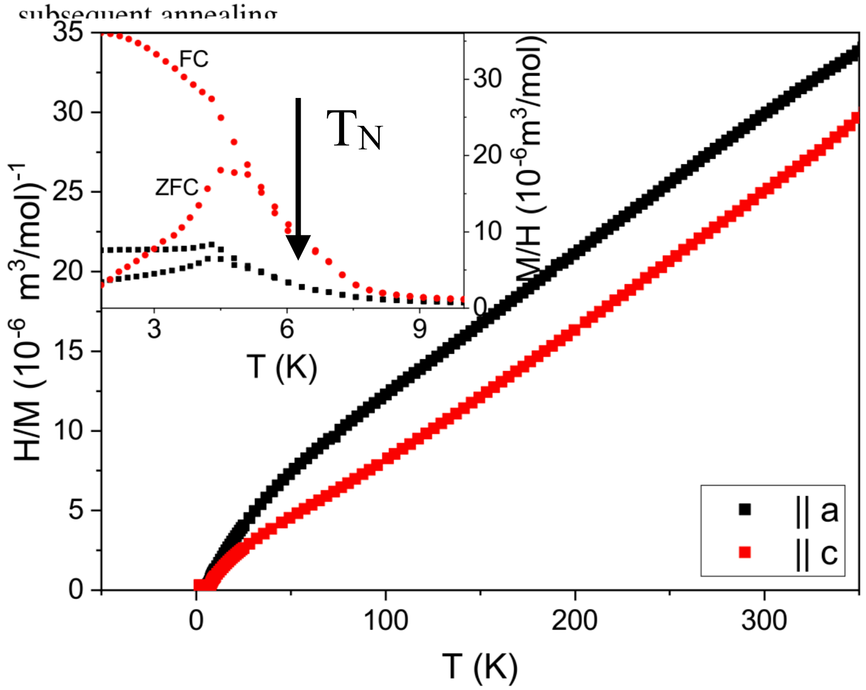

FIG. 8. Magnetic data obtained on a floating-zone-grown CeAlGe single crystal with a mass of 125.4 mg. The magnetic

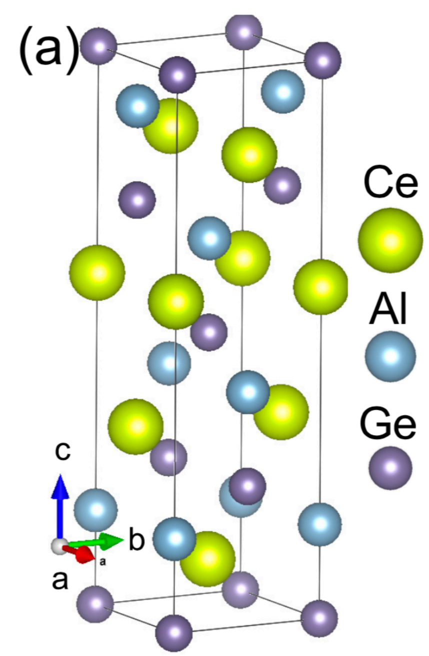

Space Group: 109 I4_1md C4v-11

non-centrosymmetric

Lattice parameters:

a=4.25717, c=14.64520

Ce1 4a (0,0,z), z=-0.41000 single magnetic Ce site

Neutron diffraction experiments: HRPT and DMC, SANS at PSI Switzerland, D33, at ILL France

Resistivity: Topologicall Hall Effect in University of Tokyo

Samples: both powder and single crystals of CeAlGe grown at PSI in Solid State Chemistry group

P. Puphal, et al, Physical Review Letters, 124, 017202 (2020)

Examples of raw experimental powder diffraction patterns for CeAlGe

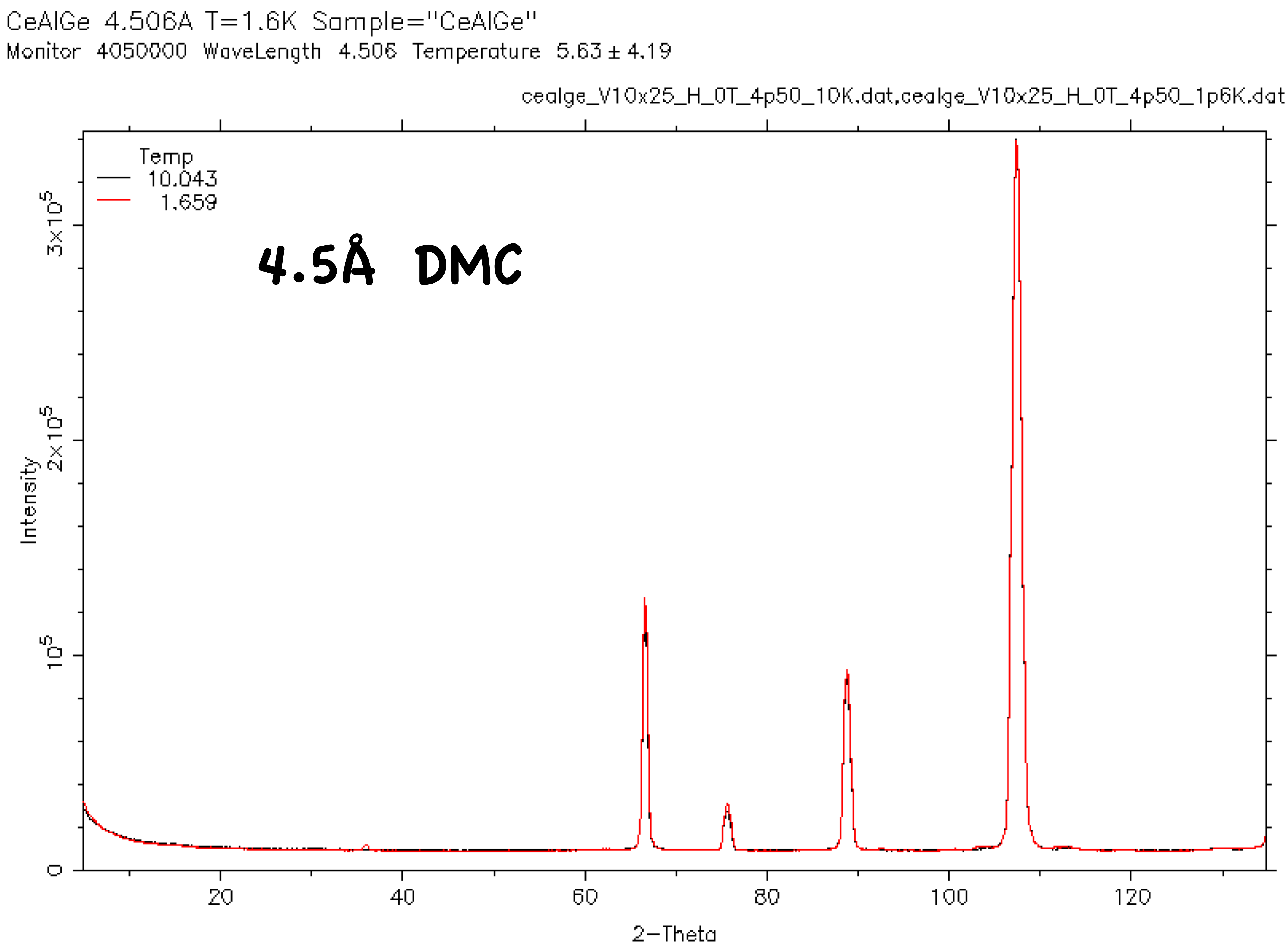

powder diffraction patterns CeAlGe

4.5Å DMC

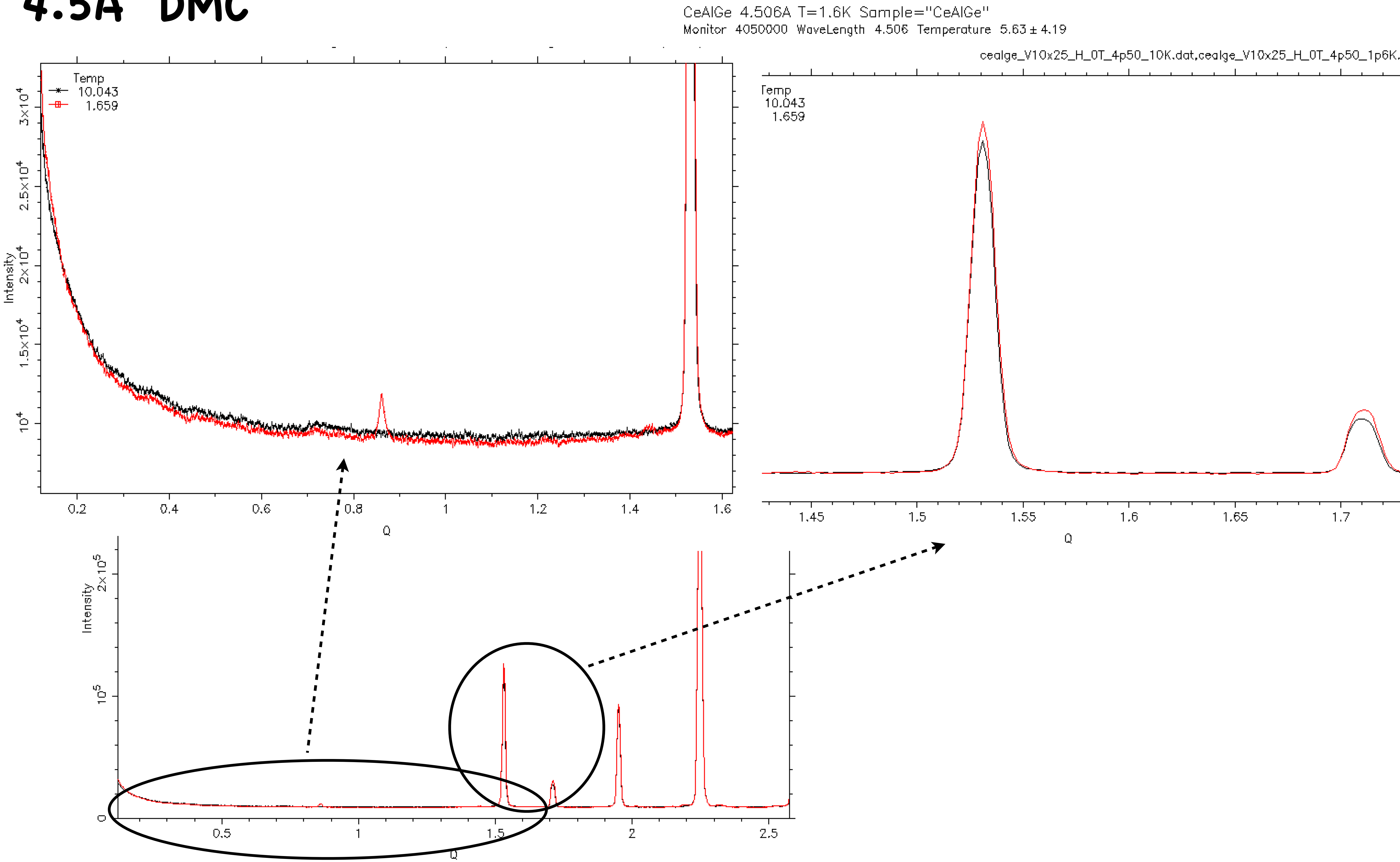

Magnetic peaks are well seen from both powder and s.c. neutron diffraction

CeAlGe

k1=[g,0,0], SM point of BZ, g=0.06503(22) ~65Å

Magnetic NPD difference profile taken between T = 1.7 K and 10 K

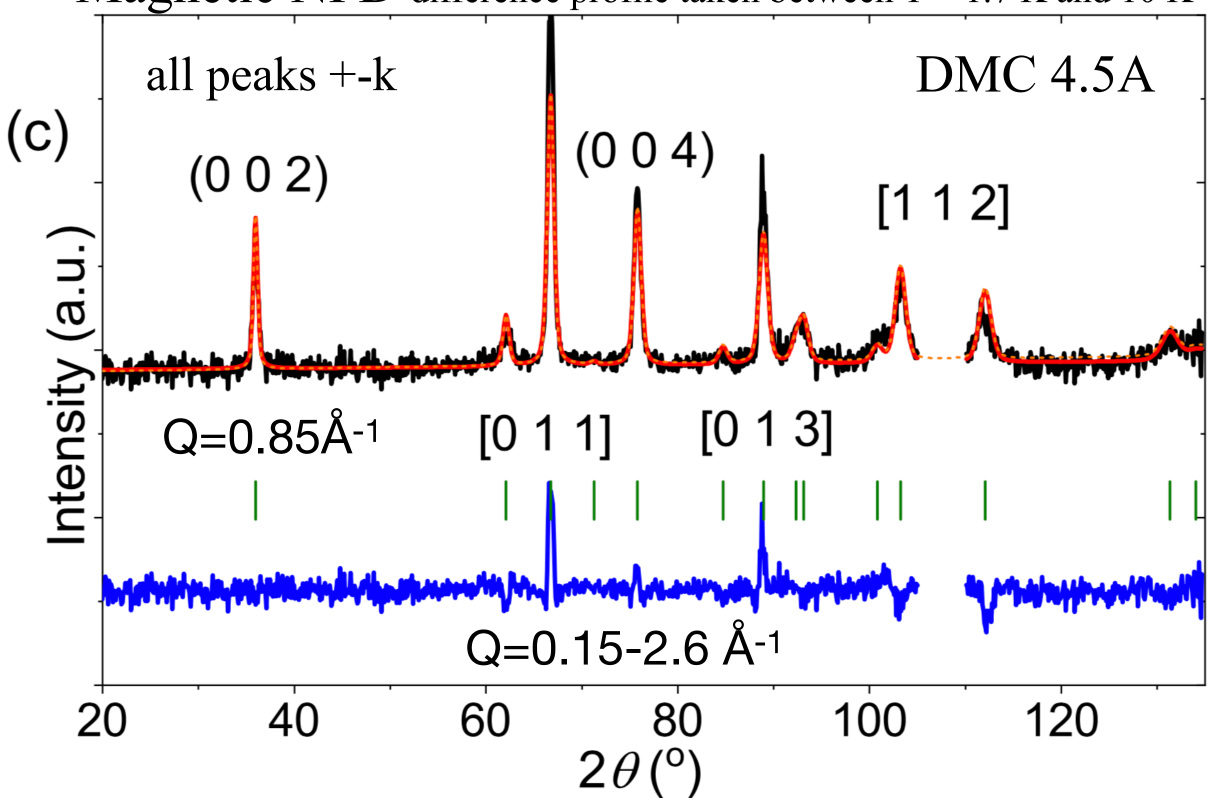

Gamma point k=0 does not fit NPD

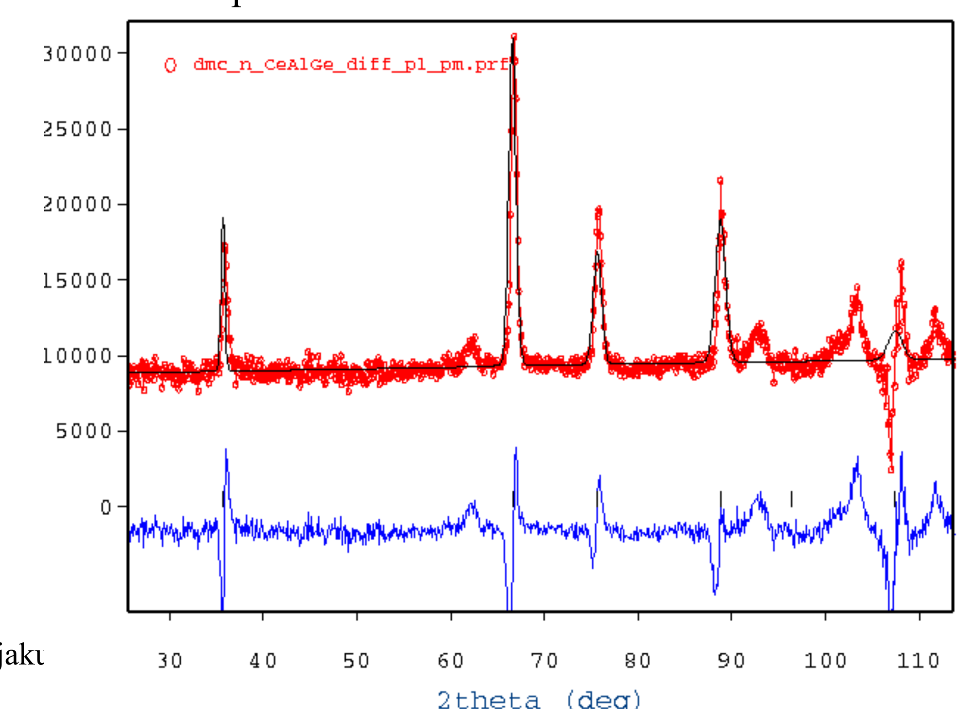

P. Puphal, et al, Physical Review Letters, 124, 017202 (2020)

Magnetic peaks are well seen from both powder and s.c. neutron diffraction

CeAlGe

k1=[g,0,0], SM point of BZ, g=0.06503(22) ~65Å

Magnetic NPD difference profile taken between T = 1.7 K and 10 K

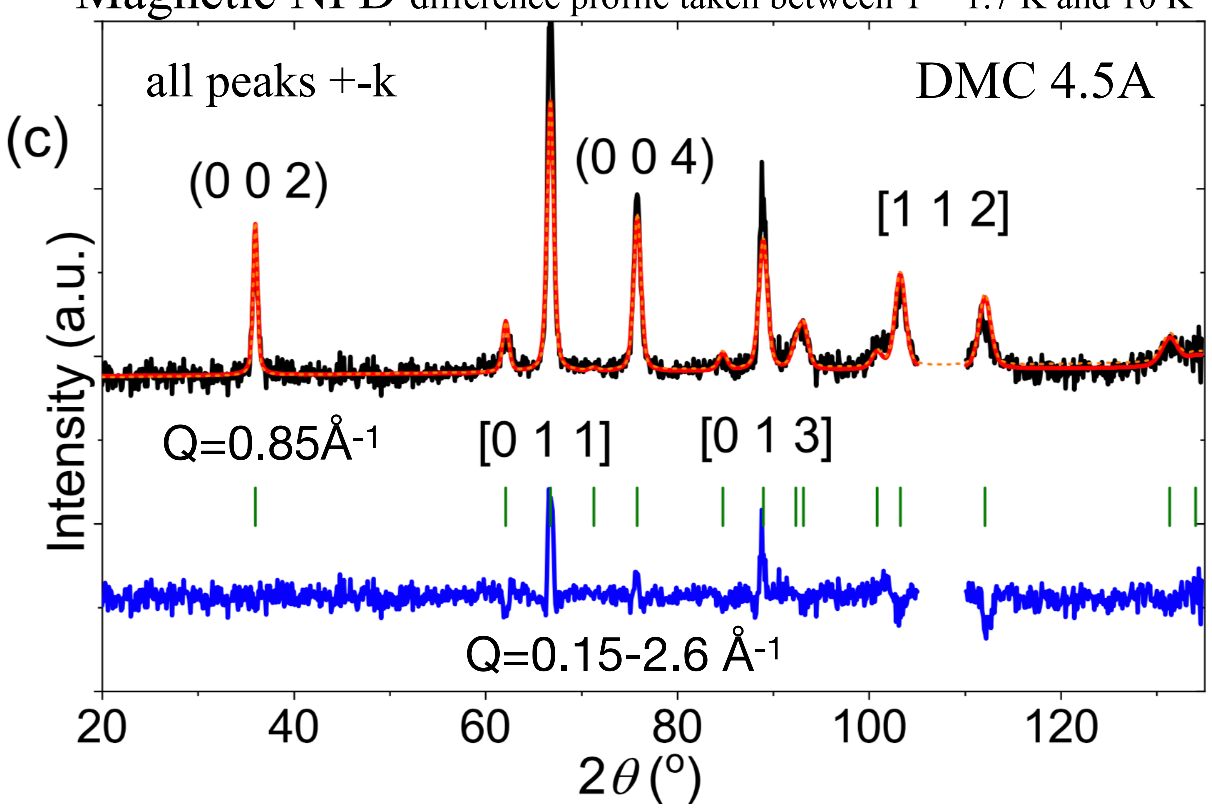

Gamma point k=0 does not fit NPD

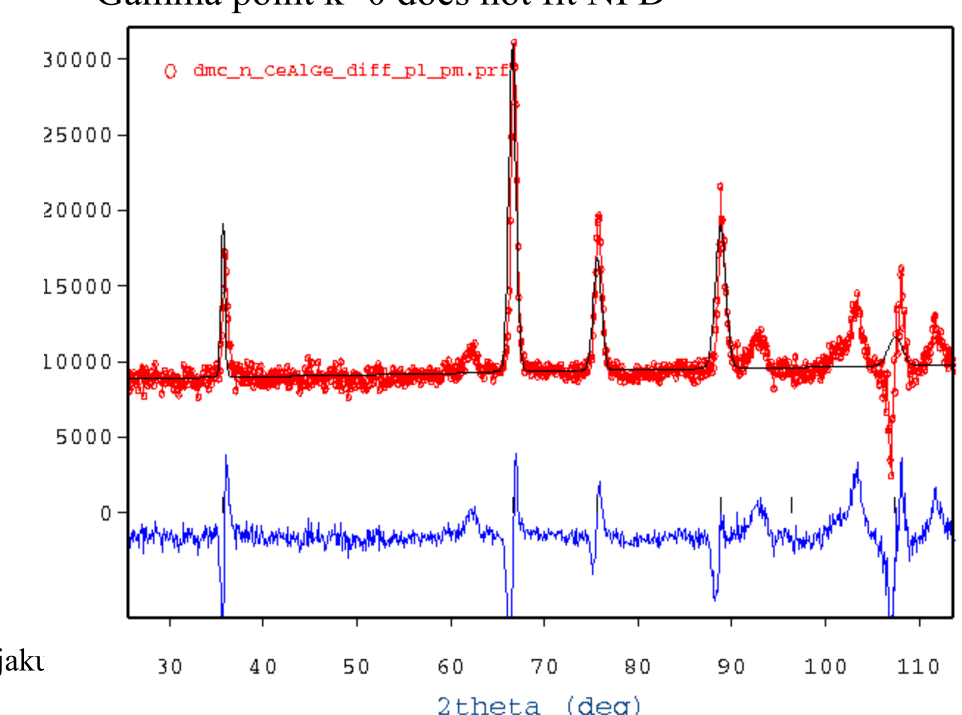

k1=[g,0,0], k2=[0,g,0]

Single crystal

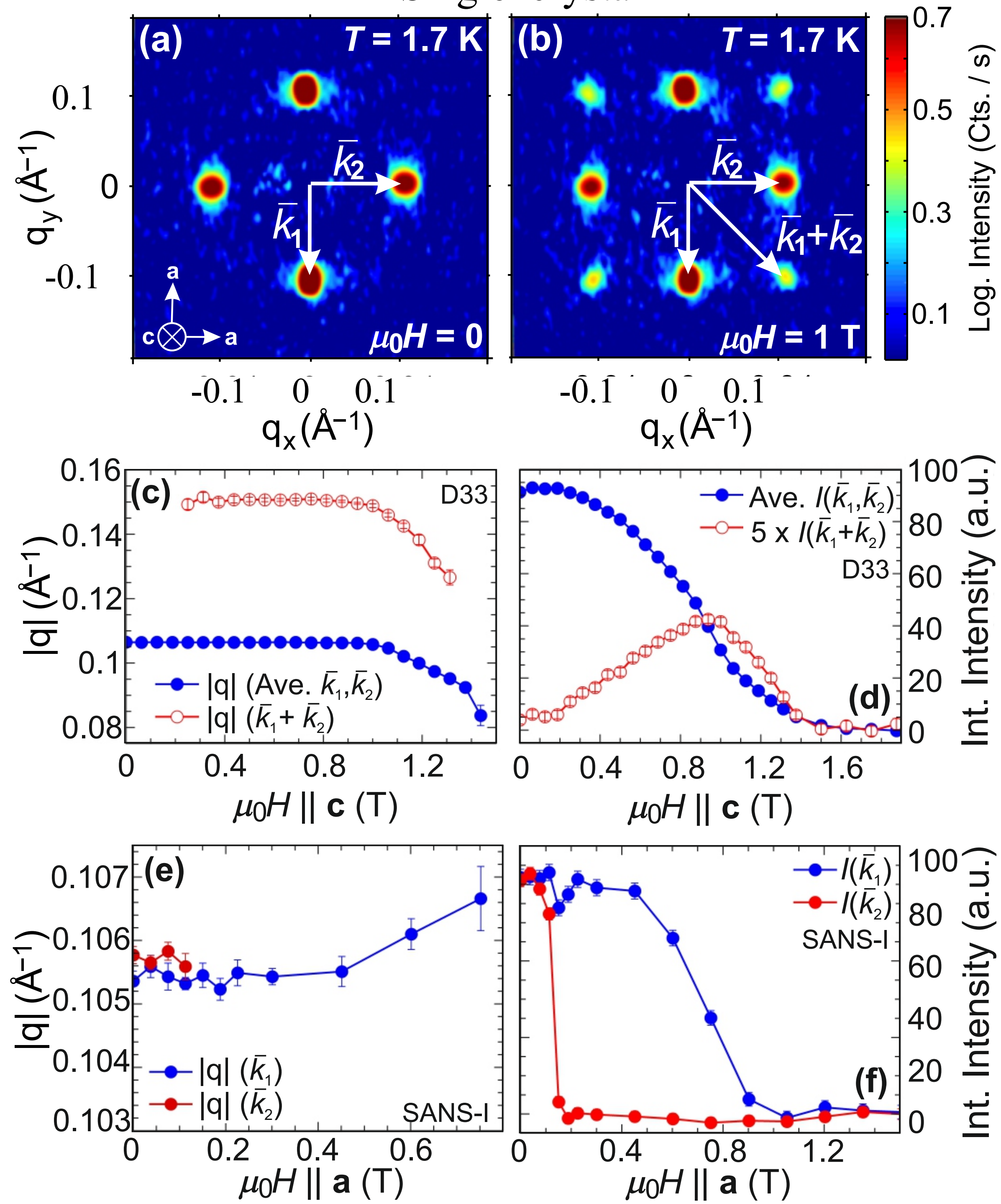

P. Puphal, et al, Physical Review Letters, 124, 017202 (2020)

Crystal structure. Magnetic atoms.

Space group $I4_1md$:
8 symops & I-centering,
Ce 4a (0,0,z) single
magnetic Ce site: 4 atoms
per cell

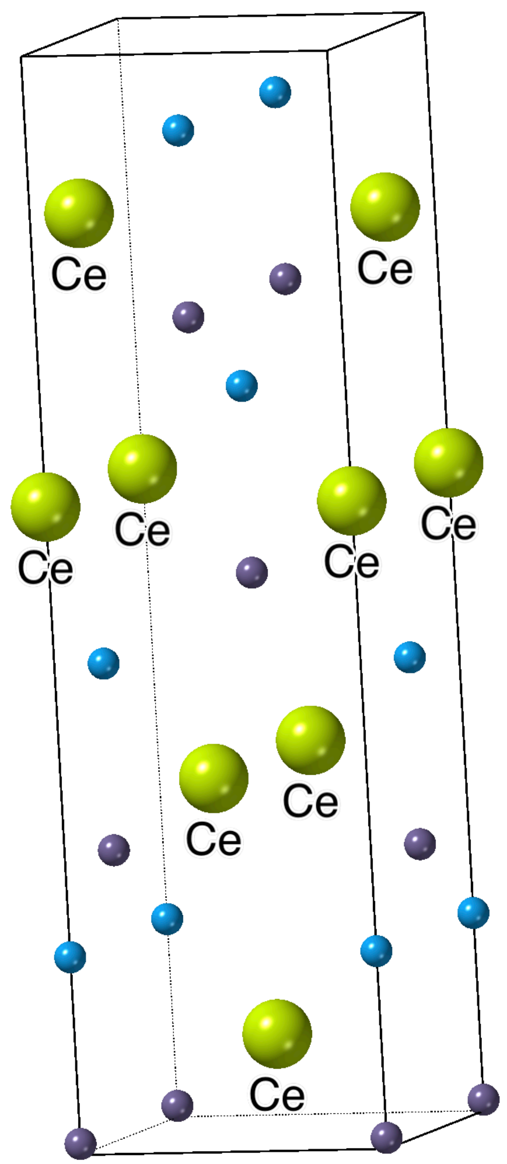

Crystal structure. Magnetic atoms.

Space group $I4_1md$:
8 symops & I-centering,
Ce 4a (0,0,z) single magnetic Ce site: 4 atoms per cell

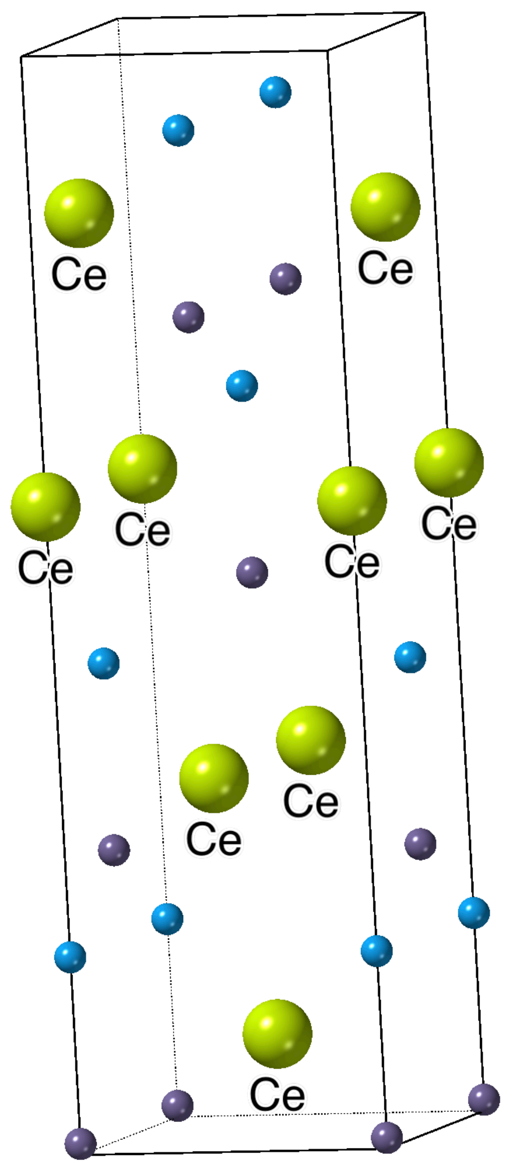

4(a) $\mathrm{Ce1}(0, 0, z)$

$\mathrm{Ce2}(0, \frac{1}{2}, z + \frac{1}{4})$

$\bar{y}, x + \frac{1}{2}, z + \frac{1}{4}$

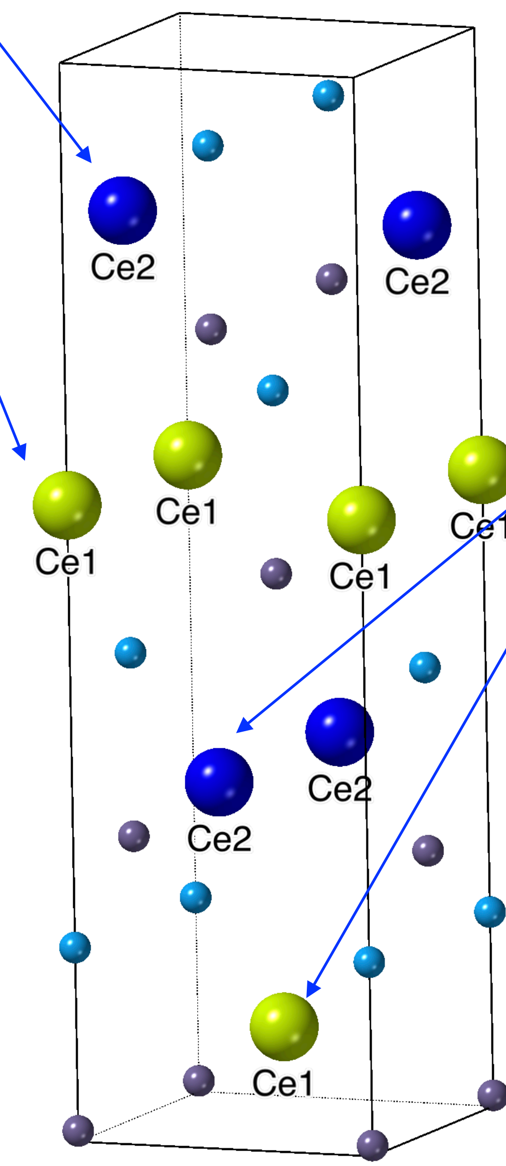

Two other Ce's are generated b I-centering translations (½, ½, ½)+

subgroup tree for I4_1md [u,0,0]+[0,u,0]

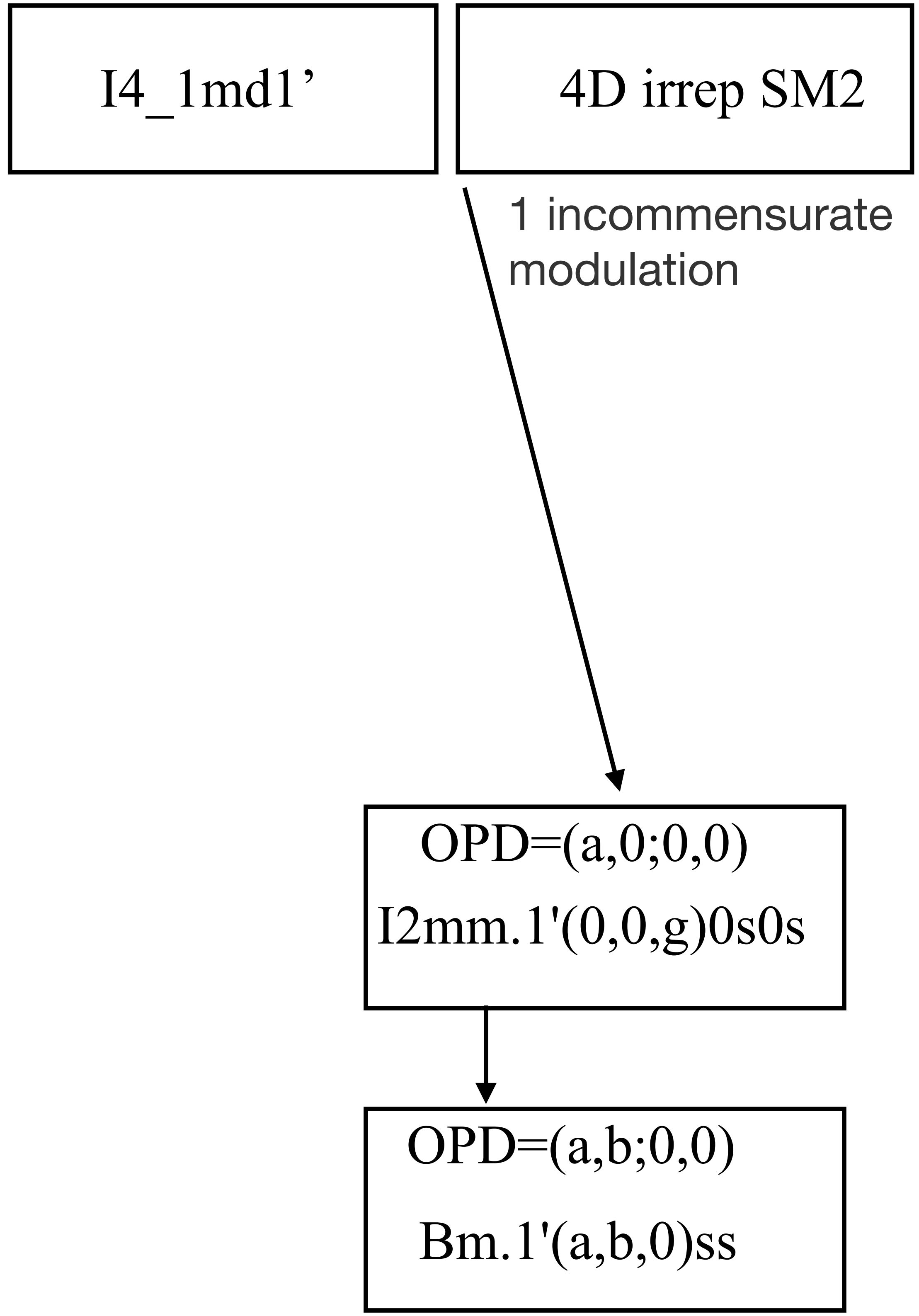

irrep OPD

$$\begin{pmatrix} 1 & 0 & 0 & 0 \\ 0 & -1 & 0 & 0 \\ 0 & 0 & 1 & 0 \\ 0 & 0 & 0 & -1 \end{pmatrix} \begin{pmatrix} a \\ b \\ c \\ d \end{pmatrix}$$

$$\begin{pmatrix} 0 & 0 & 1 & 0 \\ 0 & 0 & 0 & -1 \\ \mathrm{Cos}(\pi u) & \mathrm{Sin}(\pi u) & 0 & 0 \\ \mathrm{Sin}(\pi u) & \mathrm{Cos}(\pi u) & 0 & 0 \end{pmatrix}$$

$$\begin{pmatrix} 0 & 0 & 1 & 0 \\ 0 & 0 & 0 & 1 \\ \mathrm{Cos}(\pi u) & -\mathrm{Sin}(\pi u) & 0 & 0 \\ \mathrm{Sin}(\pi u) & -\mathrm{Cos}(\pi u) & 0 & 0 \end{pmatrix}$$

$$\begin{pmatrix} -1 & 0 & 0 & 0 \\ 0 & -1 & 0 & 0 \\ 0 & 0 & -1 & 0 \\ 0 & 0 & 0 & 1 \end{pmatrix}$$

subgroup tree for I4_1md [u,0,0]+[0,u,0]

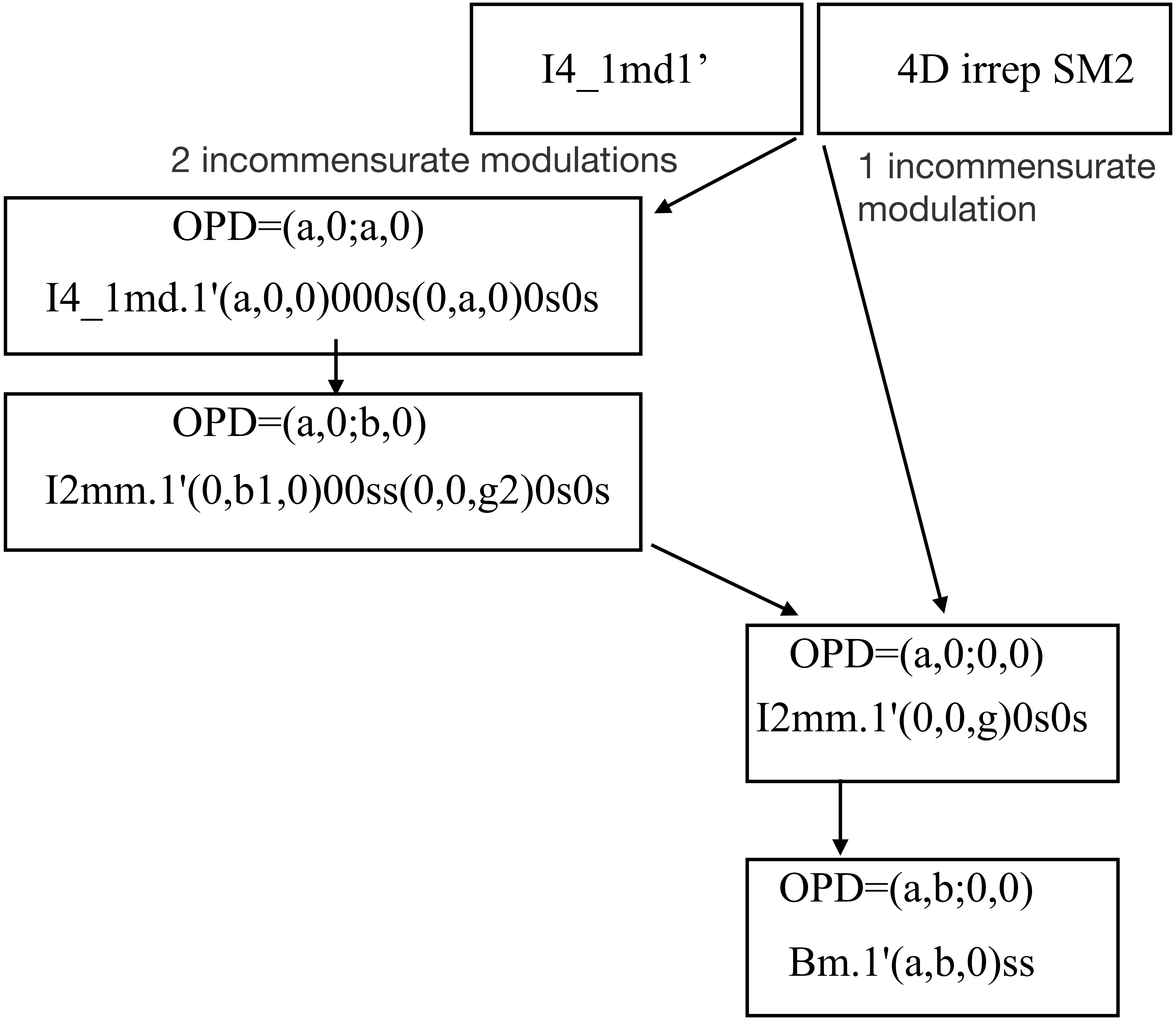

irrep OPD

$$\begin{pmatrix} 1 & 0 & 0 & 0 \\ 0 & -1 & 0 & 0 \\ 0 & 0 & 1 & 0 \\ 0 & 0 & 0 & -1 \end{pmatrix} \begin{pmatrix} a \\ b \\ c \\ d \end{pmatrix}$$

$$\begin{pmatrix} 0 & 0 & 1 & 0 \\ 0 & 0 & 0 & -1 \\ \cos(\pi u) & \sin(\pi u) & 0 & 0 \\ \sin(\pi u) & \cos(\pi u) & 0 & 0 \end{pmatrix}$$

$$\begin{pmatrix} 0 & 0 & 1 & 0 \\ 0 & 0 & 0 & 1 \\ \cos(\pi u) & -\sin(\pi u) & 0 & 0 \\ \sin(\pi u) & -\cos(\pi u) & 0 & 0 \end{pmatrix}$$

$$\begin{pmatrix} -1 & 0 & 0 & 0 \\ 0 & -1 & 0 & 0 \\ 0 & 0 & -1 & 0 \\ 0 & 0 & 0 & 1 \end{pmatrix}$$

CeAlGe: Maximal symmetry full star superspace 3D+2 magnetic group I4_1md1'(a00)000s(0a0)0s0s

$I4_1md1'$ IR: mSM2 , k-active= (g,0,0),(0,g,0)

I4_1md1'(a,0,0)000s(0,a,0)0s0s
single Ce site: Ce1 and Ce2 equivalent

View along the z-(c-)axis of the magnetic structure of CeAlGe. The x- and y-axes are in units of in-plane lattice parameter a.

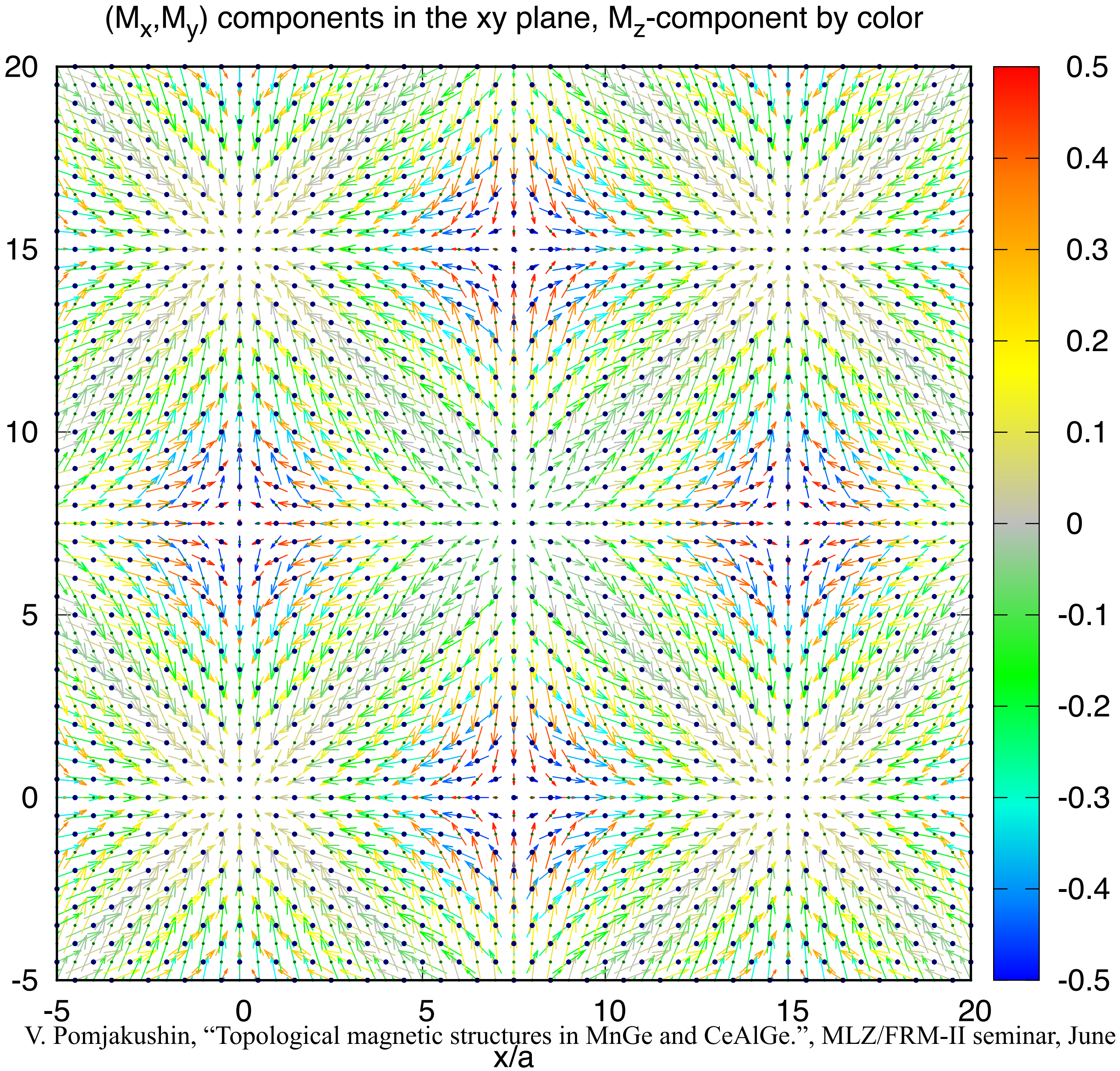

k1=[g,0,0], SM point of BZ, g=0.06503(22): four arms

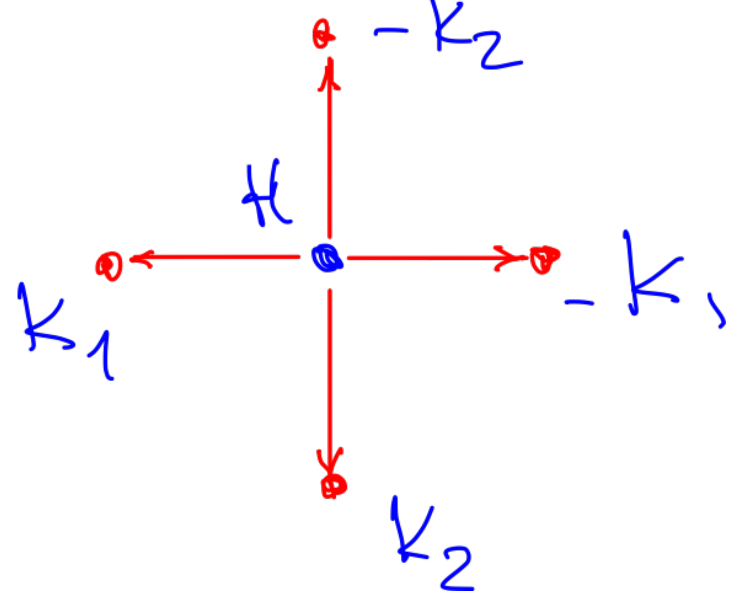

CeAlGe: Maximal symmetry full star superspace 3D+2 magnetic group I4_1md1'(a00)000s(0a0)0s0s

I4$_1$md1'   IR: mSM2 , k-active= (g,0,0),(0,g,0)

↓

I4_1md1'(a,0,0)000s(0,a,0)0s0s
single Ce site: Ce1 and Ce2 equivalent

View along the z-(c-)axis of the magnetic structure of CeAlGe. The x- and y-axes are in units of in-plane lattice parameter a.

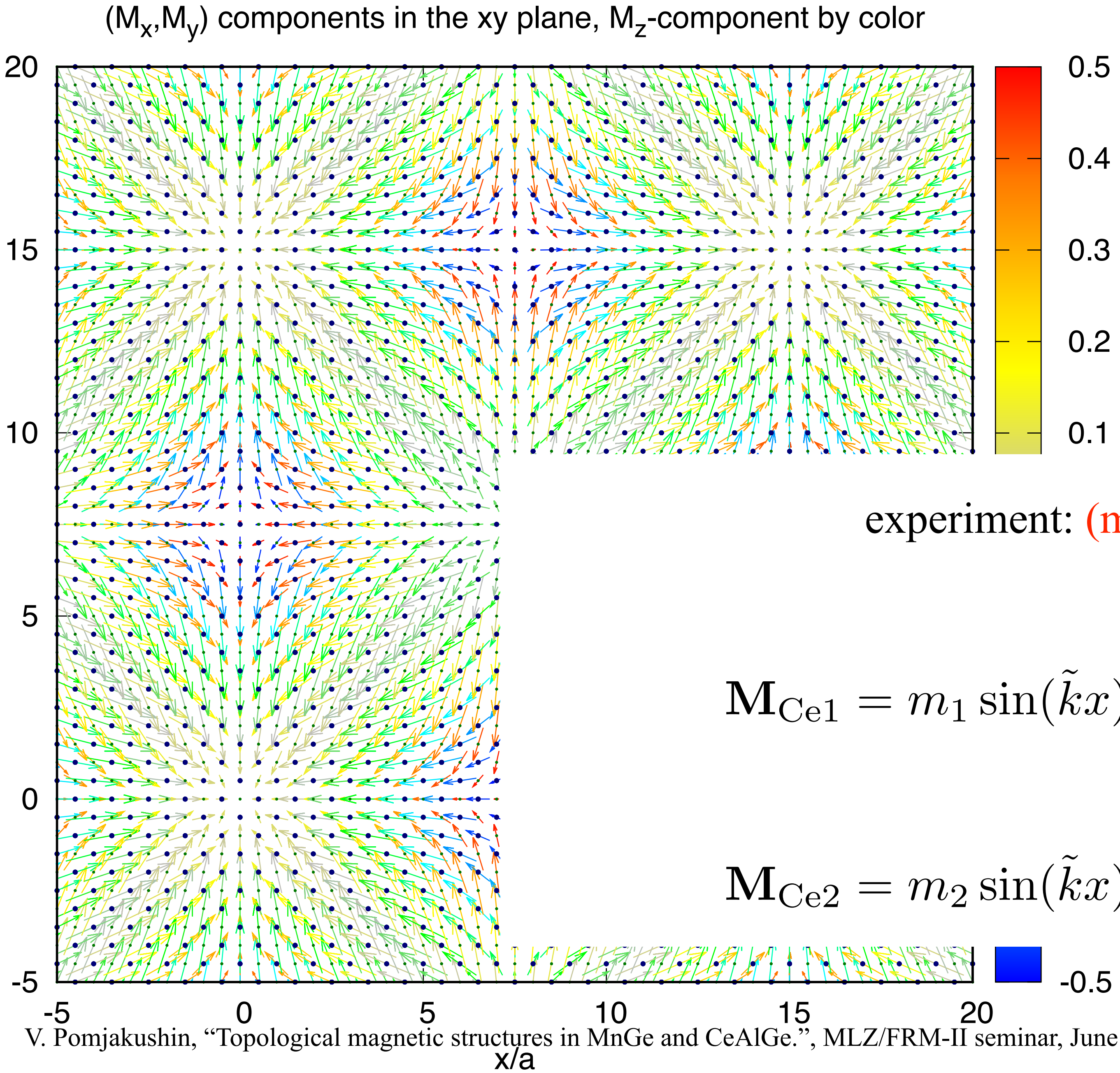

k1=[g,0,0], SM point of BZ, g=0.06503(22): four arms

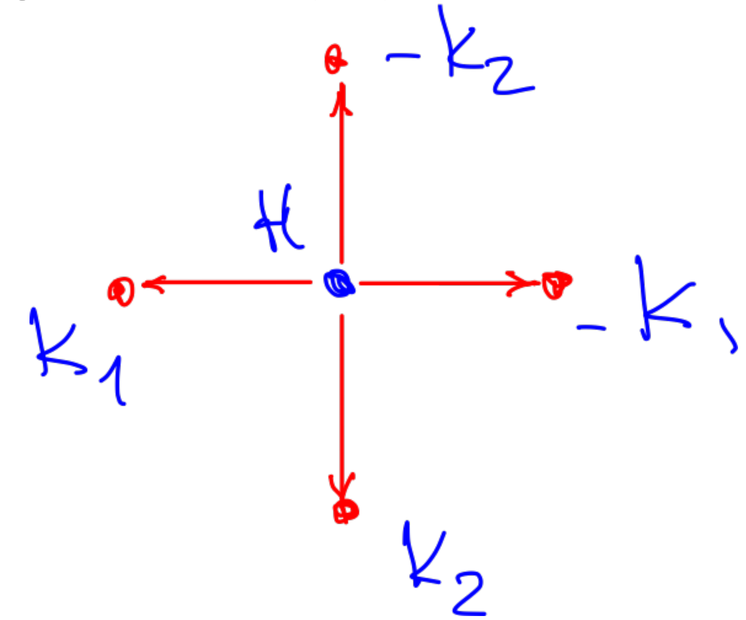

All Ce are equivalent and their moments are given symmetrically by 4 parameters

experiment: (m1,m2,m3,m4) = (0.44(1), 1.02(1), −0.21(5), 0.29(7)) μ_B.

$$\tilde{k}=2\pi|\boldsymbol{k}_1|=2\pi|\boldsymbol{k}_2|=2\pi g$$

$$\mathbf{M}_{\text{Ce1}} = m_1 \sin(\tilde{k}x)\mathbf{e}_{\boldsymbol{x}} + m_2 \sin(\tilde{k}y)\mathbf{e}_{\boldsymbol{y}} + \Big(m_3 \cos(\tilde{k}x) + m_4 \cos(\tilde{k}y)\Big)\,\mathbf{e}_{\boldsymbol{z}}$$

$$\mathbf{M}_{\text{Ce2}} = m_2 \sin(\tilde{k}x)\mathbf{e}_{\boldsymbol{x}} + m_1 \sin(\tilde{k}y)\mathbf{e}_{\boldsymbol{y}} + \Big(m_4 \cos(\tilde{k}x) + m_3 \cos(\tilde{k}y)\Big)\,\mathbf{e}_{\boldsymbol{z}}$$

CeAlGe: Maximal symmetry full star superspace 3D+2 magnetic group I4_1md1'(a00)000s(0a0)0s0s

$I4_1md1'$ IR: mSM2 , k-active= (g,0,0),(0,g,0)

↓

I4_1md1'(a,0,0)000s(0,a,0)0s0s
single Ce site: Ce1 and Ce2 equivalent

k1=[g,0,0], SM point of BZ, g=0.06503(22): four arms

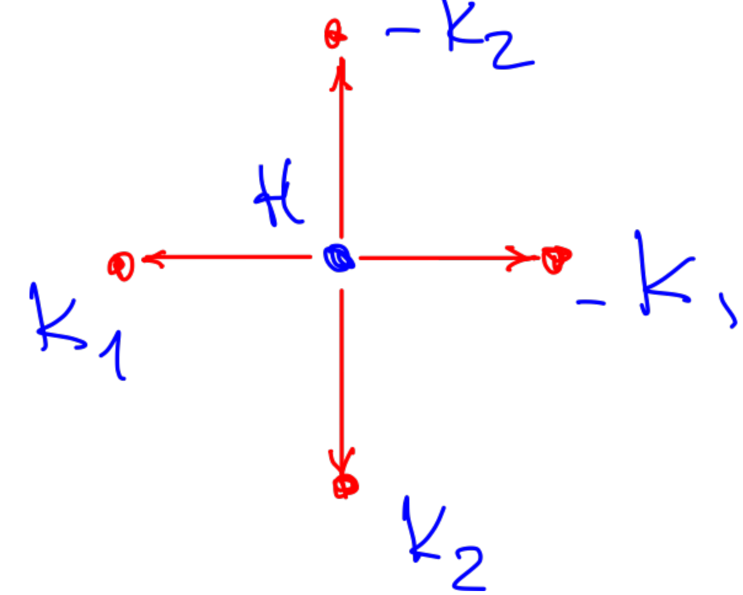

View along the z-(c-)axis of the magnetic structure of CeAlGe. The x- and y-axes are in units of in-plane lattice parameter a.

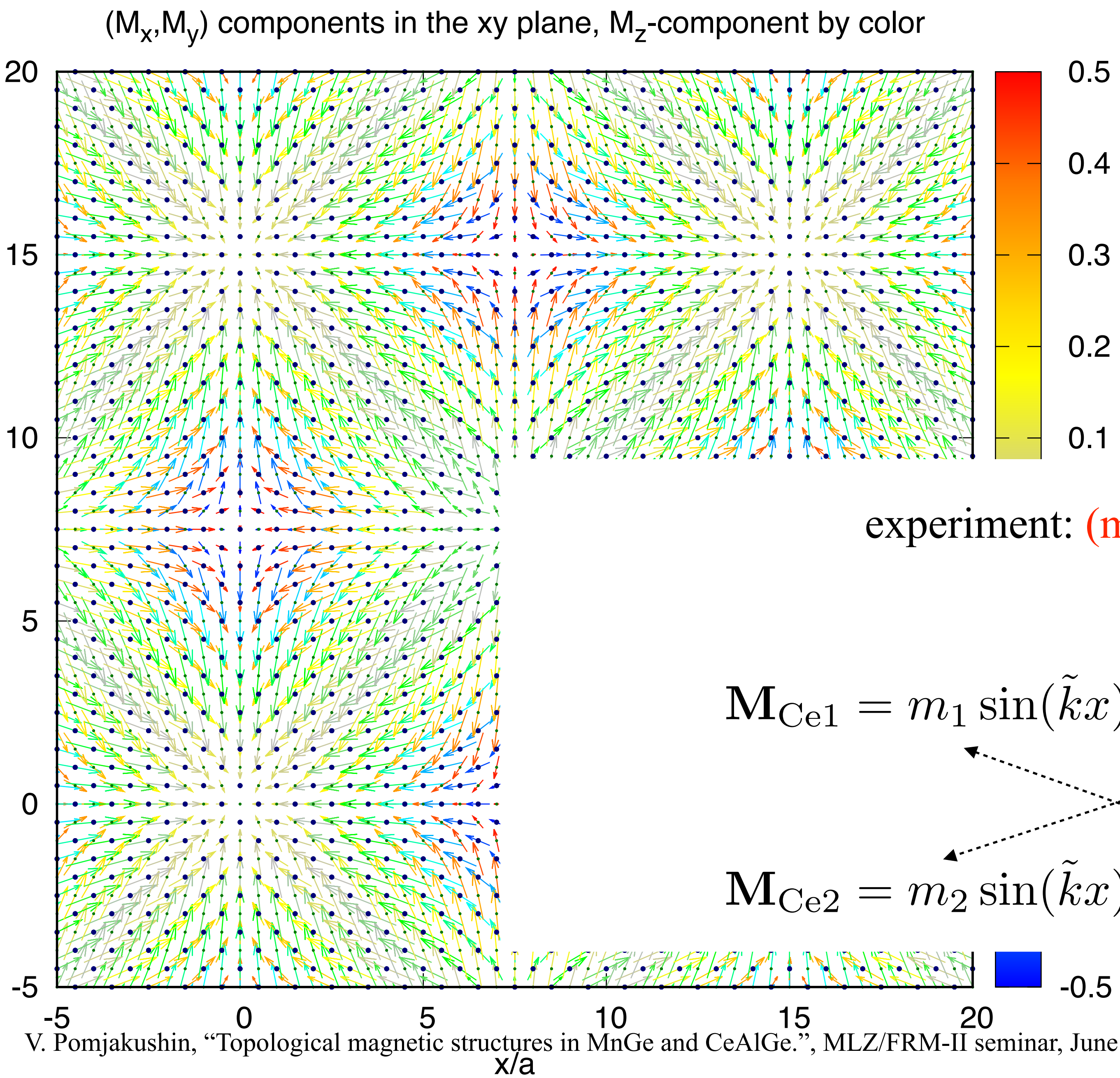

All Ce are equivalent and their moments are given symmetrically by 4 parameters

experiment: (m1,m2,m3,m4) = (0.44(1), 1.02(1), −0.21(5), 0.29(7)) μ_B.

$$\tilde{k}=2\pi|\boldsymbol{k}_1|=2\pi|\boldsymbol{k}_2|=2\pi g$$

$$\mathbf{M}_{\mathrm{Ce1}} = m_1 \sin(\tilde{k}x)\mathbf{e}_{\boldsymbol{x}} + m_2 \sin(\tilde{k}y)\mathbf{e}_{\boldsymbol{y}} + \left(m_3 \cos(\tilde{k}x) + m_4 \cos(\tilde{k}y)\right)\mathbf{e}_{\boldsymbol{z}}$$

$$\mathbf{M}_{\mathrm{Ce2}} = m_2 \sin(\tilde{k}x)\mathbf{e}_{\boldsymbol{x}} + m_1 \sin(\tilde{k}y)\mathbf{e}_{\boldsymbol{y}} + \left(m_4 \cos(\tilde{k}x) + m_3 \cos(\tilde{k}y)\right)\mathbf{e}_{\boldsymbol{z}}$$

CeAlGe: Maximal symmetry full star superspace 3D+2 magnetic group I4_1md1'(a00)000s(0a0)0s0s

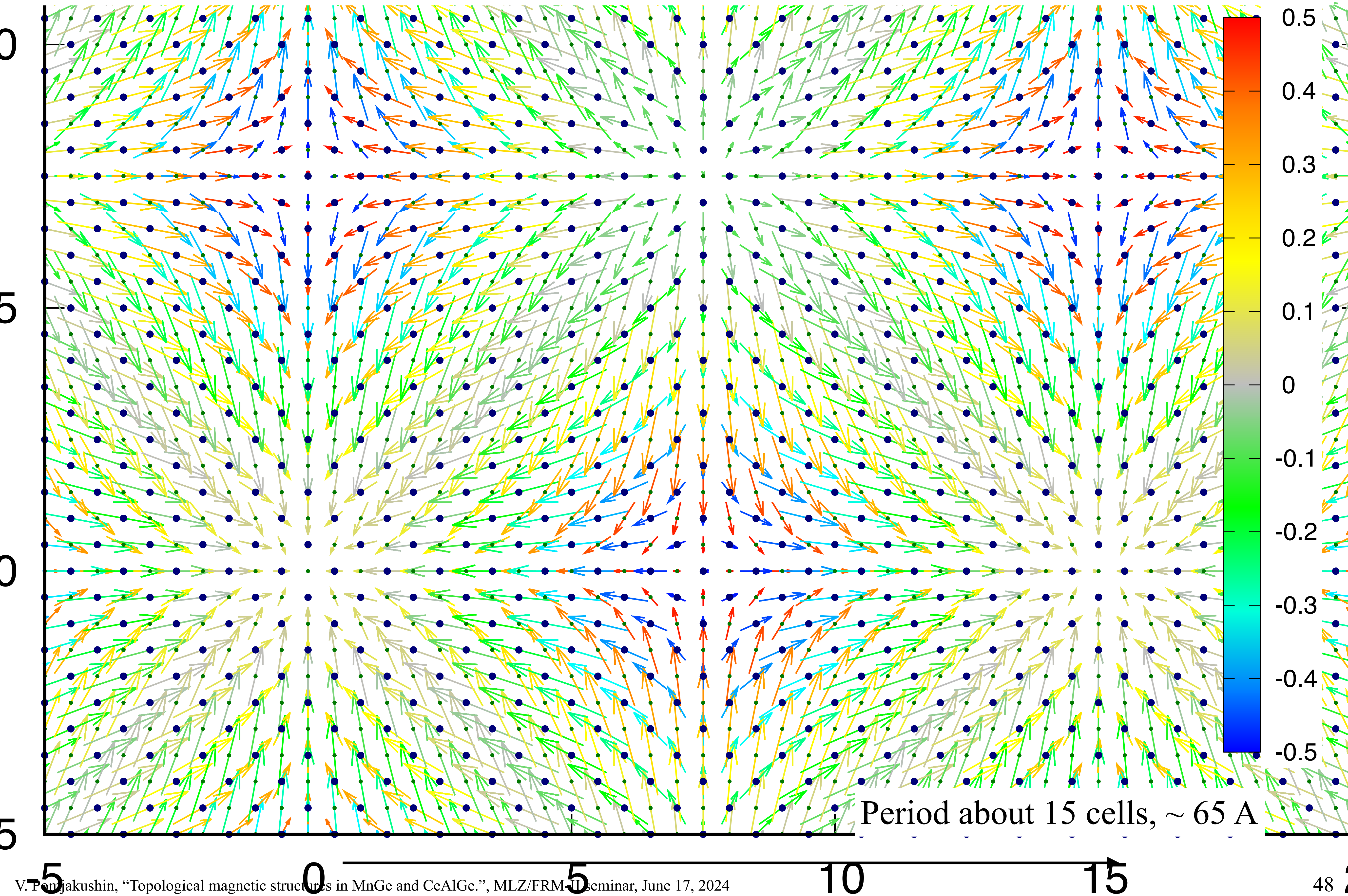

Period about 15 cells, ~ 65 A

non-continuos case: magnetic merons in CeAlGe

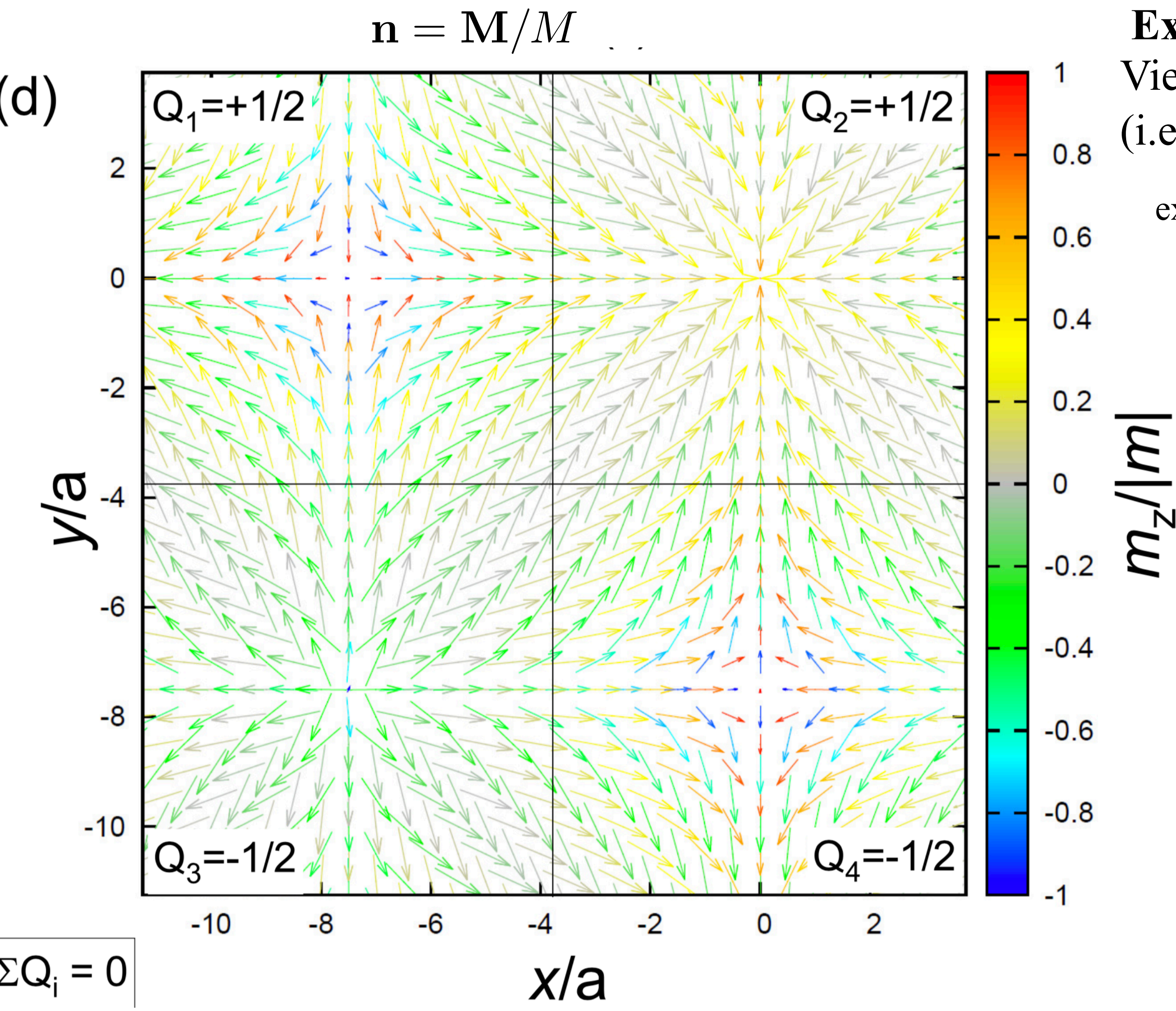

Experimentally observed multi-k magnetic structure.

View along the z-(c-)axis of the normalized (i.e. $\vec{n} = \vec{M}/|\vec{M}|$, where $\vec{M}$ is the local Ce moment)

experiment: (m1,m2,m3,m4) = (0.44(1), 1.02(1), −0.21(5), 0.29(7)) μ_B.

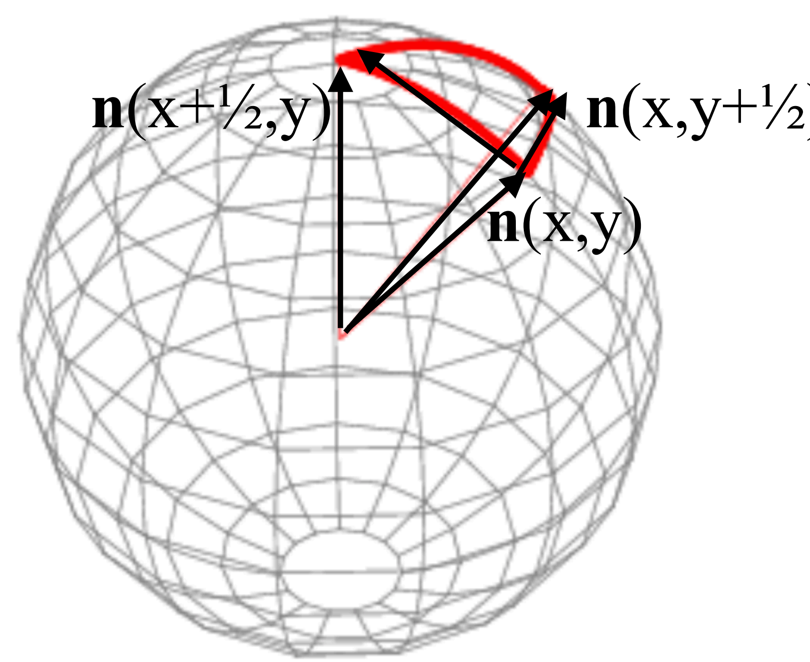

topological density/winding ~ solid angle

$$\omega(x,y) = \frac{1}{4\pi}(\mathbf{n}\cdot[\frac{\partial \mathbf{n}}{\partial x} \times \frac{\partial \mathbf{n}}{\partial y}]) \quad \mathbf{n} = \mathbf{M}/M$$

Topological number/charge over S

$$Q = \iint_{S\subset\mathbb{R}^2} \omega(x,y)dxdy$$

non-continuos case: magnetic merons in CeAlGe

$\mathbf{n} = \mathbf{M}/M$

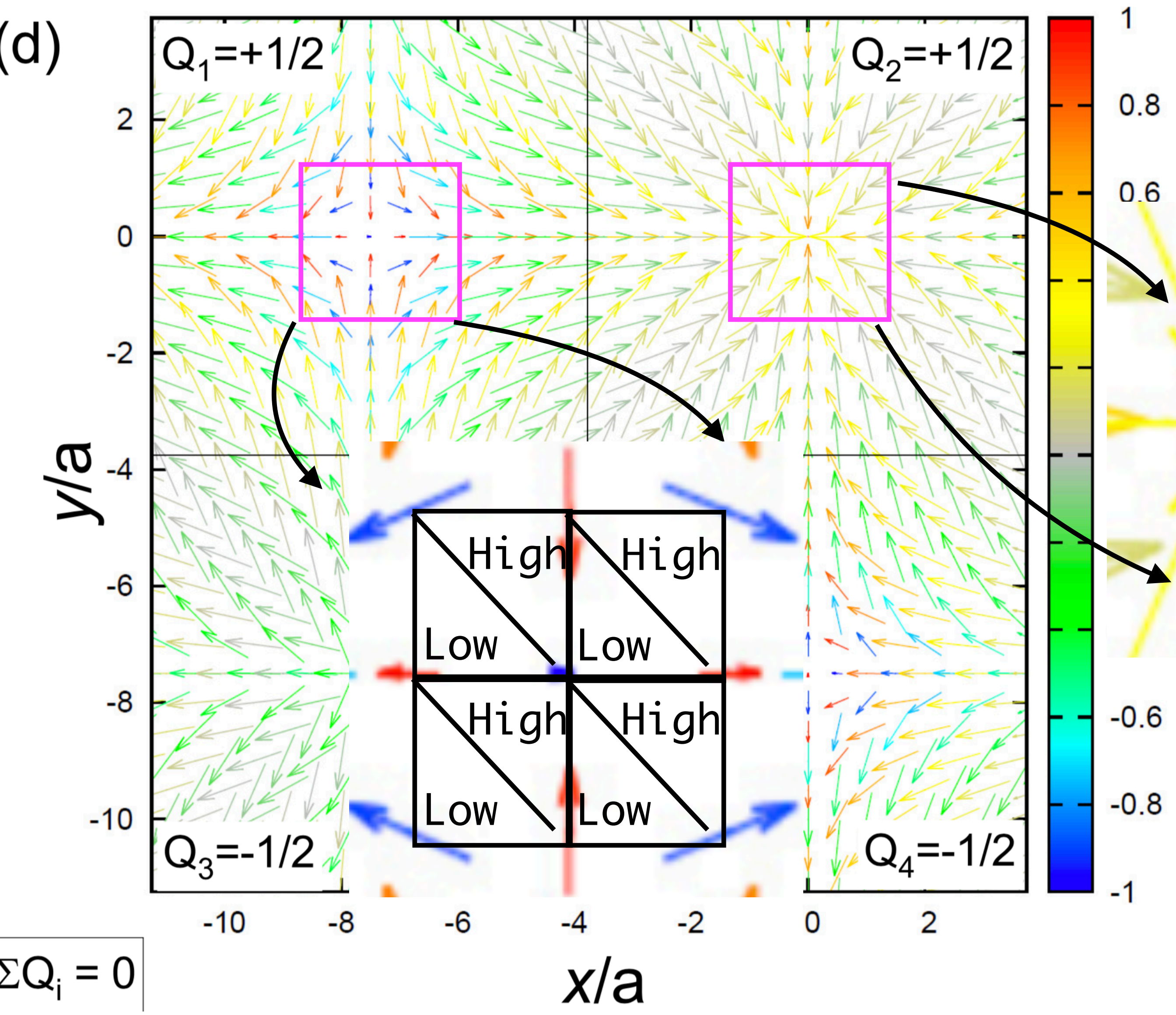

Experimentally observed multi-k magnetic structure.
View along the z-(c-)axis of the normalized (i.e. $\vec{n} = \vec{M}/|\vec{M}|$, where $\vec{M}$ is the local Ce moment)

experiment: (m1,m2,m3,m4) = (0.44(1), 1.02(1), −0.21(5), 0.29(7)) μ_B.

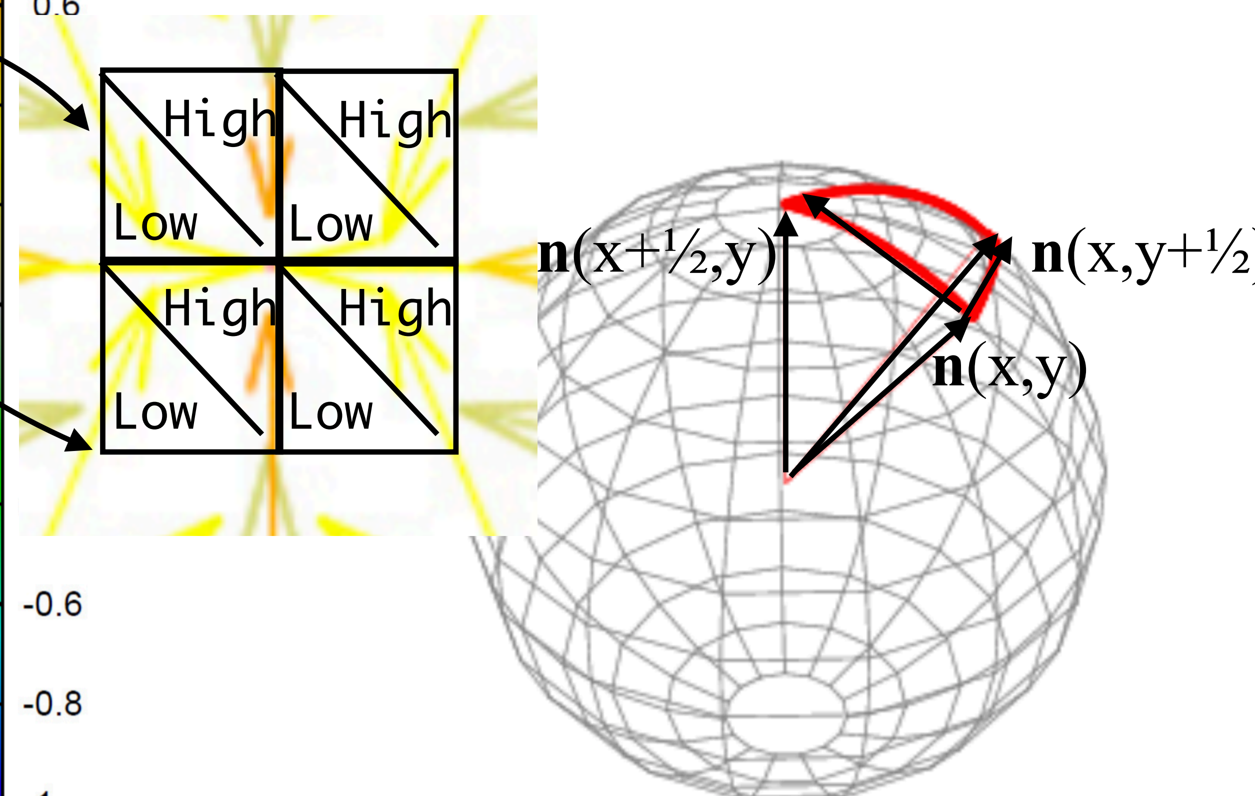

topological density/winding ~ solid angle

$$\omega(x,y) = \frac{1}{4\pi}\left(\mathbf{n}\cdot\left[\frac{\partial \mathbf{n}}{\partial x}\times\frac{\partial \mathbf{n}}{\partial y}\right]\right) \quad \mathbf{n} = \mathbf{M}/M$$

Topological number/charge over S

$$Q = \iint_{S\subset\mathbb{R}^2} \omega(x,y)\,dx\,dy$$

non-continuos case: magnetic merons in CeAlGe

$\mathbf{n} = \mathbf{M}/M$

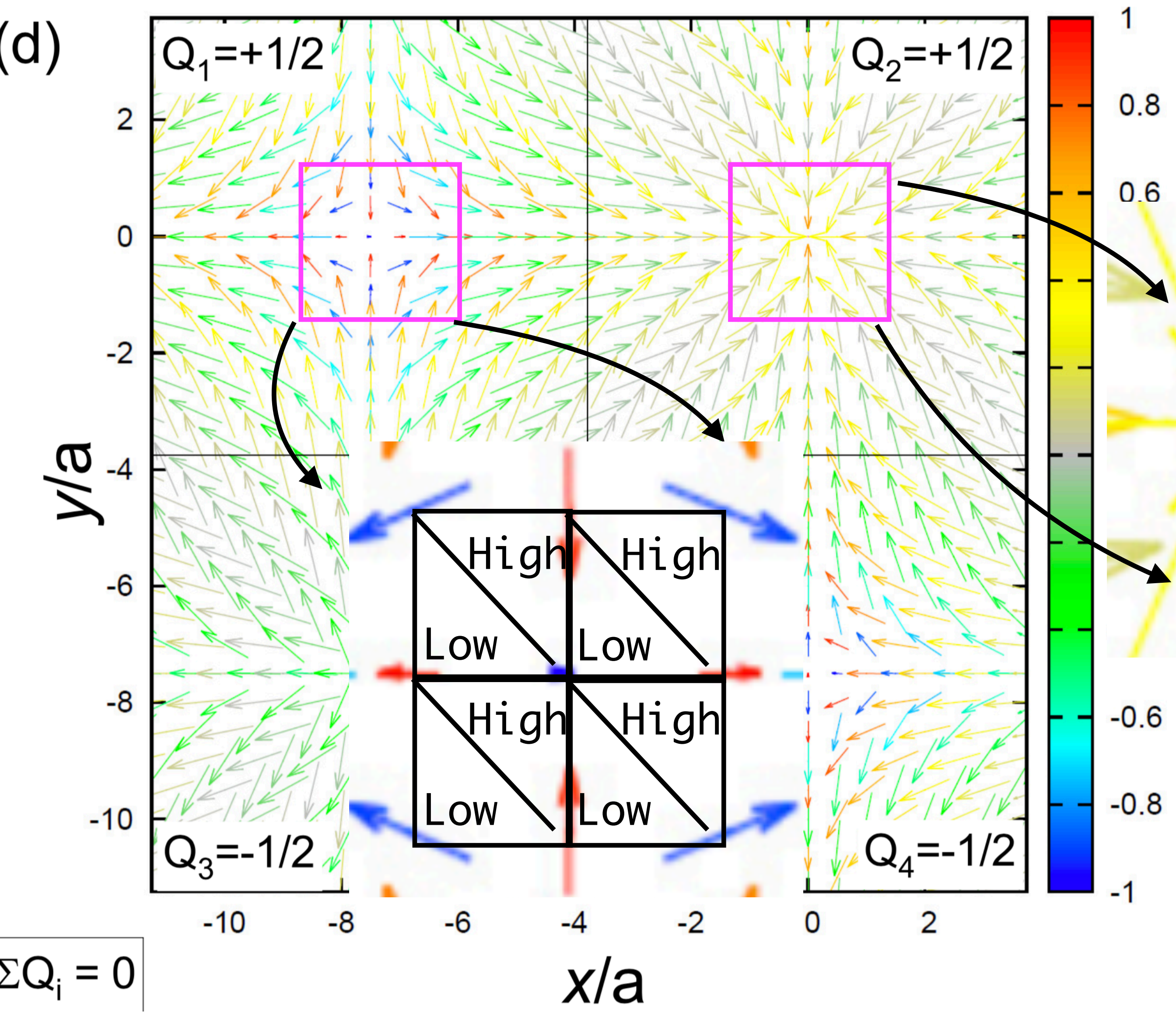

$\Sigma Q_i = 0$

Experimentally observed multi-k magnetic structure.
View along the z-(c-)axis of the normalized (i.e. $\vec{n} = \vec{M}/|\vec{M}|$, where $\vec{M}$ is the local Ce moment)

experiment: (m1,m2,m3,m4) = (0.44(1), 1.02(1), −0.21(5), 0.29(7)) μ_B.

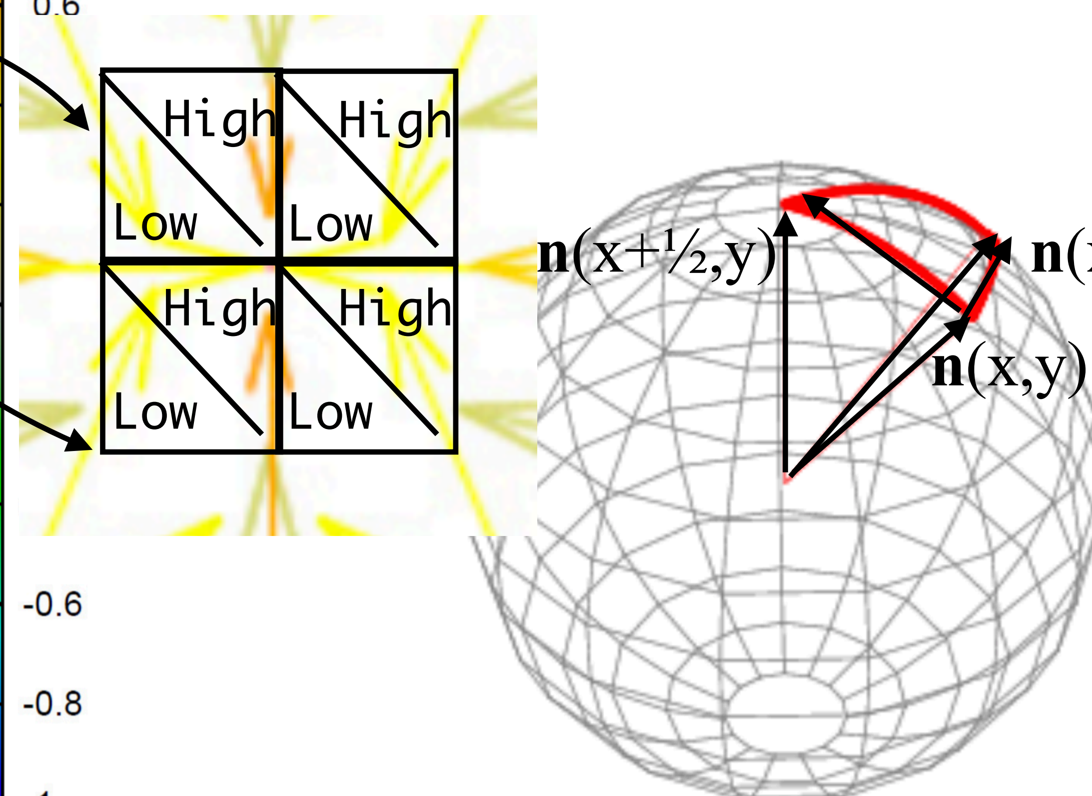

topological density/winding ~ solid angle

$$\omega(x,y) = \frac{1}{4\pi}(\mathbf{n}\cdot[\frac{\partial \mathbf{n}}{\partial x}\times\frac{\partial \mathbf{n}}{\partial y}]) \quad \mathbf{n} = \mathbf{M}/M$$

→ $$\Delta w(x,y) = \frac{1}{4\pi}\left(\Delta\Omega_{\text{low}} + \Delta\Omega_{\text{high}}\right)^{\star}$$

solid angle per square placket

Topological number/charge over S

$$Q = \iint_{S\subset\mathbb{R}^2} \omega(x,y)\,dxdy$$

→ $$Q = \sum_{x,y} \Delta w(x,y)$$

$$^{\star}\ \tan\left(\frac{1}{2}\Omega\right) = \frac{\mathbf{a}\cdot(\mathbf{b}\times\mathbf{c})}{abc + (\mathbf{a}\cdot\mathbf{b})\,c + (\mathbf{a}\cdot\mathbf{c})\,b + (\mathbf{b}\cdot\mathbf{c})\,a}$$

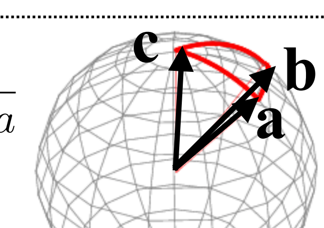

Topological density and charge. H=0

experiment: (m1,m2,m3,m4) = (0.44(1), 1.02(1), −0.21(5), 0.29(7)) μ_B.

$$\mathbf{n} = \mathbf{M}/M$$

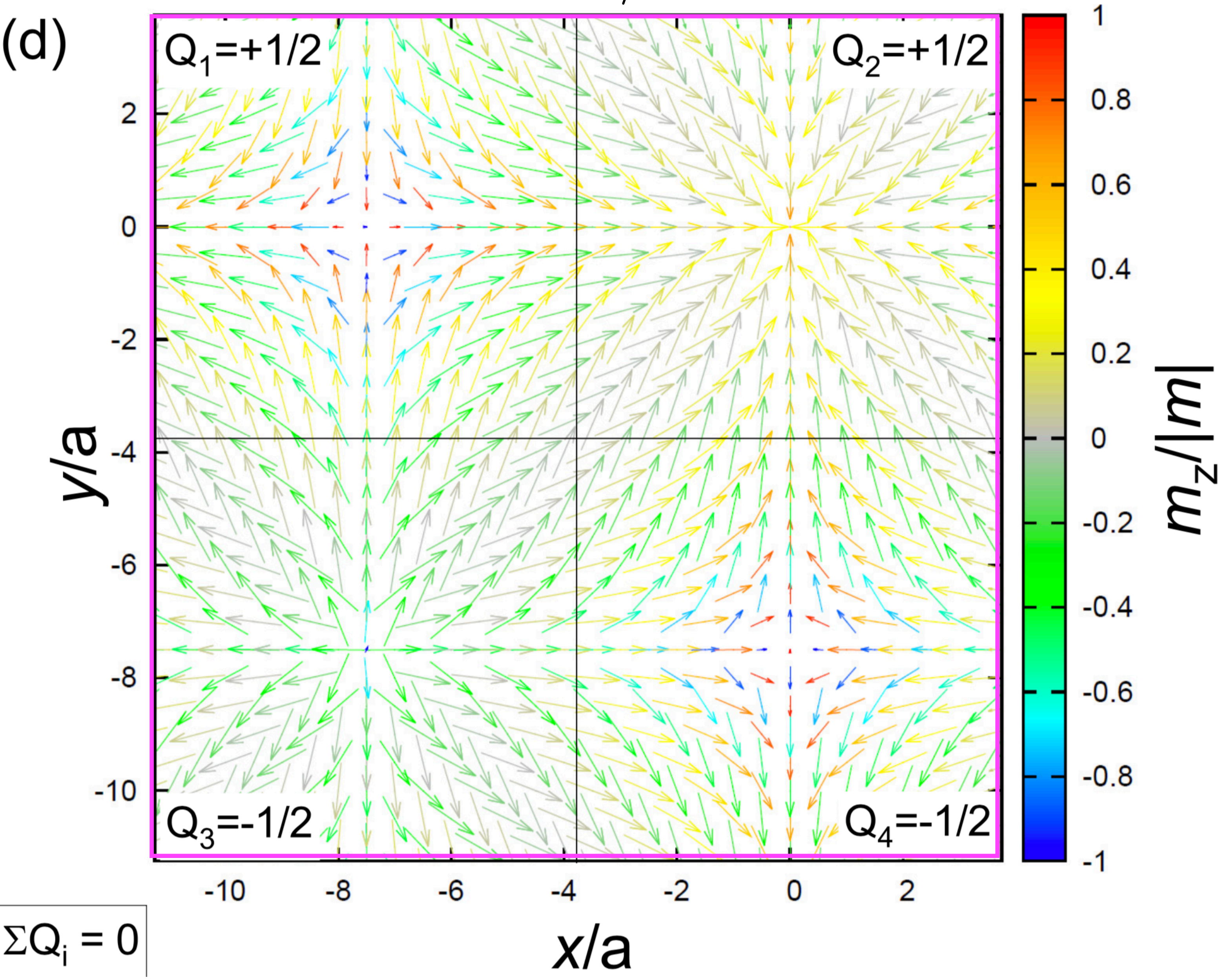

$$\Delta w(x,y) = \frac{1}{4\pi}\left(\mathbf{n}\cdot[\Delta\mathbf{n}_x \times \Delta\mathbf{n}_y]\right)$$

solid angle per square placket

$$Q = \sum_{x,y} \Delta w(x,y)$$

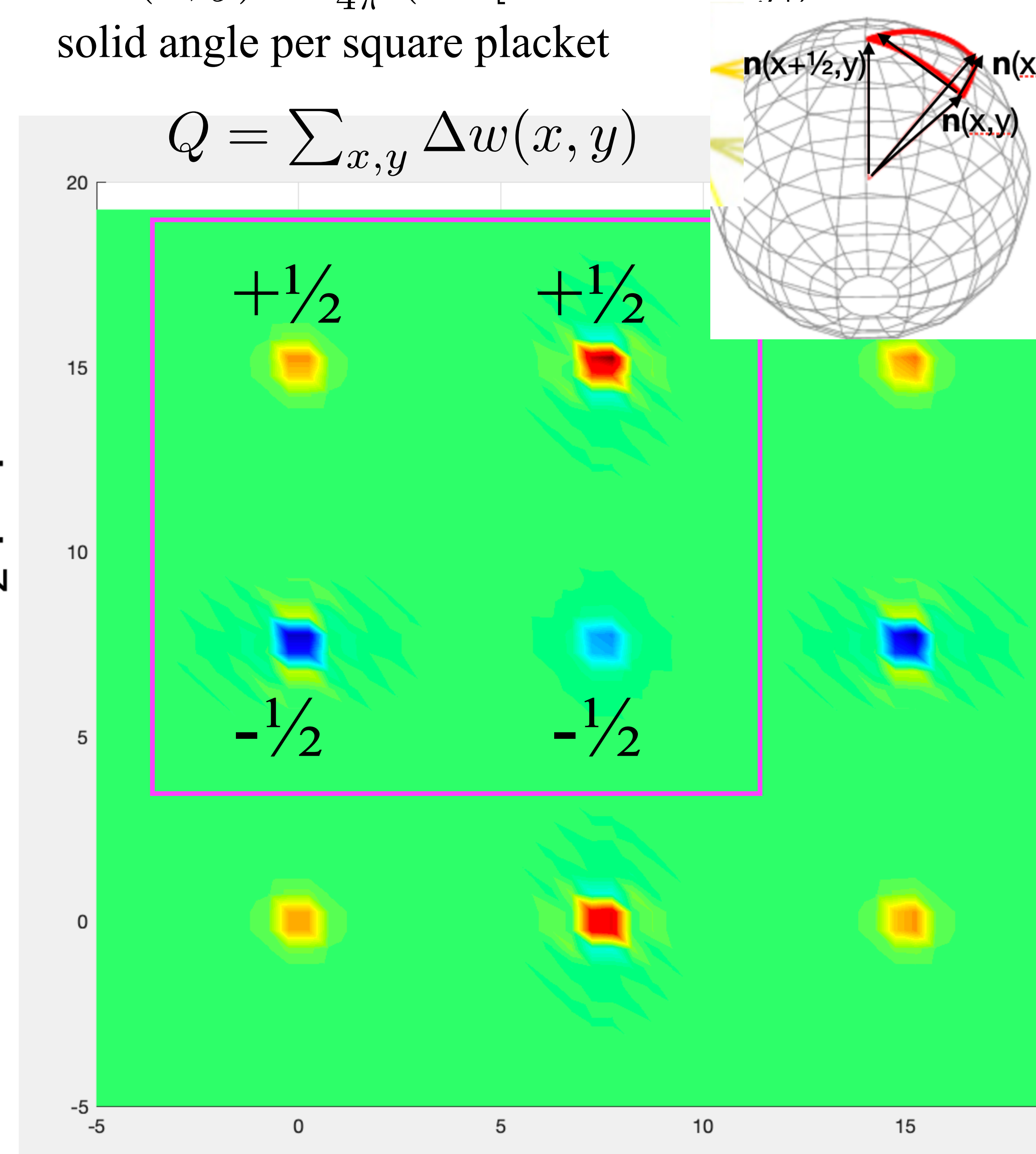

$$\mathbf{M}_{\mathrm{Ce2}} = m_2 \sin(\tilde{k}x)\mathbf{e}_{\boldsymbol{x}} + m_1 \sin(\tilde{k}y)\mathbf{e}_{\boldsymbol{y}} + \left(m_4 \cos(\tilde{k}x) + m_3 \cos(\tilde{k}y)\right)\mathbf{e}_{\boldsymbol{z}}$$

$$\mathbf{M}_{\mathrm{Ce1}} = m_1 \sin(\tilde{k}x)\mathbf{e}_{\boldsymbol{x}} + m_2 \sin(\tilde{k}y)\mathbf{e}_{\boldsymbol{y}} + \left(m_3 \cos(\tilde{k}x) + m_4 \cos(\tilde{k}y)\right)\mathbf{e}_{\boldsymbol{z}}$$

$\tilde{k}=2\pi|\boldsymbol{k}_1|=2\pi|\boldsymbol{k}_2|=2\pi g$

Simulation of external field ~ FM component along z-axis

experiment: (m1,m2,m3,m4) = (0.44(1), 1.02(1), −0.21(5), 0.29(7)) μB.

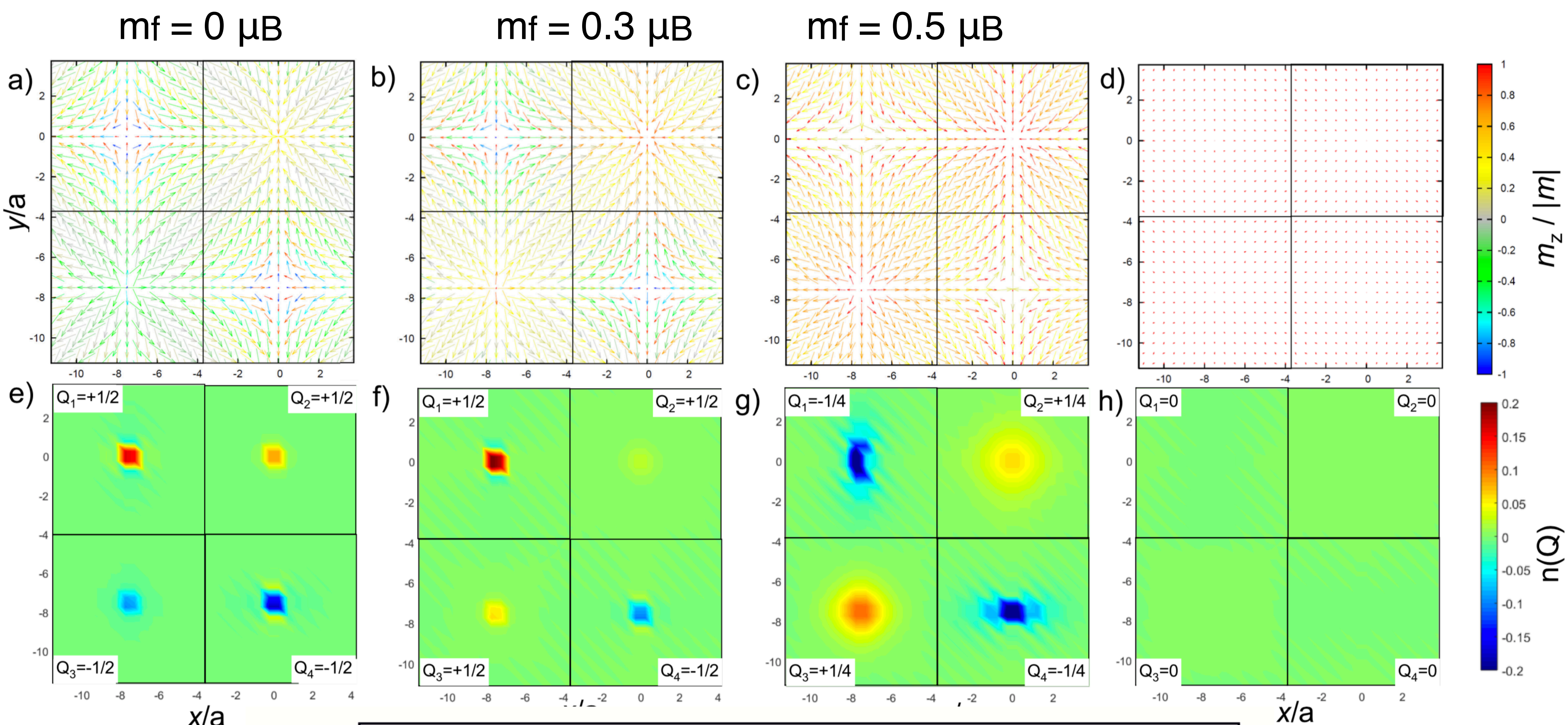

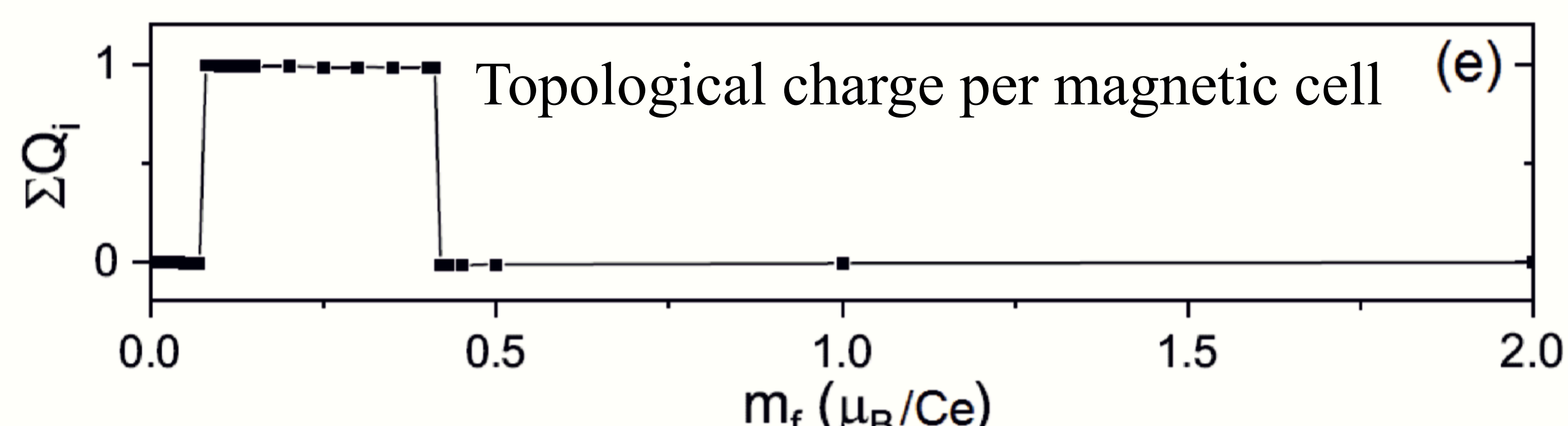

Figure 10. Compari… g canting fields along th…
z-direction out of th… μ_B. a-d) The first row …
images shows the vi… $m_f = 0.2\,\mu_B$ (b) are th…
same ones shown in … plane lattice parameter …

Experimental proof comes from behaviour in external field

Topological Hall Effect THE

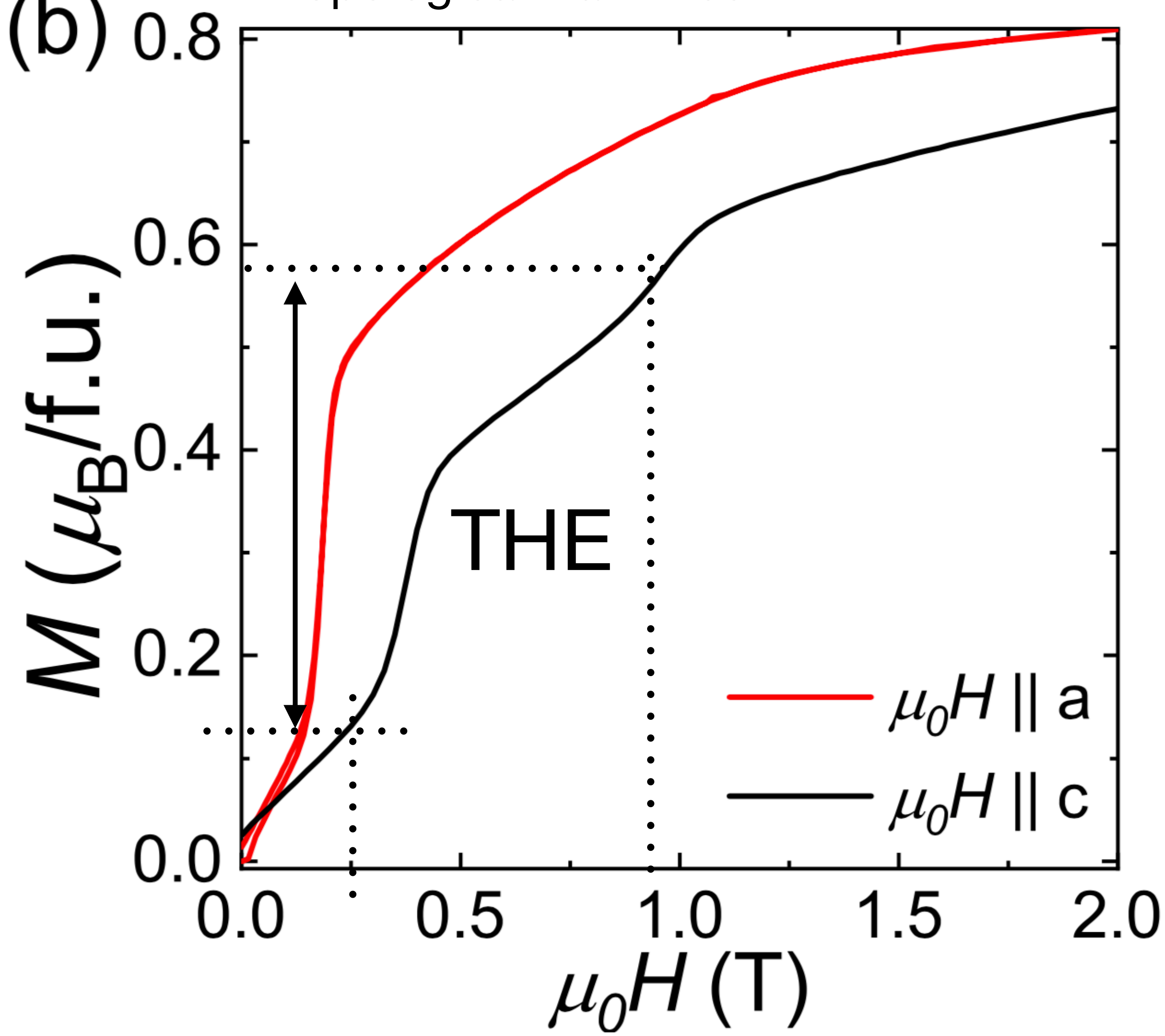

SANS diffraction: k1+k2+0 is 3rd order harmonics in external field

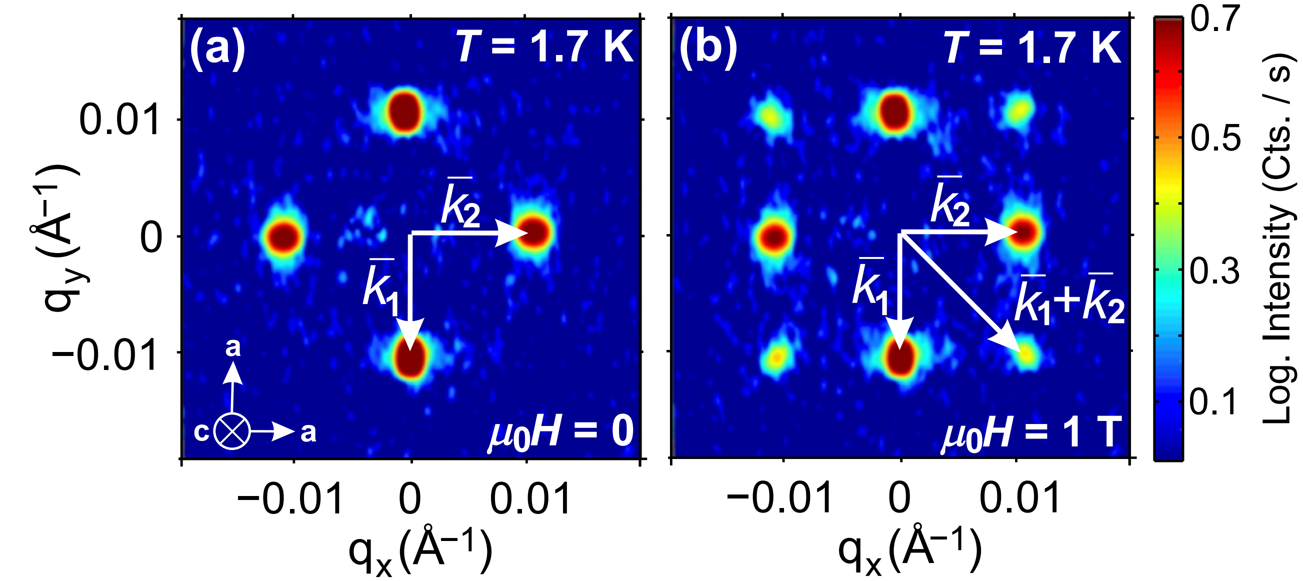

Topological charge per magnetic cell

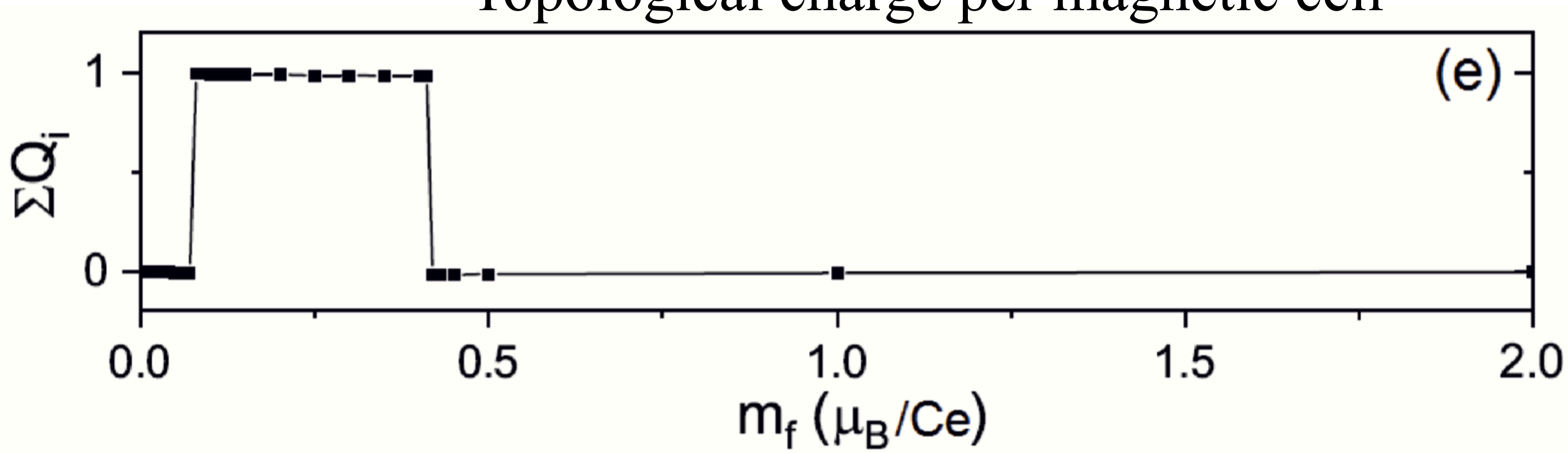

Topological magnetic structures in MnGe: Neutron diffraction and symmetry analysis

The motivation: apply a state-of-the-art analysis of all possible magnetic superspace structures allowed by the crystal symmetry in metallic MnGe (P213) that are consistent with neutron diffraction data. *MnGe has been long-studied for its remarkable phenomena related to its topological magnetic order, but surprisingly, the detailed magnetic structure underlying such phenomena was not addressed before this study.*

Several maximal crystallographic symmetry magnetic structures are found to fit the data equally well. Among them: Topological multi-**k** 3**k**-hedgehog and 2**k**-meron structures that can account for the topological Hall effect should be preferable over the single-**k** helical- or AM-structures.

New route to synthesize MnGe at ambient pressures and moderate temperatures, in addition to the traditional high pressure synthesis.

$P2_13.1'(a,0,0)00s(0,a,0)00s(0,0,a)00s$

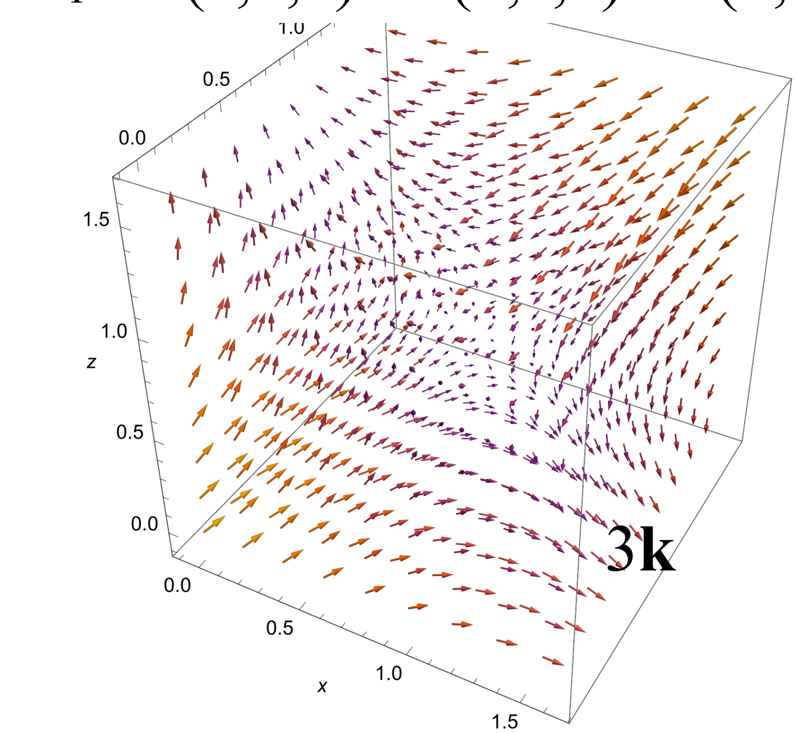

$P2_12_12_1.1'(0,b1,0)000s(0,0,g2)000s$

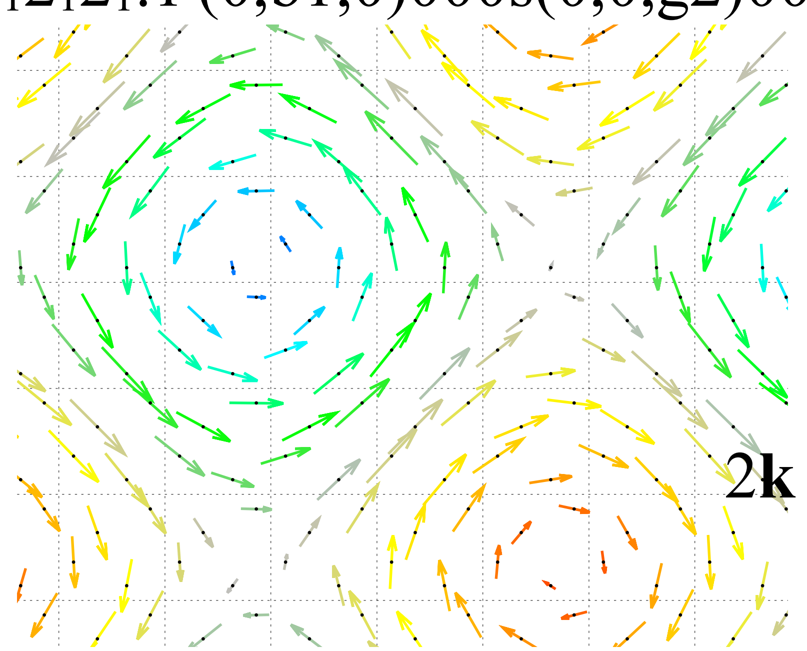

$P2_12_12_1.1'(0,0,g)000s$

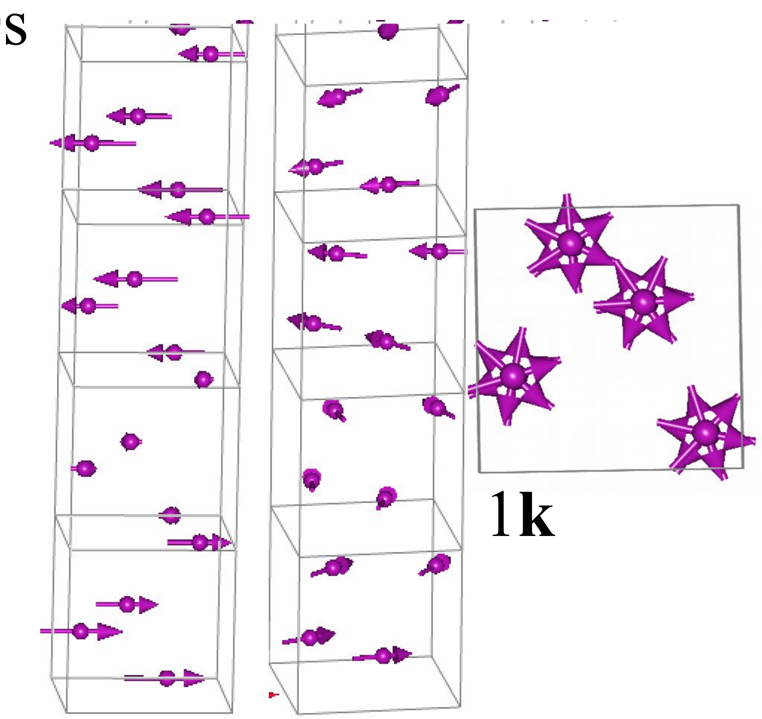

Summary on CeAlGe

- We report the discovery of topological magnetic order in the polar tetragonal magnetic Weyl semimetal candidate CeAlGe.
- CeAlGe has an incommensurate magnetic structure modulation length 70 Å [3D+2 group *I4_1md.1’(a,0,0)000s(0,a,0)0s0s*] hosting a lattice of magnetic particle-like objects called (anti)merons with half-integer topological numbers Q=±1/2. 1k-structure cycloid structure in *I2mm.1’(0,0,g)0s0s* fit the data as well
- At intermediate magnetic fields H parallel to the c-axis one of merons flips sign leading to total Q=±1 in accordance with the observation of a topological Hall effect (THE) in the same range of H.

Thank you!

Crystal structure below T_N=170K P2_12_12_1

(222) is not split in both groups

(320) is <u>split</u> in $P2_12_12_1$

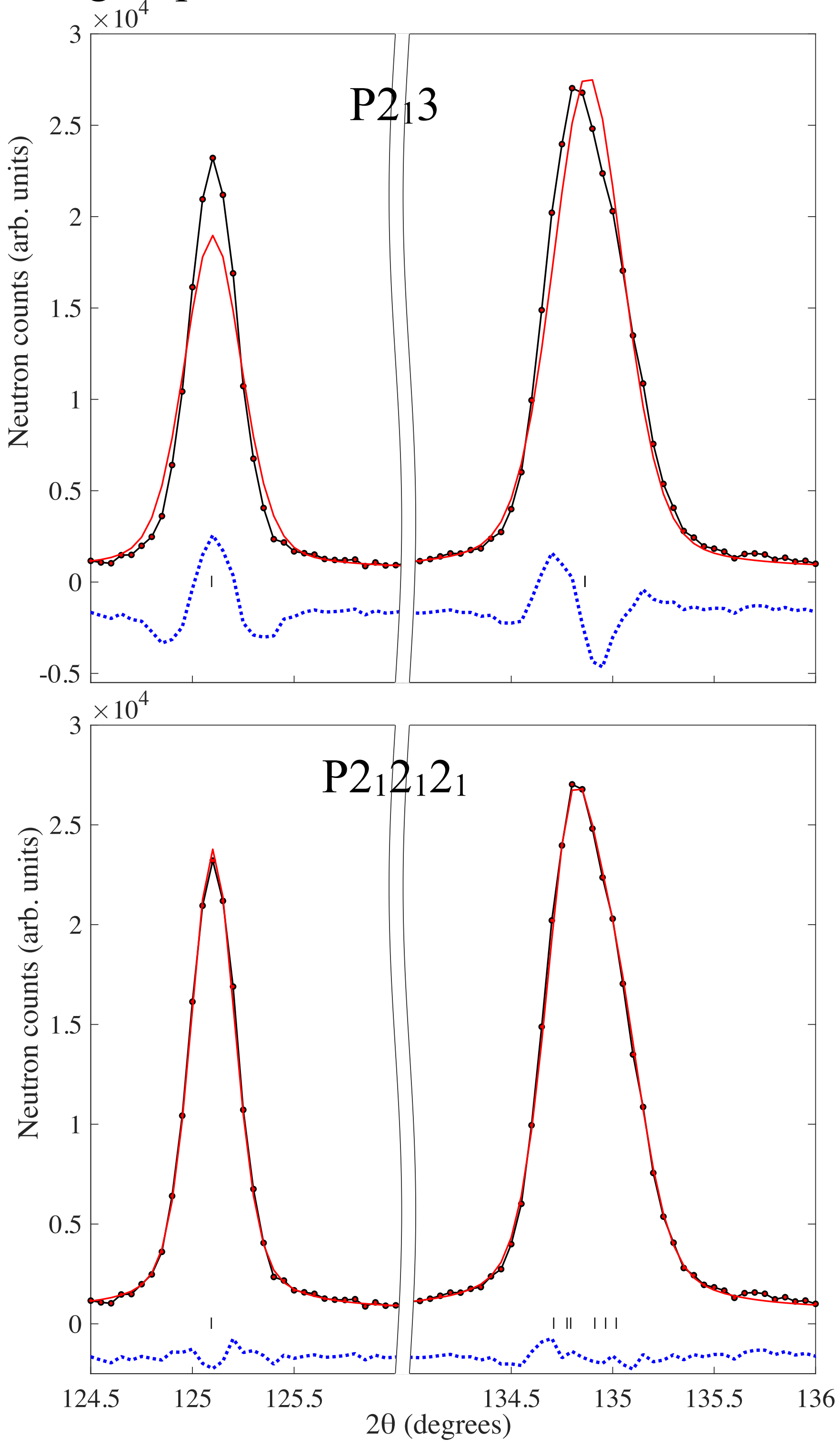

HR mode at HRPT with the wavelength λ = 2.45 Å at T = 1.8 K

Crystal structure below T_N=170K P2_12_12_1

(222) is not split in both groups

(320) is split in $P2_12_12_1$

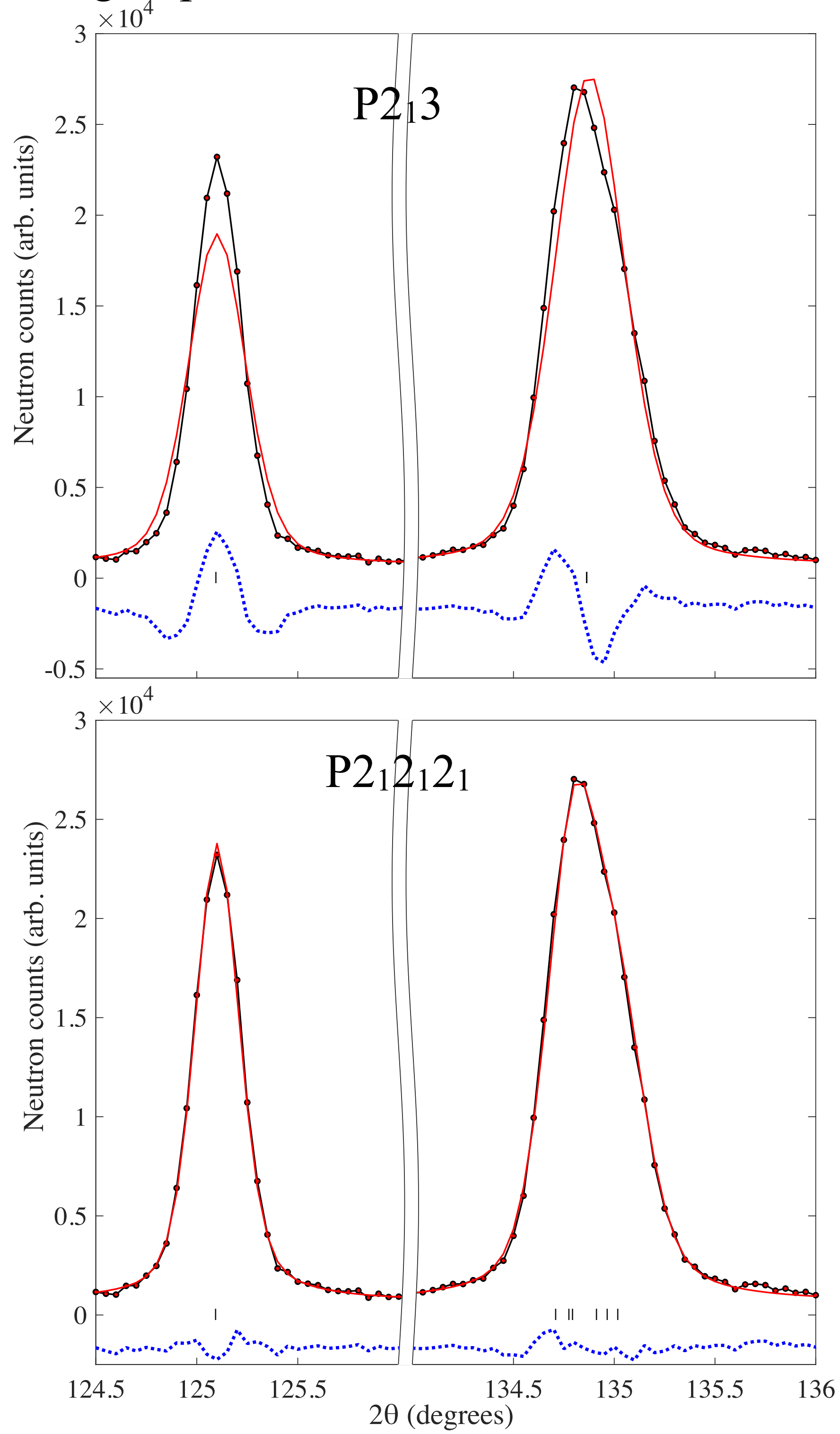

HR mode at HRPT with the wavelength λ = 2.45 Å at T = 1.8 K

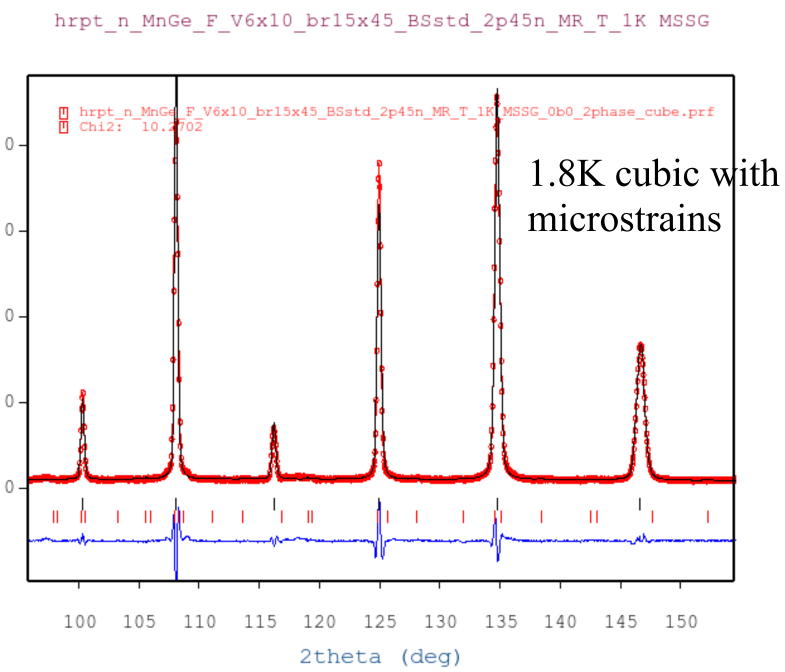

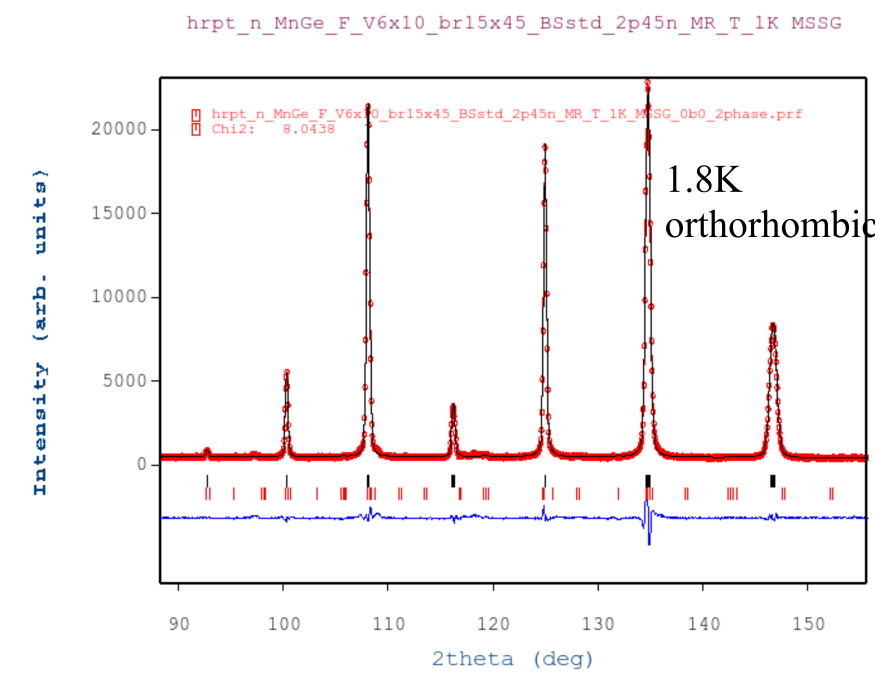

The fit of the combined MR and HR data sets using both wavelengths 1.49 Å and 2.45 Å is well converged to $P2_12_12_1$ model.

Orth-metrics: 0.1% and 0.16% along the b and c axes with respect to the a axis

Bloch vs. Neel

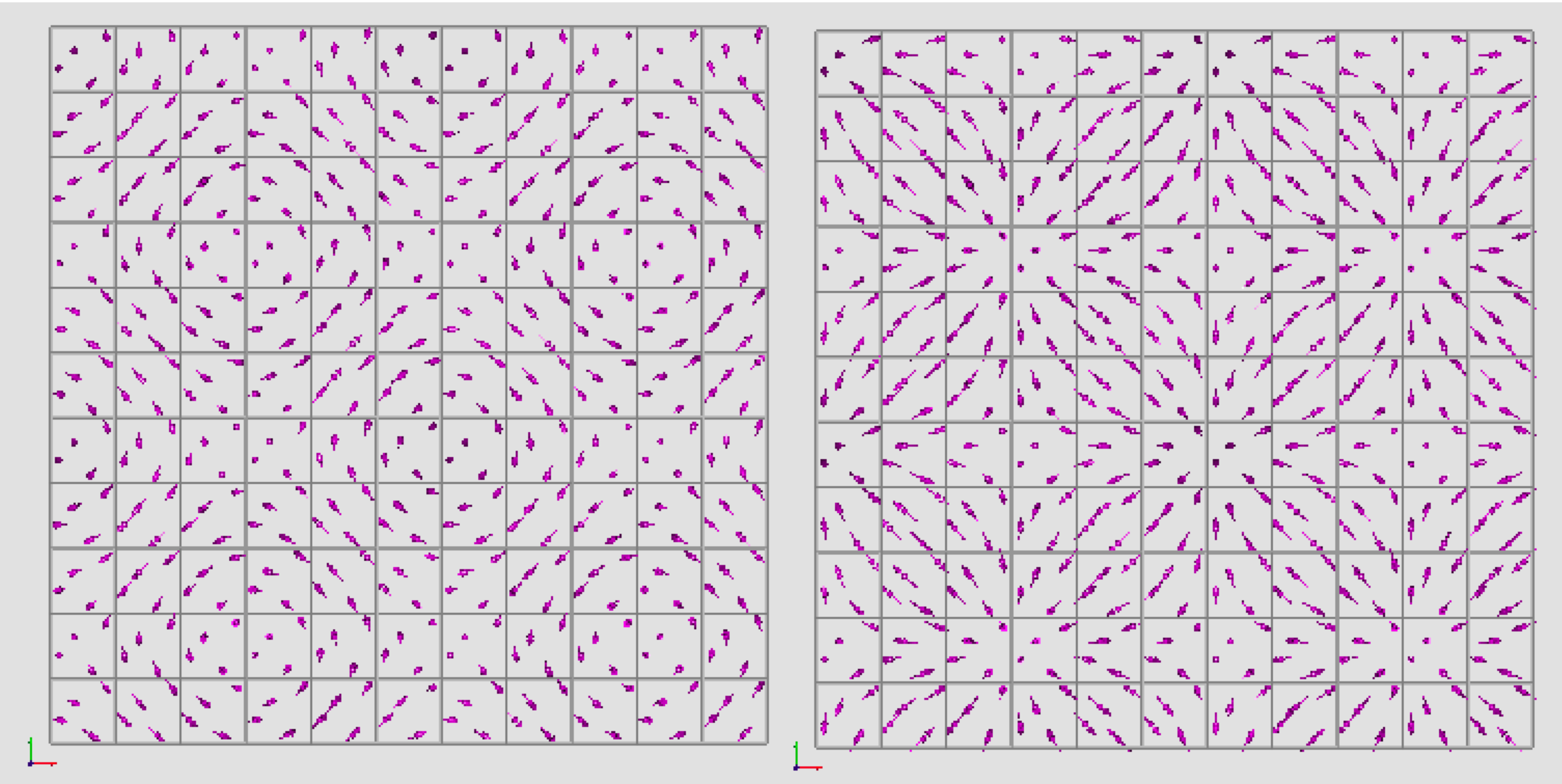

Note on continuous limit of modulated structures

“true” topological charge $Q = (1/4\pi) \int \vec{n}(\partial\vec{n}/\partial x \times \partial\vec{n}/\partial y)dxdy$

there is a principal difficulty in the realisation of the continuous limit related to the crystallographic symmetries like rotations by the large crystallographic angles, such as 180, 120, 90, or 60 deg.

Note on continuous limit of modulated structures

k=0.3 one atom in unit cell

$$y = 1, 2, 3...$$

$$M(y) = m\cos(2\pi k y)$$

$$\tilde{y} = 2\pi k y$$

Note on continuous limit of modulated structures

k=0.3

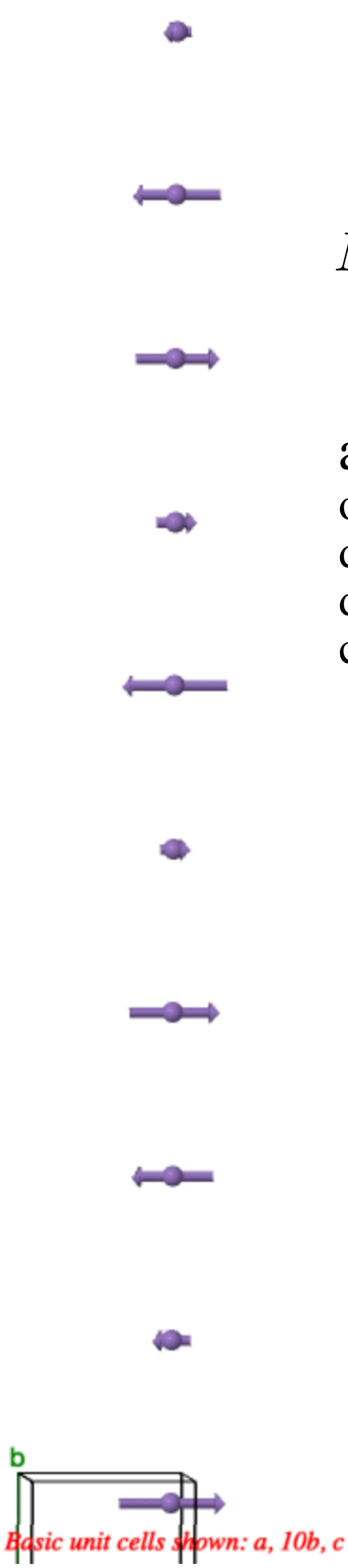

one atom in unit cell

$$y = 1, 2, 3...$$

$$M(y) = m\cos(2\pi ky)$$

$$\tilde{y} = 2\pi ky$$

and in the limit of k $\rightarrow$ 0
one can approximate the distribution of the magnetization density to be spatially continuous.

derivatives $\dfrac{\partial \mathbf{n}}{\partial \tilde{y}}$ are no problem!

k=0.03

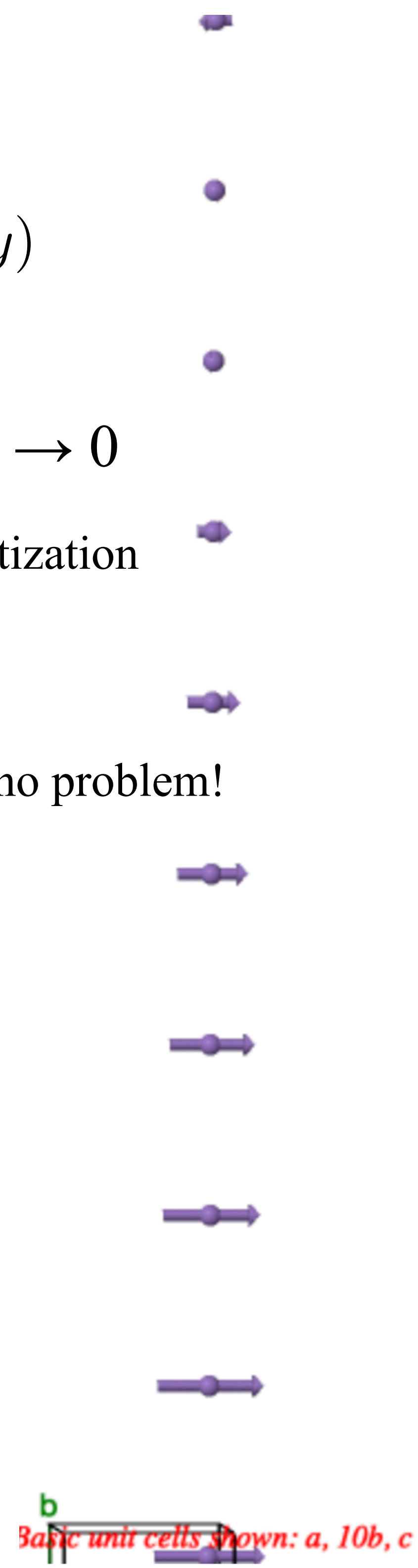

Note on continuous limit of modulated structures

k=0.3 one atom in unit cell k=0.03

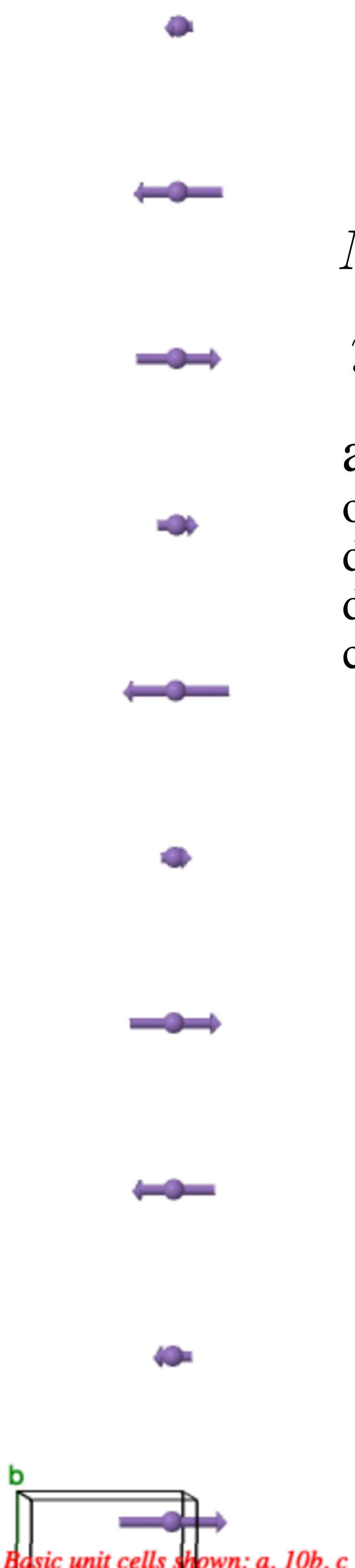

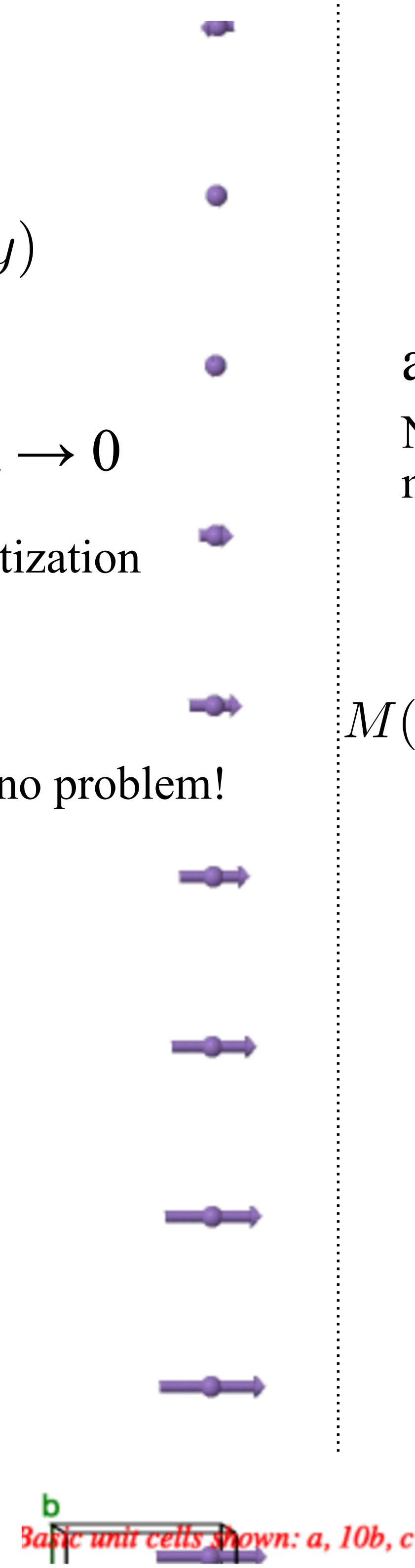

$$y = 1, 2, 3 \ldots$$

$$M(y) = m\cos(2\pi k y)$$

$$\tilde{y} = 2\pi k y$$

and in the limit of k → 0
one can approximate the distribution of the magnetization density to be spatially continuous.

derivatives $\frac{\partial \mathbf{n}}{\partial \tilde{y}}$ are no problem!

MnGe with artificially small k

k=0.03 four atoms in unit cell, related by 2_x 2_y 2_z

$\alpha_1 = \pi/2$

and in the limit of k → 0
NO spatially continuous magnetization density

$$M(y) = \begin{cases} m_1 \cos(\tilde{y} + \alpha_1) = -\sin\tilde{y} \\ m_1 \cos(\tilde{y} - \alpha_1) = +\sin\tilde{y} \\ m_1 \cos(\tilde{y} + \alpha_1) \\ m_1 \cos(\tilde{y} - \alpha_1) \end{cases}$$

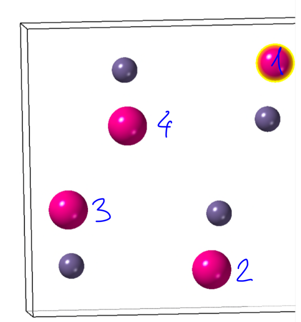

$$\tilde{y} = 2\pi k y$$

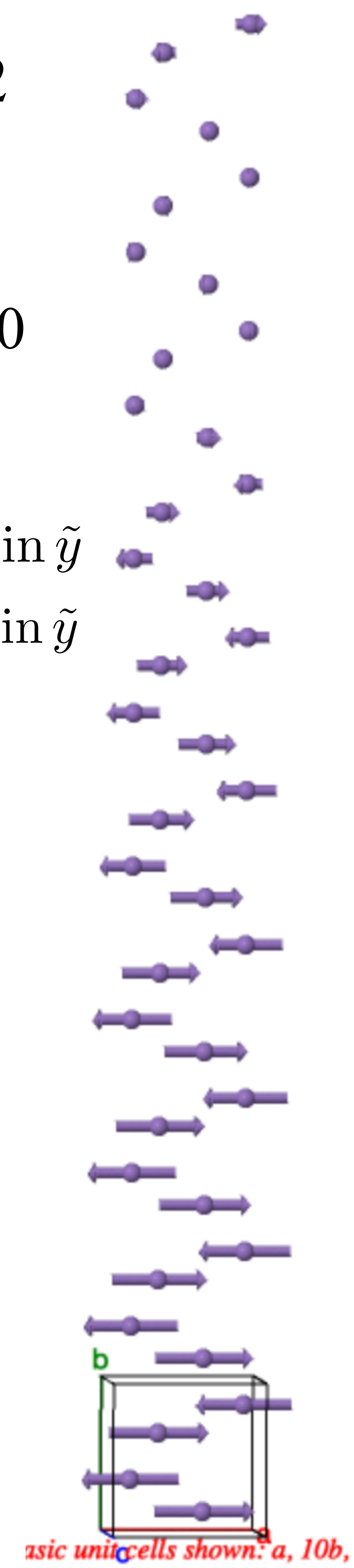

Note on continuous limit of modulated structures

k=0.3 one atom in unit cell k=0.03

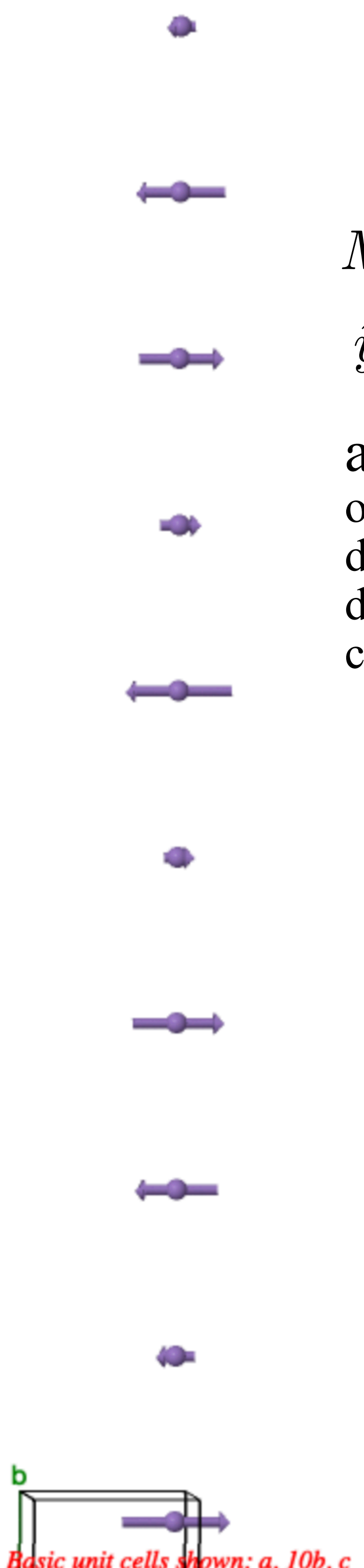

$$y = 1, 2, 3...$$

$$M(y) = m\cos(2\pi k y)$$

$$\tilde{y} = 2\pi k y$$

and in the limit of k → 0
one can approximate the distribution of the magnetization density to be spatially continuous.

derivatives $\frac{\partial \mathbf{n}}{\partial \tilde{y}}$ are no problem!

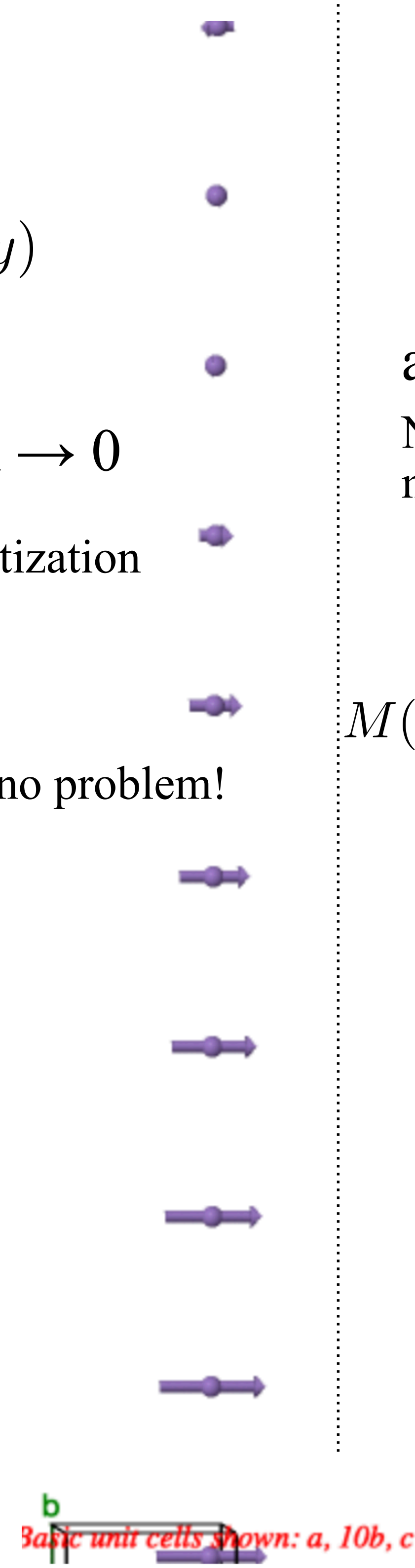

MnGe with artificially small k

k=0.03 four atoms in unit cell, related by 2_x 2_y 2_z

$\alpha_1=\pi/2$ $\alpha_1=0$

and in the limit of k → 0
NO spatially continuous magnetization density

$$M(y) = \begin{array}{l} m_1\cos(\tilde{y}+\alpha_1) = -\sin\tilde{y} \\ m_1\cos(\tilde{y}-\alpha_1) = +\sin\tilde{y} \\ m_1\cos(\tilde{y}+\alpha_1) \\ m_1\cos(\tilde{y}-\alpha_1) \end{array}$$

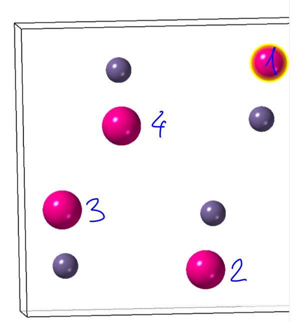

$$\tilde{y} = 2\pi k y$$

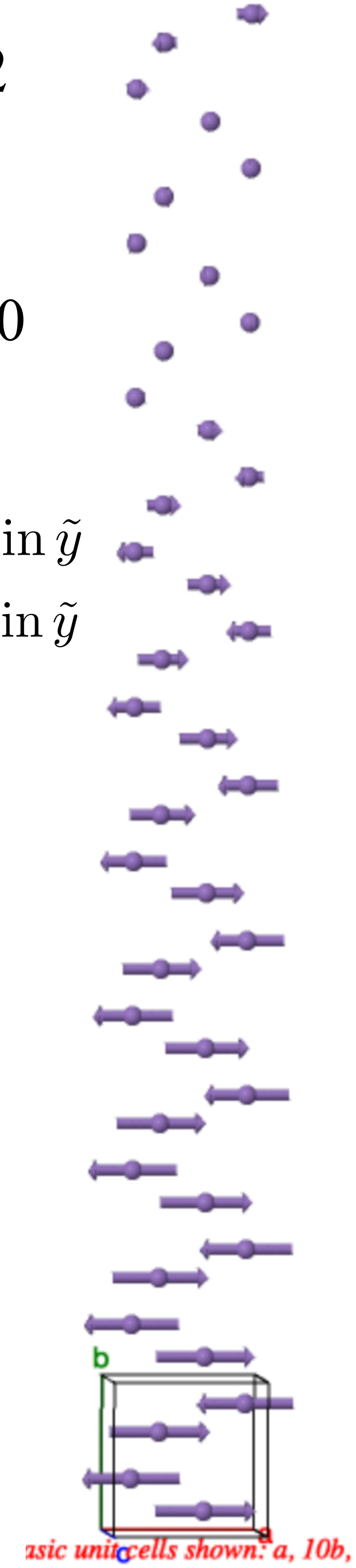

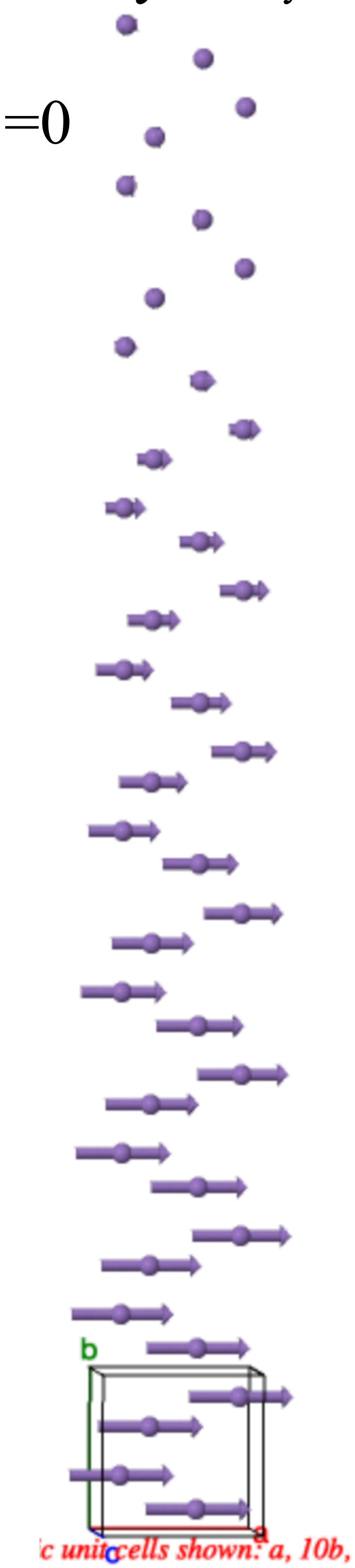

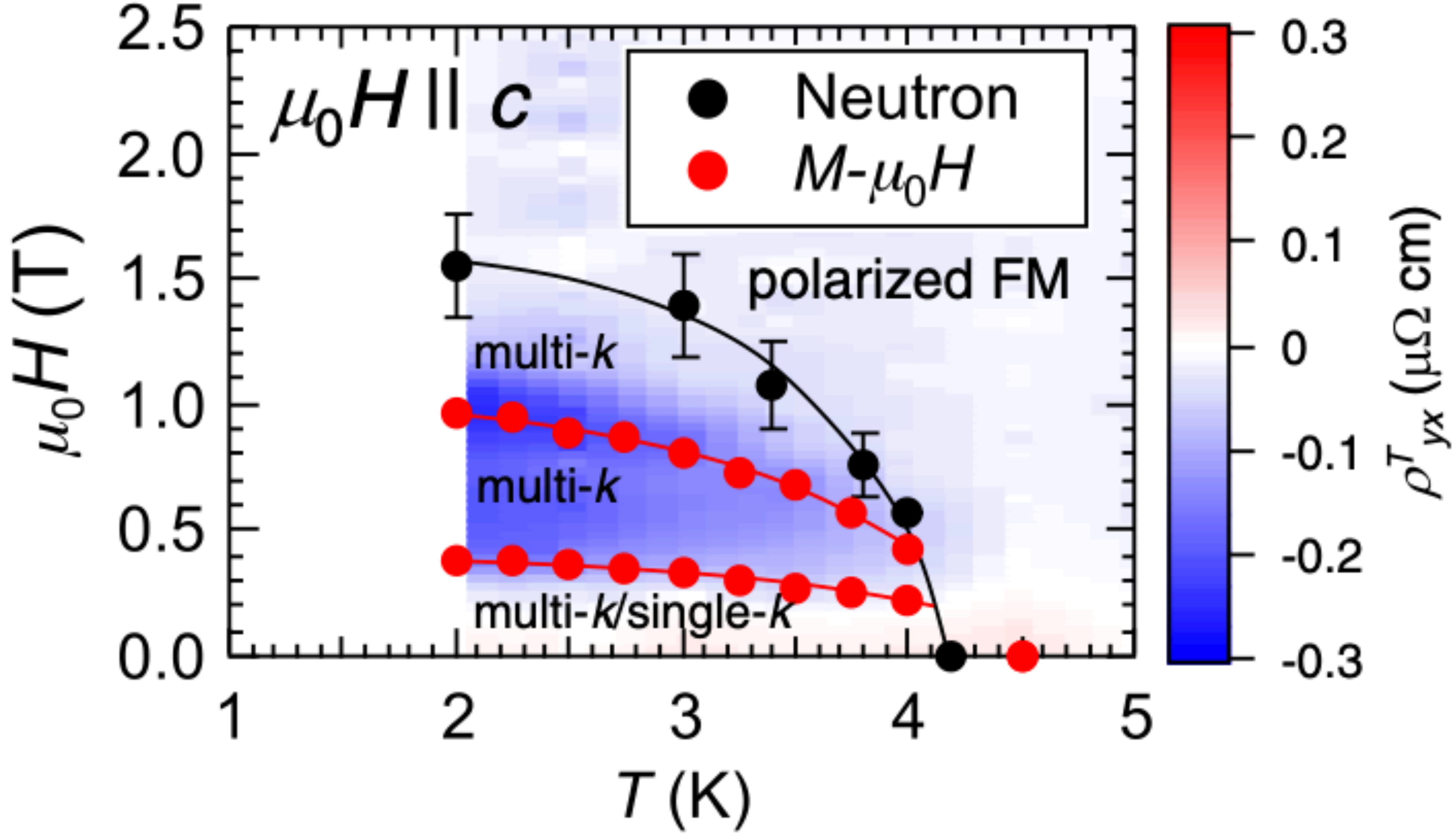

FIG. 4. CeAlGe magnetic phase diagram for $\mu_0 H \| c$. Black symbols are determined from SANS data [36], and red symbols from peaks in dM/dH denoted as H_1 and H_2 in Fig. 3(c). ρ^T_{yx} data are included as a color map. Solid lines are guides for the eye.

One k-case, standard representation analysis without magnetic group symmetry arguments: Space group $I4_1md$, Ce 4a (0,0,z)

Solution: SM2 irreducible representation

- **Cycloid in ac-plane for k1=[g,0,0]**, in bc=lane for k2=[0,g,0]
- two magnetic domains (twins)

Lowest monoclinic MSSG
8.1.4.2.m33.2 Bm.1'(a,b,0)ss

$k=|\boldsymbol{k}_1|=|\boldsymbol{k}_2|=g$

$$\mathbf{M}_{Ce(i)} = m_{ix}\sin(2\pi kx)\mathbf{e}_{\boldsymbol{x}} + m_{iz}\sin(2\pi kx+\varphi_i)\mathbf{e}_{\boldsymbol{z}}, \quad i=1,2$$

Experimental values (μ_B) :
Ce1: m_{1x}= -0.64(1), m_{1z} =-0.30(6)
Ce2: m_{2x}= -1.50(2), m_{2z} = 0.46(8)

$\varphi_1=\varphi_2\approx 90°$

$Ce1(0,0,z)$
$Ce2(0,\frac{1}{2},z+\frac{1}{4})$

Two independent sites. No symmetry relations between Ce1 and Ce2

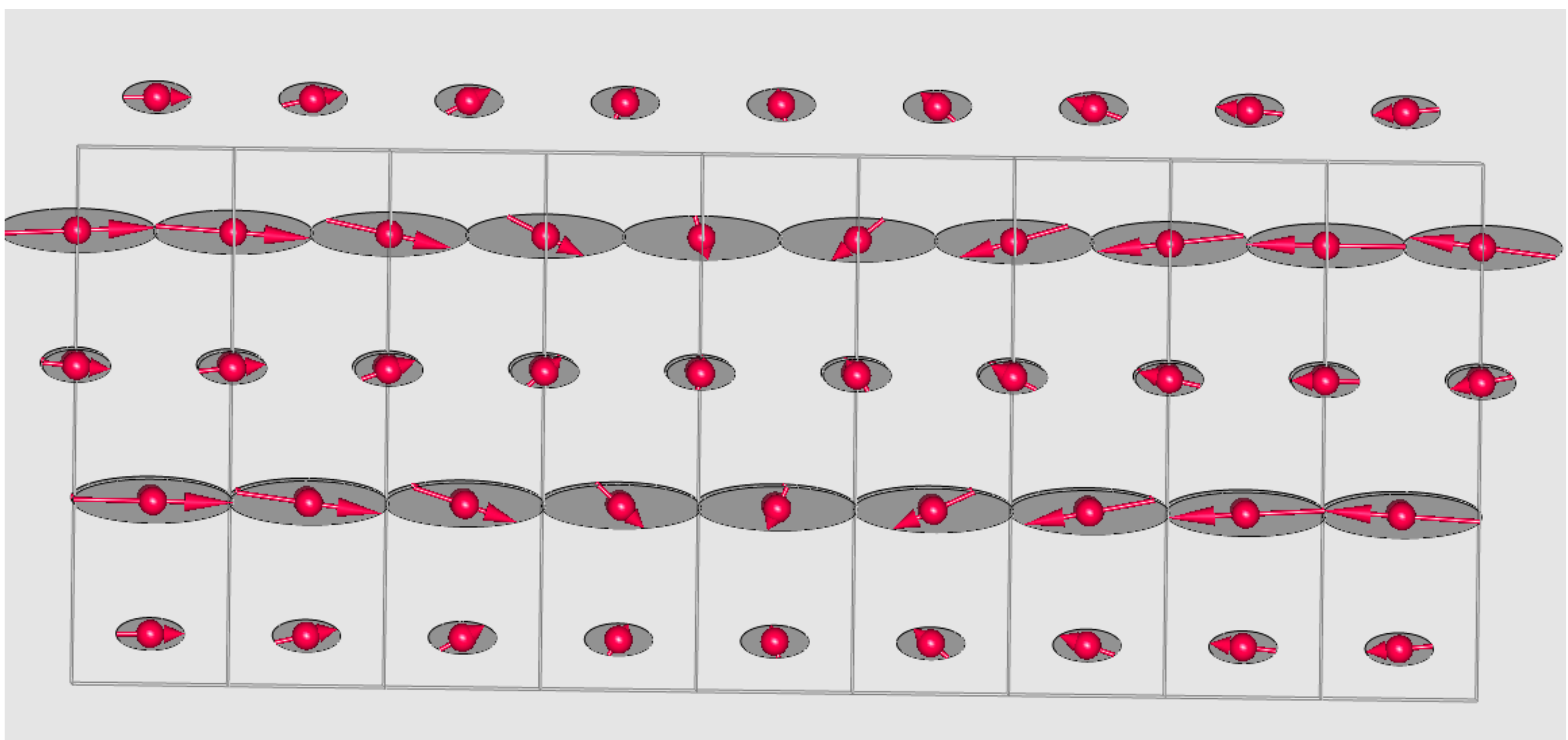

One k-case, standard representation analysis without magnetic group symmetry arguments: Space group $I4_1md$, Ce 4a (0,0,z)

Solution: SM2 irreducible representation

- **Cycloid in ac-plane for k1=[g,0,0]**, in bc=lane for k2=[0,g,0]
- two magnetic domains (twins)

Lowest monoclinic MSSG
8.1.4.2.m33.2 Bm.1'(a,b,0)ss

$k=|\boldsymbol{k}_1|=|\boldsymbol{k}_2|=g$

$$\mathbf{M}_{Ce(i)} = m_{ix}\sin(2\pi kx)\mathbf{e}_{\boldsymbol{x}} + m_{iz}\sin(2\pi kx+\varphi_i)\mathbf{e}_{\boldsymbol{z}}, \quad i=1,2$$

Experimental values (μ_B) :
Ce1: m_{1x}= -0.64(1), m_{1z} =-0.30(6)
Ce2: m_{2x}= -1.50(2), m_{2z} = 0.46(8)

$\varphi_1=\varphi_2\approx 90°$

$Ce1(0,0,z)$
$Ce2(0,\frac{1}{2},z+\frac{1}{4})$

Two independent sites. No symmetry relations between Ce1 and Ce2

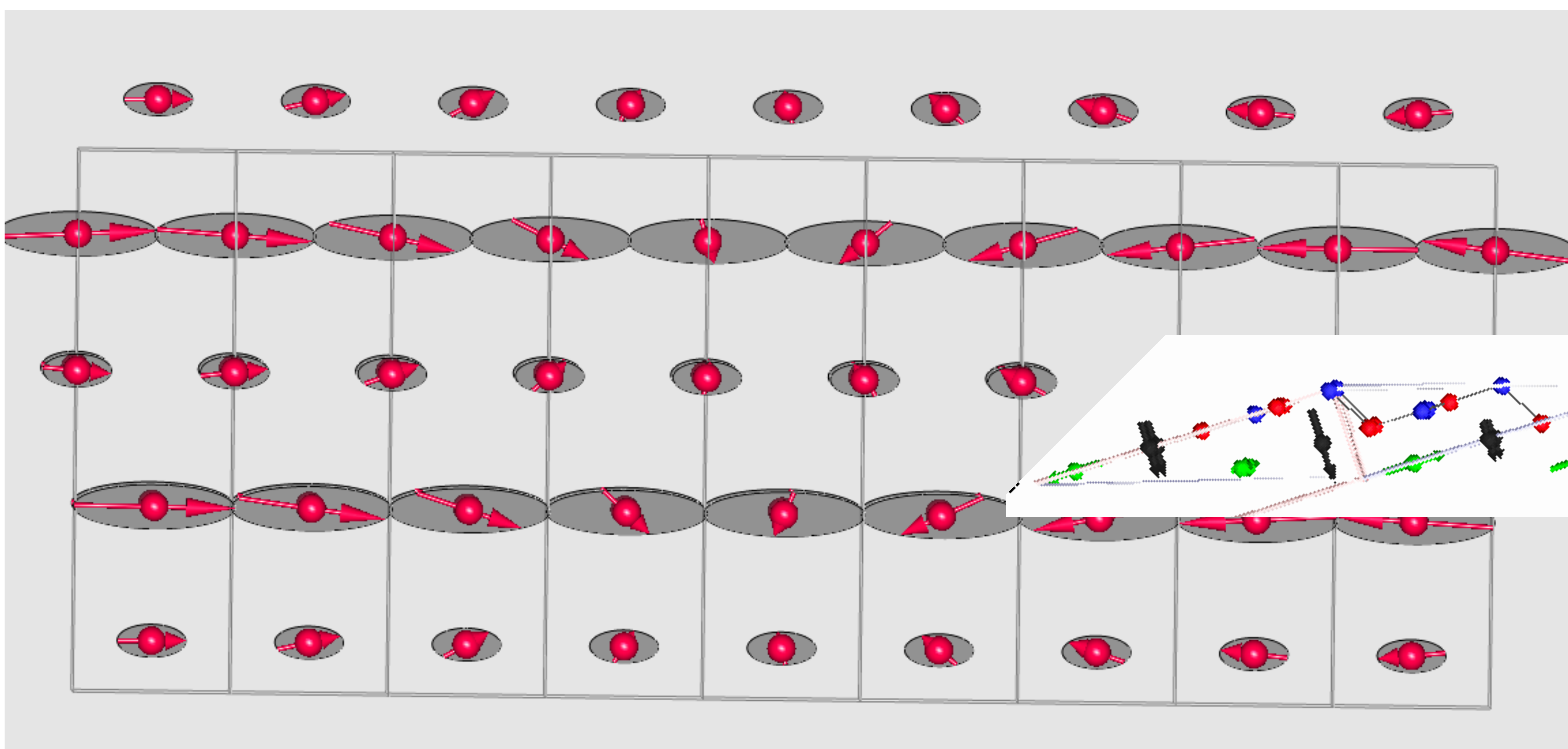

Note: if $\varphi_1=\varphi_2=0 \rightarrow$ amplitude modulation, different symmetry

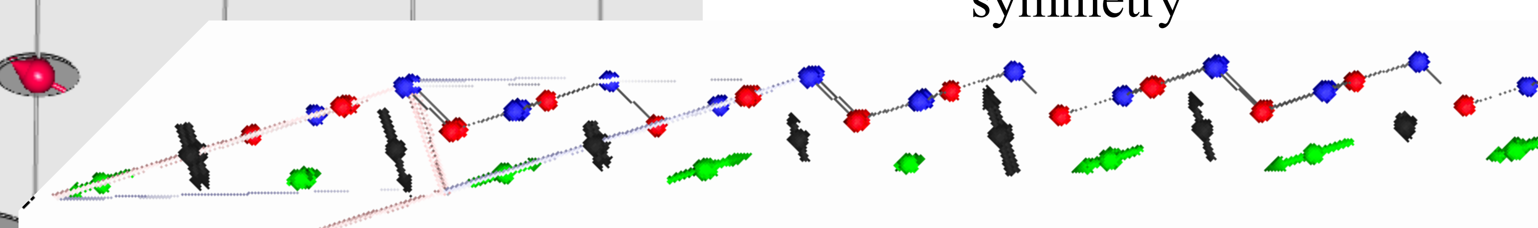

Symmetry of cycloid. 3D+1 superspace group for SM2 irrep

$I4_1md1'$ Advantage of magnetic symmetry when keeping {+**k**,-**k**}

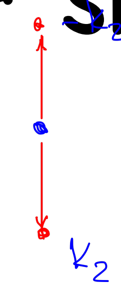

or

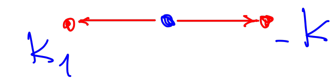

I2mm1'(0,0,g)0s0s

$$\mathbf{M}_{Ce(i)} = m_{ix}\sin(2\pi kx)\mathbf{e}_{\boldsymbol{x}} + m_{iz}\cos(2\pi kx)\mathbf{e}_{\boldsymbol{z}}, \quad i = 1, 2$$

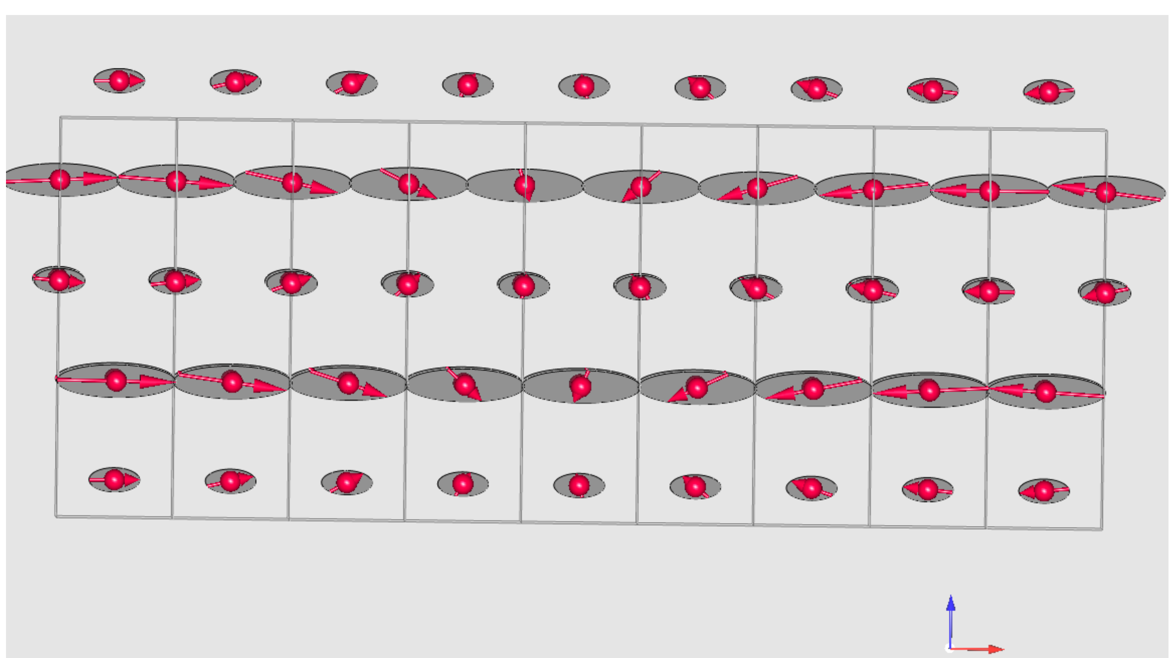

Experimental values:
Ce1: m_{1x}= -0.64(1), m_{1z} =-0.30(6)
Ce2: m_{2x}= -1.50(2), m2z = 0.46(8)

Symmetry of cycloid. 3D+1 superspace group for SM2 irrep

$I4_1md1'$ Advantage of magnetic symmetry when keeping {+**k**,-**k**}

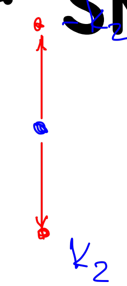

or

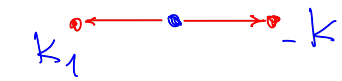

I2mm1'(0,0,g)0s0s

$$\mathbf{M}_{Ce(i)} = m_{ix}\sin(2\pi kx)\mathbf{e}_{\boldsymbol{x}} + m_{iz}\cos(2\pi kx)\mathbf{e}_{\boldsymbol{z}}, \quad i = 1, 2$$

phase shift 90 degrees between x and y-components is fixed by symmetry!

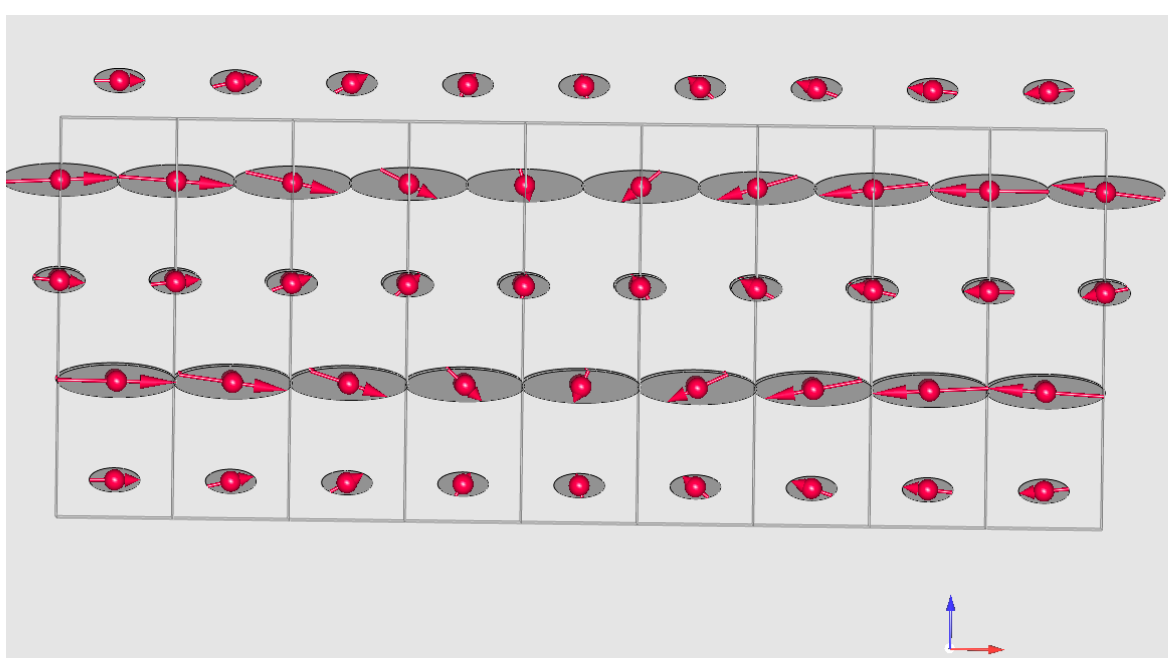

Experimental values:
Ce1: m_{1x}= -0.64(1), m_{1z} =-0.30(6)
Ce2: m_{2x}= -1.50(2), m2z = 0.46(8)

Topological density and charge. H=0

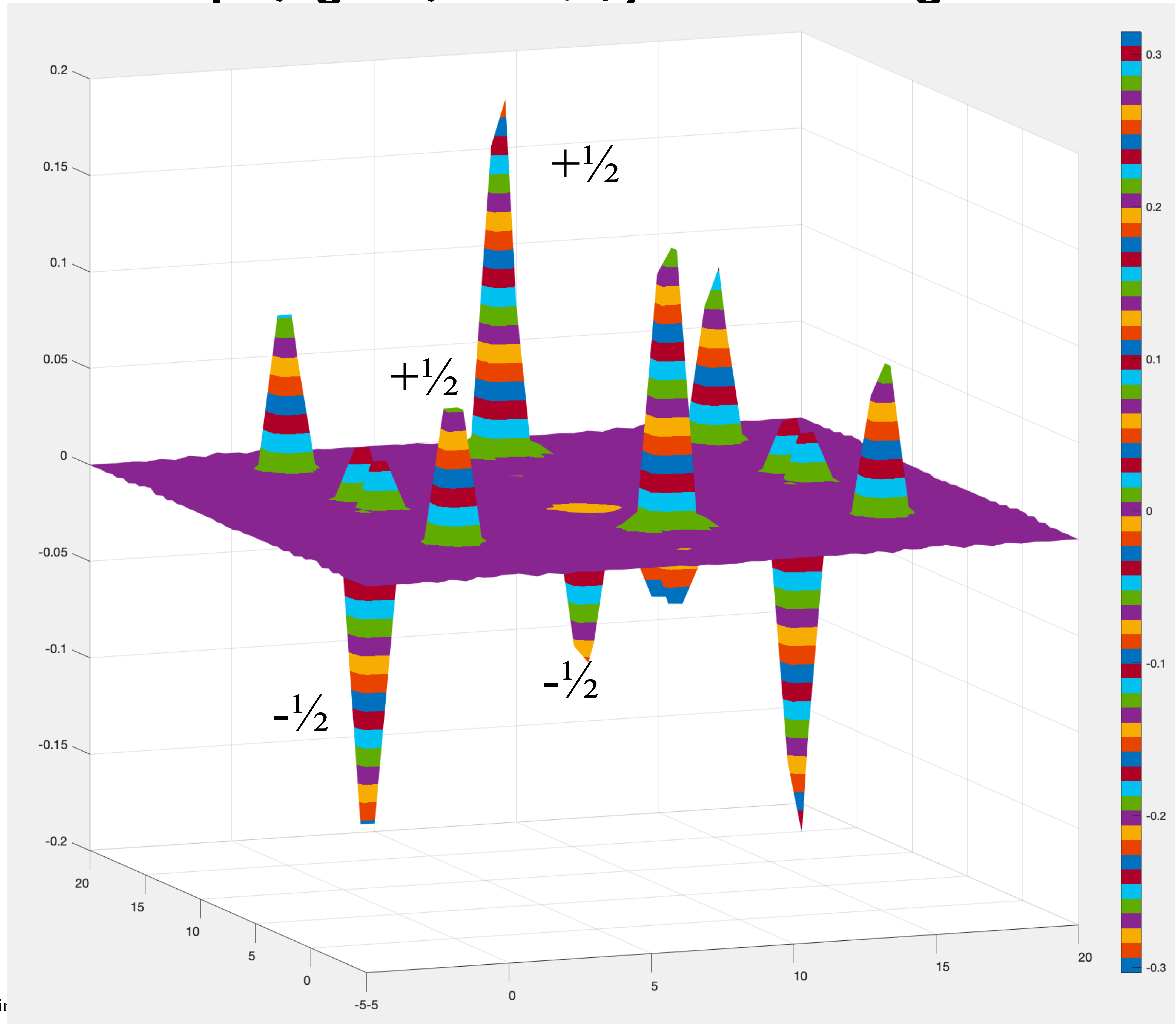

MnGe synthesized by two different methods. Crystal structure.

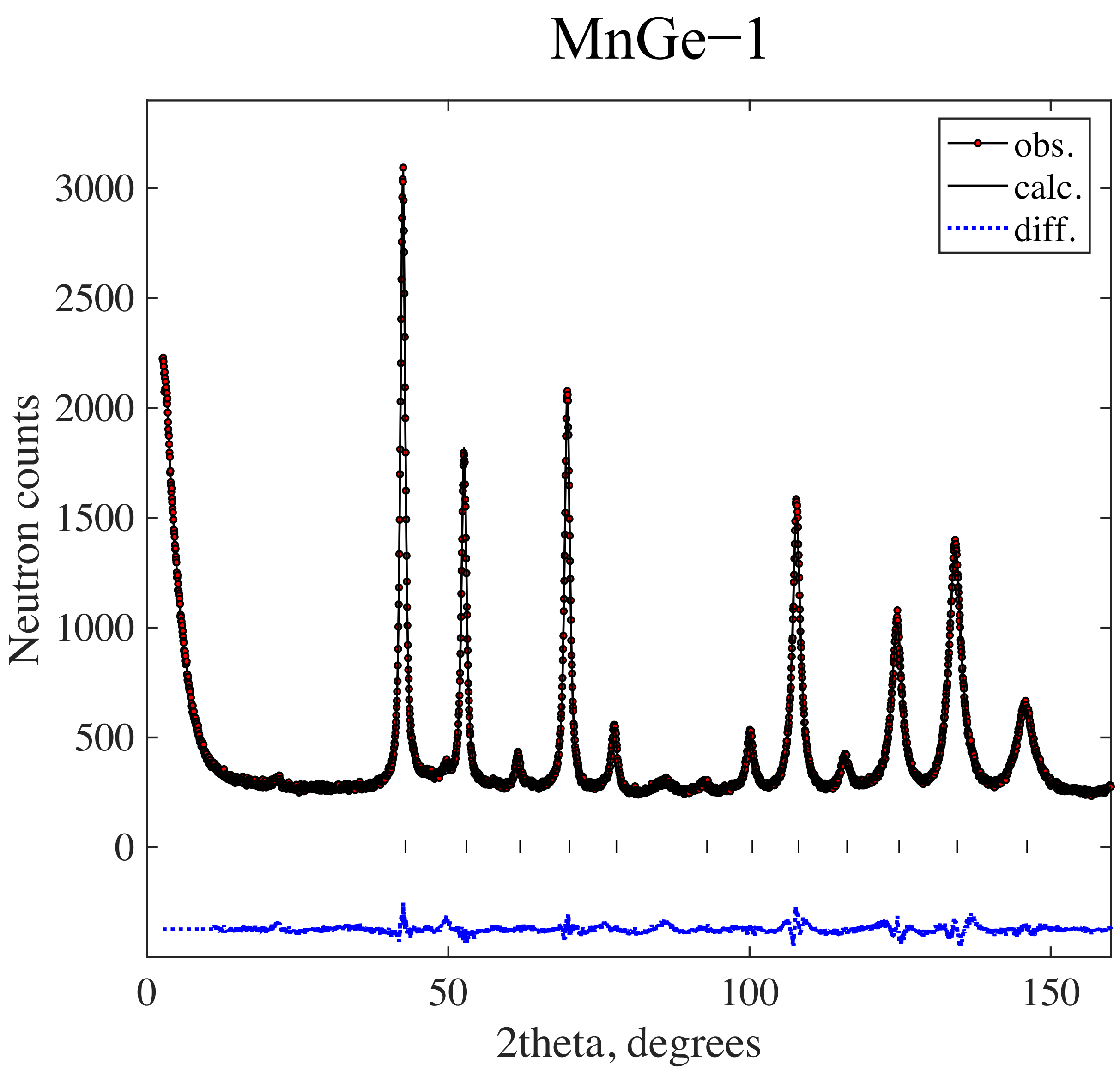

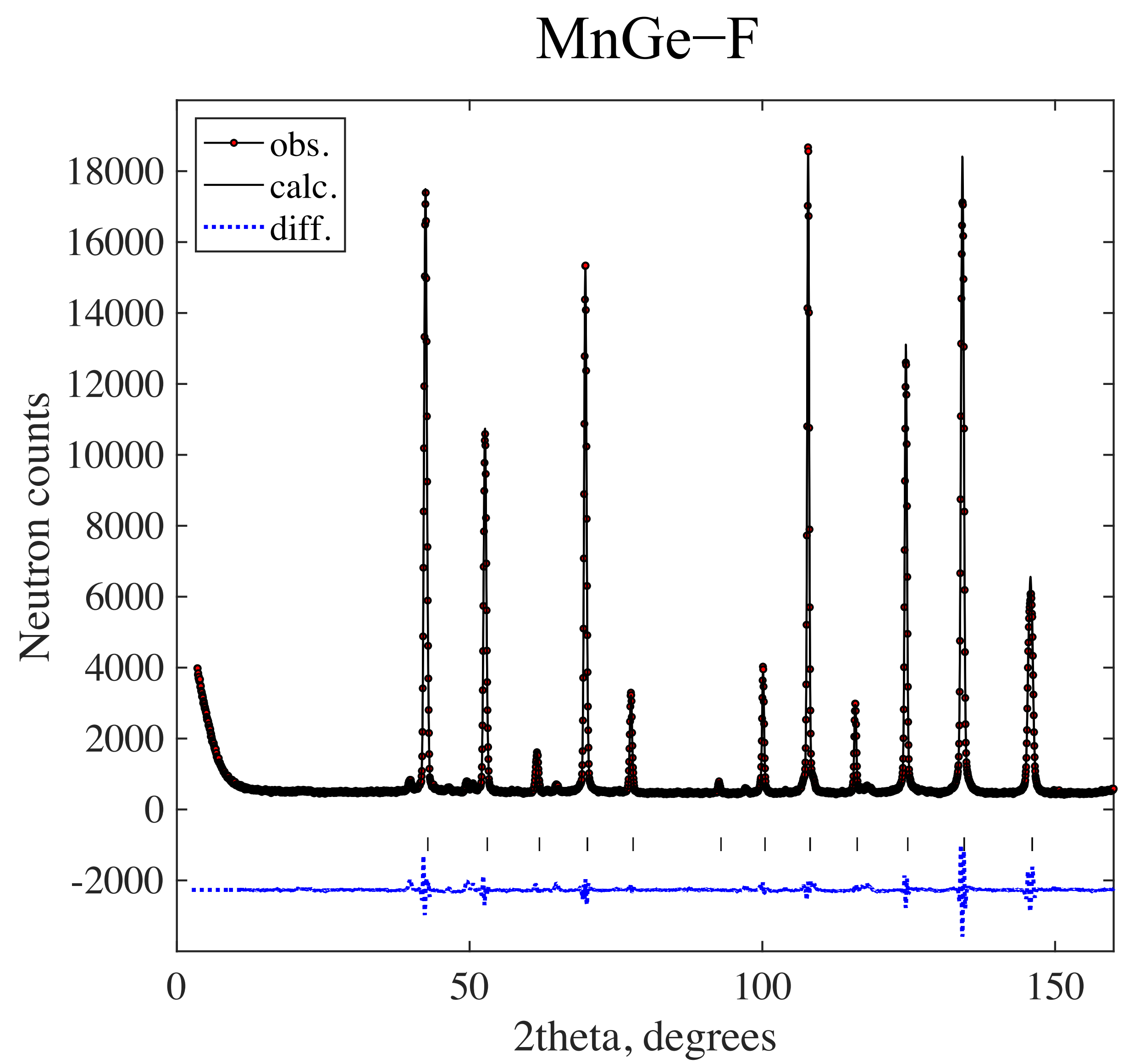

The coherently scattering domains (or crystalline sizes)

~150 Å

>2000 Å

MnGe synthesized by two different methods. Magnetic structure.

MnGe−1

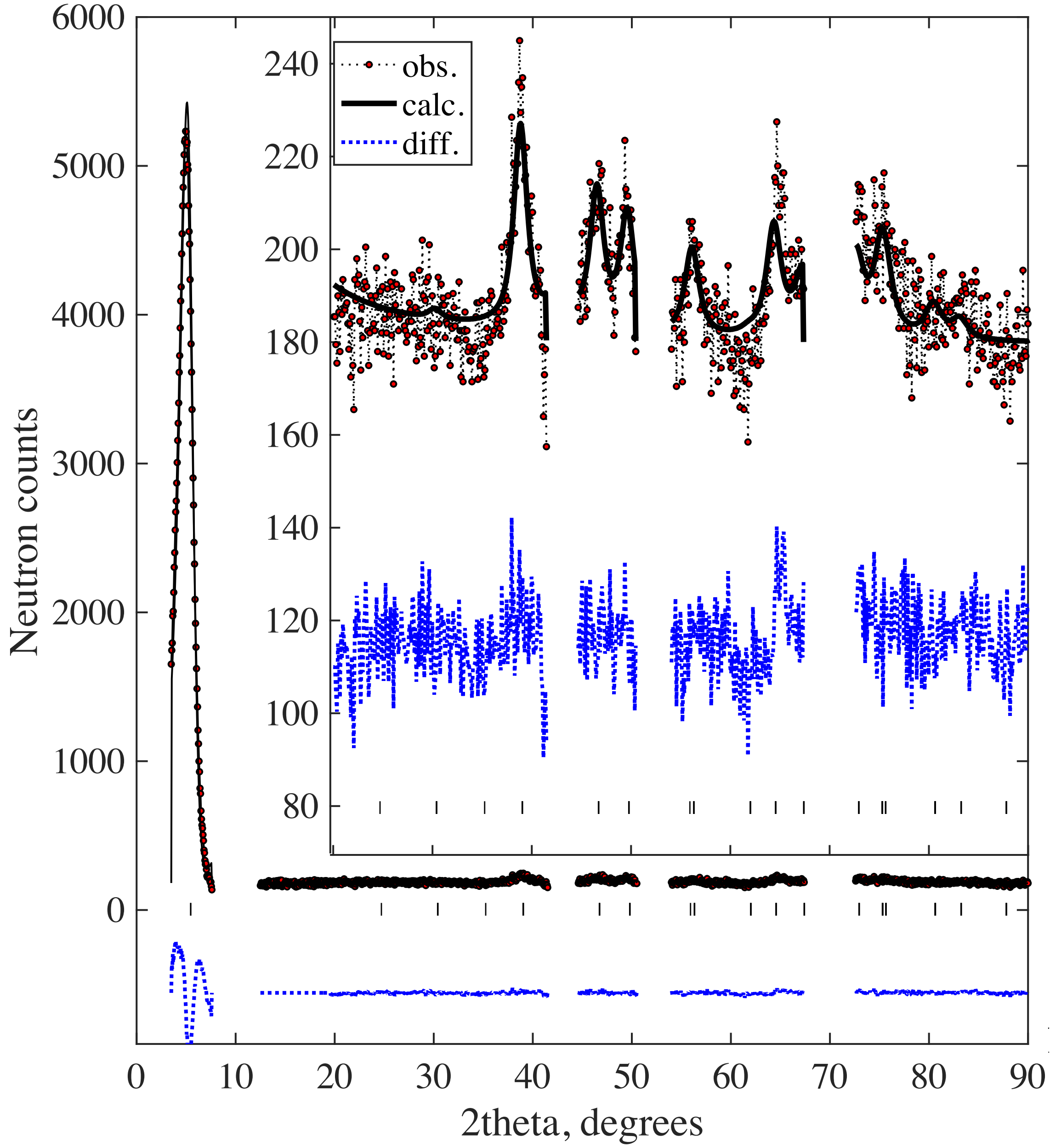

2.33 μ_B

MnGe−F

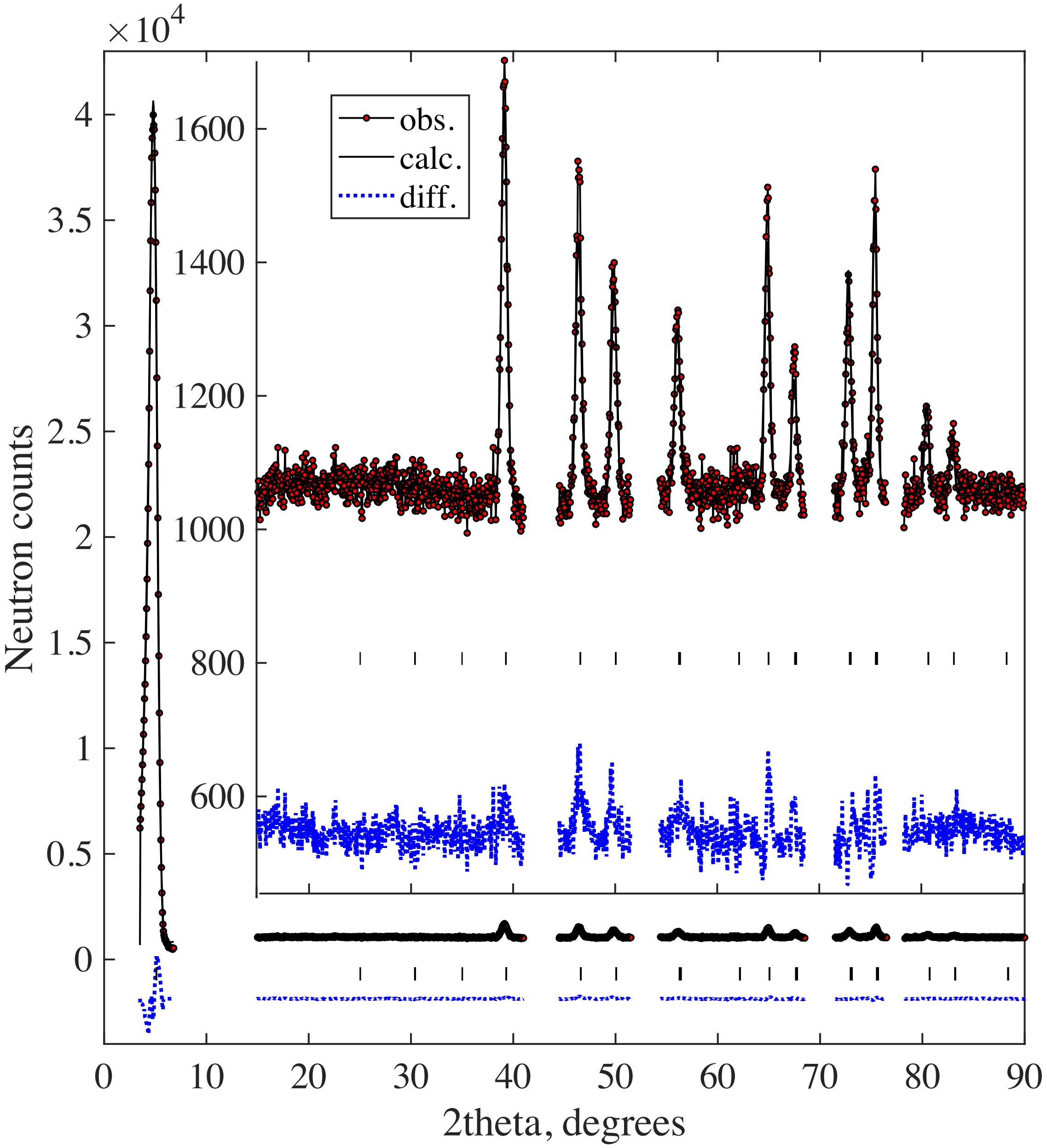

2.57 μ_B

Continuous limit k->0 artificial full star magnetic structure

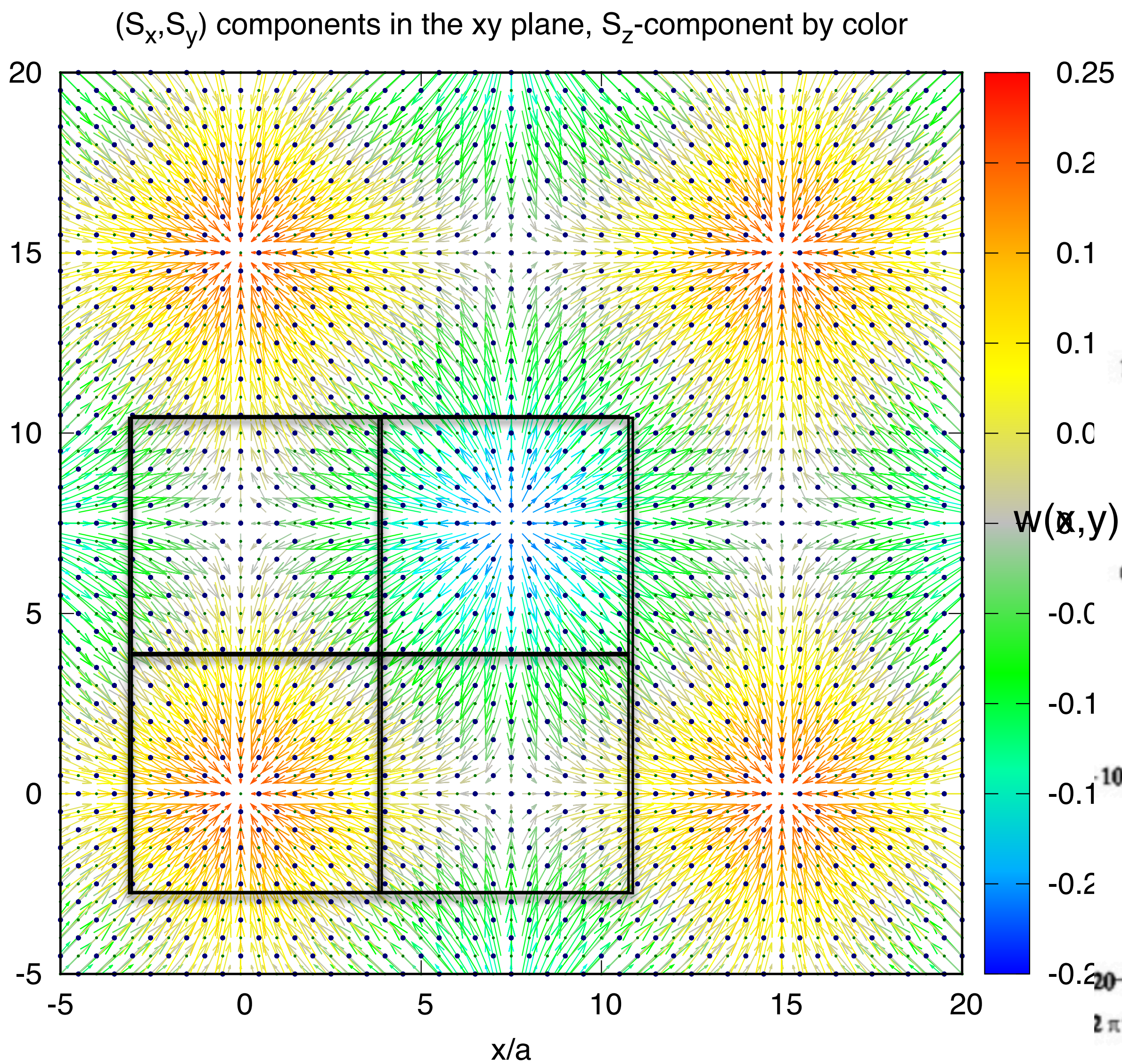

topological density/winding ~ solid angle

$$w(x,y) = \frac{1}{4\pi}(\mathbf{n}\cdot[\frac{\partial \mathbf{n}}{\partial x} \times \frac{\partial \mathbf{n}}{\partial y}]), \quad \mathbf{n} = \mathbf{M}/M$$

Topological number/charge

$$Q = \int\int w(x,y)dxdy$$

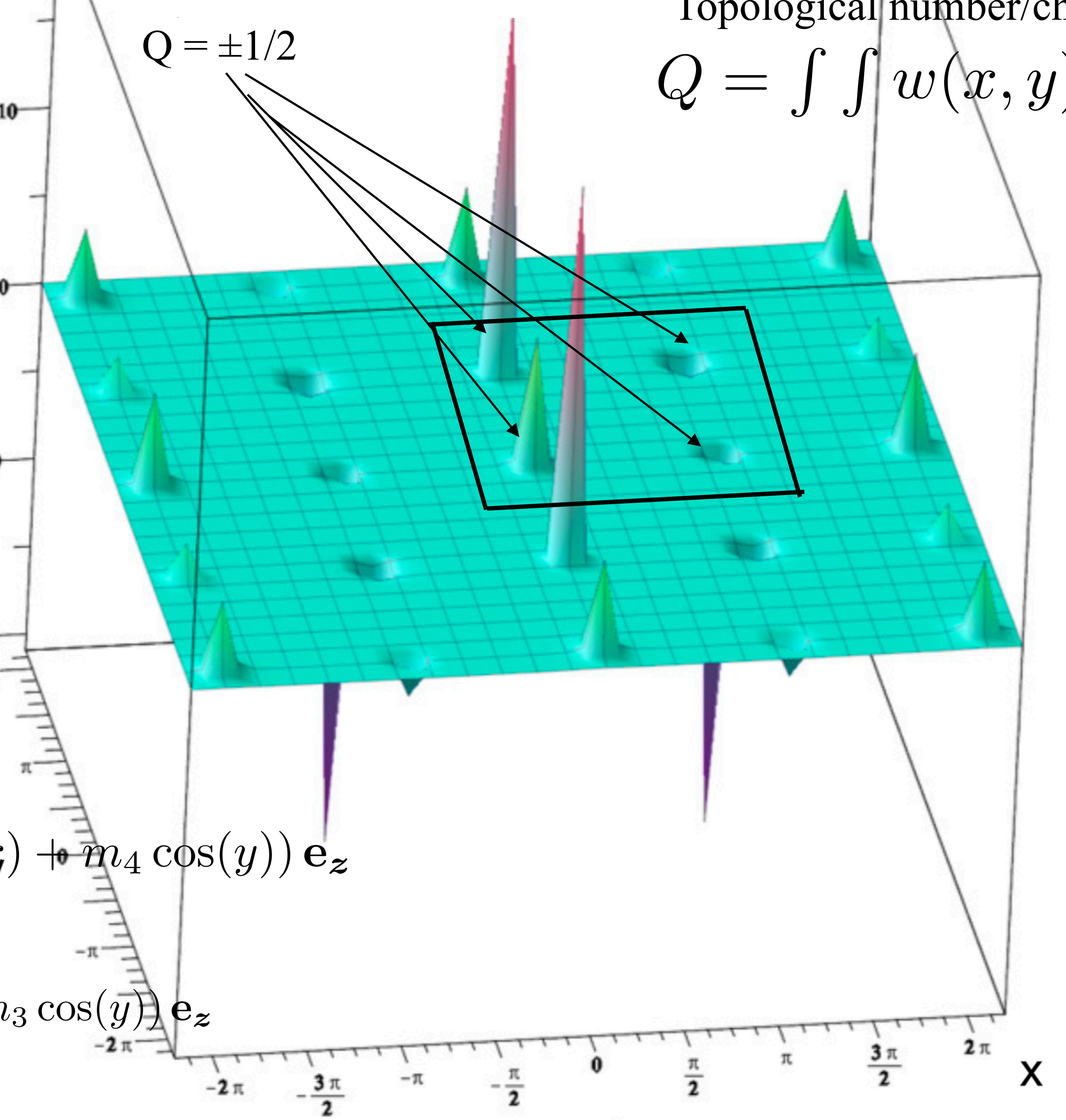

$$\mathbf{M}_{\mathrm{Ce1}} = m_1 \sin(x)\mathbf{e}_{\boldsymbol{x}} + m_2 \sin(y)\mathbf{e}_{\boldsymbol{y}} + (m_3 \cos(x) + m_4 \cos(y))\,\mathbf{e}_{\boldsymbol{z}}$$

m1=m2=2 and m3=0.1, m4=0.11

$$\mathbf{M}_{\mathrm{Ce2}} = m_2 \sin(x)\mathbf{e}_{\boldsymbol{x}} + m_1 \sin(y)\mathbf{e}_{\boldsymbol{y}} + (m_4 \cos(x) + m_3 \cos(y))\,\mathbf{e}_{\boldsymbol{z}}$$

Continuous limit k->0 artificial full star magnetic structure

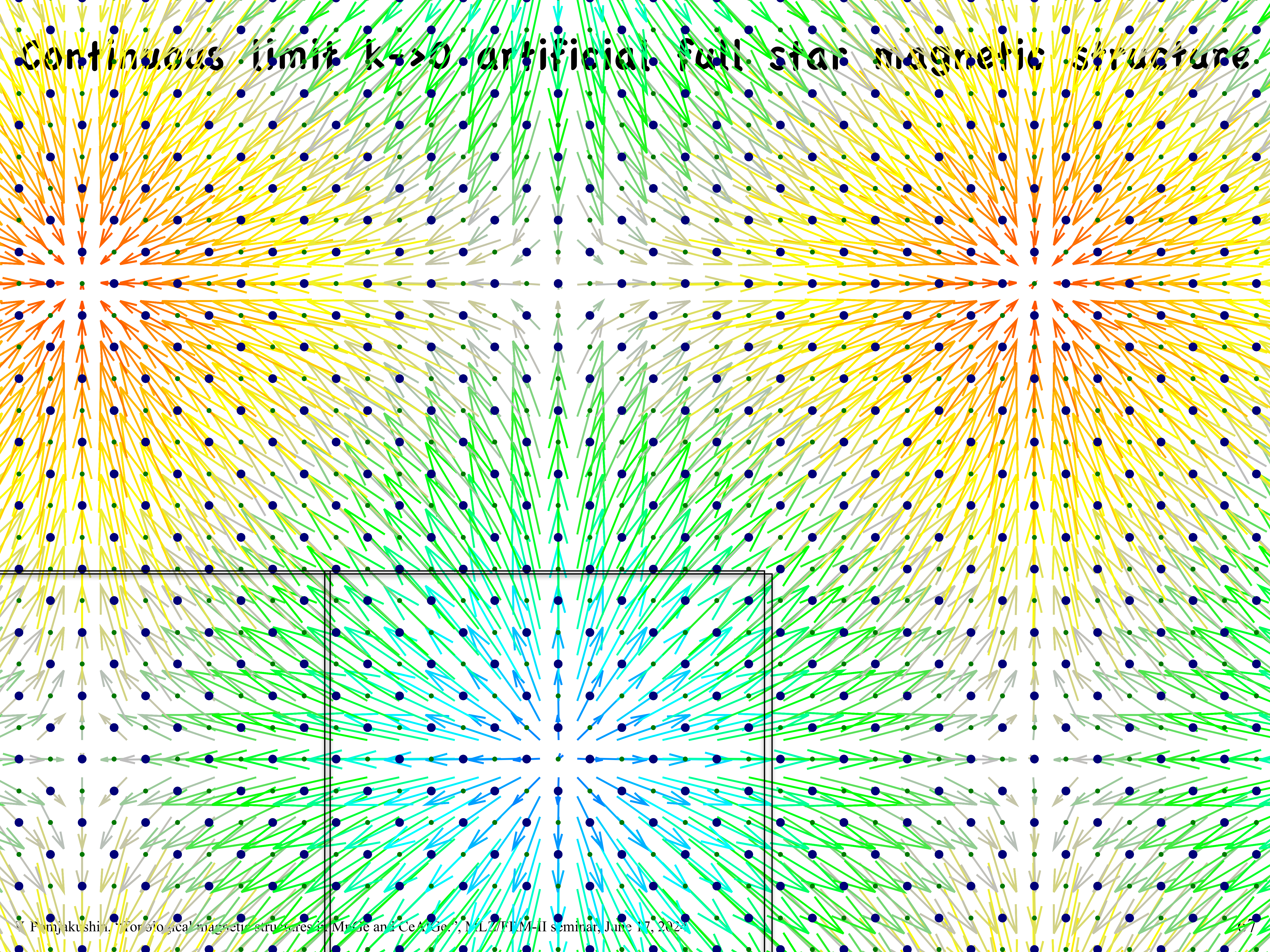

Extrema can be both in |M|=0 and at max |Mz|

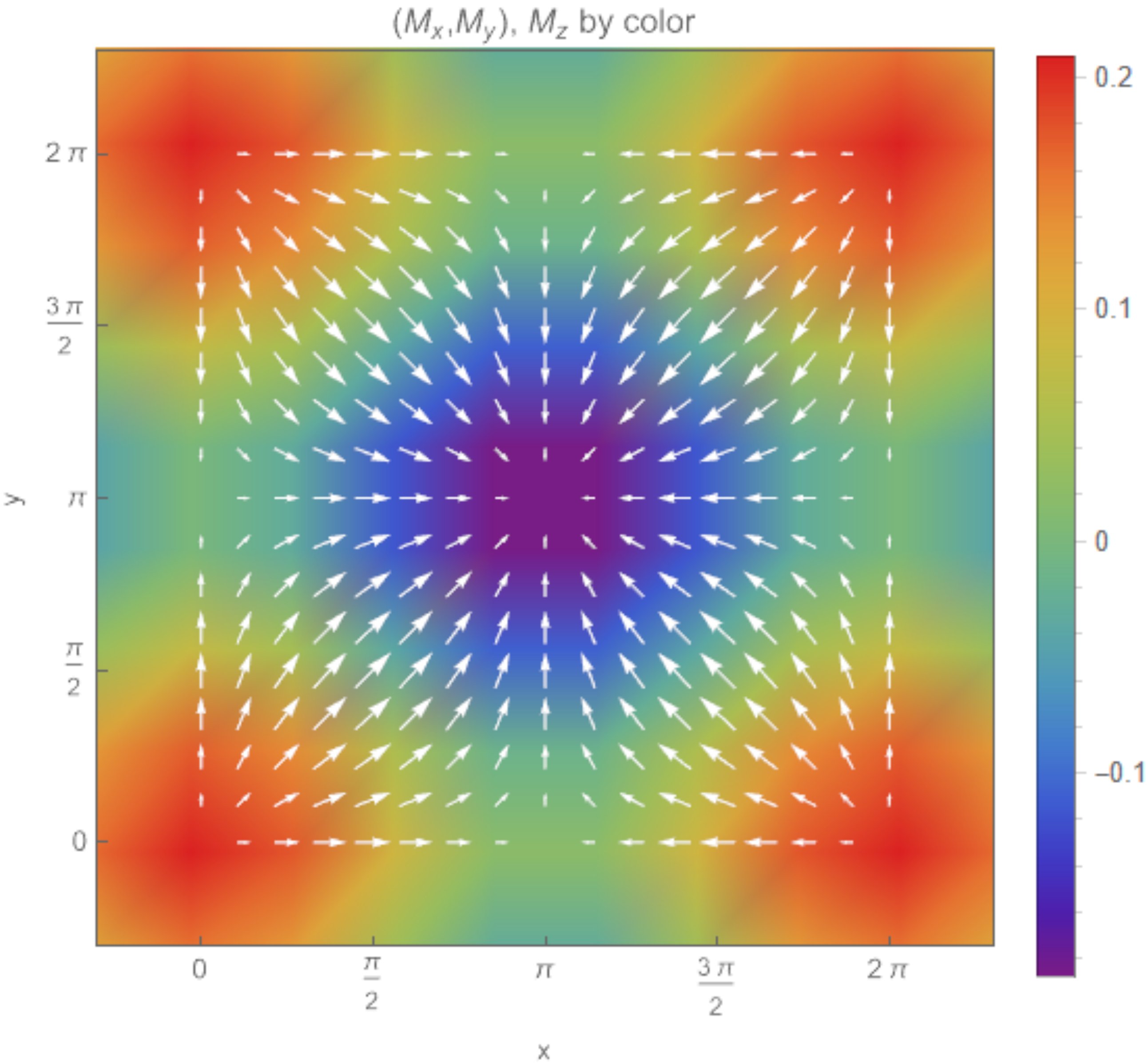

,

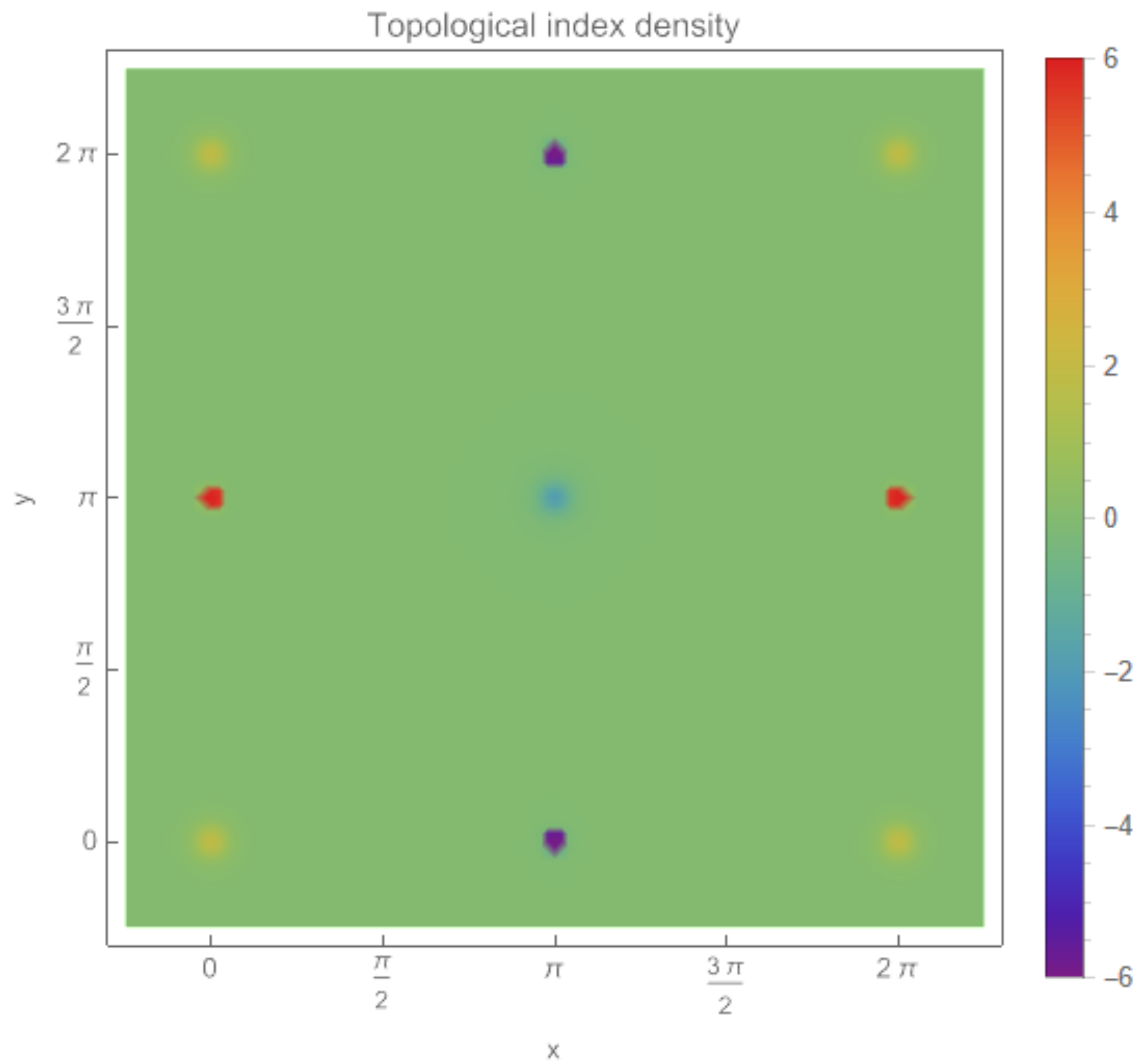

in CeAlGe for Ce1 (mx, my, mz) = [sin y, sin x, 0.5(0.11 cos x +0.11cos y)].

singularities and Bloch/Neel

{Mx , My} vs. {x,y}, Mz by color

Extrema can be only in |M|=0

```
9]:= {fig1, fig2} // Row
```

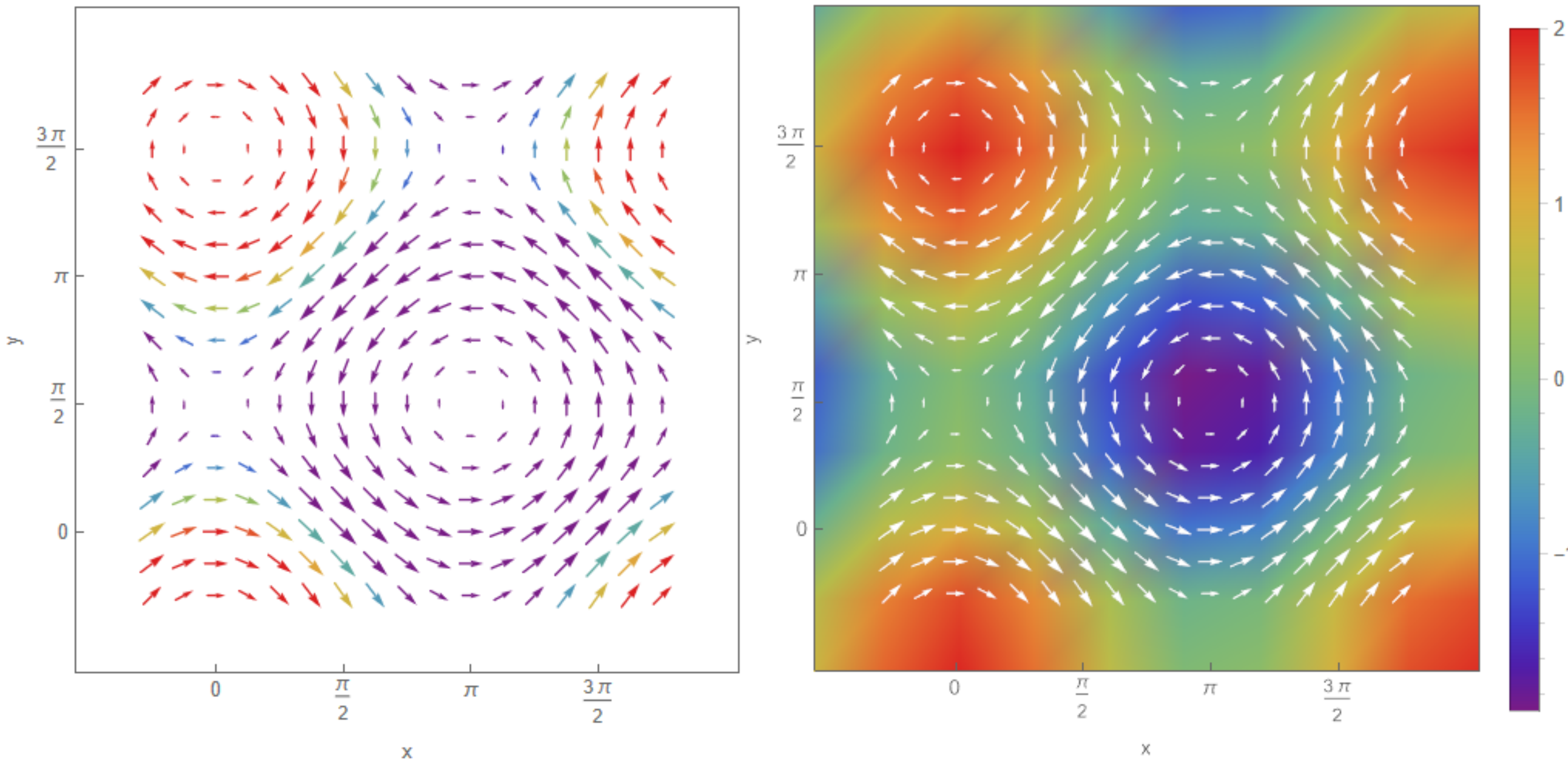

$(mx, my, mz) = (\cos y, -\sin x, -\sin y + 1.001\cos x)$.

in CeAlGe for Ce1 $(mx, my, mz) = [\sin y,\ \sin x,\ 0.5(0.11 \cos x + 0.11\cos y)]$.

Skyrmions

Neel skyrmion Q = 1

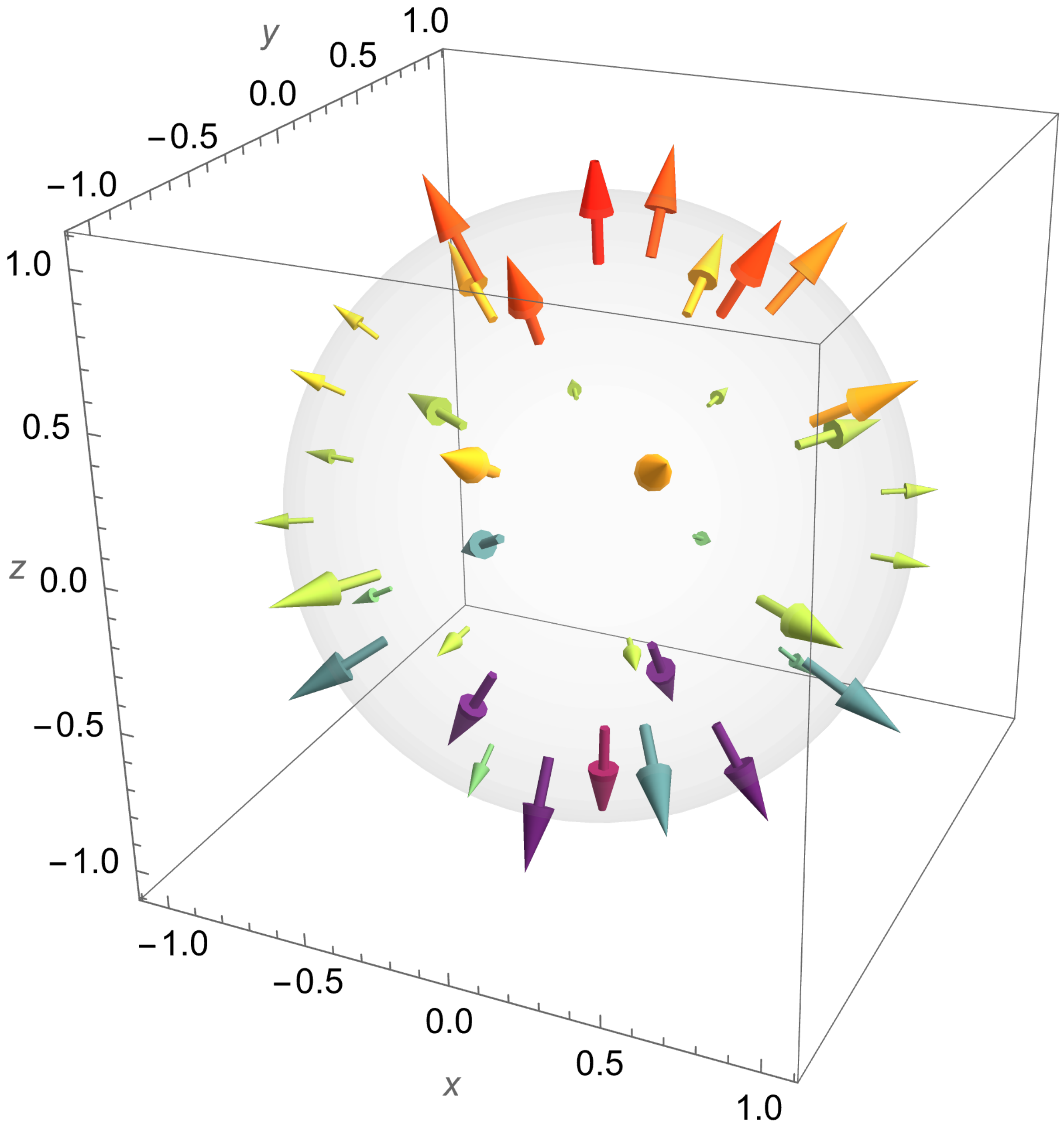

Neel skyrmion Q=-1

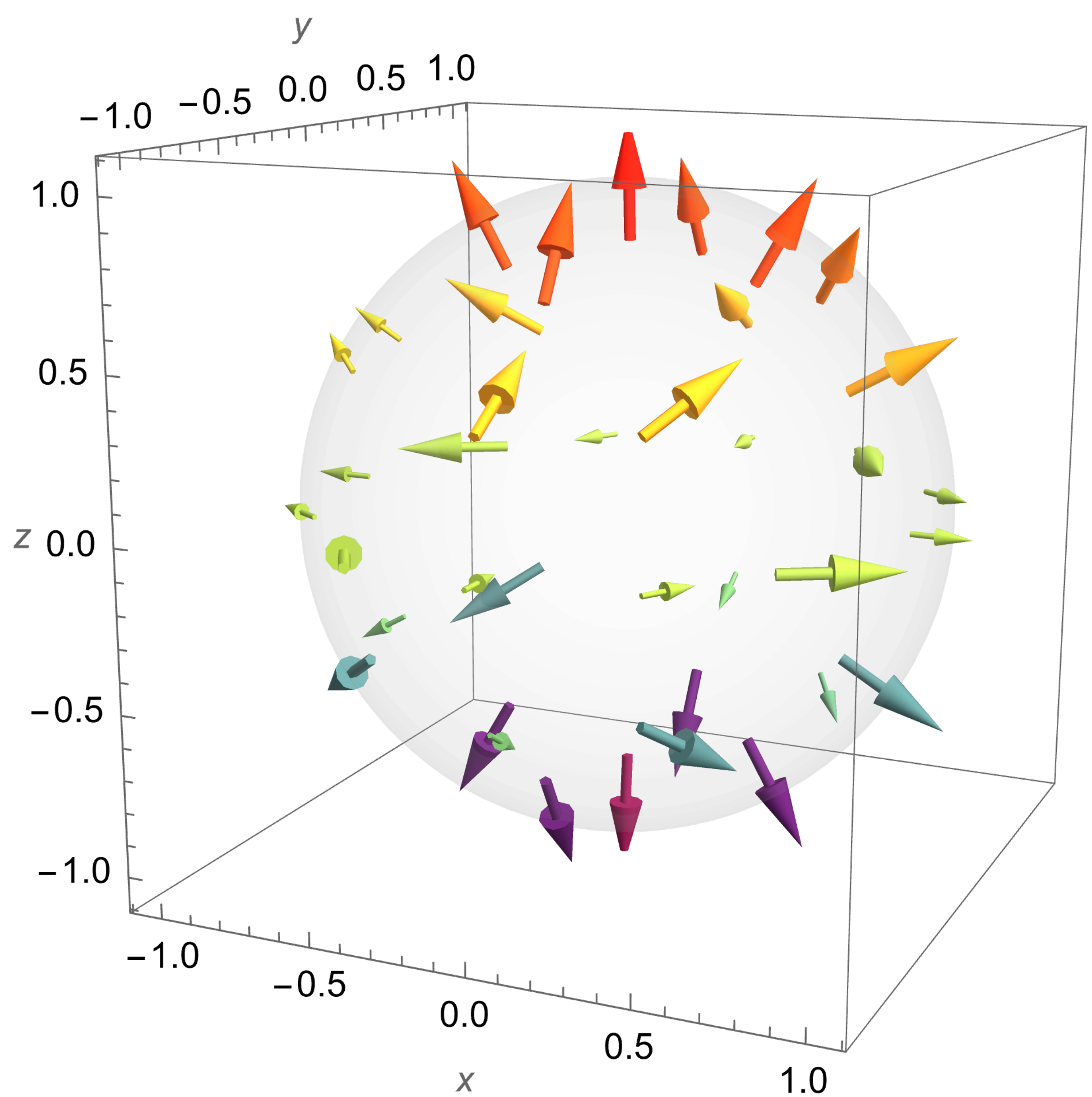

Merons

Neel meron Q = 1/2

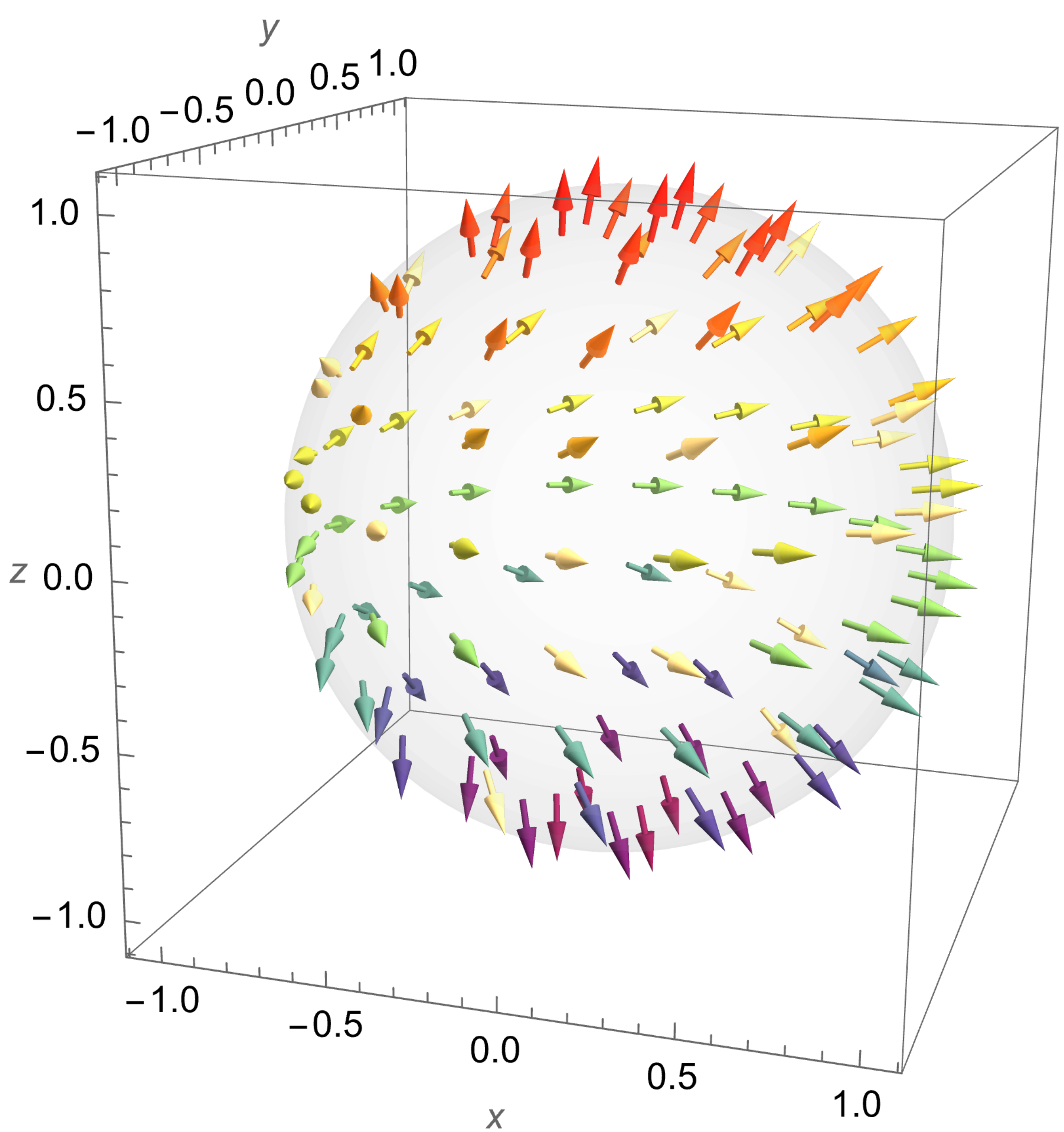

Neel meron Q = -1/2

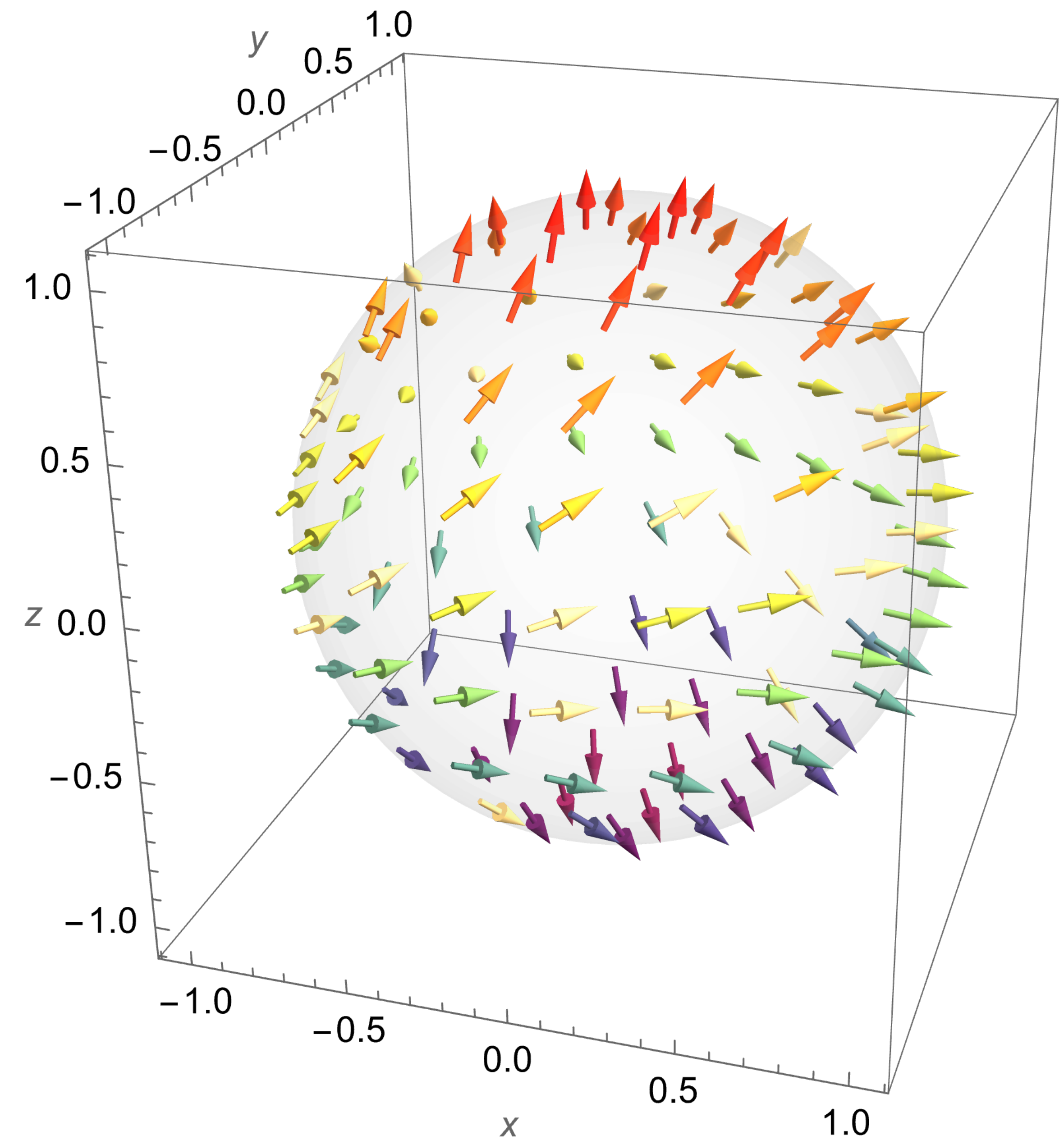

non linear M(x,y). Q=+-1!

Mapping $N: R^2 \longrightarrow S^2$

```
In[◦]:= n[{u_, v_}] := {2*u, 2*v, -1+u^2+v^2}/(1+u^2+v^2)
```

Periodic mapping $P: R^2 \longrightarrow R^2$

```
In[◦]:= p[{x_, y_}] := {Sin[x], Sin[y]}/(Cos[x]^2*Cos[y]^2 + ϵ)
```

Peiodic mapping $f = N \circ P: R^2 \longrightarrow S^2$